SYNTHESIS OF NOVEL POTENT DRUG MOLECULES ACTIVE AGAINST PROSTATE CANCER AND INVESTIGATION OF BIOACTIVE PROPERTIES OF CYCLOPOLYMERS OBTAINED BY RAFT POLYMERIZATION

by

Selda Erkoç

B.S., Chemistry, İstanbul University, 2001

M.S., Chemistry, Boğaziçi University, 2005

Submitted to the Institute for Graduate Studies in
Science and Engineering in partial fulfillment of
the requirements for the degree of
Doctor of Philosophy

Graduate Program in Chemistry

Boğaziçi University

2011

SYNTHESIS OF NOVEL POTENT DRUG MOLECULES ACTIVE AGAINST PROSTATE CANCER AND INVESTIGATION OF BIOACTIVE PROPERTIES OF CYCLOPOLYMERS OBTAINED BY RAFT POLYMERIZATION

APPROVED BY:

Assoc. Prof. A. Ersin Acar (Thesis Supervisor)	.....
Prof. Duygu Avcı	.....
Prof. İlknur Doğan	.....
Prof. Selim Küsefoğlu	.....
Prof. Ümit Tunca	.....

DATE OF APPROVAL: 22.12.2011

Aileme...

ACKNOWLEDGEMENTS

I would like to express my gratitude to my thesis supervisor Assoc. Prof. A. Ersin Acar for his guidance during my study. I belive that being a part of Acar Reseach Group has been an invaluable exprience for me.

I would like to thank my committe members Prof. Duygu Avcı, Prof. İlknur Doğan, Prof. Selim Küsefoğlu and Prof. Ümit Tunca for spending their time in reviewing my thesis.

I am grateful to Prof. Metin Türkay and Assoc. Prof. İ. Halil Kavaklı from Koç University for their contributions to my thesis.

I would like to thank Prof. Alpay Taralp and Gönül Kendirci from Sabancı University for the antibacterial tests.

I would like to thank Ayla Türkekul and Burcu Selen Çağlayan for the NMR analyses.

I want to thank my all laboratory friends; first of all to Sezgin Bayrak and Nurdan Meraklı for their friendships and helps to my study and Ahmet Köseoğlu, Engin Doğan, Aydın Can, Erhan Özkal, Gülhan Kocasakal, Berçem Dutağacı, Kanykey Ryskulova, Tuba Şahin, Turhan Gül, Nariye Çavuşoğlu, Şükrü Eren, Turgay Yıldırım and Özgün Can Önder for their friendships. I also especially would like to thank Şule Erol, Zeynep Saraylı, Sevgi Sarıgül, Jesmi Çavuşoğlu and Nergiz Cengiz for their enjoylable friendships and motivating words through my study. I would like to extend my thanks to all members of Chemistry Department.

Finally, I would like to express my gratitude to my family; my mother Aysel Erkoç, my father Lütfi İhsan Erkoç and my sisters Temha Erkoç and Fatma Çağla Erkoç for their everlasting support, encouragement and unconditional love. And my special thanks go to Serkan İlter for his endless support and love.

The projects were funded by Boğaziçi University Research Fund (BAP) and The Scientific and Technological Research Council of Turkey (TÜBİTAK, Project No: 109T431 and 104M261).

ABSTRACT

SYNTHESIS OF NOVEL POTENT DRUG MOLECULES ACTIVE AGAINST PROSTATE CANCER AND INVESTIGATION OF BIOACTIVE PROPERTIES OF CYCLOPOLYMERS OBTAINED BY RAFT POLYMERIZATION

The first part of the thesis includes synthesis of novel potent drug molecules active against prostate cancer. Structure-based drug design (SBDD) approach was used to discover novel lead compounds active against CYP17 by the researchers Prof. Metin Türkay and Assoc. Prof. İ. Halil Kavaklı from the Koç University. They found a non-steroidal lead compound with the IC_{50} value of 35.65 μM. In this study, in order to increase the activity of the lead compound against the CYP17, lead optimization studies were done. Lead compound derivatives were evaluated on the computer generated model of CYP17. The compounds that have favorable energy values in docking studies were synthesized to be effective in nanomolar concentrations. Some of the synthesized compounds were subjected to biological tests in order to measure inhibitory effects of them on CYP17. IC_{50} value of the compounds that displayed favorable inhibitory activity on human CYP17 were calculated. As a result, a new compound with the IC_{50} value of 2.3 μM was discovered. The activity of this compound is about fifteen times higher than the activity of the lead compound.

The second part of the thesis includes the investigation of bioactive properties of cyclopolymers obtained by Reversible Addition Fragmentation Chain Transfer (RAFT) Polymerization. In this study, RAFT polymerization was applied to symmetrical difunctional monomers, alkyl α-(hydroxymethyl)acrylate (RHMA) ether dimers (R=alkyl (ethyl, *n*-butyl, *tert*-butyl, cyclohexyl, isobornyl)). The livingness of the obtained cyclopolymers with *tert*-butyl and isobornyl ester groups was shown through successful block copolymerization studies with *n*-butyl acrylate where the former was used as the macro-chain transfer agent (macroCTA). Finally, the antibacterial activities of the obtained cyclopolymers were investigated using *Staphylococcus aureus* and *Escherichia coli* as test organisms.

ÖZET

PROSTAT KANSERİNE KARŞI AKTİF YENİ İLAÇ MOLEKÜLLERİNİN SENTEZİ VE RAFT POLİMERLEŞME YÖNTEMİ İLE ELDE EDİLEN SİKLOPOLİMERLERİN BİYOAKTİF ÖZELLİKLERİNİN ARAŞTIRILMASI

Tezin ilk bölümünde prostat kanserine karşı aktif yeni ilaç moleküllerinin sentezi yer almaktadır. Koç Üniversitesi'nde çalışan araştırmacılar Prof. Metin Türkay ve Doç. Dr. İbrahim Halil Kavaklı CYP17 enziminin aktivitesini önleyebilecek yeni ilaç aday moleküllerinin keşfi icin yapıya dayalı ilaç tasarımı yöntemini kullandılar ve steroid yapıda olmayan, IC_{50} değeri 35.65 μM olan yeni bir aday molekül buldular. Bu çalışmada, aday molekülün CYP17 enzimine karşı aktivitesini arttırmak için, aday molekül iyileştirme çalışmaları yapıldı. Bazı aday molekül türevleri CYP17 enziminin bilgisayar modeli üzerinde değerlendirildi. Bilgisayar çalışmalarında uygun enerji değerlerine sahip aday molekül türevleri nM seviyede etkili olabilmek amacı ile sentezlendi. Sentezlenen bileşiklerden bazılarının CYP17 enzimi üzerinde önleyici etkilerini ölçmek için biolojik testleri yapıldı. Enzim üzerinde uygun önleyici etki gösteren bileşiklerin IC_{50} değerleri hesaplandı. Sonuç olarak IC_{50} değeri 2.3 μM olan ve steroid yapıda olmayan yeni bir molekül bulundu. Bu molekülün aktivitesi aday molekülün aktivitesinden yaklaşık on beş kat daha fazladır.

Tezin ikinci bölümünde Tersinir Eklenme Ayrılma Zincir Transfer (RAFT) Polimerleşme yöntemi ile elde edilen siklopolimerlerin bioaktif özelliklerinin araştırılması yer almaktadır. Bu çalışmada, RAFT polimerleşme yöntemi simetrik difonksiyonlu monomerlere uygulandı. Bu monomerler alkil α-(hidroksimetil)akrilat (RHMA) eter dimerleri (R=alkil (etil, *n*-butil, *tert*-butil, sikloheksil, isobornil)) dir. *Tert*-bütil ve isobornil ester gruplu siklopolimerlerin yaşayan uç gruplara sahip olduğu başarılı blok kopolimerleşme çalışmaları ile gösterildi. Polimerler makroRAFT ajanı olarak, *n*-bütil akrilat da ikinci monomer olarak kullanıldı. Son olarak elde edilen kontrollü siklopolimerlerin antibakteriyel özellikleri *Staphylococcus aureus* ve *Escherichia coli* test organizmaları kullanılarak araştırıldı.

TABLE OF CONTENTS

ACKNOWLEDGEMENTS iv

ABSTRACT vi

ÖZET vii

LIST OF FIGURES xiv

LIST OF TABLES xx

LIST OF ACRONYMS/ABBREVIATIONS xxi

PART I: SYNTHESIS OF NOVEL POTENT DRUG MOLECULES ACTIVE AGAINST PROSTATE CANCER 23

1. INTRODUCTION 24

1.1. Prostate Cancer 24

1.2. Role of Androgens in Prostate Cancer 24

1.3. Alternative Treatments for Prostate Cancer 25

1.4. Novel Target for the Therapy of Prostate Cancer 27

1.5. Reactions Catalyzed by the CYP17 28

1.6. Inhibition of the Target Enzyme (CYP17) 29

1.7. CYP17 Inhibitors 30

1.7.1. Steroidal CYP17 Inhibitors 31

1.7.2. Nonsteroidal CYP17 Inhibitors 32

1.8. Discovery of Novel CYP17 Inhibitors 33

1.8.1. Computational Modeling of the Target Enzyme (CYP17) 33

1.8.2. Evaluation of the Model with Natural Substrates 34

1.8.3. Virtual Screening, Detailed Docking and Selection of Candidates 35

1.8.4. Biological Effects of the Candidates on Human CYP17 Activity 35

1.8.5. Lead Compound....36
2. OBJECTIVES....37
2.1. Lead Optimization....37
2.2. Docking Studies of the Lead Compound Derivatives....38
3. RESULTS AND DISCUSSION....41
3.1. Syntheses....42
3.1.1. Simple Synthesis of the Lead Compound Derivatives from Available Starting Materials....42
3.1.2. Synthesis of the Lead Compound Derivatives from Alkoxy and *ortho*-Diamino Substituted Phenyl Derivatives....45
3.1.3. Synthesis of the Lead Compound Derivatives from Alkyl and *ortho*-Dihidroxy Substituted Phenyl Derivatives....49
3.1.4. Synthesis of the Lead Compound Derivatives from Alkyl and *meta*-Dihidroxy Substituted Phenyl Derivatives....50
3.1.5. Synthesis of the Lead Compound Derivatives from Alkyl and *ortho*-Diamino Substituted Phenyl Derivatives....52
3.1.6. Synthesis of the Lead Compound Derivatives from Alkyl, Methoxy and Amino Substituted Phenyl Derivatives....55
3.2. Biological Evaluation of the Lead Compound Derivatives....56
4. EXPERIMENTAL SECTION....62
4.1. Materials....62
4.2. Instrumentation....62
4.3. Syntheses....62
4.3.1. Synthesis of 2-naphthoyl chloride (2)....62
4.3.2. Synthesis of *N*-(4-butylphenyl)-2-naphthamide (6)....62

4.3.3. Synthesis of *N*-(4-butoxyphenyl)-2-naphthamide (7).....63

4.3.4. Synthesis of 4-butoxyphenyl 2-naphthoate (8).....63

4.3.5. Synthesis of *N*-(4-butylphenyl)-6-methoxy-2-naphthamide (10).....64

4.3.6. Synthesis of *N*-(4-butoxyphenyl)-6-methoxy-2-naphthamide (11).....64

4.3.7. Synthesis of 4-butoxyphenyl 6-methoxy-2-naphthoate (12).....65

4.3.8. Synthesis of *N*-(4-butylphenyl)-5,6,7,8-tetrahydronaphthalene-2-carboxamide (18).....66

4.3.9. Synthesis of *N*-(4-butylphenyl)-1-naphthamide (19).....66

4.3.10. Synthesis of *N*-(4-butylphenyl)-6-fluoro-2-naphthamide (20).....67

4.3.11. Synthesis of *N*-(4-butylphenyl)-3,5-dimethoxy-2-naphthamide (21).....67

4.3.12. Synthesis of *N*-(4-butylphenyl)-3-methoxy-2-naphthamide (22).....68

4.3.13. Synthesis of *N*-(4-hydroxy-2-nitrophenyl)acetamide (24).....69

4.3.14. Synthesis of *N*-(4-butoxy-2-nitrophenyl)acetamide (25).....69

4.3.15. Synthesis of 4-butoxy-2-nitroaniline (26).....69

4.3.16. Synthesis of 4-butoxybenzene-1,2-diamine (27).....70

4.3.17. Synthesis of *N*-(2-amino-4-butoxyphenyl)-2-naphthamide (28a).....70

4.3.18. Synthesis of *N*-(4-butoxy-2-nitrophenyl)-2-naphthamide (30).....71

4.3.19. Synthesis of *N*-(2-amino-4-butoxyphenyl)-2-naphthamide (28a) and *N*-(2-amino-5-butoxyphenyl)-2-naphthamide (28b).....72

4.3.20. Synthesis of 4-(bromomethyl)-1,2-dimethoxybenzene (32).....72

4.3.21. Synthesis of 1,2-dimethoxy-4-pentylbenzene (33).....73

4.3.22. Synthesis of 1,2-dihydroxy-4-pentylbenzene (34).....73

4.3.23. Synthesis of 2-hydroxy-4-pentylphenyl 2-naphthoate (35a) and 2-hydroxy-5-pentylphenyl 2-naphthoate (35b).....74

4.3.24. Synthesis of 1,3-dimethoxy-5-pentylbenzene (38).....74

4.3.25. Synthesis of 5-pentylbenzene-1,3-diol (39) 75
4.3.26. Synthesis of 3-hydroxy-5-pentylphenyl 2-naphthoate (40) 76
4.3.27. Synthesis of *N*-(4-butylphenyl)acetamide (43) 76
4.3.28. Synthesis of *N*-(4-butyl-2-nitrophenyl)acetamide (44) 77
4.3.29. Synthesis of 4-butyl-2-nitroaniline (45) 77
4.3.30. Synthesis of 4-butylbenzene-1,2-diamine (46) 78
4.3.31. Synthesis of *N*-(2-amino-4-butylphenyl)-2-naphthamide (47a) 78
4.3.32. Synthesis of *N*-(4-butyl-2-nitrophenyl)-2-naphthamide (49) 79
4.3.33. Synthesis of *N*-(2-amino-4-butylphenyl)-2-naphthamide (47a) and *N*-(2-amino-5-butylphenyl)-2-naphthamide (47a) 79
4.3.34. Synthesis of methyl 4-amino-3-methoxybenzoate (51) 80
4.3.35. Synthesis of methyl 4-acetamido-3-methoxybenzoate (52) 81
4.3.36. Synthesis of *N*-(4-(hydroxymethyl)-2-methoxyphenyl)acetamide (53) 81
4.3.37. Synthesis of *N*-(4-(bromomethyl)-2-methoxyphenyl)acetamide (54) 82
4.3.38. Synthesis of *N*-(2-methoxy-4-pentylphenyl)acetamide (55) 82
4.3.39. Synthesis of 2-methoxy-4-pentylaniline (56) 83
4.3.40. Synthesis of *N*-(2-methoxy-4-pentylphenyl)-2-naphthamide (57) 83
5. CONCLUSIONS 85
PART II: INVESTIGATION OF BIOACTIVE PROPERTIES OF CYCLOPOLYMERS OBTAINED BY RAFT POLYMERIZATION 86
6. INTRODUCTION 87
6.1. Conventional Radical Polymerization 87
6.2. Living Radical Polymerization 88
6.3. RAFT Polymerization 89
6.3.1. The Mechanism 90

6.3.2. RAFT Agents 91
6.4. Cyclopolymers of Alkyl α-(Hydroxymethyl)acrylate (RHMA) Ether Dimers 93
6.4.1. Factors Affecting Cyclization 94
6.4.2. Apparent and Effective Bulkiness 95
7. OBJECTIVES 96
8. RESULTS AND DISCUSSION 97
8.1. Synthesis of the RAFT Agent (CDB) 97
8.2. Synthesis of the Monomers 98
8.3. RAFT Cyclopolymerization of the TBHMA Ether Dimer 99
8.3.1. The Effect of CDB and AIBN Concentrations 102
8.3.2. The Effect of Temperature 104
8.4. The Effect of Ester Substituent on the RAFT Cyclopolymerization System (The Importance of Apparent and Effective Bulkiness) 106
8.5. RAFT Polymerization of the Monomers with Primary Central Ester Carbon 107
8.6. RAFT Polymerization of the Monomers with Secondary Central Ester Carbon 107
8.6.1. RAFT Cyclopolymerization of the CHHMA Ether Dimer 108
8.6.2. RAFT Cyclopolymerization of the IBHMA Ether Dimer 109
8.7. Block Copolymerization Studies 110
8.8. Antibacterial Properties of the Cyclopolymers 112
9. EXPERIMENTAL SECTION 115
9.1. Materials 115
9.2. Instrumentation 115
9.3. Synthesis of RAFT Agent (CDB) 115
9.3.1. Step 1: Synthesis of Dithiobenzoic Acid (DTBA) 115
9.3.2. Step 2: Synthesis of Cumyl Dithiobenzoate (CDB) 116

9.4. Syntheses of Monomers 116
9.4.1. Synthesis of Ethyl α-(Hydroxymethyl) Acrylate (EHMA) Ether Dimer 116
9.4.2. Synthesis of *n*-Butyl α-(Hydroxymethyl) Acrylate (BHMA) Ether Dimer 117
9.4.3. Synthesis of *tert*-Butyl α-(Hydroxymethyl) Acrylate (TBHMA) Ether Dimer 117
9.4.4. Synthesis of Cyclohexyl α-(Hydroxymethyl) Acrylate (CHHMA) Ether Dimer 118
9.4.5. Synthesis of Isobornyl α-(Hydroxymethyl) Acrylate (IBHMA) Ether Dimer 118
9.5. Syntheses of Polymers 119
9.5.1. Raft Solution Polymerization of TBHMA Ether Dimer (Table 8.1, Entry 3) 119
9.5.2. Conventional Free Radical Polymerization of TBHMA Ether Dimer (Table 8.1, Entry 12) 120
9.5.3. Bulk Block Copolymerization of Poly(TBHMA Ether Dimer) with *n*-BA (Table 8.4, Entry 4) 120
10. CONCLUSIONS 122
APPENDIX A: SPECTROSCOPY DATA 124
REFERENCES 205

LIST OF FIGURES

Figure 1.1. Structures of testosterone (T) and dihydrotestosterone (DHT). 25

Figure 1.2. Postate cancer agents and regulation of androgens. 26

Figure 1.3. Examples of antiandrogens. 27

Figure 1.4. Biological reactions leading to the formation of androgens. 28

Figure 1.5. Reactions catalyzed by CYP17. 29

Figure 1.6. Active site of CYP17 (heme and substrate binding site). A1: binding of progesterone; A2: binding of a competitive inhibitor. 30

Figure 1.7. Steroidal CYP17 inhibitors. 31

Figure 1.8. Nonsteroidal CYP17 inhibitors. 32

Figure 1.9. Iterative process of structure-based drug design (SBDD). 33

Figure 1.10. Computer generated model with PDB ID code 2c17. 34

Figure 1.11. Docking conformations of known substrates of CYP17. 34

Figure 1.12. Structure of the lead compound. 36

Figure 2.1. Substituents on the lead compound and their possible functions. 37

Figure 3.1. Parts of the lead compound derivatives. 41

Figure 3.2. Commercially available naphthoic acid and its derivatives. 42

Figure 3.3. Commercially available phenyl derivatives. 42

Figure 3.4. Simple synthesis of the lead compound derivatives by the first method. 43

Figure 3.5. Simple synthesis of the lead compound derivatives by the second method. 44

Figure 3.6. Simple synthesis of the lead compound derivatives by the third method. 45

Figure 3.7. Synthesis of alkoxy and *ortho*-diamino substituted phenyl derivative. 46

Figure 3.8. Synthesis of the lead compound derivatives from alkoxy and *ortho*-diamino substituted phenyl derivative. 47

Figure 3.9. Synthesis and reduction of the compound 30.....48

Figure 3.10. Synthesis of alkyl and *ortho*-dihydroxy substituted phenyl derivative.....49

Figure 3.11. Synthesis of the lead compound derivatives from alkyl and *ortho*-dihydroxy substituted phenyl derivative.....50

Figure 3.12. Synthesis of alkyl and *meta*-dihydroxy substituted phenyl derivative.....51

Figure 3.13. Synthesis of the lead compound derivatives from alkyl and *meta*-dihydroxy substituted phenyl derivative.....51

Figure 3.14. Synthesis of alkyl and *ortho*-diamino substituted phenyl derivative. 52

Figure 3.15. Synthesis of the lead compound derivatives from alkyl and *ortho*-diamino substituted phenyl derivative. 53

Figure 3.16. Synthesis and reduction of the compound 49.....54

Figure 3.17. Synthesis of alkyl, methoxy and amino substituted phenyl derivative. 55

Figure 3.18. Synthesis of the lead compound derivatives from alkyl, methoxy and amino substituted phenyl derivative. 56

Figure 5.1. Derivatization of the lead compound. 85

Figure 6.1. Conventional radical polymerization. 87

Figure 6.2. Reversible deactivation. 88

Figure 6.3. Reversible chain transfer. 88

Figure 6.4. Overall reaction in the RAFT polymerization.....89

Figure 6.5. The mechanism of the RAFT polymerization.....91

Figure 6.6. Examples of thiocarbonylthio RAFT agents. 91

Figure 6.7. Structural features of thiocarbonylthio RAFT agent. 92

Figure 6.8. Cyclopolymers of RHMA ether dimers. 93

Figure 6.9. Intra- and intermolecular reactions leading to cyclization and crosslinking. ...94

Figure 8.1. RAFT cyclopolmerization of RHMA ether dimers.....97

Figure 8.2. Synthesis of RAFT agent (CDB).....98

Figure 8.3. Synthesis of RHMA ether dimers *via* Baylis-Hillman reaction. 98

Figure 8.4. Kinetic studies of the RAFT cyclopolymerization of TBHMA ether dimer in xylene at 70 ^{o}C and various [M]/[CDB] ratios.....101

Figure 8.5. Kinetic studies of the RAFT cyclopolymerization of TBHMA ether dimer in xylene at 70 ^{o}C and various CDB and AIBN concentrations.....103

Figure 8.6. Kinetic studies of the RAFT cyclopolymerization of TBHMA ether dimer in xylene at 70 and 80 ^{o}C. 106

Figure 8.7. ^{1}H-NMR spectrum of poly(CHHMA ether dimer) obtained by RAFT polymerization at 80 ^{o}C. 109

Figure 8.8. ^{1}H-NMR spectrum of poly(IBHMA ether dimer) obtained by RAFT polymerization at 70 ^{o}C. 110

Figure 8.9. Size-exclusion chromatography (SEC) traces of the copolymerization studies in bulk using *tert*-butyl (a) and isobornyl (b) α-(hydroxymethyl) acrylate ether dimers derived cyclopolymers as the macroCTA and *n*-butyl acrylate as the co-monomer (Table 8.7, Entries 4 and 6).....112

Figure 9.1. Summary on the effect of the apparent and effective bulkiness on the RAFT cyclopolymerization.....122

Figure A.1. ^{1}H-NMR ($CDCl_3$) spectrum of compound 6. 125

Figure A.2. ^{13}C-NMR ($CDCl_3$) spectrum of compound 6. 126

Figure A.3. ^{1}H-NMR ($CDCl_3$) spectrum of compound 7. 127

Figure A.4. ^{13}C-NMR ($CDCl_3$) spectrum of compound 7. 128

Figure A.5. ^{1}H-NMR ($CDCl_3$) spectrum of compound 8. 129

Figure A.6. ^{13}C-NMR ($CDCl_3$) spectrum of compound 8. 130

Figure A.7. ^{1}H-NMR ($CDCl_3$) spectrum of compound 10. 131

Figure A.8. ^{13}C-NMR ($CDCl_3$) spectrum of compound 10. 132

Figure A.9. ^{1}H-NMR ($CDCl_3$) spectrum of compound 11. 133

Figure A.10. ^{13}C-NMR ($CDCl_3$) spectrum of compound 11. 134

Figure A.11. ^{1}H-NMR ($CDCl_3$) spectrum of compound 12. 135

Figure A.12. ^{13}C-NMR ($CDCl_3$) spectrum of compound 12. 136

Figure A.13. ^{1}H-NMR ($CDCl_3$) spectrum of compound 18. 137

Figure A.14. ^{13}C-NMR ($CDCl_3$) spectrum of compound 18. 138

Figure A.15. ^{1}H-NMR ($CDCl_3$) spectrum of compound 19. 139

Figure A.16. ^{13}C-NMR ($CDCl_3$) spectrum of compound 19. 140

Figure A.17. ^{1}H-NMR ($CDCl_3$) spectrum of compound 20. 141

Figure A.18. ^{13}C-NMR ($CDCl_3$) spectrum of compound 20. 142

Figure A.19. ^{1}H-NMR ($CDCl_3$) spectrum of compound 21. 143

Figure A.20. ^{13}C-NMR ($CDCl_3$) spectrum of compound 21. 144

Figure A.21. ^{1}H-NMR ($CDCl_3$) spectrum of compound 22. 145

Figure A.22. ^{13}C-NMR ($CDCl_3$) spectrum of compound 22. 146

Figure A.23. ^{1}H-NMR (DMSO-d_6) spectrum of compound 24.....147

Figure A.24. ^{13}C-NMR (DMSO-d_6) spectrum of compound 24.....148

Figure A.25. ^{1}H-NMR (DMSO-d_6) spectrum of compound 25.....149

Figure A.26. ^{13}C-NMR (DMSO-d_6) spectrum of compound 25.....150

Figure A.27. ^{1}H-NMR (DMSO-d_6) spectrum of compound 26.....151

Figure A.28. ^{13}C-NMR (DMSO-d_6) spectrum of compound 26.....152

Figure A.29. ^{1}H-NMR (DMSO-d_6) spectrum of compound 27.....153

Figure A.30. ^{13}C-NMR (DMSO-d_6) spectrum of compound 27.....154

Figure A.31. ^{1}H-NMR (DMSO-d_6) spectrum of compound 28a. 155

Figure A.32. ^{13}C-NMR (DMSO-d_6) spectrum of compound 28a. 156

Figure A.33. ^{1}H-NMR ($CDCl_3$) spectrum of compound 28a and 28b. 157

Figure A.34. ^{1}H-NMR ($CDCl_3$) spectrum of compound 30. 158

Figure A.35. ^{13}C-NMR ($CDCl_3$) spectrum of compound 30. 159

Figure A.36. ^{1}H-NMR ($CDCl_3$) spectrum of compound 32. 160

Figure A.37. ^{13}C-NMR ($CDCl_3$) spectrum of compound 32. 161

Figure A.38. ^{1}H-NMR ($CDCl_3$) spectrum of compound 33. 162

Figure A.39. ^{13}C-NMR ($CDCl_3$) spectrum of compound 33. 163

Figure A.40. ^{1}H-NMR ($CDCl_3$) spectrum of compound 34. 164

Figure A.41. ^{13}C-NMR ($CDCl_3$) spectrum of compound 34. 165

Figure A.42. ^{1}H-NMR ($CDCl_3$) spectrum of compound 35a and 35b. 166

Figure A.43. ^{13}C-NMR ($CDCl_3$) spectrum of compound 35a and 35b. 167

Figure A.44. ^{1}H-NMR ($CDCl_3$) spectrum of compound 36. 168

Figure A.45. ^{1}H-NMR ($CDCl_3$) spectrum of compound 38. 169

Figure A.46. ^{13}C-NMR ($CDCl_3$) spectrum of compound 38. 170

Figure A.47. ^{1}H-NMR ($CDCl_3$) spectrum of compound 39. 171

Figure A.48. ^{13}C-NMR ($CDCl_3$) spectrum of compound 39. 172

Figure A.49. ^{1}H-NMR ($CDCl_3$) spectrum of compound 40. 173

Figure A.50. ^{13}C-NMR ($CDCl_3$) spectrum of compound 40. 174

Figure A.51. ^{1}H-NMR ($CDCl_3$) spectrum of compound 41. 175

Figure A.52. ^{1}H-NMR ($CDCl_3$) spectrum of compound 43. 176

Figure A.53. ^{13}C-NMR ($CDCl_3$) spectrum of compound 43. 177

Figure A.54. ^{1}H-NMR ($CDCl_3$) spectrum of compound 44. 178

Figure A.55. ^{13}C-NMR ($CDCl_3$) spectrum of compound 44. 179

Figure A.56. ^{1}H-NMR ($CDCl_3$) spectrum of compound 45. 180

Figure A.57. ^{13}C-NMR ($CDCl_3$) spectrum of compound 45. 181

Figure A.58. ^{1}H-NMR ($CDCl_3$) spectrum of compound 46. 182

Figure A.59. ^{1}H-NMR ($CDCl_3$) spectrum of compound 47a. 183

Figure A.60. ^{13}C-NMR ($CDCl_3$) spectrum of compound 47a. 184

Figure A.61. ^{1}H-NMR ($CDCl_3$) spectrum of compound 47a and 47b. 185

Figure A.62. ^{1}H-NMR ($CDCl_3$) spectrum of compound 48. 186

Figure A.63. ^{1}H-NMR ($CDCl_3$) spectrum of compound 49. 187

Figure A.64. ^{13}C-NMR ($CDCl_3$) spectrum of compound 49. 188

Figure A.65. ^{1}H-NMR ($CDCl_3$) spectrum of compound 51. 189

Figure A.66. ^{13}C-NMR ($CDCl_3$) spectrum of compound 51. 190

Figure A.67. ^{1}H-NMR ($CDCl_3$) spectrum of compound 52. 191

Figure A.68. ^{13}C-NMR ($CDCl_3$) spectrum of compound 52. 192

Figure A.69. ^{1}H-NMR ($CDCl_3$) spectrum of compound 53. 193

Figure A.70. ^{13}C-NMR ($CDCl_3$) spectrum of compound 53. 194

Figure A.71. ^{1}H-NMR ($CDCl_3$) spectrum of compound 54. 195

Figure A.72. ^{13}C-NMR ($CDCl_3$) spectrum of compound 54. 196

Figure A.73. ^{1}H-NMR ($CDCl_3$) spectrum of compound 55. 197

Figure A.74. ^{13}C-NMR ($CDCl_3$) spectrum of compound 55. 198

Figure A.75. ^{1}H-NMR ($CDCl_3$) spectrum of compound 56. 199

Figure A.76. ^{13}C-NMR ($CDCl_3$) spectrum of compound 56. 200

Figure A.77. ^{1}H-NMR ($CDCl_3$) spectrum of compound 57. 201

Figure A.78. ^{13}C-NMR ($CDCl_3$) spectrum of compound 57. 202

Figure A.79. ^{1}H-NMR ($CDCl_3$) spectrum of RAFT agent (CDB). 203

Figure A.80. ^{13}C-NMR ($CDCl_3$) spectrum of RAFT agent (CDB). 204

LIST OF TABLES

Table 1.1. Docking energies for natural substrates of CYP17.....35

Table 2.1. Possible changes on the substituents of the lead compound.....38

Table 2.2. Docking and binding energies of the lead compound and its some derivatives.....39

Table 3.1. Inhibition activities of the lead compound derivatives on human CYP17. 58

Table 8.1. Results from the RAFT cyclopolymerization of TBHMA ether dimer in xylene at 70 ^{o}C.....100

Table 8.2. Effect of CDB and AIBN concentrations on the RAFT cyclopolymerization of TBHMA ether dimer in xylene at 70 ^{o}C.....103

Table 8.3. Effect of temperature on the RAFT cyclopolymerization of TBHMA ether dimer in xylene. 105

Table 8.4. Results from the RAFT polymerization of EHMA and BHMA ether dimers in xylene at 80 ^{o}C.....107

Table 8.5. Results from the RAFT polymerization of CHHMA ether dimer in xylene. ..108

Table 8.6. Results from the RAFT polymerization of IBHMA ether dimer in xylene.....110

Table 8.7. Synthesis of block copolymers in bulk using the TBHMA ether dimer and IBHMA ether dimer derived cyclopolymers as the macroCTAs and *n*-butyl acrylate as the co-monomer. 111

Table 8.8. Antibacterial activities of the cyclopolymers. 114

LIST OF ACRONYMS/ABBREVIATIONS

Ac_2O	Acetic Anhydride
AIBN	*N,N'*-Azobis(isobutyronitrile)
AR	Androgen Receptor
ATRP	Atom Transfer Radical Polymerization
BFE	Binding Free Energy
BHMA	*n*-Butyl α-(Hydroxymethyl)acrylate
CAB	Combined Androgen Blockade
CDB	Cumyl Dithiobenzoate
CHHMA	Cyclohexyl α-(Hydroxymethyl)acrylate
CPR	Controlled Radical Polymerization
CTA	Chain Transfer Agent
CYP17	17α-hydroxylase-C17, C20 lyase
DABCO	1,4-Diazabicyclo[2.2.2] octane
DCC	*N,N'*-Dicyclohexylcarbodiimide
DHEA	Dehydroepiandrosterone
DHT	Dihydrotestosterone
DMAP	*N,N'*-Dimethylaminopyridine
DMF	Dimethylformamide
DMSO	Dimethyl Sulfoxide
EHMA	Ethyl α-(Hydroxymethyl)acrylate
Et_3N	Triethylamine
EtOAc	Ethyl Acetate

FSH	Follicle Stimulating Hormones
GnRH	Gonadotropin Releasing Hormones
GPC	Gel Permeation Chromatography
IBHMA	Isobornyl α-(Hydroxymethyl)acrylate
IC_{50}	Inhibitory Concentration
LH	Luteinizing Hormones
LHRH	Luteinizing Releasing Hormones
NMP	Nitroxide Mediated Polymerization
NMR	Nuclear Magnetic Resonance
P450	CYP cytochrome
PC	Prostate Cancer
PDI	Polydispersity Index
RAFT	Reversible Addition Fragmentation Chain Transfer
RHMA	Alkyl α-(Hydroxymethyl)acrylate
rt	room temperature
SBDD	Structure Based Drug Design
SEC	Size Exclusion Chromatography
T	Testosterone
TBHMA	*tert*-Butyl α-(Hydroxymethyl)acrylate
TC_{50}	Toxicity Concentration
TEA	Triethylamine
T_g	Glass Transition Temperature
THF	Tetrahydrofuran
TLC	Thin Layer Chromatography

PART I

SYNTHESIS OF NOVEL POTENT DRUG MOLECULES ACTIVE AGAINST PROSTATE CANCER

1. INTRODUCTION

1.1. Prostate Cancer

Prostate cancer (PC) is the most common malignancy and age-related cause of cancer deaths among male worlwide [1]. In many countries, apart from skin cancer, it is one of the most common cancers among men. Apart from lung cancer, it is the second leading cause of death from cancer in both the USA and Australia [2-4].

Several factors can increase or reduce the risk of prostate cancer. The following factors are believed to increase the risk of prostate cancer [5]:

- *Age*: Being over especially 65 age
- *Family history*: Having a father or brother diagnosed with prostate cancer doubles the risk
- *Race*: Afro-Americans are at a higher risk of being prostate cancer than white Americans and Europen men
- *Geography*: Prostate cancer is rarer in Asia, Africa, and South America
- *Weight, physical inactivity*: Overweight and inactive men have higher risk of prostate cancer
- *Diet*: Eating high-fat foods and red meats, and not eating enough vegetables, fruits, and fibre increases the risk

1.2. Role of Androgens in Prostate Cancer

About 80 % of prostate cancers are androgen dependent. Androgens are steroid based compounds that affect masculine characters in males. They play an important role in the development, growth, and progression of the prostate cancer cells [6]. At the molecular level, androgens bind to androgen receptor in target cells and initiate transcription of genes involved in cell proliferation and survival. The two most important androgens in this regard are testosterone (T) and dihydrotestosterone (DHT) (Figure 1.1).

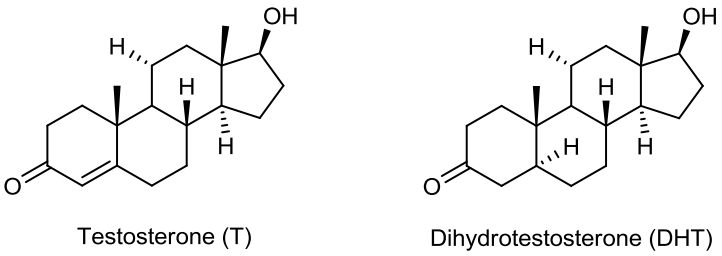


Figure 1.1. Structures of testosterone (T) and dihydrotestosterone (DHT).

The testes synthesize about 90 % of testosterone, and the rest (10 %) is synthesized by the adrenal glands. Testosterone (T) is further converted to the more potent androgen dihydrotestosterone (DHT) by the enzyme 5α-reductase that is localized primarily in the prostate [7].

A number of studies indicate a correlation between serum testosterone levels and increased risk of prostate cancer. Therefore, many treatments focus on reducing or blocking androgen biosynthesis in the body.

1.3. Alternative Treatments for Prostate Cancer

Few patients in early stages can be cured by local therapy, like *prostatectomy* (removal of prostate tissue) or *radiotherapy*. Most, especially the ones with metastates, are treated with hormone therapy. Since tumors are sensitive to androgen deprivation, unspecific *chemotherapy* can be avoided in most cases [8]. *Endocrine therapy* (androgen deprivation therapy (ADT), hormone therapy) with fewer side effects can be used instead [9, 10].

Estrogens show their activity on the hypothalamic level by reducing the level of gonadotropin releasing hormones (GnRH) [11]. GnRH causes the release of other hormones like the luteinizing hormones (LH) and follicle-stimulating hormones (FSH) (LH and FSH control development in children and fertility in adults) in the pituitary gland. As a consequence, the reduced pituitary LH/FSH formation results in a decrease of the testicular androgen production (Figure 1.2). However, estrogen therapy has become less important due to its considerable cardiovascular side effects.

Another endocrine strategy that results in the reduction of androgen formation is *orchidectomy* (surgical castration, removal of testes), usually applied to patients under 70 years old.

The reduction of testicular androgen production by *gonadotropin releasing hormone (GnRH) agonists* or *luteinizing releasing hormone (LHRH) agonists* (medical castration) is often preferred over the surgical one and can also be used for treating older patients [12]. However, adrenal androgen formation is not affected (Figure 1.2).

Nevertheless, surgical or medical castration reduces maximally 90 % of the daily testosterone production, which is often not enough to stop the tumor from growing. The remaining 10 % of the androgens are produced in adrenal glands.

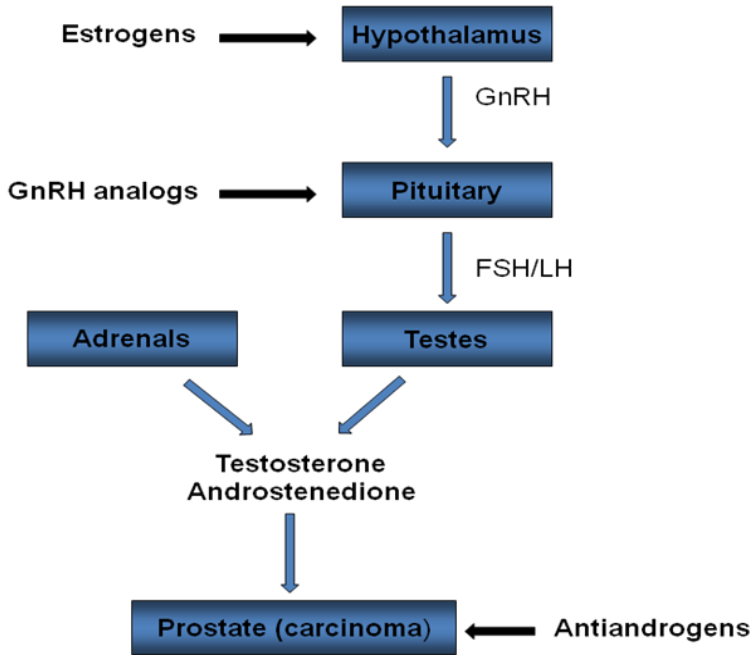
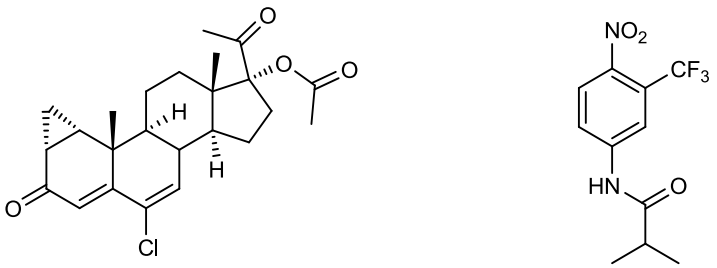


Figure 1.2. Postate cancer agents and regulation of androgens [11].

Anti-androgens (androgen receptor antagonists) interact with the androgen receptor (AR). Thus, they prevent the physiological androgens from unfolding their tumor stimulating activity [13]. Examples of this mechanism of action are cyproterone acetate (a steroid derivative) and flutamide (a non-steroidal compound) (Figure 1.3). These are well known drugs that have been in use for more than two decades.



Cyproterone acetate Flutamide

Figure 1.3. Examples of antiandrogens.

Currently, the standard therapy for prostate cancer is the "combined androgen blockade" (CAB), which means surgical or chemical castration combined with androgen receptor antagonists [14]. In CAB therapy, orchidectomy or GnRH treatment is employed to annihilate testicular androgen production and consequently to reduce plasma androgen concentration. However, about 10 % of the androgens are produced in adrenal glands, which is still sufficient to prompt cancer growth. To solve this problem, androgen receptor (AR) antagonists are additionally applied to prevent adrogen stimulation. Nonetheless, mutations in androgen receptor are the reason for emerging resistance to this therapy. A promising alternative to CAB is the total blockage of androgen biosynthesis in testes and adrenals.

1.4. Novel Target for the Therapy of Prostate Cancer

As stated before, androgens are major growth factors in the normal prostate and they determine the overall number of prostate cancer cells. The two most important androgens in this regard are testosterone (T) and dihydrotestosterone (DHT) (Figure 1.1).

The biosynthesis of androgens starts in testes and adrenal glands from cholesterol (Figure 1.4). Several enzymatic transformations of this precursor sterol finally lead to the formation of androgenic steroids. The last step of androgen biosynthesis in testes and adrenal glands involves two key sequential reactions that are catalyzed by a single enzyme, 17α-hydroxylase-C17, C20 lyase (CYP17), a cytochrome P450 monooxygenase [15, 16]. Strong and selective inhibition of the CYP17 will decrease the production of testicular as well as the adrenal androgens since it is responsible for the production of androgens in

both organs. Therefore, CYP17 enzyme is the key enzyme of androgen biosynthesis and the new therapeutic target for the treatment of the prostate cancer.

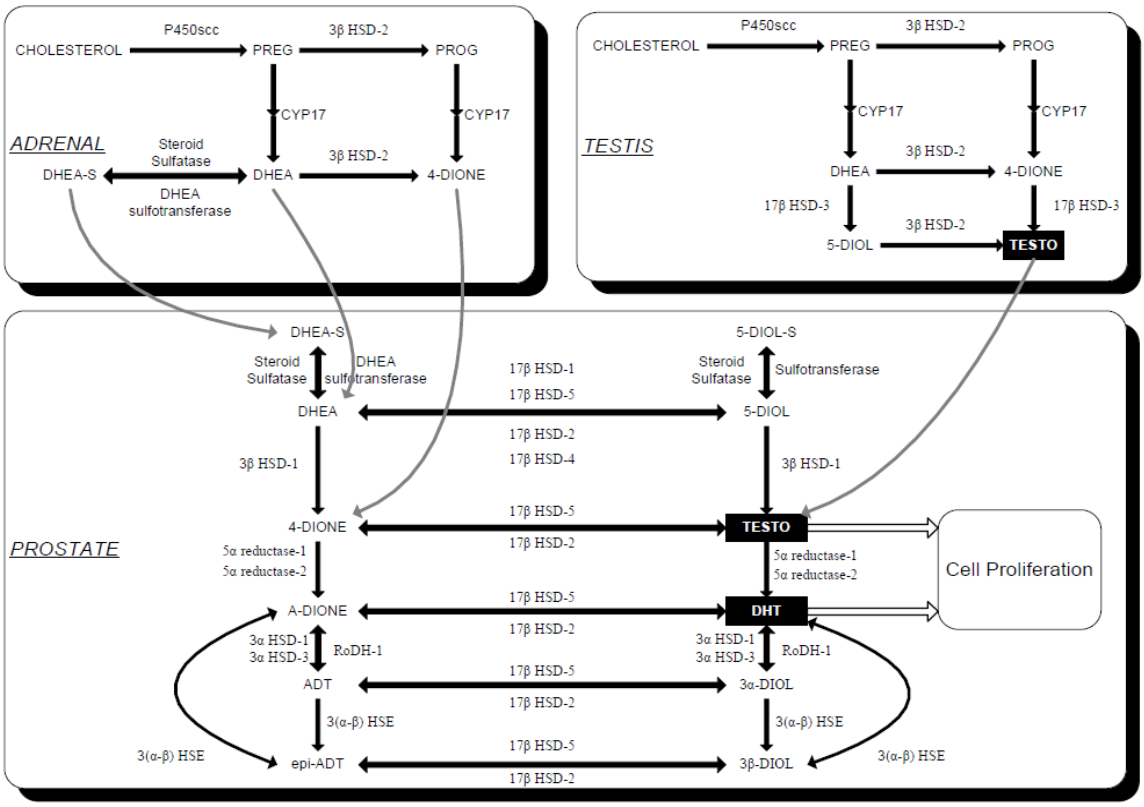


Figure 1.4. Biological reactions leading to the formation of androgens [15,16].

1.5. Reactions Catalyzed by the CYP17

Figure 1.5 gives a representation of the reactions in androgen biosynthesis catalyzed by CYP17. CYP17 first hydroxylates pregnenolone and progesterone in 17α-position (17α-hydroxylase activity). Subsequently, the acetyl group is cleaved (C17, C20 lyase activity) and the 17-keto-androgens dehydroepiandrosterone (DHEA) and androstenedione are produced [17]. These are further transformed enzymatically into testosterone and dihydrotestosterone, steroids with even higher androgenic potency [18].

The inhibition of the CYP17 enzyme by using drug molecules reduce the levels of androgens, which is the novel treatment strategy for the prostate cancer [11, 19].

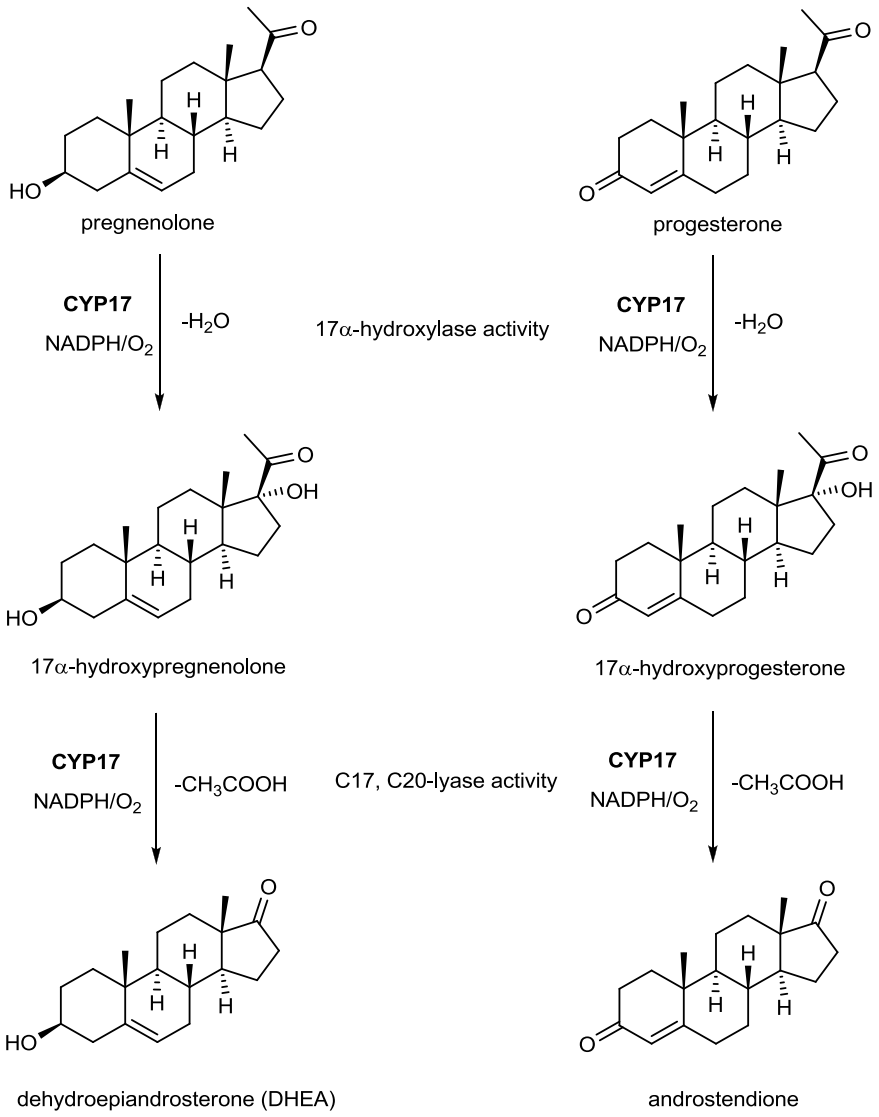


Figure 1.5. Reactions catalyzed by CYP17 [15,16].

1.6. Inhibition of the Target Enzyme (CYP17)

An enzyme catalyses a reaction by providing a specific area to which a substrate can bind. This area is called the active site of the enzyme. When an inhibitor reversibly binds to the active site of the enzyme, it blocks access of the natural substrate to the active site and stops the catalytic reaction as long as it is there. This is known as competitive inhibition. Inhibitor competes with the natural substrates for binding to the active site.

In order to understand how drugs interact with the target enzymes, the structure of the enzymes should be well-known. CYP17, CYP19 and four other enzymes (CYP11A1, CYP11B1, CYP11B2, CYP21) of steroid hormone biosynthesis are P450 (CYP) enzymes [20]. The function of most CYP enzymes is to catalyze the oxidation of organic substances. As a prosthetic group, they consist of a heme moiety, i.e. a porphyrin ring with a central iron (Figure 1.6). The function of iron is to activate molecular oxygen, which is a prerequisite for the subsequent conversion of the substrate. In the development process of CYP17 inhibitors, designed compounds should be capable of complexing the heme iron that the original substrates (pregnenolone and progesterone) are supposed to complex, thus preventing oxygen activation (Figure 1.6). In addition, a high affinity for the apoprotein should be achieved [11].

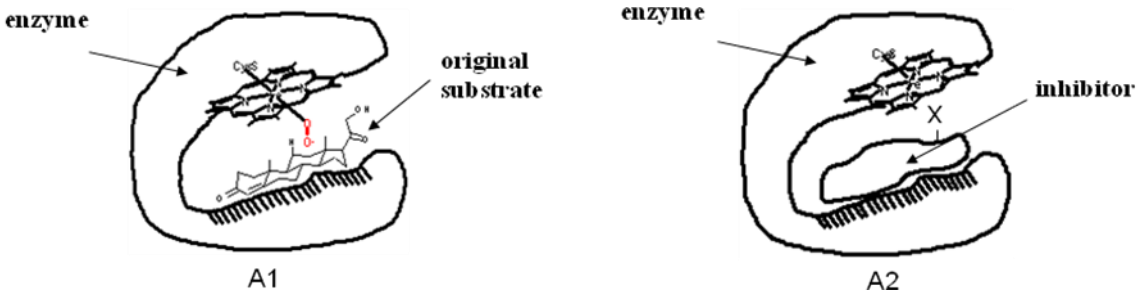


Figure 1.6. Active site of CYP17 (heme and substrate binding site). A1: binding of progesterone; A2: binding of a competitive inhibitor [11].

The decisive factor for the binding affinity is the interaction of the drug with the amino acids that are located in the enzyme's active site. Cytochrome P450 enzymes are all membrane bound proteins, so no X-ray data are available. The structure of the active site is not yet known and a "key-lock" design of an inhibitor is not posssible.

1.7. CYP17 Inhibitors

In the literature, several steroidal and nonsteroidal compounds were synthesized and evaluated as CYP17 inhibitors [21].

1.7.1. Steroidal Inhibitors

As a starting point steroidal CYP17 inhibitors were synthesized by modifying natural CYP17 substrates (pregnenolone, progesterone) [22, 23]. The steroid backbone was changed by attaching a heme iron complexing functional group into the 17-position. This modification prevented P450 17 to catalyze the hydroxylation step. For example Hartmann *et al.* prepared various nitrogen bearing derivatives [11, 21]. Among them the aziridine derivative (1) is shown in Figure 1.7. Despite its high *in vivo* activity, 1 became not an appropriate drug candidate due to its acid instability, which resulted in the hydrolysis of the aziridine ring [21]. However, this compound was used as a template in the design of new structures.

In the last years, several steroidal inhibitors were developed. Compounds having a 3-pyridyl group in the 17-position, like abiraterone (2) in Figure 1.7 were the most active ones. Abiraterone (2) was the only steroidal compound in the clinical trial [24].

Recently, Hartmann *et al.* reported on the potent inhibitory activity of the pyrimidyl derivatives (3 and 4) shown in Figure 1.7 [11, 21]. These compounds could be promising candidates for clinical evaluation. The compounds 3 (IC_{50}=38 nM) and 4 (IC_{50}=24 nM) revealed to be two to three times more active than the steroidal inhibitor abiraterone (2) (IC_{50}=73 nM).

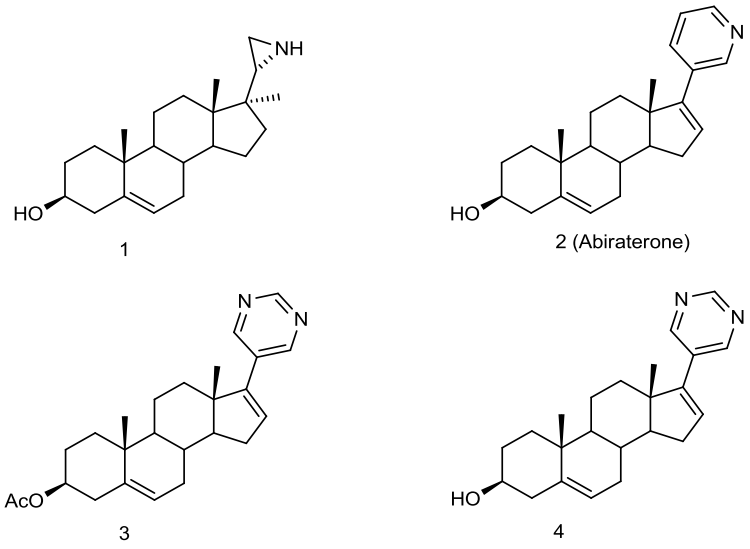


Figure 1.7. Steroidal CYP17 inhibitors.

Nevertheless, there are good reasons to replace steroidal drugs by non-steroidal drugs. Independent of their mode of action, steroidal compounds often show some affinity towards one or several steroid receptors (estrogen-, gestagen-, androgen-, mimeralocorticoid-, or glucocorticoid-receptors), acting as an agonist or antagonist. Side effects due to this insufficient selectivity are the results.

1.7.2. Nonsteroidal Inhibitors

The first compound to be identified as a P450 17 inhibitor was the well-known antimycotic ketoconazole (5) (IC_{50}=740 μM), shown in Figure 1.8. Ketoconazol (5) was demonstrated to be active against prostate cancer in a clinical study [25]. However, due to its low selectivity, it was not well suited for the treatment of the prostate cancer. Bifonazole (6), a long known antimycotic had shown weak rat P450 17 inhibitory activity due to its action as a mimic of the A- and C-ring of progesterone (Figure 1.8). Based on the results of the steroidal inhibitor 1 shown in Figure 1.7, Hartmann *et al*. designed different classes of non-steroidal compounds acting as mimics of 1. In the class of dihydronaphthalenes, two highly active *in vitro* inhibitors of P450 17, 7 (IC_{50}=36 nM) and 8 (IC_{50}=110 nM) were found (Figure 1.8). The derivatives 7 and 8 revealed not only a high inhibitory activity, but also a high selectivity towards P450 17 (CYP17) in comparison with four other enzymes of steroid hormone biosynthesis [15, 16].

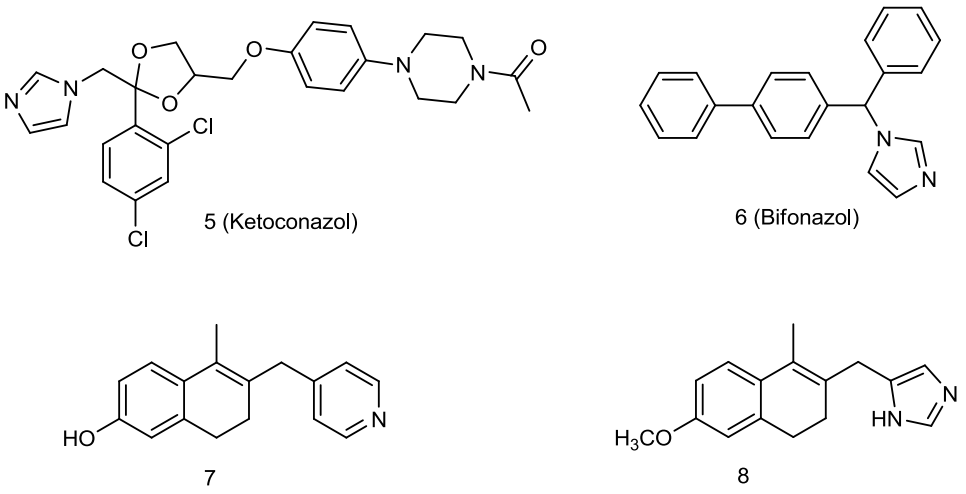


Figure 1.8. Nonsteroidal CYP17 inhibitors.

1.8. Discovery of Novel CYP17 Inhibitors

Structure-based drug design (SBDD) approach was used to discover novel lead compounds active against CYP17 by the researchers Prof. Metin Türkay and Assoc. Prof. İbrahim Halil Kavaklı from Koç University [26].

SBDD is an iterative process (Figure 1.9) that starts with the identification of the target molecule [27, 28]. The discovery of the lead compounds for the target is the key step in structure based drug design. A lead compound is a compound that shows a useful pharmacological activity and is the starting point for the drug design. Then, lead optimization and development studies follow.

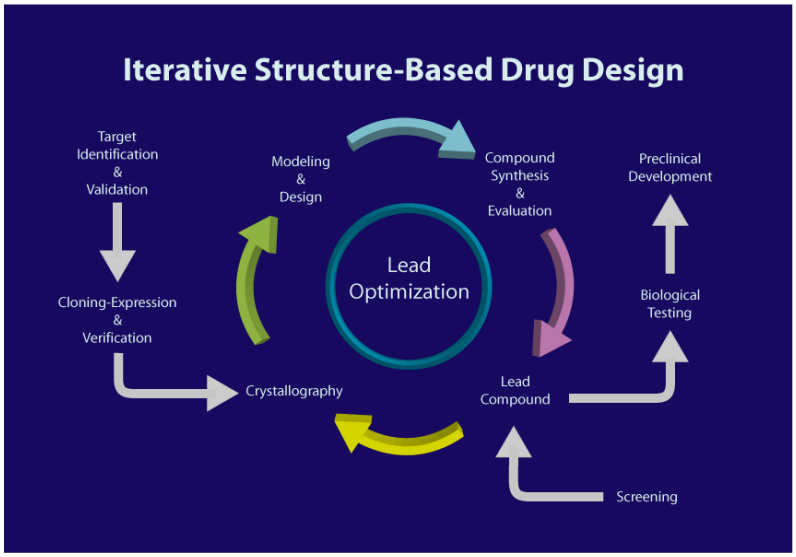


Figure 1.9. Iterative process of structure-based drug design (SBDD) [28].

1.8.1. Computational Modeling of the Target Enzyme (CYP17)

Enzyme structure is important for understanding the catalytic activities, substrate and reaction selectivity. Therefore, knowing the structure of CYP17 is required in designing specific drugs to inhibit the catalytic activities of the enzyme. Although a crystal structure of CYP17 has not been reported in the literature or databases, a computer generated model of the protein structure by Auchus *et al.* exists as shown in Figure 1.10 with PDB ID code 2c17 [29]. This model is based on a class II P450 crystal structure,

P450BMP. CYP17 enzyme consists of a hydrophobic region and a heme group which is common in all P450 enzymes.



Figure 1.10. Computer generated model with PDB ID code 2c17 [29].

The researchers at Koc University showed that the computer generated model of the CYP17 by Auchus *et al.*can be successfully applied to identify novel CYP17 inhibitors. They improved the protein structure by Auchus *et al.* for further use in docking studies [26].

1.8.2. Evaluation of the Model with Natural Substrates

In order to validate the protein structure model, computational chemists at Koç University conducted docking studies with natural substrates of CYP17 (Figure 1.11). Docking energies for all substrate molecules were in the range of -10 kcal/mol (Table 1.1). These results indicate a strong affinity of substrates towards CYP17 [26].

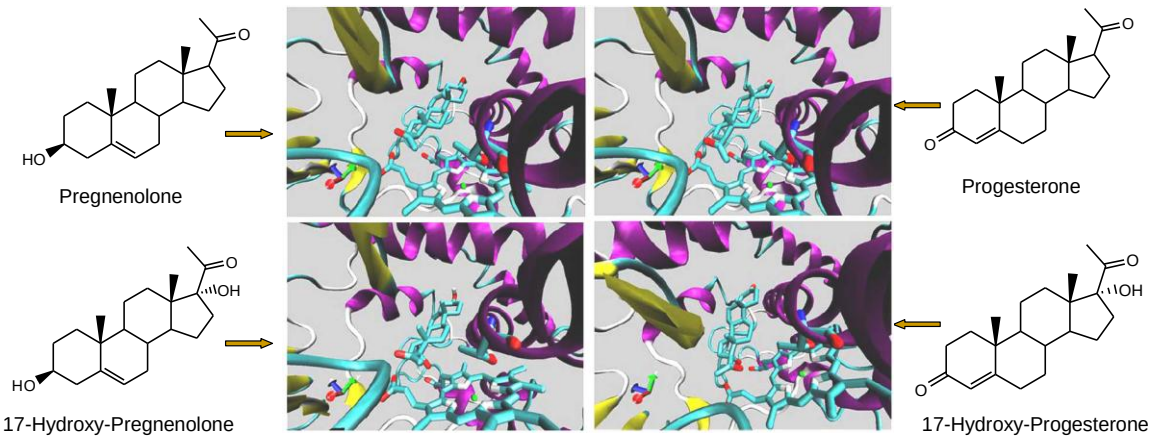


Figure 1.11. Docking conformations of known substrates of CYP17 [26].

Table 1.1. Docking energies for natural substrates of CYP17 [26].

Substrate	Docking Energy
Pregnenolone	-10.12 kcal/mol
17-Hydroxy-Pregnenolone	-9.88 kcal/mol
Progesterone	-10.39 kcal/mol
17-Hydroxy-Progesterone	-10.42 kcal/mol

1.8.3. Virtual Screening, Detailed Docking and Selection of Candidates

In virtual screening phase about 50000 compounds provided by Ambinter SARL were screened by the researchers at Koç University [26].

Autodock computational program was used to determine the best energy conformation of the ligand molecules. The docking and binding energies for all the compounds in the virtual library were determined. Compounds with best docking and binding energies were subjected to detailed docking analysis and biological tests.

1.8.4. Biological Effects of the Candidates on Human CYP17 Activity

Compounds that displayed inhibitory activity on human CYP17 were picked to calculate IC_{50} value. IC_{50} is the inhibitory concentration that required to reduce enzyme activity by 50 %.

Toxicity of a drug candidate is as important as its inhibition potential; therefore, cell viability assays were performed for the compounds. According to the results of viability assay, TC_{50} values were calculated. TC_{50} represents the concentration of a test compound at which 50 % of the cells are killed. For lead compounds, toxicity values lower than 25 μM are not favored.

1.8.5. Lead Compound

After all above calculations, screenings and biological tests, the non-steroidal compound in Figure 1.12 was found as a lead compound for the inhibition of CYP17. The docking and binding energy values of the compound are -9.60 kcal/mol and -7.70 kcal/mol respectively and its IC_{50} value is 35.65 μM [26].

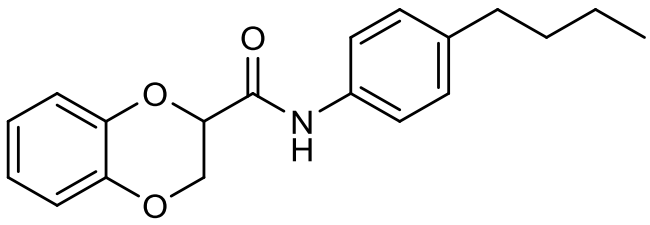


Figure 1.12. Structure of the lead compound [28].

The lead compound has good viability scores above its IC_{50} value. The TC_{50} is calculated to be 271 μM for the 12 hours assay and 397 μM for the 24 hours assay, which is very promising. Therefore, it can be used for further optimization studies to improve inhibition efficiency and reduce toxicity [26].

2. OBJECTIVES

2.1. Lead Optimization

From the docking studies, the role of substituents on the lead compound during the interaction with CYP17 was estimated. According to results, the lead compound has oxygen and nitrogen atom well oriented with the heme iron and threonine oxygen atom. There is a strong interaction of ring and short carbon tail with residues 254 and 255 of I-helix. These residues are glycine and alanine, and their overall hydrophobicity would help stabilize drug molecule in the active site [26].

Figure 2.1 shows substituents on the lead compound and their possible functions.

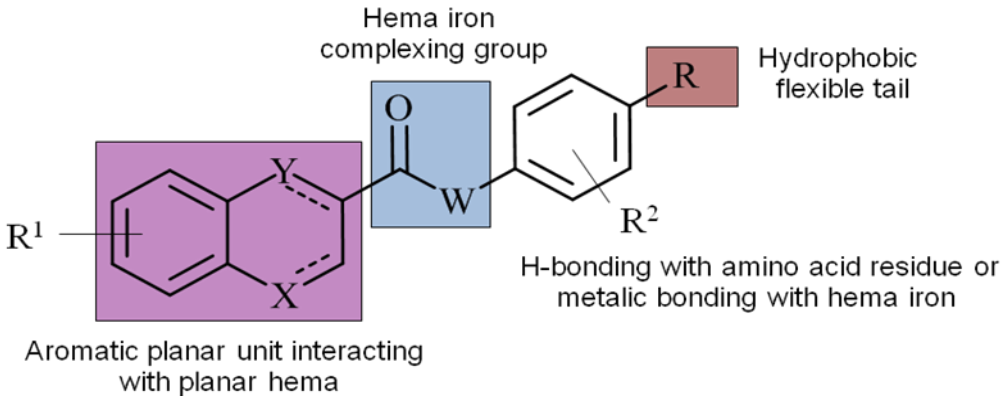


Figure 2.1. Substituents on the lead compound and their possible functions.

Table 2.1 shows the possible changes that can be done on the lead compound. For example, hema iron complexing group can be changed with ester or keton groups instead of the amide group. It is estimated that the left side of the molecule should be planer to fit the active site of the enzyme. Here are hydrophobic interactions with planar hema. In the lead compound, X and Y atoms are O atoms. In the derivatization, they can be O or C atoms with saturated or unsaturated bonds. In the right hand side, there is a hydrophobic flexible tail (R). Different R groups such as alkyl, alkoxy or branched alkyl groups can be attached to the phenyl ring to increase the selectivity of the molecule towards the enzyme.

Similarly, different R^1 and R^2 groups as shown in Table 2.1 can be attached to naphthyl and phenyl rings at different positions in order to see the effect of changing electron density on the rings or increase the interactions between molecule and the enzyme via H-bonds, metalic bonds etc.

Table 2.1. Possible changes on the substituents of the lead compound.

X and Y atoms	C, O
W atom	N, O, C
R	C2-C6 alkyl or alkoxy, brached alkyl
R^1	-OMe, -OH, -F (at different positions)
R^2	-OMe, -OH, $-NH_2$, $-NO_2$ (at different positions)

Such changes on lead compound may increase the affinity and selectivity of the lead compound towards CYP17 and reduce IC_{50} value to nM levels. This stage also may be considered as a part of the lead optimization step.

2.2. Docking Studies of the Lead Compound Derivatives

Docking and binding energy calculations of some considered lead compound derivatives were done by using AutoDock computational program (Table 2.2). Binding energy is the strength of interaction between the enzyme and the candidate drug molecule. Docking energy is related to the approach of the candidate drug molecule to the enzyme.

The results show that some lead compound derivatives had favorable docking and binding energies in compared to the energy values of the lead compound (Table 2.2). The aim of the study is to synthesize lead compound derivatives that have favorable energy values in order to be effective in nanomolar concentrations (at least 35 nm). These new compounds may be used as chemotherapeutic agents for the treatment of the prostate cancer.

Compounds with the naphthyl unit at the left side gave better energy values than the other ones. Therefore, we decided to synthesize compounds including naphyl groups at

the left side. An additional amino or hydroxy group on the phenyl ring increased the energy values (Table 2.2).

Table 2.2. Docking and binding energies of the lead compound and its some derivatives.

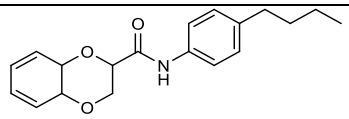
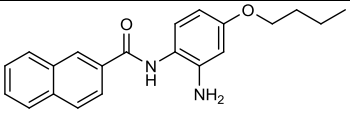
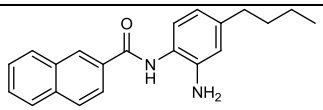
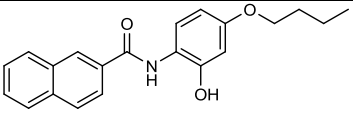
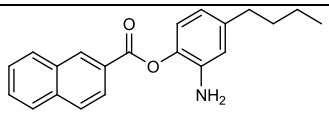
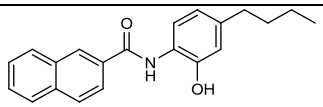
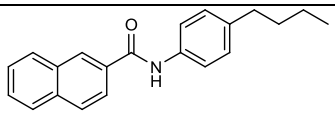
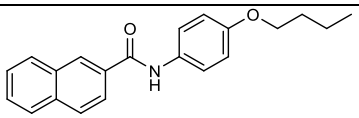
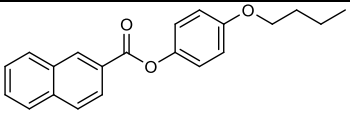
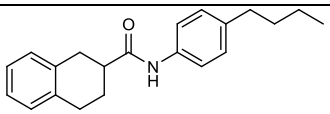
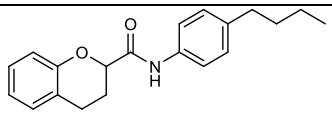
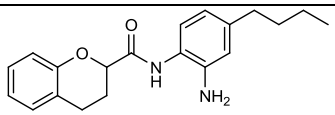
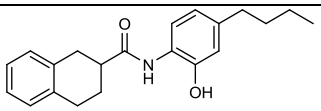
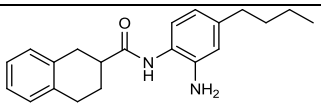
Lead Compound	Docking Energy (kcal/mol)	Binding Energy (kcal/mol)
	-9.60	-7.70
Lead Compound Derivatives	Docking Energy (kcal/mol)	Binding Energy (kcal/mol)
	-10.66	-8.39
	-10.56	-8.47
	-10.38	-8.10
	-10.14	-8.26
	-10.13	-8.05
	-9.89	-7.77
	-9.85	-7.63
	-9.55	-7.87
	-9.50	-8.85

Table 2.2. Docking and binding energies of the lead compound and its some derivatives (cont.).

	-9.43	-7.61
	-9.31	-7.33
	-9.29	-7.60
	-9.28	-7.46

3. RESULTS AND DISCUSSION

The lead compound derivatives can be considered to have two parts; naphthyl group at the left hand side and phenyl group at the right hand side (Figure 3.1). Thus, the lead compound derivatives can be synthesized by coupling of naphthyl groups with phenyl groups via amide or ester bonds.

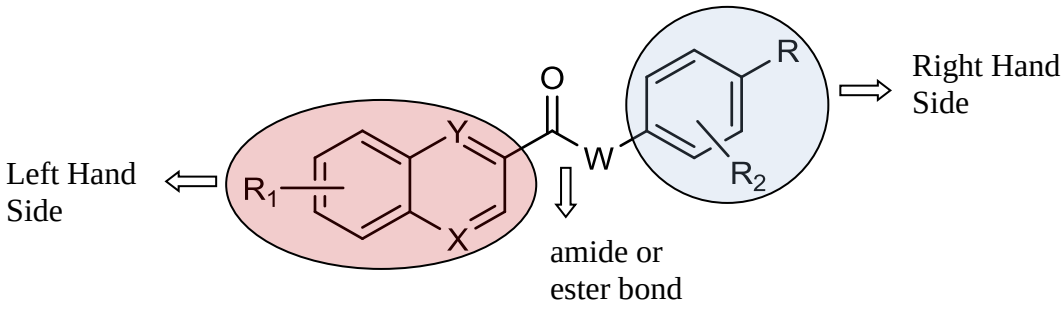


Figure 3.1. Parts of the lead compound derivatives.

In this part of the project, X and Y atoms were decided to be unsaturated carbon atoms because such compounds gave better energy values (Table 2.2). Thus, the left hand side consisted of naphthyl group and its derivatives such as mehoxy or fluoride (R_1) substituted naphthyls. For the right hand side, linear alkyl or alkoxy (R) substituted phenyl derivatives were used. In some phenyl derivatives, R_2 groups such as -NH_2, -OH, -OMe, -NO_2 were attached to the phenyl ring as well. Napthyl and phenyl parts were coupled via ester or amide bonds (W atom= N or O atom) as seen in Figure 3.1.

In the study, commercially available naphthoic acid and its derivatives were used for the left hand side (Figure 3.2). They were coupled with various phenyl derivatives to obtain the final products. Initially, commercially available phenyl derivatives that had desired substituents were used for the right hand side (Figure 3.3). Some phenyl derivatives which are not commercially available were synthesized *via* multistep reactions. The synthesized phenyl derivatives can be summarized as follows:

- Alkoxy and Diamine Substituted Phenyl Derivatives
- Alkyl and *ortho*-Dihydroxy Substituted Phenyl Derivatives
- Alkyl and *meta*-Dihydroxy Substituted Phenyl Derivatives
- Alkyl and Diamine Substituted Phenyl Derivatives
- Alkyl, Methoxy/Hydoxy and Amine Substituted Phenyl Derivatives

3.1. Syntheses

3.1.1. Simple Synthesis of the Lead Compound Derivatives from Available Starting Materials

The commercially available naphthoic acid and phenyl derivatives that had the desired substituents were used as the starting materials. The structures of used naphthoic acid and phenyl derivatives can be seen in the Figure 3.2 and 3.3. The coupling of these compounds via ester or amide bonds gave the final products.

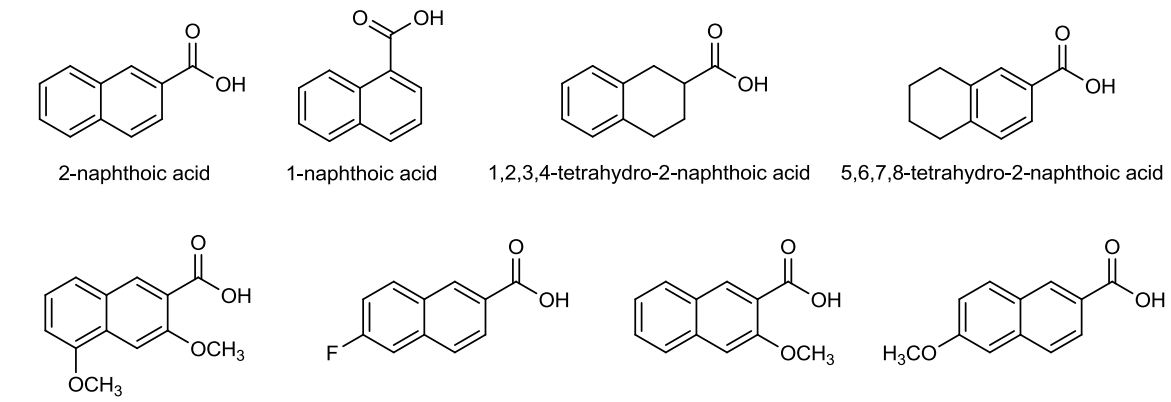


Figure 3.2. Commercially available naphthoic acid and its derivatives.

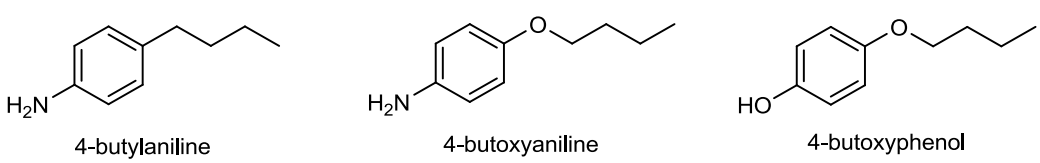


Figure 3.3. Commercially available phenyl derivatives.

Three different coupling methods were used. In the first one, naphthoic acid (1) was converted to naphthoyl chloride (2) by using thionyl chloride ($SOCl_2$) [30] and then coupled with phenyl derivatives 4-butylaniline (3), 4-butoxyaniline (4) and 4-butoxyphenol (5) via ester or amide bonds in the presence of triethylamine (Figure 3.4) [31]. As a result, compounds 6, 7 and 8 were synthesized as seen in Figure 3.4.

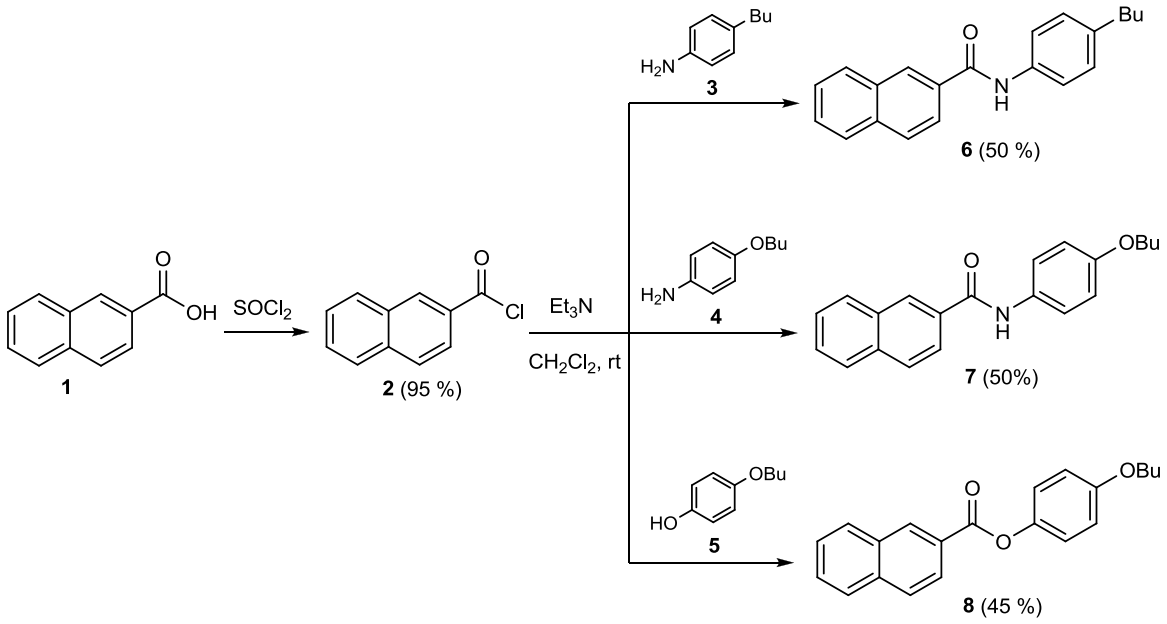


Figure 3.4. Simple synthesis of the lead compound derivatives by the first method.

Compounds 6, 7 and 8 were synthesized to see the differences between amide and ester bonds (compounds 7 and 8) or differences between butyl and butoxy groups (compounds 6 and 7) in the biological activity.

In the second method, 6-methoxy-2-naphthoic acid (9) was coupled with phenyl derivatives 4-butylaniline (3), 4-butoxyaniline (4) and 4-butoxyphenol (5) by using *N,N'*-dicyclohexylcarbodiimide (DCC) and *N,N'*-Dimethylaminopyridine (DMAP) in one pot (Figure 3.5) [32]. Finally, the compounds 10, 11 and 12 were synthesized (Figure 3.5). They were synthesized in order to see the effect of electron donating methoxy group on the naphthyl unit.

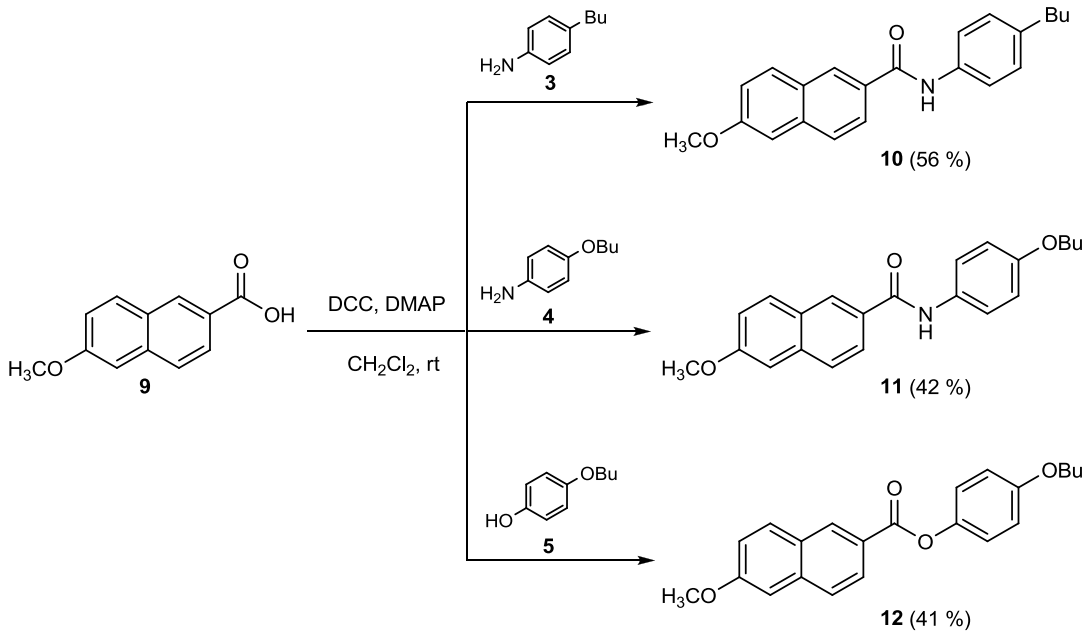


Figure 3.5. Simple synthesis of the lead compound derivatives by the second method.

The third approach was the *in-situ* conversion of the naphthoic acid derivatives (13, 14, 15, 16 and 17) to the corresponding naphthoyl bromides with PBr_3 and then coupling with 4-butylaniline (3) in the presence of triethylamine in one pot (Figure 3.6) [33]. The compounds 18, 19, 20, 21 and 22 were synthesized by this approach (Figure 3.6).

In the compounds 18, 19, 20, 21 and 22, naphthyl groups at the left side are different whereas the phenyl groups at the right side are same. These compounds were synthesized to see the effects of different substituents such as electron donating metoxy and electron withdrawing F group on the naphthyl unit, saturated bonds *etc.* in the biological activity.

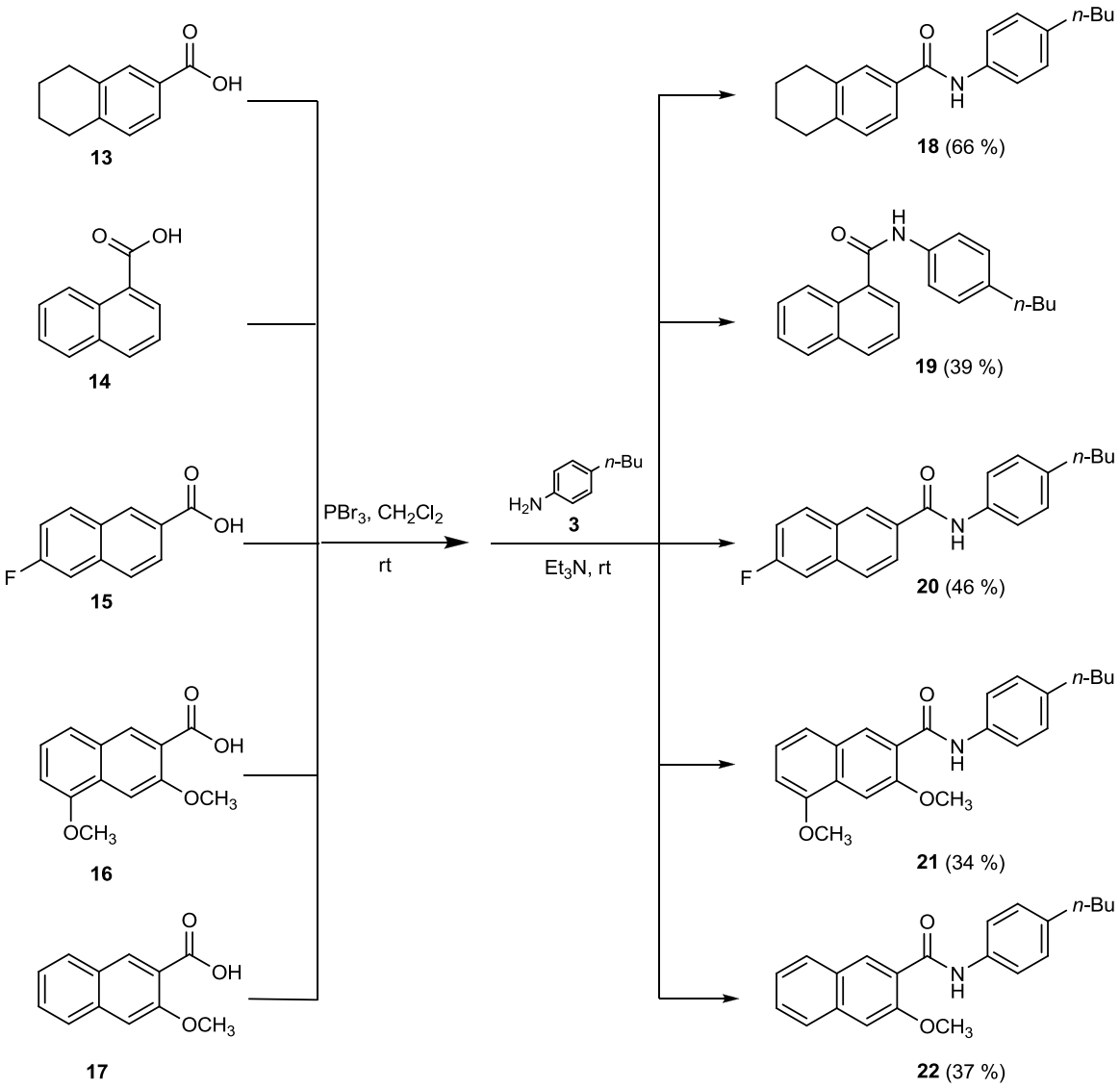


Figure 3.6. Simple synthesis of the lead compound derivatives by the third method.

3.1.2. Synthesis of the Lead Compound Derivatives from Alkoxy and *ortho*-Diamino Substituted Phenyl Derivatives

In addition to the amide forming amine and alkoxy group, an extra amine group on the phenyl ring could increase the affinity of the compound towards the enzyme by creating H-bond interactions with amino acid residues or changing the electron density of the phenyl ring. Such compounds gave favorable energy values in docking studies (Table 2.2). Therefore, alkoxy and *ortho*-diamino substituted phenyl compound was synthesized.

Figure 3.7 shows the synthetic approach used in the synthesis of alkoxy and *ortho*-diamino substituted phenyl compound.

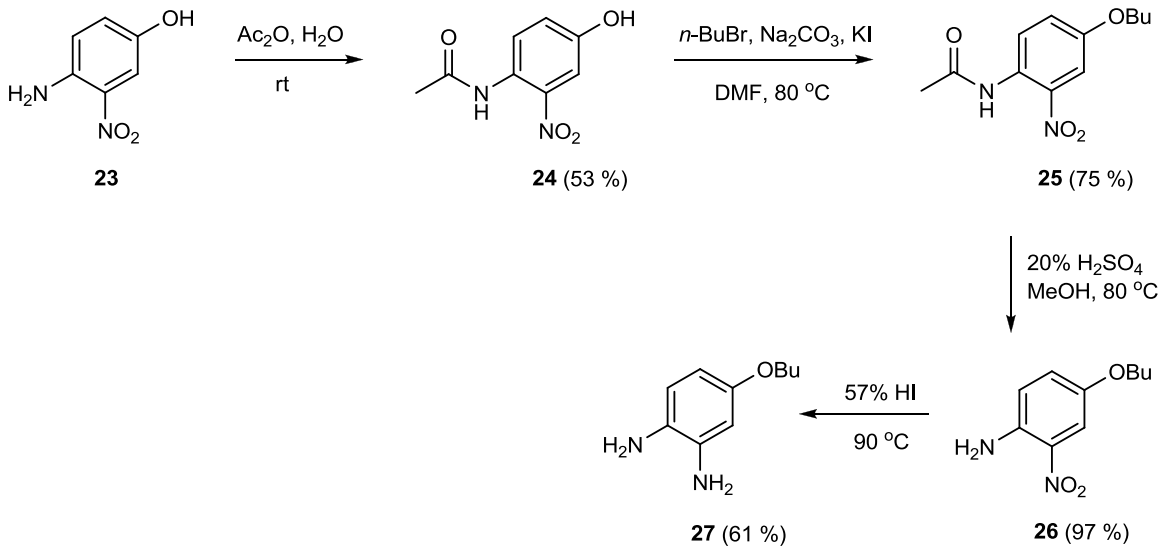


Figure 3.7. Synthesis of alkoxy and *ortho*-diamino substituted phenyl derivative.

For the synthesis of alkoxy and *ortho*-diamino substituted phenyl derivative, compound 4-amino-3-nitro phenol (compound 23) was selected as the starting material. Initially, the amino group in the compound 23 was protected by using acetic anhydride [34] to inhibit side reactions in the next step. Then, hydroxy group in the compound 24 was converted to alkoxy group with *n*-BuBr in the presence of Na_2CO_3 and KI [35]. In this reaction, by using different alkyl bromides, different alkoxy compounds can also be obtained. Acetamide group in the compound 25 was again converted to amino group with 20 % H_2SO_4. The reduction of the nitro group in compund 26 with 57 % HI gave the desired phenyl derivative (compound 27) [36].

In order to obtain lead compound derivative, the naphthoyl chloride (2) was coupled with compound 27 in the presence of triethyl amine (Figure 3.8). To provide coupling reaction with one of the two amine groups in the compound 27, reactants were used at 1:1 equivalent and naphthoyl chloride was added to the amine compound drop by drop. As a result, two products were obtained; the compound including one amide group as

the major product (compound 28a) and the compound including two amide groups as the minor product (compound 29).

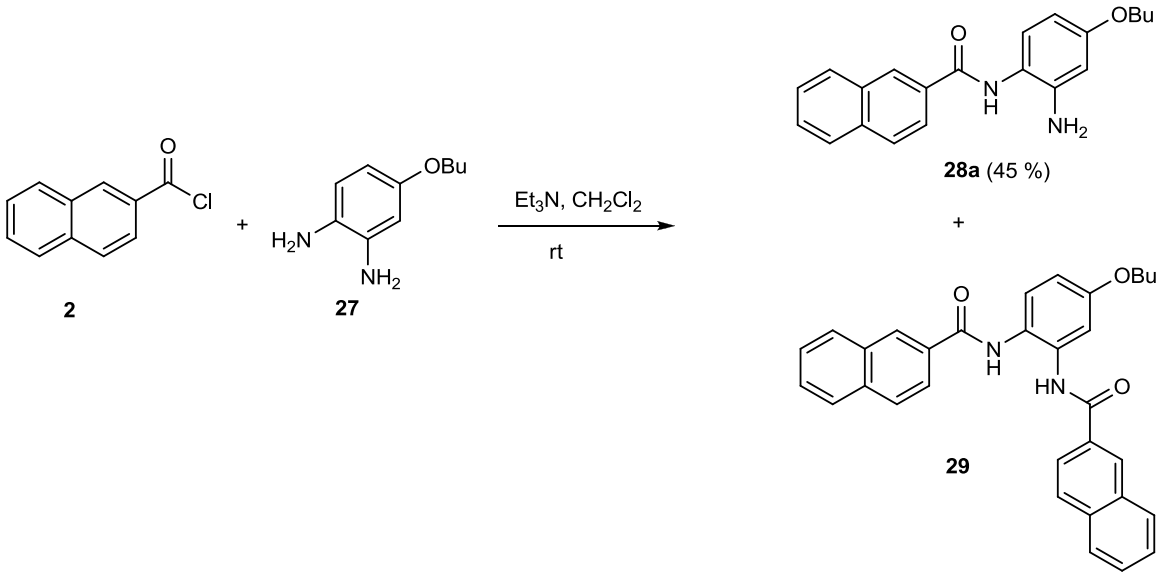


Figure 3.8. Synthesis of the lead compound derivatives from alkoxy and *ortho*-diamino substituted phenyl derivative.

It was considered that formed amide group in the major product was at the *para* position to the butoxy group as seen in the compound 28a. To prove this, compound 26 (4-butoxy-2-nitroaniline) was coupled with naphthoic acid (1) to give compound 30 as a lead compound derivative (Figure 3.9). Thus, the reduction of the nitro group in the compound 30 gives the compound 28a.

Two different reduction methods were used (Figure 3.9). In the first one, $SnCl_2.2H_2O$ and $NaBH_4$ were used to obtain the reduction product (compound 28a). In this reaction, two products (compounds 28a and 28b) were surprisingly obtained as a mixture as shown in Figure 3.9. The products were indistinguishable on TLC plate and not separated by column chromotography. Therefore, they were obtained as a mixture with 28a:28b=42:31 ratio by ^{1}H-NMR analysis. In the reaction, firstly compound 28a formed most probably, then equilibrium amide exchange reactions (transamidation) in the presence of lewis acidic metal catalyst ($SnCl_2$) gave the mixture of compounds 28a and 28b [37]. The similar ratios between the products obtained for reactions conducted in both forward

and reverse directions demonstrate that equilibrium was achieved between compounds 28a and 28b.

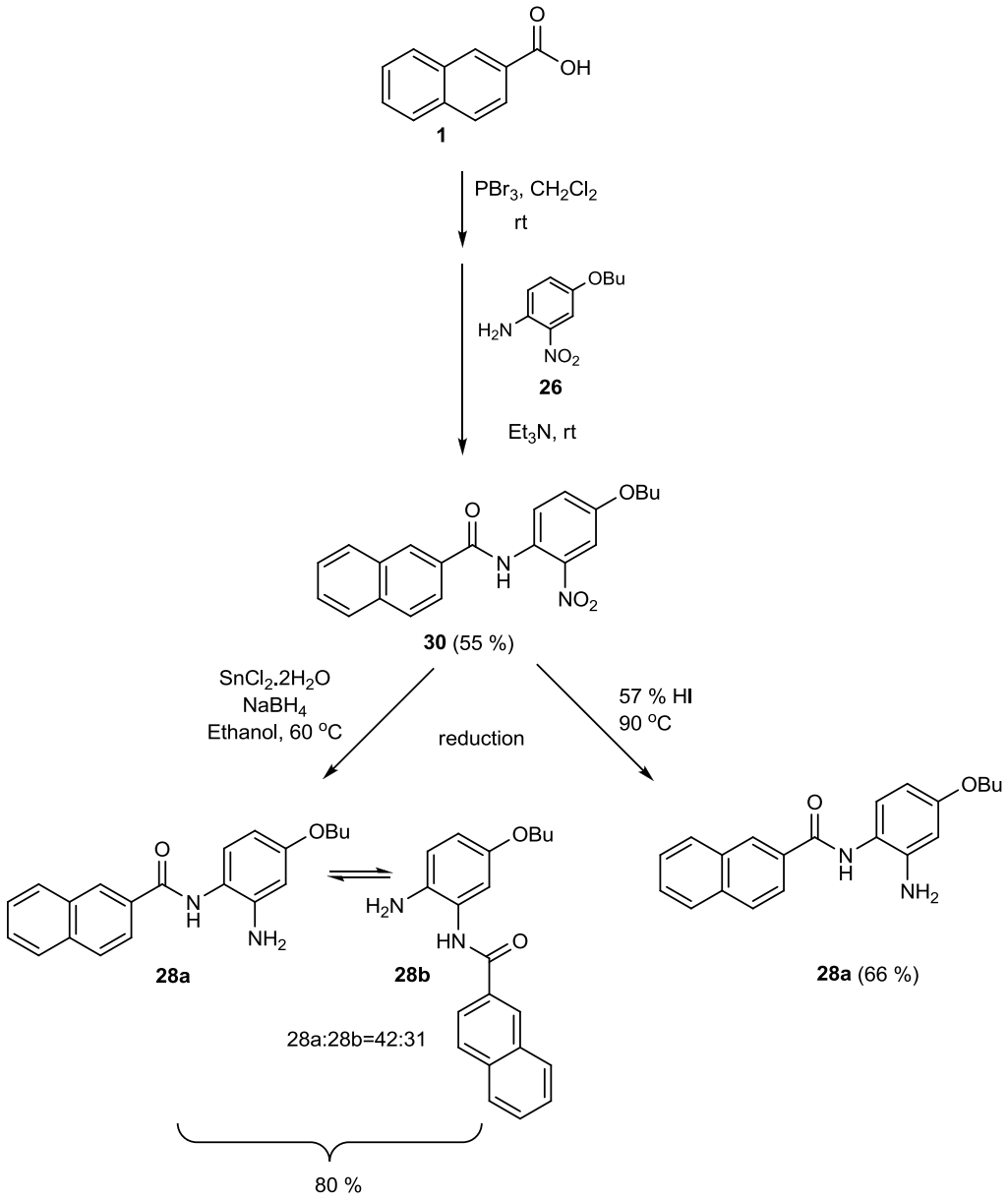


Figure 3.9. Synthesis and reduction of the compound 30.

In the literature, there are examples of facile amide exchange reactions which enabled the synthesis of important new amide-based molecules and polyamide materials under equilibrium-controlled conditions [37-45]. Equilibrium transamidation can be achieved between anilines and *N*-aryl amides as well, although somewhat more forcing conditions are required. Both metal amide complexes (Ti and Al) display activity;

however, in this case, the titanium catalyst is more effective. $Sc(OTf)_3$ as Lewis acid catalyst fails to promote these nearly thermoneutral reactions [37].

In the second method, the nitro group in the compound 30 was reduced by HI (Figure 3.9). It was seen that compound 28a was obtained as expected, which was provided by ^{1}H and ^{13}C NMR analyses.

3.1.3. Synthesis of the Lead Compound Derivatives from Alkyl and *ortho*-Dihydroxy Substituted Phenyl Derivatives

To see the effect of an additional hydroxy group together with alkyl and ester forming hydroxy on the phenyl ring, the synthesis of alkyl and *ortho*-dihydroxy substituted phenyl compound was planned.

Figure 3.10 shows the synthetic approach used in the synthesis of alkyl and *ortho*-dihydroxy substituted phenyl derivative. Compound 31 was used as the starting material. Hydroxyl group at the benzylic position in compound 31 was converted to bromine with PBr_3 to give compound 32 [46]. Then, alkylation was done at the benzylic position by using grignard reagent (*n*-BuMgBr) at -78 ^{o}C, which gave compound 33 [47]. Finally, the desired compound 34 was obtained by the conversion of methoxy groups to hydroxy groups by using BBr_3 [48].

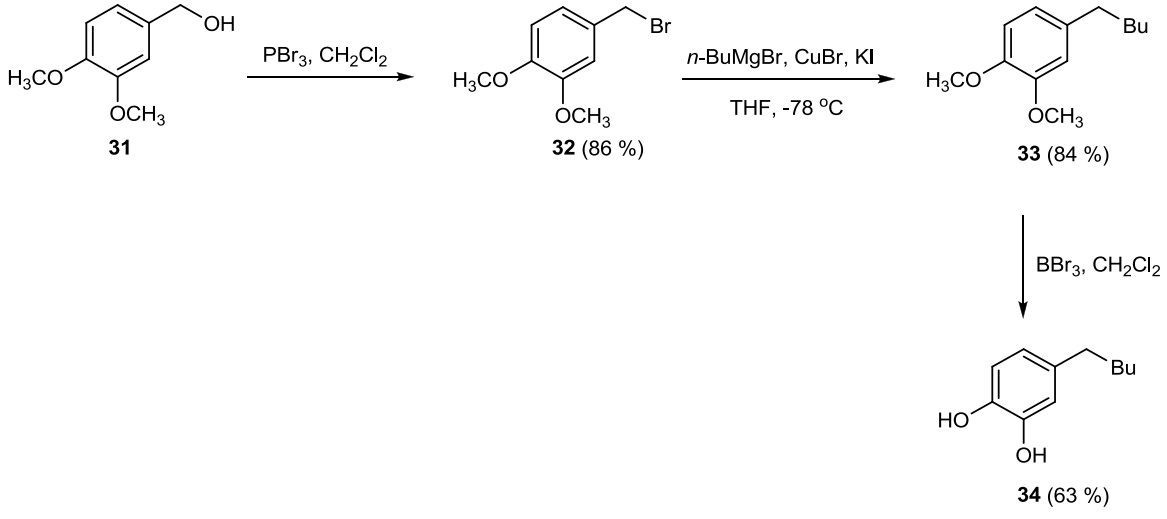


Figure 3.10. Synthesis of alkyl and *ortho*-dihydroxy substituted phenyl derivative.

The ester coupling reaction of compound 34 with the naphthoic acid (1) in the presence of DCC and DMAP gave the lead compound derivatives 35a and 35b as a mixture (Figure 3.11). These compounds include one ester group at para or meta positions to the alkyl group. The ratio of these compounds was 35a:35b=3:2 as determined by ^{1}H-NMR analysis. In this reaction, in addition to the desired lead compound derivatives (compounds 35a and 35b), compound 36 including two ester groups was also obtained as by-product in low yield.

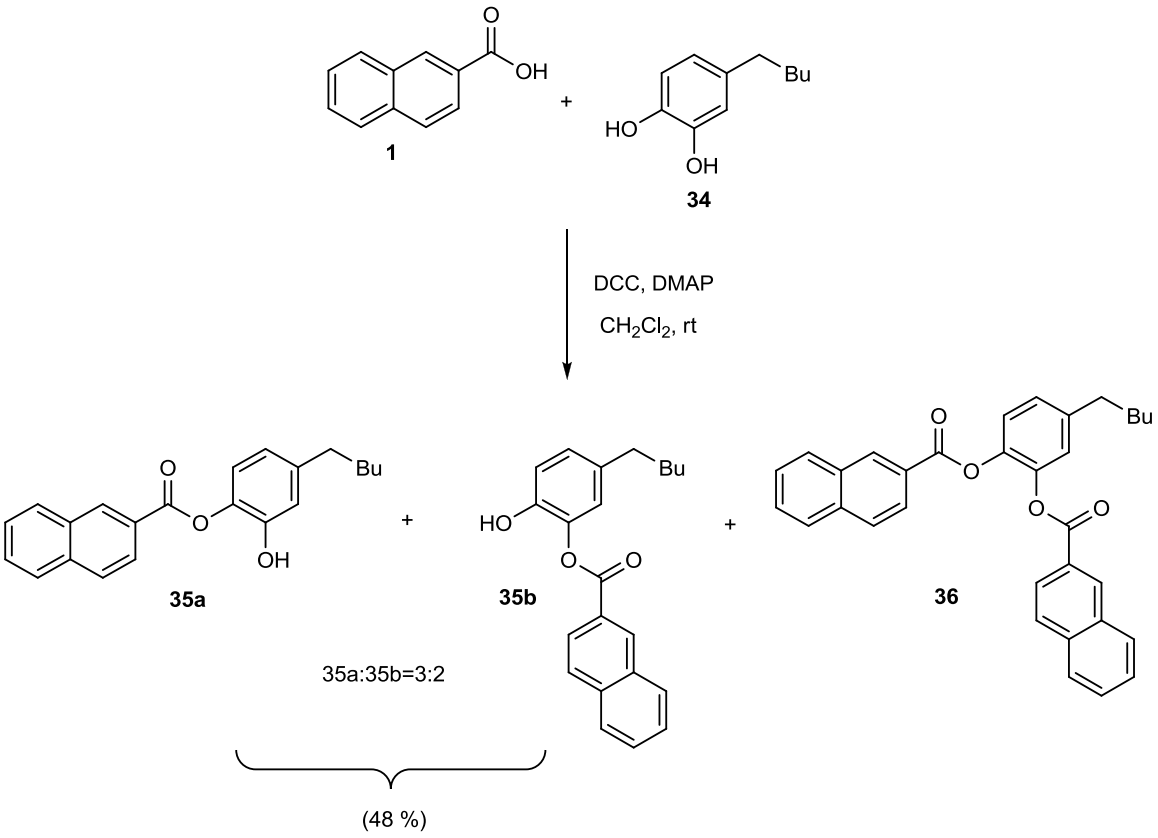


Figure 3.11. Synthesis of the lead compound derivatives from alkyl and *ortho*-dihydroxy substituted phenyl derivative.

3.1.4. Synthesis of the Lead Compound Derivatives from Alkyl and *meta*-Dihydroxy Substituted Phenyl Derivatives

To see the effects of the positions of alkyl and hydroxy group on the phenyl ring, alkyl and *meta*-dihydroxy substituted phenyl compound was also synthesized.

Synthesis of alkyl and *meta*-dihydroxy substituted phenyl compound is shown in Figure 3.12. Compound 37 was used as the starting material and the final product (compound 39) was obtained following a similar approach to the method shown in Figure 3.10.

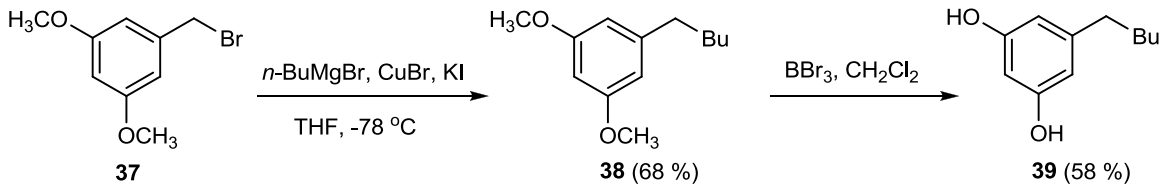


Figure 3.12. Synthesis of alkyl and *meta*-dihydroxy substituted phenyl derivative.

The ester coupling reaction of compound 39 with the naphthoic acid in the presence of DCC and DMAP gave the lead compound derivative (compound 40) (Figure 3.13). In this reaction, in addition to desired lead compound derivative (compound 40), the compound including two ester groups (compound 41) was obtained as by-product in low yield.

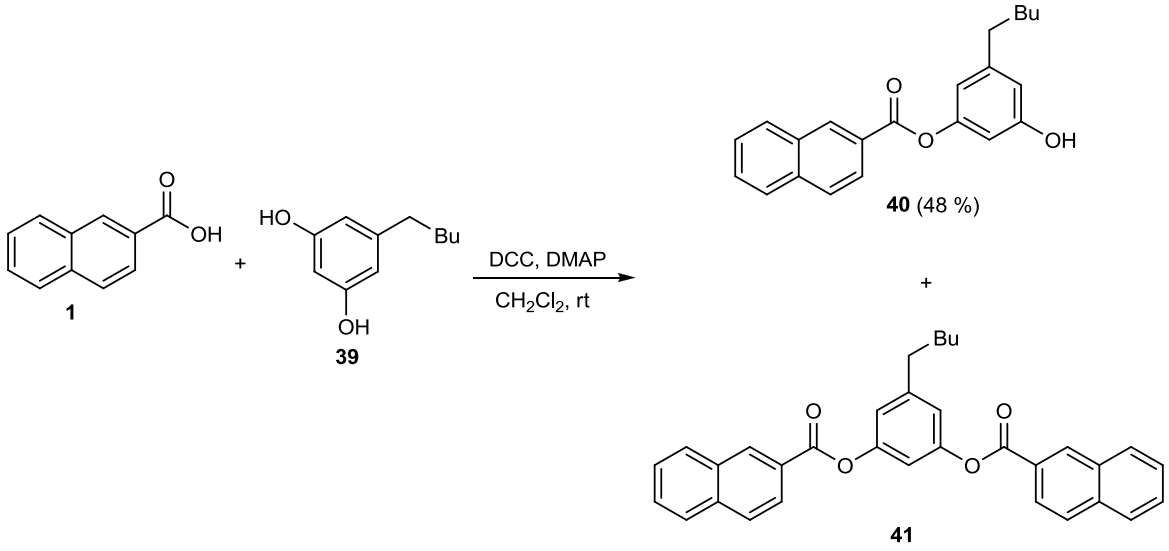


Figure 3.13. Synthesis of the lead compound derivatives from alkyl and *meta*-dihydroxy substituted phenyl derivative.

3.1.5. Synthesis of the Lead Compound Derivatives from Alkyl and *ortho*-Diamino Substituted Phenyl Derivatives

To see the effect of an additional amine group together with alkyl and amide forming amine on the phenyl ring, alkyl and *ortho*-diamino substituted phenyl compound was also synthesized.

The synthesis of alkyl and *ortho*-diamino substituted phenyl compound was successfully carried out by the synthetic approach shown in Figure 3.14. 4-Butyl aniline (compound 42) was used as the starting material. After the protection of the amine group by using acetic anhydride, compound 44 was obtained by the nitration of compound 43 using nitric acid and sulfiric acid [49]. Acetamide group in the compound 44 was again converted to amine group with 20 % H_2SO_4 to obtain compound 45. The reduction of the nitro group in compound 45 with HI gave the desired alkyl and *ortho*-diamino substituted phenyl derivative (compound 46)

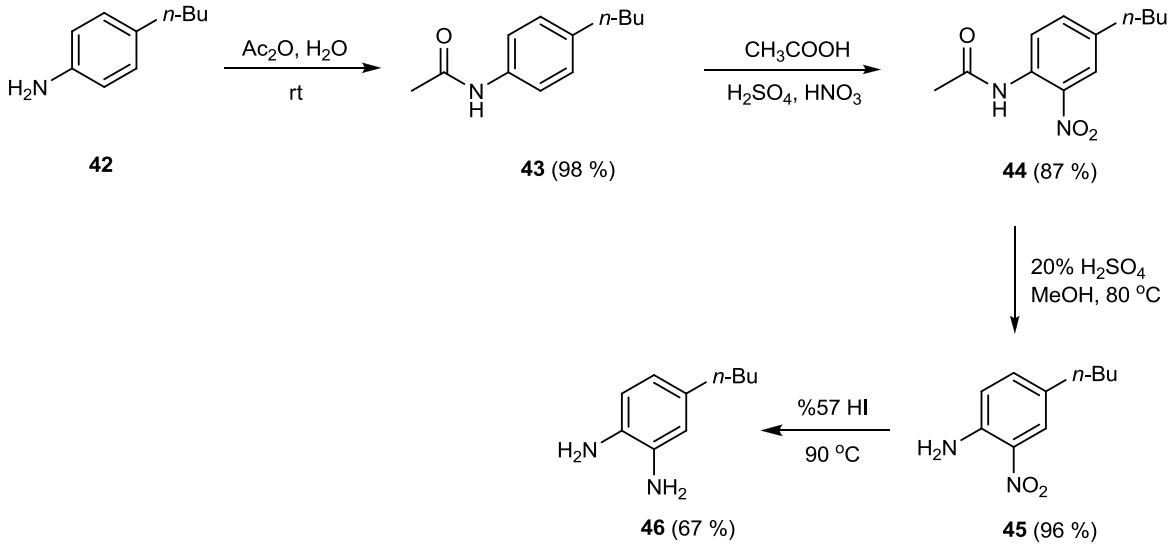


Figure 3.14. Synthesis of alkyl and *ortho*-diamino substituted phenyl derivative.

In order to obtain the lead compound derivative, the naphthoyl chloride (2) was coupled with compound 46 in the presence of triethyl amine (Figure 3.15). To provide coupling reaction with one of the two amine groups in the compound 46, reactants were

used at 1:1 equivalent and naphthoyl chloride was added to the amine compound drop by drop. As a result, two products were obtained; the compound including one amide group as the major product (compound 47a) and the compound including two amide groups as the minor product (compound 48).

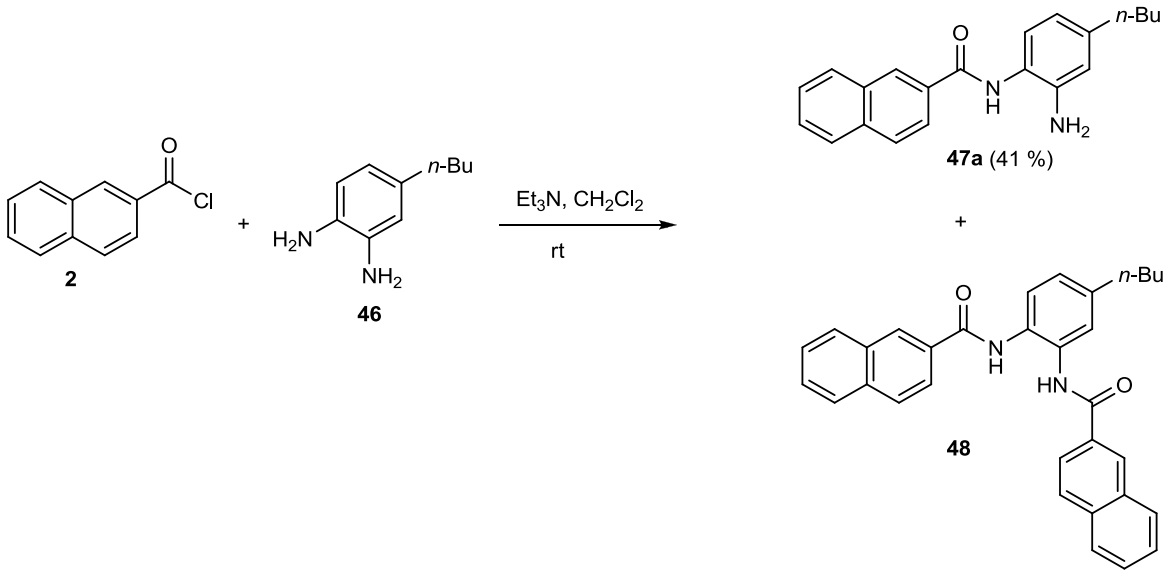


Figure 3.15. Synthesis of the lead compound derivatives from alkyl and *ortho*-diamino substituted phenyl derivative.

It was considered that formed amide group in the major product was at the *para* position to the butyl group as seen in the compound 47a. To prove this, compound 45 (4-butyl-2-nitroaniline) was coupled with naphthoic acid (1) to give compound 49 as a lead compound derivative (Figure 3.9). Thus, the reduction of the nitro group in the compound 49 gives the compound 47a.

Two different reduction methods were again used (Figure 3.16). In the first one, $SnCl_2.2H_2O$ and $NaBH_4$ were used to obtain the reduction product (compound 47a). In this reaction, two products (compounds 47a and 47b) were obtained as a mixture as shown in Figure 3.16. The products were indistinguishable on TLC plate and not separated by column chromotography. Therefore, they were obtained as a mixture with 47a:47b=69:53 ratio by ^{1}H-NMR analysis. In the reaction, firstly compound 48a formed most probably,

then equilibrium amide exchange reactions (transamidation) in the presence of lewis acidic metal catalyst ($SnCl_2$) gave the mixture of compounds 47a and 47b [37-45].

In the second method, nitro group in the compound 49 was reduced by 57 % HI (Figure 3.16). It was seen that compound 47a was obtained as expected, which was provided by ^{1}H and ^{13}C NMR analyses.

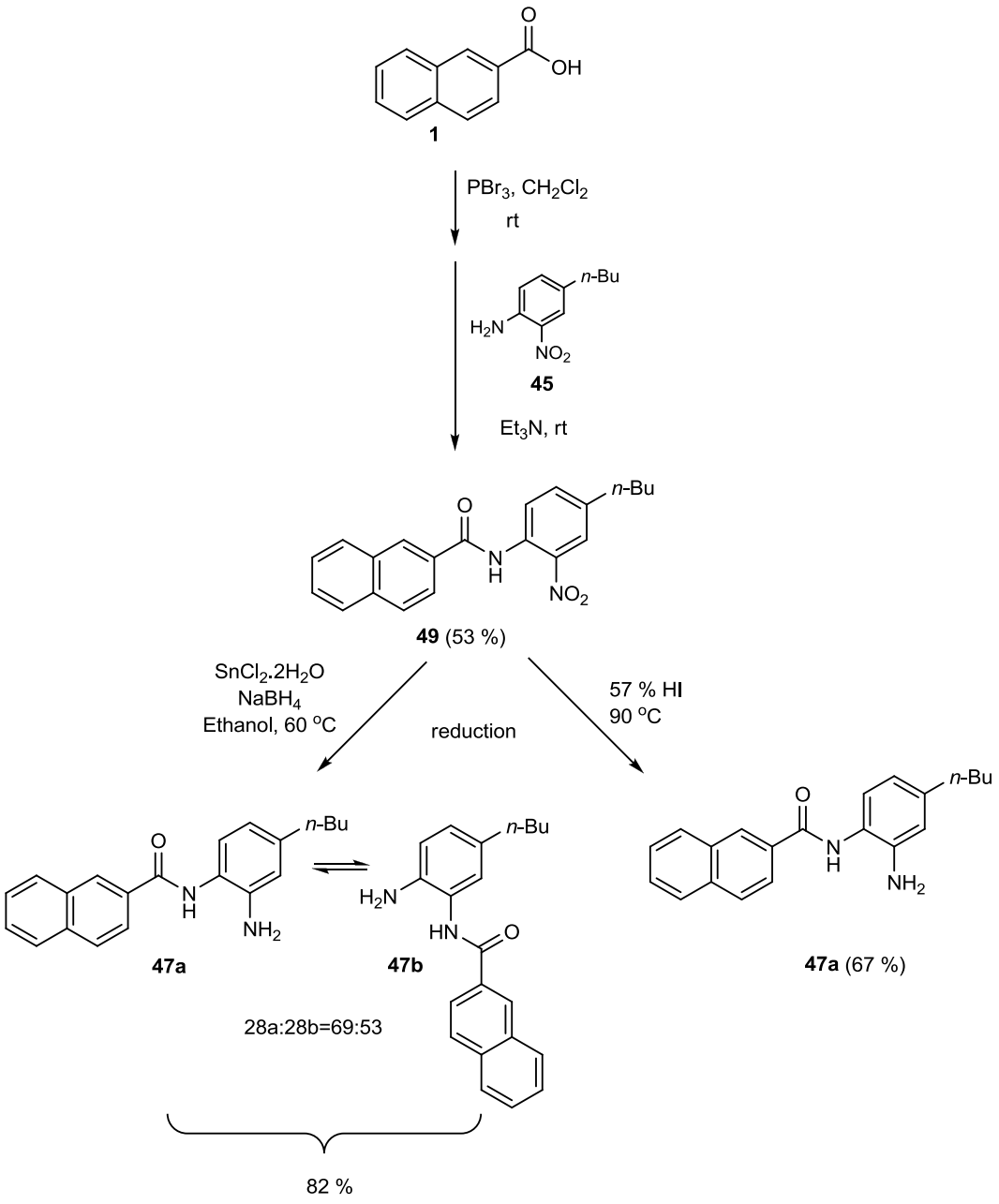


Figure 3.16. Synthesis and reduction of the compound 49.

3.1.6. Synthesis of the Lead Compound Derivatives from Alkyl, Methoxy and Amino Substituted Phenyl Derivatives

Finally, to see the effect of an additional metoxy or hydroxyl group together with alkyl and amide forming amine on the phenyl ring, alkyl, amino and metoxy substituted phenyl compound was synthesized.

Alkyl, amino and methoxy substituted phenyl derivative was synthesized according to the synthetic way shown in Figure 3.17. The general strategy followed in the synthesis was as follows; compound 50 that had the desired substituents was used as the starting material and was converted to the corresponding methyl ester by Fisher Esterification method to obtain compound 51. Second implementation became the protection of the aromatic amine so that side reactions may be avoided in the next step. Protection of the amine was done by using acetic anhydride in the presence of water.

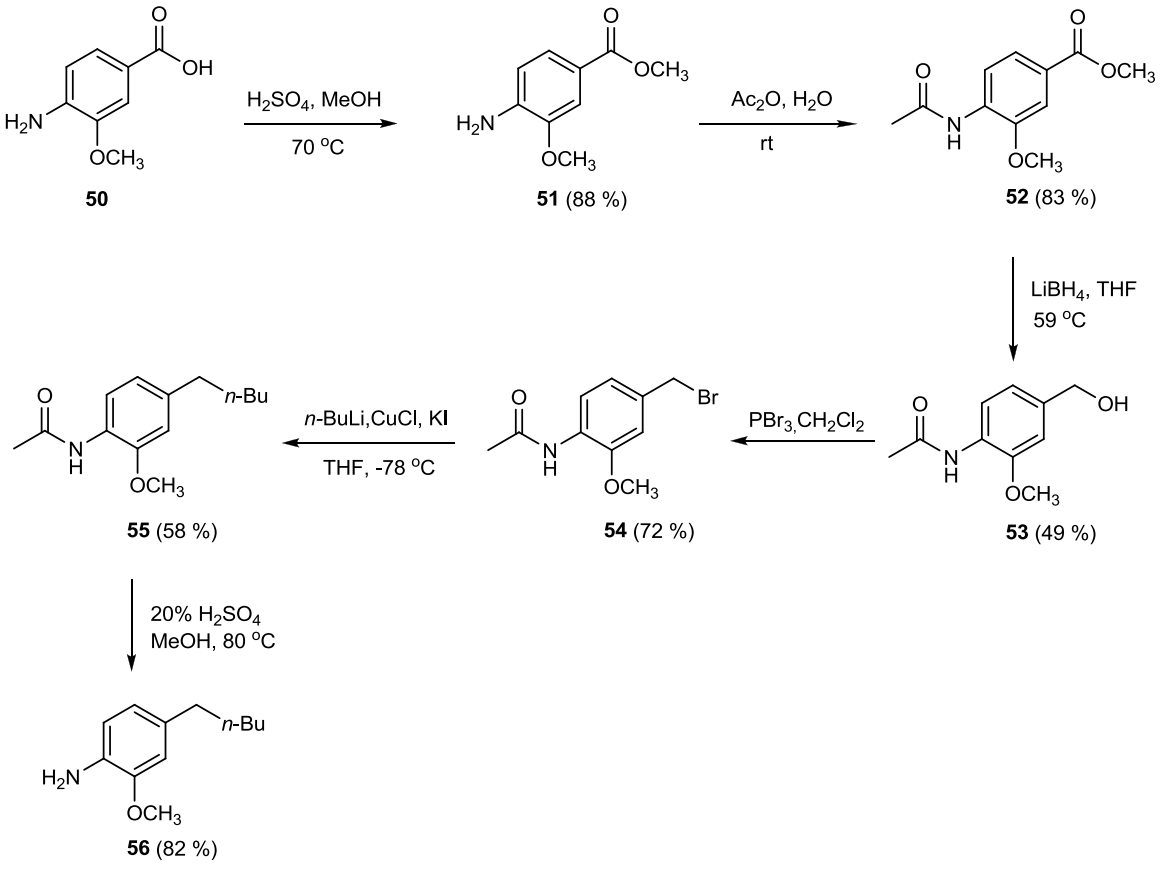


Figure 3.17. Synthesis of alkyl, methoxy and amino substituted phenyl derivative.

After the amine protection, the ester group was reduced to benzylic alcohol by $LiBH_4$ [50]. To achieve alkyl substitution, benzylic alcohol group was converted benzyl bromide with PBr_3. Then, alkylation was done with *n*-BuLi. After the synthesis of compound 55, a deprotection was done by using 20 % sulphuric acid to obtain compound 56 (Figure 3.17).

Compound 56 was coupled with naphthoic acid to form compound 57 as a lead compound derivative (Figure 3.18). Then the methoxy group on compound 57 can be converted to hydroxyl group by using BBr_3. If this reaction is done before coupling with naphthoic acid, there will be a competition between nitrogen and oxygen atoms about the attack to the naphthoyl chloride. Therefore this reaction was planned to be the last step to of the synthesis to avoid the competition.

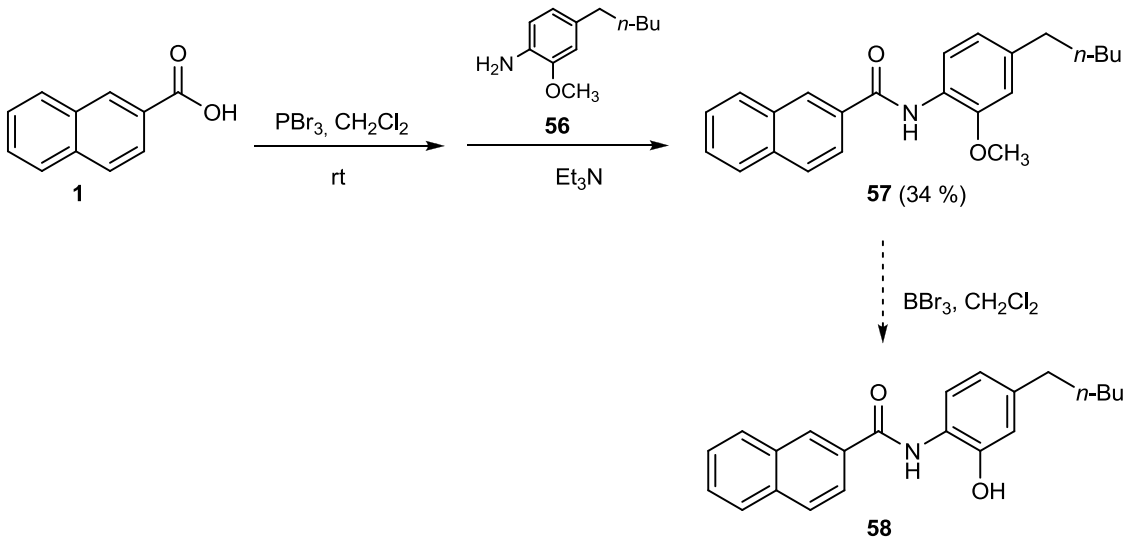


Figure 3.18. Synthesis of the lead compound derivatives from alkyl, methoxy and amino substituted phenyl derivative.

3.2. Biological Evaluation of the Lead Compound Derivatives

Some synthesized compounds were subjected to biological tests in order to measure inhibitory effects of them on human CYP17. Biological tests were done at Koç University

by Türkay and Kavaklı research groups. These efforts are still going on. In the study, the compounds that displayed favorable inhibitory activity on human CYP17 are picked to calculate IC_{50} value.

The compounds 6, 7, 8, 28a and 29 were tested together at 5 μM (Table 3.1). Among them, compound 6 showed highest inhibition activity with 79 % inhibition. Therefore, its IC_{50} value was determined. IC_{50} value of the compound 6 was found to be 2300 nM, which means that this compound is about fifteen times more active than the lead compound. The compound 6 includes an alkyl group on the phenyl ring unlike the other ones (Table 3.1). Therefore, an alkyl substituent in stead of alkoxy on the phenyl ring may be better in the biological activity.

The compounds 10, 11, 12, 35a and 35b, and 36 were tested together at 2 μM (Table 3.1). Among them, only the compound 10 showed inhibition activity with 40 % inhibition value. The other ones showed no inhibition. They include alkoxy substituent or ester bond. Therefore, it can be considered that the use of amide bond instead of ester bond in the derivatization of the lead compound should be better for the biological activity. Methoxy group at six position on the naphtyl unit may be used in the derivatization.

The compounds 18, 19, 20, and 21 were tested together at 1 μM (Table 3.1). Among them, only the compound 21 showed inhibition activity. It has electron donating metoxy groups at 3 and 5 positions on the naphtyl unit. Saturated bonds, amide group at 1 position and electron withdrawing F group on the naphtyl ring were not appropriate for inhibition.

Table 3.1. Inhibition activities of the lead compound derivatives on human CYP17.

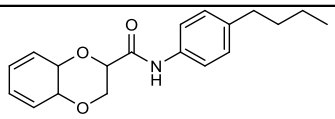
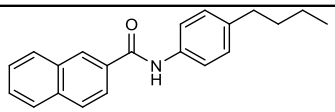
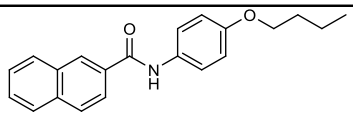
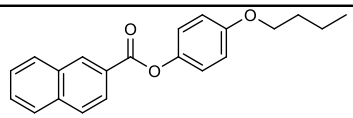
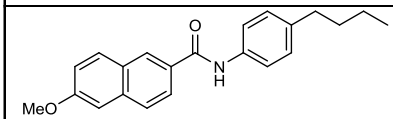
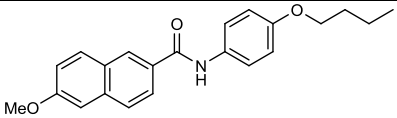
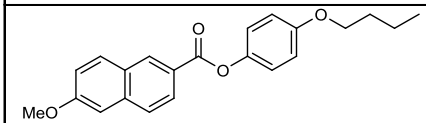
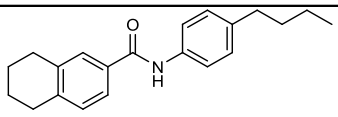
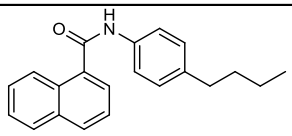
Compounds	% inhibation at 5 μM	% inhibation at 2 μM	% inhibition at 1 μM	IC_{50} (nM)[a]
 Lead compound	-[b]	-	-	35650
 6	79	-	-	2300
 7	65	-	-	-
 8	74	-	-	-
 10	-	40	-	-
 11	-	ni[c]	-	-
 12	-	ni	-	-
 18	-	-	ni	-
 19	-	-	5	-

Table 3.1. Inhibition activities of the lead compound derivatives on human CYP17 (cont.).

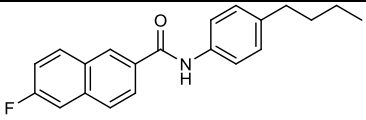
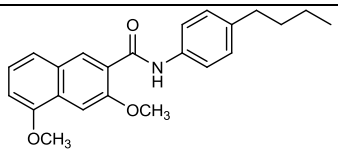
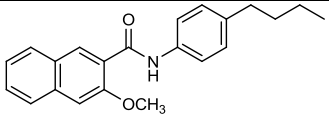
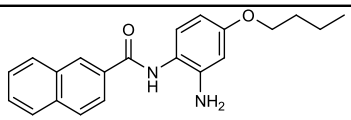
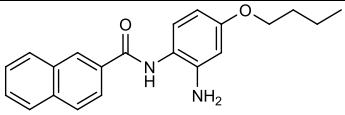
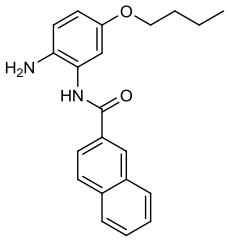
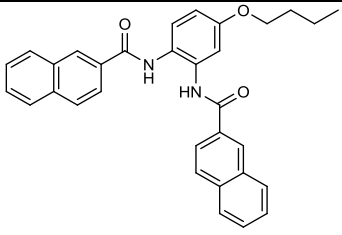
Compounds	% inhibation at 5 μM	% inhibation at 2 μM	% inhibition at 1 μM	IC_{50} (nM)[a]
 20	-	-	ni	-
 21	-	-	33	-
 22	-	-	-	-
 28a	54	-	-	-
 28a and  28b	-	-	-	-
 29	ni	-	-	-

Table 3.1. Inhibition activities of the lead compound derivatives on human CYP17 (cont.).

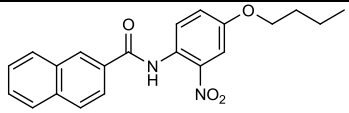
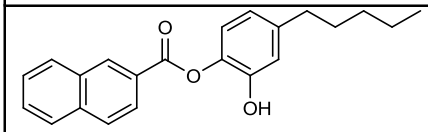
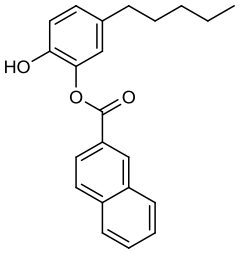
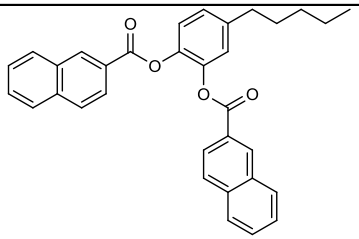
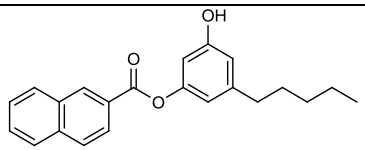
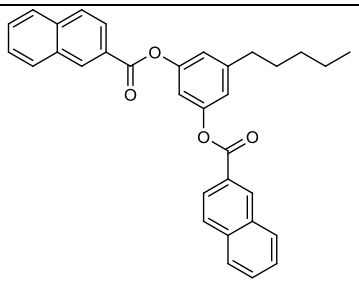
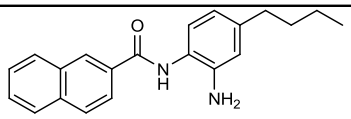
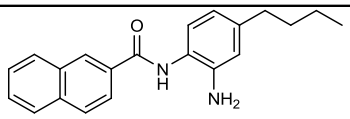
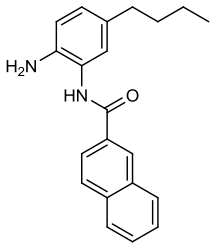
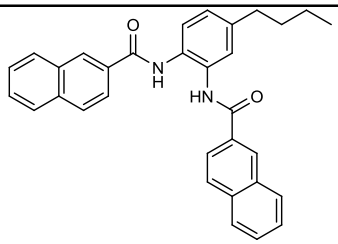
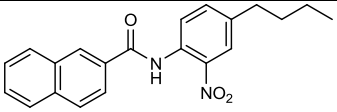
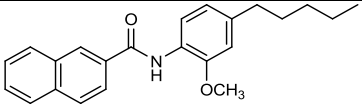
Compounds	% inhibation at 5 μM	% inhibation at 2 μM	% inhibition at 1 μM	IC_{50} (nM)[a]
 30	-	-	-	-
 35a and  35b	-	ni	-	-
 36	-	ni	-	-
 40	-	ni	-	-
 41	-	ni	-	-

Table 3.1. Inhibition activities of the lead compound derivatives on human CYP17 (cont.).

Compounds	% inhibation at 5 μM	% inhibation at 2 μM	% inhibition at 1 μM	IC_{50} (nM)[a]
 47a	-	-	-	-
 47a and  47b	-	-	-	-
 48	-	-	-	-
 49	-	-	-	-
 57	-	-	-	-

[a]Concentration of inhibitors required to give 50% inhibition. The assay was run with human CYP17 expressed in *E. coli* using 17α-(21-hydroxypregnenolone) as substrate. [b] "-": not determined. [c] "ni": no inhibition.

4. EXPERIMENTAL SECTION

4.1. Materials

All chemicals were used as received from the manufacturers (Merck, Aldrich, Alfa Aesar, Riedel de Haen). Dry solvents (CH_2Cl_2, THF, toluene) were obtained from ScimatCo Purification System.

4.2. Instrumentation

Thin layer chromatograhy plates were viewed under 254 nm UV lamp. ^{1}H-NMR and ^{13}C-NMR spectra were recorded on Varian 400-MHz NMR spectrometer (Varian Associates, Palo Alto, CA).

4.3. Syntheses

4.3.1. Synthesis of 2-naphthoyl chloride (2)

A 50 mL round-bottom flask was charged with 2-naphthoic acid (2.00 g, 11.6 mmol) and thionyl chloride $SOCl_2$ (15.0 mL). The solution was refluxed at 80 ^{o}C for 4 hours and then concentrated to give the product as a yellow solid, which was used without further purification. (2.11 g, 95.5 % yield). ^{1}H NMR ($CDCl_3$), δ : 7.66 (m, 2H, Ar*H*s), 7.93 (d, *J*=8.9 Hz, 2H, Ar*H*s), 8.04 (m, 2H, Ar*H*s), 8.76 (s, 1H, Ar*H*) ppm.

4.3.2. Synthesis of *N*-(4-butylphenyl)-2-naphthamide (6)

2-Naphthoyl Chloride (0.22 g, 1.13 mmol) was dissolved in anhydrous dichloromethane (5 mL) in a 25 mL round-bottom flask. Triethylamine (0.17 g, 1.70 mmol, 1.5 equiv) and 4-butylaniline (0.17 g, 1.13 mmol, 1.0 equiv) were added. Then the reaction mixture was stirred at room temperature overnight. After this time, the solvent of resulting homogeneous solution was evaporated to give crude product. Column

chromatography on silica with dichloromethane as eluent gave the pure product as a white solid (0.17 g, 49.6 % yield). ^{1}H NMR ($CDCl_3$), δ : 0.84 (t, *J*=7.3 Hz, 3H, C*H*$_3$), 1.27 (m, 2H, C*H*$_2$CH$_3$), 1.52 (m, 2H, C*H*$_2$CH$_2$CH$_3$), 2.52 (t, *J*=7.7 Hz, 2H, C*H*$_2$), 7.11 (d, *J*=8.4 Hz, 2H, Ar*H*s), 7.49 (m, 4H, Ar*H*s), 7.85 (m, 5H, Ar*H*s), 8.28 (s, 1H, N*H*) ppm. ^{13}C NMR ($CDCl_3$), δ : 13.95 (*C*H$_3$), 22.29 (*C*H$_2$CH$_3$), 33.66 (*C*H$_2$CH$_2$CH$_3$), 35.09 (O*C*H$_2$), 120.29 (Ar*C*), 123.56 (Ar*C*), 126.90 (Ar*C*), 127.45 (Ar*C*), 127.80 (Ar*C*), 127.83 (Ar*C*), 128.71 (Ar*C*), 128.95 (Ar*C*), 129.00 (Ar*C*), 132.31 (Ar*C*), 132.62 (Ar*C*), 134.82 (Ar*C*), 135.57 (Ar*C*), 139.38 (Ar*C*), 165.71 (*C*=O) ppm.

4.3.3. Synthesis of *N*-(4-butoxyphenyl)-2-naphthamide (7)

2-Naphthoyl chloride (0.37 g, 1.95 mmol) was dissolved in anhydrous dichloromethane (8 mL) in a 25 mL round-bottom flask. Triethylamine (0.29 g, 2.93 mmol, 1.5 equiv) and 4-butoxyaniline (0.32 g, 1.95 mmol, 1.0 equiv) were added. Then the reaction mixture was stirred at room temperature overnight. After this time, a solid precipitated out of solution and this was filtered and washed with several portions of dichloromethane to give pure product as a white crystalline solid (0.31 g, 49.9 % yield). ^{1}H NMR ($CDCl_3$), δ : 0.98 (t, *J*=7.4 Hz, 3H, C*H*$_3$), 1.50 (m, 2H, C*H*$_2$CH$_3$), 1.78 (m, 2H, C*H*$_2$CH$_2$CH$_3$), 3.97 (t, *J*=6.5 Hz, 2H, OC*H*$_2$), 6.92 (d, *J*=9.0 Hz, 2H, Ar*H*s), 7.57 (m, 4H, Ar*H*s), 7.91 (m, 5H, Ar*H*s), 8.37 (s, 1H, N*H*) ppm. ^{13}C NMR ($CDCl_3$), δ : 14.24 (*C*H$_3$), 19.62 (*C*H$_2$CH$_3$), 31.71 (*C*H$_2$CH$_2$CH$_3$), 68.38 (O*C*H$_2$), 115.28 (Ar*C*), 122.47 (Ar*C*), 123.94 (Ar*C*), 127.27 (Ar*C*), 127.79 (Ar*C*), 128.17 (Ar*C*), 129.06 (Ar*C*), 129.21 (Ar*C*), 131.23 (Ar*C*), 132.64 (Ar*C*), 133.01 (Ar*C*), 135.17 (Ar*C*), 156.63 (Ar*C*), 166.01 (*C*=O) ppm.

4.3.4. Synthesis of 4-butoxyphenyl 2-naphthoate (8)

2-Naphthoyl chloride (0.20 g, 1.05 mmol) was dissolved in anhydrous dichloromethane (5 mL) in a 25 mL round-bottom flask. Triethylamine (0.16 g, 1.57 mmol, 1.5 equiv) and 4-butoxyphenol (0.17 g, 1.05 mmol, 1.0 equiv) were added. Then the reaction mixture was stirred at room temperature overnight. After this time, the solvent of resulting homogeneous solution was evaporated to give crude product. Column chromatography on silica with dichloromethane as eluent gave the pure product as a light yellow powder solid (0.15 g, 45.3 % yield). ^{1}H NMR ($CDCl_3$), δ : 0.92 (t, *J*=7.4 Hz, 3H,

C*H*$_3$), 1.44 (m, 2H, C*H*$_2$CH$_3$), 1.72 (m, 2H, C*H*$_2$CH$_2$CH$_3$), 3.92 (t, *J*=6.5 Hz, 2H, OC*H*$_3$), 6.88 (d, *J*=9.0 Hz, 2H, Ar*H*s), 7.10 (d, *J*=8.5 Hz, 2H, Ar*H*s), 7.54 (m, 2H, Ar*H*s), 7.86 (t, *J*=9.0 Hz, 2H, Ar*H*s), 7.93 (d, *J*=8.0 Hz, 1H, Ar*H*), 8.12 (dd, *J*=8.6, 1.6, 1H, Ar*H*), 8.71 (s, 1H, Ar*H*) ppm. ^{13}C NMR ($CDCl_3$), δ: 13.85 (*C*H$_3$), 19.25 (*C*H$_2$CH$_3$), 31.33 (*C*H$_2$CH$_2$CH$_3$), 68.11 (O*C*H$_2$), 115.14 (Ar*C*), 122.43 (Ar*C*), 125.48 (Ar*C*), 126.80 (Ar*C*), 126.89 (Ar*C*), 127.82 (Ar*C*), 128.34 (Ar*C*), 128.56 (Ar*C*), 129.47 (Ar*C*), 131.83 (Ar*C*), 132.51 (Ar*C*), 135.78 (Ar*C*), 144.32 (Ar*C*), 156.94 (Ar*C*), 165.74 (*C*=O) ppm.

4.3.5. Synthesis of *N*-(4-butylphenyl)-6-methoxy-2-naphthamide (10)

4-Butylaniline (89.5 mg, 0.6 mmol) and DMAP (48.9 mg, 0.4 mmol, 0.6 equiv) were dissolved in anhydrous CH_2Cl_2 (5 mL). To this solution at room temperature under nitrogen atmosphere was added 6-metoxy-2-naphthoic acid (121.3 mg, 0.6 mmol) and DCC (148.6 mg, 0.72 mmol, 1.2 equiv) in CH_2Cl_2 (5 mL) over a period of 2 hours. The reaction mixture was stirred at room temperature for 24 hours. Resulting precipitate was filtered. Solution was concentrated to give crude product. The crude product was purified by filtration through silica gel using CH_2Cl_2 as solvent and recrystallization from methanol-water (5:1, v/v) to give pure product as a solid (112.6 mg, 56.4 % yield). ^{1}H NMR ($CDCl_3$), δ: 0.87 (t, *J*=7.3 Hz, 3H, C*H*$_3$), 1.30 (m, 2H, C*H*$_2$CH$_3$), 1.54 (m, 2H, C*H*$_2$CH$_2$CH$_3$), 2.54 (t, *J*=7.6 Hz, 2H, ArC*H*$_2$), 3.89 (s, 3H, OC*H*$_3$), 7.10-7.17 (m, 4H, Ar*H*s), 7.51 (d, *J*=8.4 Hz, 2H, Ar*H*s), 7.74-7.84 (m, 4H. Ar*H*s), 8.24 (s, 1H, N*H*) ppm. ^{13}C NMR ($CDCl_3$), δ: 13.95 (*C*H$_3$), 22.28 (*C*H$_2$CH$_3$), 33.65 (*C*H$_2$CH$_2$CH$_3$), 35.09 (Ar*C*H$_2$), 55.40 (O*C*H$_3$), 105.67 (Ar*C*), 119.90 (Ar*C*), 120.23 (Ar*C*), 124.16 (Ar*C*), 127.31 (Ar*C*), 127.37 (Ar*C*), 128.02 (Ar*C*), 128.98 (Ar*C*), 130.02 (Ar*C*), 130.49 (Ar*C*), 135.65 (Ar*C*), 136.39 (Ar*C*), 139.24 (Ar*C*), 159.21 (Ar*C*), 165.69 (*C*=O) ppm.

4.3.6. Synthesis of *N*-(4-butoxyphenyl)-6-methoxy-2-naphthamide (11)

4-Butoxyaniline (99.1 mg, 0.6 mmol) and DMAP (48.9 mg, 0.4 mmol, 0.6 equiv) were dissolved in anhydrous CH_2Cl_2 (5 mL). To this solution at room temperature under nitrogen atmosphere was added 6-metoxy-2-naphthoic acid (121.3 mg, 0.6 mmol) and DCC (148.6 mg, 0.72 mmol, 1.2 equiv) in CH_2Cl_2 (5 mL) over a period of 2 hours. The reaction mixture was stirred at room temperature for 24 hours. Resulting precipitate was

filtered. Solution was concentrated to give crude product. The crude product was purified by filtration through silica gel using CH_2Cl_2 as solvent and recrystallization from CH_2Cl_2-hexane (9:1, v/v) to give pure product as a white solid (87.5 mg, 41.7 % yield). ^{1}H NMR ($CDCl_3$), δ: 0.98 (t, *J*=7.4 Hz, 3H, C*H*$_3$), 1.50 (m, 2H, C*H*$_2$CH$_3$), 1.77 (m, 2H, C*H*$_2$CH$_2$CH$_3$), 3.95 (s, 3H, OC*H*$_3$), 3.97 (t, *J*=6.5 Hz, 2H, ArOC*H*$_2$), 6.91 (d, *J*=8.9 Hz, 2H, Ar*H*s), 7.17 (d, *J*=2.4 Hz, 1H, Ar*H*), 7.21 (dd, *J*=8.9, 2.4 Hz, 1H, Ar*H*), 7.56 (d, *J*=8.9 Hz, 1H, Ar*H*), 7.79-7.89 (m, 4H, Ar*H*s), 8.30 (s, 1H, N*H*) ppm. ^{13}C NMR ($CDCl_3$), δ: 13.86 (*C*H$_3$), 19.24 (*C*H$_2$CH$_3$), 31.33 (*C*H$_2$CH$_2$CH$_3$), 55.40 (OCH$_3$), 68.00 (ArOCH$_2$), 105.66 (Ar*C*), 114.89 (Ar*C*), 119.90 (Ar*C*), 122.04 (Ar*C*), 124.16 (Ar*C*), 127.27 (Ar*C*), 127.35 (Ar*C*), 128.02 (Ar*C*), 129.98 (Ar*C*), 130.46 (Ar*C*), 130.96 (Ar*C*), 136.35 (Ar*C*), 156.16 (Ar*C*), 159.18 (Ar*C*), 165.65 (*C*=O) ppm.

4.3.7. Synthesis of 4-butoxyphenyl 6-methoxy-2-naphthoate (12)

4-Butoxyphenol (41.6 mg, 0.25 mmol) and DMAP (18.5 mg, 0.15 mmol, 0.6 equiv) were dissolved in anhydrous CH_2Cl_2 (2 mL). To this solution at room temperature under nitrogen atmosphere was added 6-metoxy-2-naphthoic acid (50.6 mg, 0.25 mmol) and DCC (61.8 mg, 0.3 mmol, 1.2 equiv) in CH_2Cl_2 (2 mL) over a period of 2 hours. The reaction mixture was stirred at room temperature for 24 hours. Resulting precipitate was filtered. Solution was concentrated to give crude product. Purification by column chromatography on silica gel using CH_2Cl_2-methanol (99:1, v/v) as eluent gave the pure product as a white solid (35.6 mg, 40.7 % yield). ^{1}H NMR ($CDCl_3$), δ: 0.99 (t, *J*=7.4 Hz, 3H, C*H*$_3$), 1.52 (m, 2H, C*H*$_2$CH$_3$), 1.78 (m, 2H, C*H*$_2$CH$_2$CH$_3$), 3.96 (s, 3H, OC*H*$_3$), 3.98 (t, *J*=6.5 Hz, 2H, OC*H*$_2$), 6.94 (d, *J*=9.1, 2H, Ar*H*s), 7.13-7.24 (m, 4H, Ar*H*s), 7.81 (d, *J*=8.7 Hz, 1H, Ar*H*), 7.88 (d, *J*=9.1 Hz, 1H, Ar*H*), 8.15 (dd, *J*=8.6, 1.7, 1H, Ar*H*), 8,69 (d, *J*=1.5 Hz, 1H, ArH) ppm. ^{13}C NMR ($CDCl_3$), δ: 13.84 (*C*H$_3$), 19.24 (*C*H$_2$CH$_3$), 31.33 (*C*H$_2$CH$_2$CH$_3$), 55.42 (OCH$_3$), 68.11 (OCH$_2$), 105.74 (Ar*C*), 115.12 (Ar*C*), 119.78 (Ar*C*), 122.45 (Ar*C*), 124.64 (Ar*C*), 126.22 (Ar*C*), 126.99 (Ar*C*), 127.91 (Ar*C*), 131.02 (Ar*C*), 131.60 (Ar*C*), 137.48 (Ar*C*), 144.39 (Ar*C*), 156.87 (Ar*C*), 159.80 (Ar*C*), 165.84 (*C*=O) ppm.

4.3.8. Synthesis of *N*-(4-butylphenyl)-5,6,7,8-tetrahydronaphthalene-2-carboxamide (18)

5,6,7,8-tetrahydro-2-naphthoic acid (176.2 mg, 1 mmol) was dissolved in anhydrous CH_2Cl_2 (3 mL). PBr_3 (0.14 mL, 1.5 mmol) was added to the solution under nitrogen. The mixture was stirred at room temperature for 3 hours. Et_3N (0.42 mL, 3 mmol) and N-butylaniline (0.16 mL, 1 mmol) were added subsequently, and after stirring for 1 hour at room temperature, the mixture was diluted with CH_2Cl_2, washed with water and dried over anhydrous $MgSO_4$. After evaporation, the crude product was purified by recrystallization from methanol-water (5:1, v/v) to give pure product as a white solid (203.4 mg, 66.2 % yield). ^{1}H NMR ($CDCl_3$), δ : 0.85 (t, *J*=7.3 Hz, 3H, C*H*$_3$), 1.28 (m, 2H, C*H*$_2$CH$_3$), 1.52 (m, 2H, C*H*$_2$CH$_2$CH$_3$), 1.75 (m, 4H, ArCCH$_2$C*H*$_2$C*H*$_2$CH$_2$ArC), 2.53 (t, *J*=7.7 Hz, 2H, ArC*H*$_2$), 2.75 (m, 4H, ArCC*H*$_2$CH$_2$CH$_2$C*H*$_2$ArC), 7.08-7.11 (m, 3H, Ar*H*s), 7.45-7.51 (m, 4H, Ar*H*s), 7.64 (s, 1H, N*H*) ppm. ^{13}C NMR ($CDCl_3$), δ : 13.98 (*C*H$_3$), 22.30 (*C*H$_2$CH$_3$), 22.88 (ArCCH$_2$*C*H$_2$CH$_2$CH$_2$ArC), 22.96 (ArCH$_2$CH$_2$*C*H$_2$CH$_2$ArC), 29.37 (ArC*C*H$_2$CH$_2$CH$_2$CH$_2$ArC), 29.44 (ArCCH$_2$CH$_2$CH$_2$*C*H$_2$ArC), 33.69 (*C*H$_2$CH$_2$CH$_3$), 35.09 (Ar*C*H$_2$), 120.19 (Ar*C*), 123.83 (Ar*C*), 127.92 (Ar*C*), 128.89 (Ar*C*), 129.41 (Ar*C*), 132.11 (Ar*C*), 135.70 (Ar*C*), 137.66 (Ar*C*), 139.03 (Ar*C*), 141.43 (Ar*C*), 165.82 (*C*=O) ppm.

4.3.9. Synthesis of *N*-(4-butylphenyl)-1-naphthamide (19)

1-Naphthoic acid (172.2 mg, 1 mmol) was dissolved in anhydrous CH_2Cl_2 (3 mL). PBr_3 (0.14 mL, 1.5 mmol) was added to the solution under nitrogen. The mixture was stirred at room temperature for 3 hours. Et_3N (0.42 mL, 3 mmol) and N-butylaniline (0.16 mL, 1 mmol) were added subsequently, and after stirring for 1 hour at room temperature, the mixture was diluted with CH_2Cl_2, washed with water and dried over anhydrous $MgSO_4$. After evaporation, the crude product was purified by column chromatography on silica gel using CH_2Cl_2-hexane (2:1, v/v) as eluent to give the pure product as a light yellow solid (119.8 mg, 39.5 % yield). ^{1}H NMR ($CDCl_3$), δ : 0.87 (t, *J*=7.3 Hz, 3H, C*H*$_3$), 1.30 (m, 2H, C*H*$_2$CH$_3$), 1.54 (m, 2H, C*H*$_2$CH$_2$CH$_3$), 2.55 (t, *J*=7.6 Hz, 2H, ArC*H*$_2$), 7.13 (d, *J*=8.1 Hz, 2H, Ar*H*s), 7.41-7.53 (m, 5H, Ar*H*s), 7.58 (bs, 1H, Ar*H*), 7.65 (d, *J*=7.0 Hz, 1H, Ar*H*), 7.82 (dd, *J*=6.8, 3.6 Hz, 1H, ArH), 7.88 (d, *J*=8.2 Hz, 1H, Ar*H*), 8.29 (d, *J*=8.7

Hz, 1H, N*H*) ppm. ^{13}C NMR ($CDCl_3$), δ: 13.95 (*C*H_3), 22.27 (*C*H_2CH_3), 33.68 (*C*$H_2CH_2CH_3$), 35.09 (Ar*C*H_2), 119.99 (Ar*C*), 124.76 (Ar*C*), 125.03 (Ar*C*), 125.30 (Ar*C*), 126.57 (Ar*C*), 127.33 (Ar*C*), 128.40 (Ar*C*), 129.04 (Ar*C*), 130.09 (Ar*C*), 130.96 (Ar*C*), 133.76 (Ar*C*), 134.64 (Ar*C*), 135.61 (Ar*C*), 139.49 (Ar*C*), 167.39 (*C*=O) ppm.

4.3.10. Synthesis of *N*-(4-butylphenyl)-6-fluoro-2-naphthamide (20)

6-Fluoro-2-naphthoic acid (190.2 mg, 1 mmol) was dissolved in anhydrous CH_2Cl_2 (3 mL). PBr_3 (0.14 mL, 1.5 mmol) was added to the solution under nitrogen. The mixture was stirred at room temperature for 3 hours. Et_3N (0.42 mL, 3 mmol) and N-butylaniline (0.16 mL, 1 mmol) were added subsequently, and after stirring for 1 hour at room temperature, the mixture was diluted with CH_2Cl_2, washed with water and dried over anhydrous $MgSO_4$. After evaporation, the crude product was purified by two times recrystallization from methanol-water (5:1, v/v) and column chromatography on silica gel using CH_2Cl_2 as eluent to give pure product as a white solid (147.4 mg, 45.9 % yield). ^{1}H NMR ($CDCl_3$), δ: 0.93 (t, *J*=7.3 Hz, 3H, C*H*$_3$), 1.36 (m, 2H, C*H*$_2$CH$_3$), 1.60 (m, 2H, C*H*$_2$CH$_2$CH$_3$), 2.61 (t, *J*=7.6 Hz, 2H, ArC*H*$_2$), 7.19 (d, *J*=8.4 Hz, 2H, Ar*H*s), 7.33 (t of d, *J*=8.7, 2.5, 1H, Ar*H*), 7.49 (dd, *J*=9.6, 2.5, 1H, Ar*H*), 7.58 (d, *J*=8.4 Hz, 2H, Ar*H*s), 7.84-7.96 (m, 4H, Ar*H*s), 8.36 (s, 1H, N*H*) ppm. ^{13}C NMR ($CDCl_3$), δ: 13.94 (*C*H_3), 22.28 (*C*H_2CH_3), 33.65 (*C*$H_2CH_2CH_3$), 35.09 (Ar*C*H_2), 111.18 (Ar*C*), 117.61 (Ar*C*), 120.31 (Ar*C*), 124.58 (Ar*C*), 127.51 (Ar*C*), 128.01 (Ar*C*), 128.06 (Ar*C*), 129.02 (Ar*C*), 129.63 (Ar*C*), 131.45 (Ar*C*), 131.54 (Ar*C*), 135.46 (Ar*C*), 139.48 (Ar*C*), 163.00 (Ar*C*), 165.38 (*C*=O) ppm.

4.3.11. Synthesis of *N*-(4-butylphenyl)-3,5-dimethoxy-2-naphthamide (21)

3,5-Dimethoxy-2-naphthoic acid (232.2 mg, 1 mmol) was dissolved in anhydrous CH_2Cl_2 (3 mL). PBr_3 (0.14 mL, 1.5 mmol) was added to the solution under nitrogen. The mixture was stirred at room temperature for 3 hours. Et_3N (0.42 mL, 3 mmol) and N-butylaniline (0.16 mL, 1 mmol) were added subsequently, and after stirring for 1 hour at room temperature, the mixture was diluted with CH_2Cl_2, washed with water and dried over anhydrous $MgSO_4$. After evaporation, the crude product was purified by column chromatography on silica gel using CH_2Cl_2-hexane (9:1, v/v) as eluent to give the pure

product as a white solid (124.8 mg, 34.4 % yield). ^{1}H NMR ($CDCl_3$), δ : 0.93 (t, *J*=7.3 Hz, 3H, C*H*$_3$), 1.36 (m, 2H, C*H*$_2$CH$_3$), 1.60 (m, 2H, C*H*$_2$CH$_2$CH$_3$), 2.61 (t, *J*=7.6 Hz, 2H, ArC*H*$_2$), 4.03 (s, 3H, OC*H*$_3$), 4.16 (s, 3H, OC*H*$_3$), 6.89 (d, *J*=7.7 Hz, 1H, Ar*H*), 7.19 (d, *J*=8.3 Hz, 2H, Ar*H*s), 7.33 (t, *J*=8.1 Hz, 1H, Ar*H*), 7.52 (d, *J*=8.1 Hz, 1H, Ar*H*), 7.62 (d, *J*=8.3 Hz, 2H, Ar*H*s), 7.68 (s, 1H, Ar*H*), 8.80 (s, 1H, Ar*H*), 9.90 (s, 1H, N*H*) ppm. ^{13}C NMR ($CDCl_3$), δ : 13.99 (*C*H$_3$), 22.32 (*C*H$_2$CH$_3$), 33.73 (*C*H$_2$CH$_2$CH$_3$), 35.12 (Ar*C*H$_2$), 55.56 (O*C*H$_3$), 56.28 (O*C*H$_3$), 101.60 (Ar*C*), 105.94 (Ar*C*), 120.53 (Ar*C*), 121.36 (Ar*C*), 122.82 (Ar*C*), 124.62 (Ar*C*), 127.76 (Ar*C*), 128.90 (Ar*C*), 129.34 (Ar*C*), 133.78 (Ar*C*), 135.97 (Ar*C*), 138.97 (Ar*C*), 154.07 (Ar*C*), 154.15 (Ar*C*), 163.00 (*C*=O) ppm.

4.3.12. Synthesis of *N*-(4-butylphenyl)-3-methoxy-2-naphthamide (22)

3-Methoxy-2-naphthoic acid (202.2 mg, 1 mmol) was dissolved in anhydrous CH_2Cl_2 (3 mL). PBr_3 (0.14 mL, 1.5 mmol) was added to the solution under nitrogen. The mixture was stirred at room temperature for 3 hours. Et_3N (0.42 mL, 3 mmol) and N-butylaniline (0.16 mL, 1 mmol) were added subsequently, and after stirring for 1 hour at room temperature, the mixture was diluted with CH_2Cl_2, washed with water and dried over anhydrous $MgSO_4$. After evaporation, the crude product was purified by recrystallization from methanol-water (5:1, v/v) and column chromatography on silica gel using hexane-CH_2Cl_2 (9:1, v/v) as eluent to give pure product as a white solid (124.5 mg, 37.4 % yield). ^{1}H NMR ($CDCl_3$), δ : 0.93 (t, *J*=7.3 Hz, 3H, C*H*$_3$), 1.36 (m, 2H, C*H*$_2$CH$_3$), 1.59 (m, 2H, C*H*$_2$CH$_2$CH$_3$), 2.58 (t, *J*=7.7 Hz, 2H, ArC*H*$_2$), 4.17 (s, 3H, OC*H*$_3$), 7.18 (dd, *J*=8.4, 1.9 Hz, 1H, Ar*H*), 7.27 (s, 1H, Ar*H*), 7.41 (m, 2H, Ar*H*s), 7.53 (m, 1H, Ar*H*s), 7.76 (d, *J*=8.2 Hz, 1H, Ar*H*), 7.92 (d, *J*=8.2 Hz, 1H, Ar*H*), 8.58 (d, *J*=8.4 Hz, 1H, Ar*H*), 8.86 (s, 1H, Ar*H*), 10.57 (s, 1H, N*H*) ppm. ^{13}C NMR ($CDCl_3$), δ : 13.92 (*C*H$_3$), 22.24 (*C*H$_2$CH$_3$), 33.44 (*C*H$_2$CH$_2$CH$_3$), 34.74 (Ar*C*H$_2$), 56.24 (O*C*H$_3$), 106.66 (Ar*C*), 113.34 (Ar*C*), 122.34 (Ar*C*), 124.72 (Ar*C*), 126.25 (Ar*C*), 128.35 (Ar*C*), 128.58 (Ar*C*), 129.30 (Ar*C*), 132.02 (Ar*C*), 134.52 (Ar*C*), 134.63 (Ar*C*), 135.95 (Ar*C*), 140.04 (Ar*C*), 154.42 (Ar*C*), 163.04 (*C*=O) ppm.

4.3.13. Synthesis of *N*-(4-hydroxy-2-nitrophenyl)acetamide (24)

4-Amino-3-nitrophenol (2.0 g, 13.0 mmol) was added to 3 mL of water with vigorous stirring. Then to it was added acetic anhydride (1.99 g, 19.5 mmol, 1.5 equiv). The reaction mixture was stirred at room temperature during two days. After this time, a solid precipitated out of solution and this was filtered by vacuum filtration and washed with several portions of ice cold methanol:water (1:1) mixture to give pure product as an orange-brown solid (1.35 g, 53.1 % yield). ^{1}H NMR (DMSO-d_6), δ : 1.98 (s, 3H, CH_3), 7.07 (dd, *J*=8.8, 2.8 Hz, 1H, Ar*H*), 7.23 (d, *J*=2.8 Hz, 1H, Ar*H*), 7.32 (d, *J*=8.8 Hz, 1H, Ar*H*), 9.90 (s, 1H, N*H*), 10.20 (br s, 1H, ArO*H*) ppm. ^{13}C NMR (DMSO-d_6), δ : 23.72 (CH_3), 111.10 (Ar*C*), 121.59 (Ar*C*), 123.26 (Ar*C*), 128.37 (Ar*C*), 144.47 (Ar*C*), 155.33 (Ar*C*), 169.03 (*C*=O) ppm.

4.3.14. Synthesis of *N*-(4-butoxy-2-nitrophenyl)acetamide (25)

A mixture of *N*-(4-Hydroxy-2-nitrophenyl)acetamide (1.10 g, 5.61 mmol), n-butyl bromide (1.15 g, 8.39 mmol, 1.5 equiv), Na_2CO_3 (1.19 g, 11.2 mmol, 2 equiv) and a catalytic amount of KI (0.19 g, 1.12 mmol) was dissolved in 10 mL DMF in a 25 mL round-bottom flask. The solution was stirred at 80 ^{o}C for 2 days. The solvent was then evaporated under reduced pressure, the residue was dissolved in water, and the product was extracted with dichloromethane. The organic layer was dried over Na_2SO_4. Evaporation of the solvent under reduced pressure gave the pure product as a yellow solid (1.06 g, 75.0 % yield). ^{1}H NMR (DMSO-d_6), δ : 0.91 (t, *J*= 7.4 Hz, 3H, CH_2CH_3), 1.42 (m, 2H, CH_2), 1.68 (m, 2H, CH_2), 1.99 (s, 1H, COCH_3), 4.02 (t, *J*= 6.5 Hz, 2H, OCH_2), 7.25 (dd, *J*=8.9, 3.0 Hz, 1H, Ar*H*), 7.41 (d, *J*=2.8 Hz, 1H, Ar*H*), 7.42 (d, *J*=8.9 Hz, 1H, Ar*H*), 10.01 (s, 1H, N*H*) ppm. ^{13}C NMR (DMSO-d_6), δ : 14.32 (CH_2CH_3), 19.31 (CH_2CH_3), 23.76 (CH_3CO), 31.17 ($CH_2CH_2CH_3$), 68.80 (OCH_2), 110.17 (Ar*C*), 121.15 (Ar*C*), 124.55 (Ar*C*), 128.06 (Ar*C*), 144.42 (Ar*C*), 156.22 (Ar*C*), 169.07 (*C*=O) ppm.

4.3.15. Synthesis of 4-butoxy-2-nitroaniline (26)

N-(4-Butoxy-2-nitropheny)acetamide (1.0 g, 3.97 mmol) was refluxed in methanol (20 mL) and 20 % H_2SO_4 (20 mL) at 80 ^{o}C for 2 hours. Then, the reaction mixture was

cooled to room temperature and made weakly alkaline by slowly adding a 5 % aquous solution of $NaHCO_3$. The resultant solution was then extracted with diethyl ether (two times). The ether layers were combined, washed with water, dried with Na_2SO_4 and filtered. Evaporation of ether gave the pure product as a red solid (0.81 g, 97.2 % yield). ^{1}H NMR (DMSO-d_6), δ : 0.90 (t, *J*=7.4 Hz, 3H, C*H*$_3$), 1.40 (m, 2H, C*H*$_2$), 1.64 (m, 2H, C*H*$_2$), 3.88 (t, *J*=6.5 Hz, 2H, OC*H*$_2$), 6.96 (d, *J*=9.2 Hz, 1H, Ar*H*), 7.13 (dd, *J*=9.2, 2,8 Hz, 1H, Ar*H*), 7.21 (br s, 2H, N*H*$_2$), 7.33 (d, *J*=2.9 Hz, 1H, Ar*H*) ppm. ^{13}C NMR (DMSO-d_6), δ : 14.37 (*C*H$_3$), 19.38 (*C*H$_2$CH$_3$), 31.33 (*C*H$_2$CH$_2$CH$_3$), 68.42 (O*C*H$_2$), 106.42 (Ar*C*), 121.39 (Ar*C*), 128.17 (Ar*C*), 129.78 (Ar*C*), 142.54 (Ar*C*), 149.22 (Ar*C*) ppm.

4.3.16. Synthesis of 4-butoxybenzene-1,2-diamine (27)

A suspension of 4-butoxy-2-nitroaniline (0.63 g, 3.0 mmol) in unstabilized 57 % HI (9 mL) was heated at 90 ^{o}C for 2-4 hours. The reaction mixture became homogeneous as the reaction progressed. After cooling to room temperature, the mixture was diluted with EtOAc (150 mL) and washed successively with saturated aqueous $Na_2S_2O_3$ (for the destruction of iodine formed), saturated aqueous $NaHCO_3$ and brine. The organic layer was dried over anhydrous $MgSO_4$, filtered and concentrated to give crude product. Column chromatography on silica with CH_2Cl_2:methanol (99:1) as eluent gave the pure product as a yellow solid (0.33 g, 61.0 % yield). ^{1}H NMR (DMSO-d_6), δ : 0.89 (t, *J*=7.4 Hz, 3H, C*H*$_3$), 1.37 (m, 2H, C*H*$_2$), 1.59 (m, 2H, C*H*$_2$), 3.73 (t, *J*=6.5 Hz, 2H, OC*H*$_2$), 3.95 (br s, 2H, N*H*$_2$), 4.43 (br s, 2H, N*H*$_2$), 5.94 (dd, *J*=8.3, 2.8 Hz, 1H, Ar*H*), 6.13 (d, *J*=2.7 Hz, 1H, Ar*H*), 6.37 (d, *J*=8.3 Hz, 1H, Ar*H*) ppm. ^{13}C NMR (DMSO-d_6), δ : 14.43 (*C*H$_3$), 19.50 (*C*H$_2$CH$_3$), 31.74 (*C*H$_2$CH$_2$CH$_3$), 67.84 (O*C*H$_2$), 102.65 (Ar*C*), 103.17 (Ar*C*), 115.00 (Ar*C*), 129.03 (Ar*C*), 137.24 (Ar*C*), 152.25 (Ar*C*) ppm.

4.3.17. Synthesis of *N*-(2-amino-4-butoxyphenyl)-2-naphthamide (28a)

1,2-Diamino-4-butoxybenzene (0.18 g, 1.0 mmol) and triethylamine (0.15 g, 1.5 mmol, 1.5 equiv) was dissolved in anhydrous dichloromethane (2 mL) in a 25 mL round-bottom flask. The reaction flask was waited under nitrogen gas for 10 minutes. 2-Naphthoyl chloride (0.19 g, 1.0 mmol, 1 equiv) was dissolved in anhydrous dichloromethane (3 mL) in a vial. This solution was added to the reaction flask drop by

drop under nitrogen. The reaction mixture was stirred under nitrogen gas overnight. The reaction mixture was diluted with dichloromethane and washed with water. The organic layer was dried over anhydrous $MgSO_4$, filtered and concentrated to give crude product. Column chromatography on neutral aluminium oxide with CH_2Cl_2:methanol (1:1) as eluent gave the pure product as a brown solid (0.15 g, 44.9 % yield). ^{1}H NMR (DMSO-d_6), δ: 0.92 (t, *J*=7.4 Hz, 3H, C*H*$_3$), 1.41 (m, 2H, C*H*$_2$), 1.66 (m, 2H, C*H*$_2$), 3.88 (t, *J*=6.5 Hz, 2H, OC*H*$_2$), 4.93 (bs, 2H, N*H*$_2$), 6.17 (dd, *J*=8.6, 2.7, 1H, Ar*H*), 6.35 (d, *J*=2.7 Hz, 1H, Ar*H*), 7.02 (d, *J*=8.6 Hz, 1H, Ar*H*), 7.56-7.63 (m, 2H, Ar*H*s), 7.97-8.05 (m, 4H, Ar*H*s), 8.58 (s, 1H, Ar*H*), 9.67 (s, 1H, N*H*) ppm. ^{13}C NMR (DMSO-d_6), δ: 14.17 (*C*H$_3$), 19.23 (*C*H$_2$CH$_3$), 31.29 (*C*H$_2$CH$_2$CH$_3$), 67.34 (O*C*H$_2$), 101.86 (Ar*C*), 103.03 (Ar*C*), 116.96 (Ar*C*), 125.06 (Ar*C*), 127.16 (Ar*C*), 128.07 (Ar*C*), 128.22 (Ar*C*), 128.32 (Ar*C*), 128.45 (Ar*C*), 129.33 (Ar*C*), 132.49 (Ar*C*), 132.57 (Ar*C*), 134.60 (Ar*C*), 145.02 (Ar*C*), 158.09 (Ar*C*), 165.97 (*C*=O) ppm.

4.3.18. Synthesis of *N*-(4-butoxy-2-nitrophenyl)-2-naphthamide (30)

2-Naphthoic acid (172.2 mg, 1 mmol) was dissolved in anhydrous CH_2Cl_2 (3 mL). PBr_3 (0.14 mL, 1.5 mmol) was added to the solution under nitrogen. The mixture was stirred at room temperature for 3 hours. Et_3N (0.42 mL,3 mmol) and 4-butoxy-2-nitroaniline (210.1 mg, 1 mmol) were added subsequently, and after stirring for 1 hour at room temperature, the mixture was diluted with CH_2Cl_2, washed with water and dried over anhydrous MgSO4. After evaporation, the crude product was purified by column chromatography on silica gel using hexane-CH_2Cl_2 (2:1, v/v) as eluent to give the pure product as a yellow solid (200.6 mg, 55.1 % yield). ^{1}H NMR ($CDCl_3$), δ : 1.00 (t, *J*=7.4 Hz, 3H, C*H*$_3$), 1.52 (m, 2H, *C*H$_2$CH$_3$), 1.81 (m, 2H, *C*H$_2$CH$_2$CH$_3$), 4.04 (t, *J*=6.4 Hz, 2H, O*C*H$_2$), 7.32 (dd, *J*=9.3, 3.0 Hz, 1H, Ar*H*), 7.61 (m, 2H, Ar*H*s), 7.75 (d, *J*=3.0 Hz, 1H, Ar*H*), 7.92 (d, *J*=7.8 Hz, 1H, Ar*H*), 7.97-8.04 (m, 3H, Ar*H*s), 8.51 (s, 1H, Ar*H*), 8.93 (d, *J*=9.3 Hz, 1H, Ar*H*), 11.28 (s, 1H, N*H*) ppm. ^{13}C NMR ($CDCl_3$), δ : 14.12 (*C*H$_3$), 19.48 (*C*H$_2$CH$_3$), 31.37 (*C*H$_2$CH$_2$CH$_3$), 68.89 (O*C*H$_2$), 109.99 (Ar*C*), 123.69 (Ar*C*), 123.99 (Ar*C*), 124.46 (Ar*C*), 127.37 (Ar*C*), 128.12 (Ar*C*), 128.58 (Ar*C*), 128.60 (Ar*C*), 129.23 (Ar*C*), 129.30 (Ar*C*), 129.62 (Ar*C*), 131.71 (Ar*C*), 132.99 (Ar*C*), 135.48 (Ar*C*), 137.40 (Ar*C*), 154.97 (Ar*C*), 165.97 (*C*=O) ppm.

4.3.19. Synthesis of *N*-(2-amino-4-butoxyphenyl)-2-naphthamide (28a) and *N*-(2-amino-5-butoxyphenyl)-2-naphthamide (28b)

Into the solution of *N*-(4-butoxy-2-nitrophenyl)-2-naphthamide (145.6 mg, 0.4 mmol) in absolute ethanol (4 mL) was added stannous chloride dihydrate (451.2 mg, 2 mmol) under nitrogen. The mixture was refluxed at 60 ^{o}C for 1 h. $NaBH_4$ (7.6 mg, 0.2 mmol) was added to it and refluxed for another 30 min. The reaction mixture was cooled, ethanol was evaporated, and the concentrate was dissolved in water. The reaction mixture was made alkaline with 40 % aqueous NaOH and extracted with ethyl acetate (3 times). The organic layer was dried with $MgSO_4$ and evaporated under reduced pressure to get crude product. Column chromatography on neutral aluminium oxide with CH_2Cl_2:methanol (1:1) as eluent gave the pure products as a brown solid (106.5 mg, 28a:28b=42:31, 79.8 % yield). ^{1}H NMR ($CDCl_3$), δ: 0.90 (m, 6H, C*H*$_3$), 1.42 (m, 4H, C*H*$_2$), 1.70 (m, 4H, C*H*$_2$), 3.85 (t, *J*=6.5 Hz, 2H, ArOC*H*$_2$), 3.92 (t, *J*=6.5 Hz, 2H, ArOC*H*$_2$), 3.90 (bs, 4H, N*H*$_2$), 6.30-8.08 (20H, Ar*H*s), 8.35 (s, 1H, N*H*), 8.40 (s, 1H, N*H*) ppm.

4.3.20. Synthesis of 4-(bromomethyl)-1,2-dimethoxybenzene (32)

3,4-(Dimethoxyphenyl)methanol (2.02 g, 12.0 mmol) was dissolved in anhydrous dichloromethane (40 mL) in a 100 mL round-bottom flask. This solution was cooled to 0 ^{o}C and PBr_3 (1.30 g, 4.80 mmol, 0.4 equiv) was added to the solution under nitrogen atmosphere. The reaction mixture was stirred at room temperature for 1 hour. Organic phase was extracted with water three times (3x10 mL). Then, organic phase was washed successively with saturated aq. $NaHCO_3$ (10 mL) and brine (10 mL). The organic layer was dried over anhydrous $MgSO_4$, filtered and concentrated to give pure product as a white solid (2.37 g, 85.7 % yield). ^{1}H NMR ($CDCl_3$), δ: 3.87 (s, 3H, OC*H*$_3$), 3.89 (s, 3H, OC*H*$_3$), 4.49 (s, 2H, C*H*$_2$), 6.80 (d, *J*=8.2 Hz, 1H, Ar*H*), 6.90 (d, *J*=2.1 Hz, 1H, Ar*H*), 6.94 (dd, *J*=8.2, 2.1 Hz, 1H, Ar*H*) ppm. ^{13}C NMR ($CDCl_3$), δ: 34.64 (*C*H$_2$Br), 56.14 (O*C*H$_3$), 56.16 (O*C*H$_3$), 111.27 (Ar*C*), 112.34(Ar*C*), 121.80 (Ar*C*), 130.48 (Ar*C*), 149.32 (Ar*C*), 149.49 (Ar*C*) ppm.

4.3.21. Synthesis of 1,2-dimethoxy-4-pentylbenzene (33)

3,4-Dimethoxybenzyl bromide (1.16 g, 5.0 mmol) was dissolved in dry THF (30 mL) in 100 mL three necked round-bottom flask. CuBr (71.7 mg, 0.50 mmol, 0.1 equiv) and KI (166 mg, 1 mmol, 0.2 equiv) were added to the reaction flask. The reaction mixture was cooled to -78 ^{o}C and 10 mL (16 mmol) of 1.6 M *n*-BuMgBr in THF was added under nitrogen atmosphere. The reaction mixture was stirred at -78 ^{o}C for 2 hours, allowed to warm to ambient temperature, and stirred for 20 hours. After cooling to 0 ^{o}C, the reaction mixture was quenched by the cautious addition of 10 mL of 1 M aqueous HCl. The resulting black slurry was filtered. Solution was extracted with three portions of ether. The combined ether layers were washed with successive portions of water and brine. Organic layer was dried over anhydrous $MgSO_4$, filtered and concentrated to give crude product. Purification by column chromatography on silica gel using hexane:CH_2Cl_2 (1:1) as eluent gave the pure product as a white solid (0.87 g, 84.0 % yield). ^{1}H NMR ($CDCl_3$), δ : 0.89 (t, *J*=6.9 Hz, 3H, C*H*$_3$), 1.33 (m, 4H, C*H*$_2$C*H*$_2$CH$_3$), 1.60 (m, 2H, C*H*$_2$CH$_2$CH$_2$CH$_3$), 2.55 (t, *J*=7.6 Hz, 2H, Ar-C*H*$_2$), 3.85 (s, 3H, OC*H*$_3$), 3.87 (s, 3H, OC*H*$_3$), 6.70-6.80 (3H, Ar*H*s) ppm. ^{13}C NMR ($CDCl_3$), δ : 14.32 (*C*H$_3$), 22.81 (*C*H$_2$CH$_3$), 31.67 (*C*H$_2$CH$_2$CH$_2$CH$_3$), 31.77 (*C*H$_2$CH$_2$CH$_3$), 35.79 (Ar-*C*H$_2$), 56.00 (O*C*H$_3$), 56.13 (O*C*H$_3$), 111.28 (Ar*C*), 11.90 (Ar*C*), 120.31 (Ar*C*), 135.86 (Ar*C*), 147.16 (Ar*C*), 148.90 (Ar*C*) ppm.

4.3.22. Synthesis of 1,2-dihydroxy-4-pentylbenzene (34)

To a solution of 1,2-Dimethoxy-4-pentylbenzene (0.39 g, 1.87 mmol) in dry CH_2Cl_2 (18 mL) at -78 ^{o}C under nitrogen atmosphere was added BBr_3 (5 mL, 1.0 M solution in CH_2Cl_2) over a period of 15 minutes. Then, the reaction temperature was gradually raised to room temperature and stirring was continued for 20 hours. The reaction mixture was cooled to 0 ^{o}C and quenched by the addition of methanol, the resulting mixture was warmed to room temperature, stirred for 40 minutes and volatiles removed under reduced pressure. The residual oil was diluted with EtOAc and solution was washed with saturated $NaHCO_3$, water and brine. Organic layer was dried over anhydrous $MgSO_4$, filtered and concentrated to give crude product. Purification by column chromatography on silica gel using EtOAc:CH_2Cl_2 (99:1) as eluent gave the pure product (0.21 g, 62.6 % yield). ^{1}H NMR ($CDCl_3$), δ : 0.89 (t, *J*=6.9 Hz, 3H, C*H*$_3$), 1.31 (m, 4H, C*H*$_2$C*H*$_2$CH$_3$),

1.55 (m, 2H, C*H*$_2$CH$_2$CH$_2$CH$_3$), 2.45 (t, *J*=7.6 Hz, 2H, Ar-C*H*$_2$), 6.61 (dd, *J*=8.0, 2.0, 1H, Ar*H*), 6.70 (d, *J*=2.0, 1H, Ar*H*), 6.77 (d, *J*=8.0, 1H, Ar*H*) ppm. ^{13}C NMR ($CDCl_3$), δ : 14.03 (*C*H$_3$), 22.5 (*C*H$_2$CH$_3$), 31.26 (*C*H$_2$CH$_2$CH$_2$CH$_3$), 31.42 (*C*H$_2$CH$_2$CH$_3$), 35.19 (Ar-*C*H$_2$), 115.29 (Ar*C*), 115.56 (Ar*C*), 120.84 (Ar*C*), 136.36 (Ar*C*), 141.12 (Ar*C*), 143.25 (Ar*C*) ppm.

4.3.23. Synthesis of 2-hydroxy-4-pentylphenyl 2-naphthoate (35a) and 2-hydroxy-5-pentylphenyl 2-naphthoate (35b)

1,2-Dihydroxy-4-pentylbenzene (0.17 g, 0.96 mmol) and DMAP (70.7 mg, 0.57 mmol, 0.6 equiv) were dissolved in anhydrous CH_2Cl_2 (8 mL). To this solution at room temperature under nitrogen atmosphere was added 2-naphthoic acid (0.16 g, 0.96 mmol, 1 equiv) and DCC (0.24 g, 1.15 mmol, 1.2 equiv) in CH_2Cl_2 (6 mL) over a period of 2 hours. The reaction mixture was stirred at room temperature for 24 hours. Resulting precipitate was filtered. Solution was concentrated to give the crude product. Purification by column chromatography on silica gel using hexane:CH_2Cl_2 (2:1) as eluent gave the products as a white solid mixture (0.15 g, 35a:35b=3:2, 47.9 % yield). ^{1}H NMR ($CDCl_3$), δ : 0.90 (m, 6H, C*H*$_3$), 1.34 (m, 8H, C*H*$_2$C*H*$_2$CH$_3$), 1.62 (m, 4H, ArC*H*$_2$), 2.58 (m, 4H, Ar-C*H*$_2$), 5.43 (s, 1H, O*H*), 5.52 (s, 1H, O*H*), 6.79-8.81 (20H, Ar*H*s) ppm. ^{13}C NMR ($CDCl_3$), δ : 14.03 (*C*H$_3$), 22.53 (*C*H$_2$), 30.94 (*C*H$_2$), 31.15 (*C*H$_2$), 31.41 (*C*H$_2$), 31.43 (*C*H$_2$), 35.00 (*C*H$_2$), 35.41 (*C*H$_2$), 122.03 (Ar*C*), 122.11 (Ar*C*), 125.42 (Ar*C*), 125.99 (Ar*C*), 126.01 (Ar*C*), 126.99 (Ar*C*), 127.07 (Ar*C*), 132.31 (Ar*C*), 132.35 (Ar*C*), 132.46 (Ar*C*), 165.30 (Ar*C*), 165.36 (Ar*C*) ppm.

Compound 36: ^{1}H NMR ($CDCl_3$), δ : 0.93 (t, *J*=7.1 Hz, 3H, C*H*$_3$), 1.38 (m, 4H, C*H*$_2$C*H*$_2$CH$_3$), 1.71 (m, 4H, ArC*H*$_2$), 2.70 (t, *J*=7.7 Hz, 2H, Ar-C*H*$_2$), 7.20 (dd, *J*=8.3, 2.1 Hz, 1H, Ar*H*), 7.30 (d, *J*=2.1 Hz, 1H, Ar*H*), 7.38 (d, *J*=8.3 Hz, 1H, Ar*H*), 7.40-8.64 (14H, Ar*H*s) ppm.

4.3.24. Synthesis of 1,3-dimethoxy-5-pentylbenzene (38)

3,5-Dimethoxybenzyl bromide (1.16 g, 5.0 mmol) was dissolved in dry THF (30 mL) in 100 mL three necked round-bottom flask. CuBr (71.7 mg, 0.5 mmol, 0.1 equiv) and

KI (166 mg, 1 mmol, 0.2 equiv) were added to the reaction flask. The reaction mixture was cooled to -78 ^{o}C and 10 mL (16 mmol) of 1.6 M *n*-BuMgBr in THF was added under nitrogen atmosphere. The reaction mixture was stirred at -78 ^{o}C for 2 hours, allowed to warm to ambient temperature, and stirred for 20 hours. After cooling to 0 ^{o}C, the reaction mixture was quenched by the cautious addition of 10 mL of 1 M aqueous HCl. The resulting black slurry was filtered. Solution was extracted with three portions of ether. The combined ether layers were washed with successive portions of water and brine. Organic layer was dried over anhydrous $MgSO_4$, filtered and concentrated to give crude product. Purification by column chromatography on silica gel using hexane:CH_2Cl_2 (2:1) as eluent gave the pure product (0.71 g, 68.3 % yield). ^{1}H NMR ($CDCl_3$), δ : 0.90 (t, *J*=6.9 Hz, 3H, C*H*$_3$), 1.33 (m, 4H, C*H*$_2$C*H*$_2$), 1.61 (m, 2H, C*H*$_2$), 2.55 (t, *J*=7.6 Hz, 2H, Ar-C*H*$_2$), 3.78 (s, 6H, OC*H*$_3$), 6.30 (1H, Ar*H*), 6.35 (2H, Ar*H*s) ppm. ^{13}C NMR ($CDCl_3$), δ : 14.02 (*C*H$_3$), 22.55 (*C*H$_2$CH$_3$), 30.96 (*C*H$_2$CH$_2$CH$_2$CH$_3$), 31.53 (*C*H$_2$CH$_2$CH$_3$), 36.28 (Ar-*C*H$_2$), 55.20 (O*C*H$_3$), 97.53 (Ar*C*), 106.47 (Ar*C*), 145.40 (Ar*C*), 160.68 (Ar*C*) ppm.

4.3.25. Synthesis of 5-pentylbenzene-1,3-diol (39)

To a solution of 1,2-dimethoxy-4-pentylbenzene (0.38 g, 1.83 mmol) in dry CH_2Cl_2 (18 mL) at -78 ^{o}C under nitrogen atmosphere was added BBr_3 (5 mL, 1.0 M solution in CH_2Cl_2) over a period of 15 minutes. Then, the reaction temperature was gradually raised to room temperature and stirring was continued for 20 hours. The reaction mixture was cooled to 0 ^{o}C and quenched by the addition of methanol, the resulting mixture was warmed to room temperature, stirred for 40 minutes and volatiles removed under reduced pressure. The residual oil was diluted with EtOAc and solution was washed with saturated $NaHCO_3$, water and brine. Organic layer was dried over anhydrous $MgSO_4$, filtered and concentrated to give crude product. Purification by column chromatography on silica gel using EtOAc:CH_2Cl_2 (99:1) as eluent gave the pure product as a yellow color oil (0.19 g, 57.7 % yield). ^{1}H NMR ($CDCl_3$), δ : 0.88 (t, *J*=6.2 Hz, 3H, C*H*$_3$), 1.31 (m, 4H, C*H*$_2$C*H*$_2$), 1.56 (m, 2H, C*H*$_2$), 2.47 (t, *J*=7.5 Hz, 2H, Ar-C*H*$_2$), 6.17 (s, 1H, Ar*H*), 6.24 (s, 2H, Ar*H*) ppm. ^{13}C NMR ($CDCl_3$), δ : 14.00 (*C*H$_3$), 22.51 (*C*H$_2$CH$_3$), 30.71 (*C*H$_2$CH$_2$CH$_2$CH$_3$), 31.44 (*C*H$_2$CH$_2$CH$_3$), 35.77 (Ar-*C*H$_2$), 100.16 (Ar*C*), 108.06 (Ar*C*), 146. 19 (Ar*C*), 156.51 (Ar*C*) ppm.

4.3.26. Synthesis of 3-hydroxy-5-pentylphenyl 2-naphthoate (40)

1,2-Dihydroxy-4-pentylbenzene (0.17 g, 0.93 mmol) and DMAP (68.8 mg, 0.56 mmol, 0.6 equiv) were dissolved in anhydrous CH_2Cl_2 (8 mL). To this solution at room temperature under nitrogen atmosphere was added 2-naphthoic acid (0.16 g, 0.93 mmol, 1 equiv) and DCC (0.23 g, 1.12 mmol, 1.2 equiv) in CH_2Cl_2 (6 mL) over a period of 2 hours. The reaction mixture was stirred at room temperature for 24 hours. Resulting precipitate was filtered. Solution was concentrated to give crude product. Purification by column chromatography on silica gel using hexane:CH_2Cl_2 (2:1) as eluent gave the pure product (0.15 g, 48.3 % yield). ^{1}H NMR ($CDCl_3$), δ : 0.89 (t, *J*=6.9 Hz, 3H, C*H*$_3$), 1.32 (m, 4H, C*H*$_2$C*H*$_2$CH$_3$), 1.62 (m, 2H, C*H*$_2$CH$_2$CH$_2$CH$_3$), 2.57 (t, *J*=7.6 Hz, 2H, Ar-C*H*$_2$), 5.45 (s, 1H, O*H*), 6.59 (s, 2H, Ar*H*s), 6.66 (t, *J*=1.6 Hz, 1H, Ar*H*), 7.55-7.65 (m, 2H, Ar*H*s), 7.92 (t, *J*=8.7 Hz, 2H, Ar*H*s), 7.99 (d, *J*=8.1 Hz, 1H, Ar*H*), 8.17 (dd, *J*=8.6, 1.7 Hz, 1H, Ar*H*), 8.77 (s, 1H, Ar*H*) ppm. ^{13}C NMR ($CDCl_3$), δ :14.12 (*C*H$_3$), 22.51 (*C*H$_2$CH$_3$), 30.69 (*C*H$_2$CH$_2$CH$_2$CH$_3$), 31.44 (*C*H$_2$CH$_2$CH$_3$), 35.78 (Ar-*C*H$_2$), 106.62 (Ar*C*), 113.29 (Ar*C*), 113.91 (Ar*C*), 125.44 (Ar*C*), 126.70 (Ar*C*), 126.84 (Ar*C*), 127.82 (Ar*C*), 128.39 (Ar*C*), 128.64 (Ar*C*), 129.49 (Ar*C*), 131.96 (Ar*C*), 132.47 (Ar*C*), 135.82 (Ar*C*), 145.92 (Ar*C*), 151.66 (Ar*C*), 156.37 (Ar*C*), 165.52 (Ar*C*) ppm.

Compound 41: ^{1}H NMR ($CDCl_3$), δ : 0.84 (t, *J*=7.0 Hz, 3H, C*H*$_3$), 1.30 (m, 4H, C*H*$_2$C*H*$_2$CH$_3$), 1.63 (m, 2H, C*H*$_2$CH$_2$CH$_2$CH$_3$), 2.63 (t, *J*=7.7 Hz, 2H, Ar-C*H*$_2$), 7.0 (d, *J*=1.7, 2H, Ar*H*s), 7.05 (s, 1H, Ar*H*s), 7.49-7.58 (m, 4H, Ar*H*s), 7.84-7.89 (m, 4H, Ar*H*s), 7.93 (d, J=8.0 Hz, 2H, Ar*H*s), 8.12 (d, J=8.6 Hz, 2H, Ar*H*s), 8.72 (s, 2H, Ar*H*s) ppm.

4.3.27. Synthesis of *N*-(4-butylphenyl)acetamide (43)

4-Butylaniline (2.98 g, 20 mmol) was added to 6 mL of water with vigorous stirring. Then acetic anhydride (3.06 g, 30 mmol, 1.5 equiv) was added to this heterogeneous solution. The reaction mixture was stirred at room temperature during 2 hours. During this time, a precipitate occured. The precipitate was filtered and washed with several portions of water and dried under vacuum to give desired product as a khaki solid (3.74 g, 97.9 % yield). ^{1}H NMR ($CDCl_3$), δ : 0.91 (t, *J*=7.3 Hz, 3H, CH$_2$C*H*$_3$), 1.33 (m, 2H, CH$_2$C*H*$_2$CH$_3$), 1.56 (m, 2H, CH$_2$C*H*$_2$CH$_2$), 2.16 (s, 3H, C*H*$_3$CO), 2.56 (t, *J*=7.6 Hz,

2H, ArC*H*$_2$), 7.12 (d, *J*=8.4 Hz, 2H, Ar*H*s), 7.19 (bs, 1H, N*H*), 7.37 (d, *J*=8.4 Hz, 2H, Ar*H*s) ppm. ^{13}C NMR ($CDCl_3$), δ: 13.92 (CH_2CH_3) , 22.26 ($CH_2CH_2CH_3$), 24.50 (CH_3CO), 33.62 ($CH_2CH_2CH_2$), 35.03 (ArCH_2), 120.01 (Ar*C*), 128.84 (Ar*C*), 135.44 (Ar*C*), 139.05 (Ar*C*), 168.25 (*C*O) ppm.

4.3.28. Synthesis of *N*-(4-butyl-2-nitrophenyl)acetamide (44)

N-(4-butylphenyl)acetamide (1.72 g, 9.0 mmol) was dissolved in 2 mL glacial acetic acid. The solution was warmed gently in order to dissolve all the solid material. Then the solution was cooled in an ice-bath. During this time some cristals can be seen again. 2.5 mL H_2SO_4 (96 %) at 5 ^{o}C was slowly added to the solution. Then the mixture of 1 mL HNO_3 (65 %) and 1 mL H_2SO_4 (96 %) at 5 ^{o}C was added with small portions. After the addition was completed, the reaction mixture was stirred at room temperature for 50 minutes. Then, viscous reaction mixture was added to the mixture of 50 mL water and 10 mL ice. Resulting precipitate was filtered and washed with ice cold water and dried under vacuum to give crude product. Purification by column chromatography on silica gel using CH_2Cl_2 as eluent gave the pure product as a yellow solid (1.84 g, 86.7 % yield). ^{1}H NMR ($CDCl_3$), δ: 0.93 (t, *J*=7.3 Hz, 3H, CH_2CH_3), 1.35 (m, 2H, $CH_2CH_2CH_3$), 1.60 (m, 2H, $CH_2CH_2CH_2$), 2.27 (s, 3H, CH_3CO), 2.63 (t, *J*=7.6 Hz, 2H, ArCH_2), 7.46 (dd, *J*=8.6, 1.8 Hz, 1H, Ar*H*), 7.99 (d, *J*=1.8 Hz, 1H, Ar*H*), 8.62 (d, *J*=8.6 Hz, 1H, Ar*H*), 10.21 (bs, 1H, N*H*) ppm. ^{13}C NMR ($CDCl_3$), δ: 13.85 (CH_2CH_3), 22.14 ($CH_2CH_2CH_3$), 25.57 (CH_3CO), 33.10 ($CH_2CH_2CH_2$), 34.55 (ArCH_2), 122.19 (Ar*C*), 124.87 (Ar*C*), 132.53 (Ar*C*), 136.24 (Ar*C*), 138.55 (Ar*C*), 168.96 (*C*O) ppm.

4.3.29. Synthesis of 4-butyl-2-nitroaniline (45)

N-(4-butyl-2-nitrophenyl)acetamide (1.84 g, 7.8 mmol) was refluxed in 40 mL methanol and 40 mL 20 % H_2SO_4 at 80 ^{o}C for 2 hours. Then, the reaction mixture was cooled to room temperature and made weakly alkaline by slowly adding a 5 % aquous solution of $NaHCO_3$. The resultant solution was then extracted with diethyl ether (two times). The ether layers were combined, washed with water, dried with Na_2SO_4 and filtered. Evaporation of ether gave the pure product as an orange-red oil (1.45 g, 95.8 % yield). ^{1}H NMR ($CDCl_3$), δ: 0.92 (t, *J*=7.3 Hz, 3H, CH_2CH_3), 1.33 (m, 2H, $CH_2CH_2CH_3$),

1.55 (m, 2H, $CH_2CH_2CH_2$), 2.52 (t, *J*=7.6 Hz, 2H, $ArCH_2$), 5.94 (bs, 2H, NH_2), 6.73 (d, *J*=8.5 Hz, 1H, Ar*H*), 7.19 (dd, *J*=8.5, 2.0 Hz, 1H, Ar*H*), 7.90 (d, *J*=1.6 Hz, 1H, Ar*H*) ppm. ^{13}C NMR ($CDCl_3$), δ: 13.87 (CH_2CH_3) , 22.12 ($CH_2CH_2CH_3$), 33.26 ($CH_2CH_2CH_2$), 34.17 ($ArCH_2$), 118.76 (Ar*C*), 124.71 (Ar*C*), 131.79 (Ar*C*), 136.55 (Ar*C*), 142.91 (Ar*C*) ppm.

4.3.30. Synthesis of 4-butylbenzene-1,2-diamine (46)

A suspension of 4-butyl-2-nitroaniline (0.58 g, 3.0 mmol) in unstabilized 57 % HI (9 mL) was heated at 90 ^oC for 3 hours. The reaction mixture became homogeneous as the reaction progressed. After cooling to room temperature, the mixture was diluted with EtOAc (150 mL) and washed successively with saturated aqueous $Na_2S_2O_3$ (for the destruction of iodine formed), saturated aqueous $NaHCO_3$ and brine. The organic layer was dried over anhydrous $MgSO_4$, filtered and concentrated to give crude product. Column chromatography on silica gel with initially CH_2Cl_2, then CH_2Cl_2:methanol (99:1, v/v) as eluent sovent gave the pure product as an orange solid (0.39 g, 67.0 % yield). ^1H NMR ($CDCl_3$), δ: 0.83 (t, *J*=7.3 Hz, 3H, CH_2CH_3), 1.25 (m, 2H, $CH_2CH_2CH_3$), 1.45 (m, 2H, $CH_2CH_2CH_2$), 2.38 (t, *J*=7.6 Hz, 2H, $ArCH_2$), 3.44 (bs, 4H, NH_2), 6.44-6.47 (2H, Ar*H*s), 7.56 (d, *J*=7.7 Hz, 1H, Ar*H*) ppm.

4.3.31. Synthesis of *N*-(2-amino-4-butylphenyl)-2-naphthamide (47a)

Into the solution of *N*-(4-butyl-2-nitrophenyl)-2-naphthamide (69.6 mg, 0.2 mmol) in absolute ethanol (2 mL) was added stannous chloride dihydrate (225.6 mg, 1 mmol, 5 equiv.). The mixture was refluxed at 60 ^oC for 1 hour. $NaBH_4$ (3.8 mg, 0.1 mmol, 0.5 equiv.) was added to it and refluxed for another 30 minutes. The reaction mixture was cooled, ethanol was evaporated, and the concentrate was dissolved in water. The reaction mixture was made alkaline with 40 % aqueous NaOH and three times extracted with ethyl acetate. The organic layer was dried with $MgSO_4$ and evaporated under reduced pressure to get crude product. Column chromatography on silica gel with CH_2Cl_2 as eluent sovent gave the pure product as a solid. (52.4 mg, 82.4 % yield). ^1H NMR ($CDCl_3$), δ: 0.93 (t, *J*=7.3 Hz, 3H, CH_3), 1.36 (m, 2H, CH_2), 1.58 (m, 2H, CH_2), 2.54 (t, *J*=7.7 Hz, 2H, $ArCH_2$), 3.41 (bs, 2H, NH_2), 6.68-8.04 (10H, Ar*H*s), 8.42 (s, 1H, N*H*) ppm. ^{13}C NMR ($CDCl_3$), δ: 14.26

(CH_2CH_3) , 22.67 ($CH_2CH_2CH_3$), 33.78 ($CH_2CH_2CH_2$), 35.57 (ArCH_2), 118.66 (Ar*C*), 120.31 (Ar*C*), 122.51 (Ar*C*), 124.03 (Ar*C*), 125.50 (Ar*C*), 127.24 (Ar*C*), 128.13 (Ar*C*), 128.22 (Ar*C*), 129.0 (Ar*C*), 129.33 (Ar*C*), 131.85 (Ar*C*), 132.99 (Ar*C*), 135.23 (Ar*C*), 140.96 (Ar*C*), 142.72 (Ar*C*), 166.21 (*C*=O) ppm.

Compound 48: ^{1}H NMR ($CDCl_3$), δ : 0.38 (t, *J*=7.2 Hz, 3H, CH_3), 0.57 (m, 2H, CH_2), 0.75 (m, 2H, CH_2), 1.72 (t, *J*=7.9 Hz, 2H, ArCH_2), 6.38 (d, *J*=8.1 Hz, 1H, Ar*H*), 7.11 (s, 1H, Ar*H*), 7.34 (d, *J*=8.1, 1H, Ar*H*), 7.49-8.63 (14H, Ar*H*s), 9.64 (s, 1H, N*H*), 9.70 (s, 1H, N*H*) ppm.

4.3.32. Synthesis of *N*-(4-butyl-2-nitrophenyl)-2-naphthamide (49)

2-Naphthoic acid (172.2 mg, 1 mmol) was dissolved in anhydrous CH_2Cl_2 (3 mL). PBr_3 (0.14 mL, 1.5 mmol) was added to the solution under nitrogen. The mixture was stirred at room temperature for 3 hours. Et_3N (0.42 mL,3 mmol) and 4-butyl-2-nitroaniline (194.1 mg, 1 mmol) were added subsequently, and after stirring for 1 hour at room temperature, the mixture was diluted with CH_2Cl_2, washed with water and dried over anhydrous MgSO4. After evaporation, the crude product was purified by filtration through silica gel using CH_2Cl_2 as solvent and recrystallization from hexane-CH_2Cl_2 (9:1, v/v) to give pure product as a yellow solid (184.9 mg, 53.1 % yield). ^{1}H NMR ($CDCl_3$), δ : 0.96 (t, *J*=7.3 Hz, 3H, CH_3), 1.39 (m, 2H, *C*H_2CH$_3$), 1.65 (m, 2H, *C*H_2CH$_2$CH$_3$), 2.69 (t, *J*=7.7 Hz, 2H, Ar*C*H_2), 7.55-7.64 (m, 3H, Ar*H*s), 7.92 (d, *J*=7.7 Hz, 1H, ArH), 7.97-8.04 (m, 3H, Ar*H*s), 8.10 (s, 1H, Ar*H*), 8.52 (s, 1H, Ar*H*), 8.93 (d, *J*=8.6 Hz, 1H, Ar*H*), 11.42 (s, 1H, N*H*) ppm. ^{13}C NMR ($CDCl_3$), δ : 13.85 (*C*H$_3$), 22.16 (*C*H_2CH$_3$), 33.11 (*C*H_2CH$_2$CH$_3$), 34.63 (Ar*C*H_2), 122.17 (Ar*C*), 123.38 (Ar*C*), 125.10 (Ar*C*), 127.06 (Ar*C*), 127.80 (Ar*C*), 128.30 (Ar*C*), 128.36 (Ar*C*), 129.01 (Ar*C*), 129.33 (Ar*C*), 131.35 (Ar*C*), 132.66 (Ar*C*), 133.16 (Ar*C*), 135.20 (Ar*C*), 136.54 (Ar*C*), 138.70 (Ar*C*), 165.77 (*C*=O) ppm.

4.3.33. Synthesis of *N*-(2-amino-4-butylphenyl)-2-naphthamide (47a) and *N*-(2-amino-5-butylphenyl)-2-naphthamide (47b)

Into the solution of *N*-(4-butyl-2-nitrophenyl)-2-naphthamide (69.6 mg, 0.2 mmol) in absolute ethanol (2 mL) was added stannous chloride dihydrate (225.6 mg, 1 mmol)

under nitrogen. The mixture was refluxed at 60 ^{o}C for 1 h. $NaBH_4$ (3.8 mg, 0.1 mmol) was added to it and refluxed for another 30 min. The reaction mixture was cooled, ethanol was evaporated, and the concentrate was dissolved in water. The reaction mixture was made alkaline with 40 % aqueous NaOH and extracted with ethyl acetate (3 times). The organic layer was dried with $MgSO_4$ and evaporated under reduced pressure to get crude product. Column chromatography on silica gel with CH_2Cl_2 as eluent sovent gave the pure products as a solid mixture (52.4 mg, 47a:47b=69:53, 82.4 % yield). ^{1}H NMR ($CDCl_3$), δ : 0.93 (m, 6H, C*H*$_3$), 1.36 (m, 4H, C*H*$_2$), 1.59 (m, 4H, C*H*$_2$), 2.54 (t, *J*=7.7 Hz, 2H, ArC*H*$_2$), 2.73 (t, *J*=7.7 Hz, 2H, ArC*H*$_2$), 3.90 (bs, 4H, N*H*$_2$), 6.67-8.17 (20H, Ar*H*s), 8.42 (s, 1H, N*H*), 8.50 (s, 1H, N*H*) ppm. ^{13}C NMR ($CDCl_3$), δ : Alkyl Hs: 13.96, 13.98, 22.31, 22.34, 13.96, 13.98, 22.31, 22.34, 33.47, 34.17, 35.24, 35.88, Aryl Hs:118.33, 119.99, 122.05, 123.65, 125.16, 125.90, 126.80, 126.95, 127.06, 127.28, 127.80, 127.83, 127.89, 127.92, 128.50, 128.71, 128.87, 129.01, 131.43, 132.60, 133.21, 133.96, 134.88, 140.65, 142.45, 165.95 (N*H*) ppm.

4.3.34. Synthesis of methyl 4-amino-3-methoxybenzoate (51)

4-Amino-3-methoxy benzoic acid (0.67 g, 4.0 mmol) and methanol (4 mL) were added to a 25 mL three necked round bottom flask fitted with a condenser and magnetic stirrer. Concentrated sulphuric acid (96 %) (0.5 mL) was added to the reaction flask. The reaction mixture was refluxed at 70 ^{o}C oil bath temperature. The mixture was stirred for 4 hours. Then, reaction mixture was cooled to room temperature and made weakly alkaline by slowly adding a 5 % aqueous solution of $NaHCO_3$. The resultant suspansion was then extracted with dichloromethane (three times). The organic layers were combined, washed with water, dried with Na_2SO_4 and filtered. Evaporation of organic phase gave the pure product as an white solid (0.64 g, 88.4 % yield). ^{1}H NMR ($CDCl_3$), δ : 3.86 (s, 3H, ArOC*H*$_3$), 3.89 (s, 3H, COOC*H*$_3$), 4.23 (bs, 2H, N*H*$_2$), 6.65 (d, *J*=8.1 Hz, 1H, Ar*H*), 7.44 (s, 1H, Ar*H*), 7.54 (d, *J*=8.9 Hz, 1H, ArH) ppm. ^{13}C NMR ($CDCl_3$), δ : 51.70 (*C*H$_3$OC=O), 55.58 (ArO*C*H$_3$), 111.13 (Ar*C*), 113.09 (Ar*C*), 119.45 (Ar*C*), 124.06 (Ar*C*), 141.11 (Ar*C*), 146.09 (Ar*C*), 167.33 (CH$_3$O*C*=O) ppm.

4.3.35. Synthesis of methyl 4-acetamido-3-methoxybenzoate (52)

Methyl 4-amino-3-methoxy benzoate (0.36 g, 2 mmol) was added to 1 mL of water with vigorous stirring. Then acetic anhydride (0.31 g, 3 mmol, 1.5 equiv.) was added to this heterogeneous solution. The reaction mixture was stirred at room temperature during 2 hours. During this time, a precipitate occured. The precipitate was filtered and washed with several portions of water and dried under vacuum to give desired product as a solid (0.37 g, 82.9 % yield). ^{1}H NMR ($CDCl_3$), δ : 2.22 (s, 3H, C*H*$_3$CO), 3.89 (s, 3H, ArOC*H*$_3$), 3.93 (s, 3H, COOC*H*$_3$), 7.53 (d, *J*=1.7 Hz, 1H, Ar*H*), 7.67 (dd, *J*=8.4, 1.7 Hz, 1H, Ar*H*), 7.92 (bs, 1H, N*H*), 8.44 (d, *J*=8.4 Hz, 1H, Ar*H*) ppm. ^{13}C NMR ($CDCl_3$), δ : 25.06 (*C*H$_3$C=O), 52.09 (*C*H$_3$OC=O), 55.92 (ArO*C*H$_3$), 110.59 (Ar*C*), 118.49 (Ar*C*), 123.42 (Ar*C*), 124.87 (Ar*C*), 131.96 (Ar*C*), 146.10 (Ar*C*), 166.76 (CH$_3$O*C*=O), 168.43 (CH$_3$*C*=O) ppm.

4.3.36. Synthesis of *N*-(4-(hydroxymethyl)-2-methoxyphenyl)acetamide (53)

Methyl 4-acetamido-3-methoxybenzoate (0.56 g, 2.5 mmol) was added to a 25 mL round bottom flask fitted with a magnetic stirrer and septum. The flask was purged with nitrogen for 15 minutes. Then dry THF was added to the flask under nitrogen. After the starting material was dissolved in THF, $LiBH_4$ (136.1 mg, 6.25 mmol, 2.5 eq) was added to the flask at room temperature. Reaction mixture was stirred under nitrogen at 58 ^{o}C for overnight. Then, the reaction mixture was cooled to room temperature and diluted with water. THF was removed under reduced pressure. Remain water phase was extracted with EtOAc three times. The organic layers were combined and dried with $MgSO_4$. After the filtration of organic layer, evaporation of organic solvent gave crude product. Column chromatography on silica with CH_2Cl_2:EtOAc (99:1) as eluent sovent mixture gave the pure product as white solid (0.24 g, 49.2 % yield). ^{1}H NMR ($CDCl_3$), δ : 1.67 (bs, 1H, O*H*), 2.19 (s, 3H, C*H*$_3$), 3.89 (s, 3H, OC*H*$_3$), 4.64 (s, 2H, C*H*$_2$OH), 6.90 (dd, *J*=8.2, 1.5 Hz, 1H, Ar*H*), 6.93 (d, *J*=1.5 Hz, 1H, Ar*H*), 7.74 (bs, 1H, N*H*), 8.30 (d, *J*=8.1 Hz, 1H, Ar*H*) ppm. ^{13}C NMR ($CDCl_3$), δ : 24.90 (*C*H$_3$), 55.69 (O*C*H$_3$), 65.25 (*C*H$_2$OH), 108.73 (Ar*C*), 119.54 (Ar*C*), 119.61 (Ar*C*), 127.08 (Ar*C*), 136.42 (Ar*C*), 147.85 (Ar*C*), 168.18 (*C*=O) ppm.

4.3.37. Synthesis of *N*-(4-(bromomethyl)-2-methoxyphenyl)acetamide (54)

3,4-(Dimethoxyphenyl)methanol (0.23 g, 1.18 mmol) was dissolved in anhydrous dichloromethane (5 mL) in a 25 mL round-bottom flask. This solution was cooled to 0 ^{o}C and PBr_3 (0.13 g, 0.47 mmol) was added to the solution under nitrogen atmosphere. The reaction mixture was stirred at room temperature for 1 hour. Organic phase was extracted with water three times (3x5 mL). Then, organic phase was washed successively with saturated aqueous $NaHCO_3$ (5 mL) and brine (5 mL). The organic layer was dried over anhydrous $MgSO_4$, filtered and concentrated to give product as a white solid (0.22 g, 72.5 % yield). ^{1}H NMR ($CDCl_3$), δ: 2.20 (s, 3H, C*H*$_3$), 3.90 (s, 3H, OC*H*$_3$), 4.48 (s, 2H, C*H*$_2$Br), 6.90 (d, *J*=1.8 Hz, 1H, Ar*H*), 6.98 (dd, *J*=8.2, 1.9 Hz, 1H, Ar*H*), 7.75 (bs, 1H, N*H*), 8.31 (d, *J*=8.2 Hz, 1H, Ar*H*) ppm. ^{13}C NMR ($CDCl_3$), δ: 24.93 (*C*H$_3$), 34.05 (C*H*$_2$Br), 55.75 (OC*H*$_3$), 110.54 (Ar*C*), 119.54 (Ar*C*), 121.86 (Ar*C*), 127.95 (Ar*C*), 132.91 (Ar*C*), 147.65 (Ar*C*), 168.15 (*C*=O) ppm.

4.3.38. Synthesis of *N*-(2-methoxy-4-pentylphenyl)acetamide (55)

N-(4-(bromomethyl)-2-methoxyphenyl)acetamide (103 mg, 0.4 mmol) was dissolved in dry THF (3 mL) in 25 mL round-bottom flask. CuCl (7.92 mg, 0.08 mmol) and KI (13.3 mg, 0.08 mmol) were added to the reaction flask. The reaction mixture was cooled to -78 ^{o}C and *n*-BuLi (2.5 M hexane solution) (0.64 mL, 1.6 mmol) was added under nitrogen atmosphere. The reaction mixture was stirred at -78 ^{o}C for 2 hours, then allowed to warm to ambient temperature, and stirred for 24 hours at this temperature. After cooling to 0 ^{o}C, the reaction mixture was quenched by the cautious addition of 1 mL of 1 M aqueous HCl. After the filtration of resulting mixture, solution was extracted with three portions of ether. The combined ether layers were washed with successive portions of water and brine. Organic layer was dried over anhydrous $MgSO_4$, filtered and concentrated to give crude product. Purification by column chromatography on silica gel using CH_2Cl_2:EtOAc (5:1, v/v) as eluent gave the pure product (55.7 mg, 58.5 % yield). ^{1}H NMR ($CDCl_3$), δ: 0.82 (t, *J*=6.8 Hz, 3H, CH_2CH_3), 1.25 (m, 4H, $CH_2CH_2CH_2CH_3$), 1.52 (m, 2H, $CH_2CH_2CH_2CH_3$), 2.11 (s, 3H, CH_3C=O), 2.49 (t, *J*=7.6 Hz, 3H, ArCH_2), 3.80 (s, 3H, OC*H*$_3$), 6.61 (d, *J*=1.5 Hz, 1H, Ar*H*), 6.70 (dd, *J*=8.2, 1.7 Hz, 1H, Ar*H*), 7.59 (bs, 1H, N*H*), 8.14 (d, *J*=8.2 Hz, 1H, Ar*H*) ppm. ^{13}C NMR ($CDCl_3$), δ: 14.02 (CH_2CH_3), 22.53

(*C*H_2CH$_3$), 24.85 (*C*H_3C=O), 31.23 (*C*H_2CH$_2$CH$_2$CH$_3$), 31.47 (*C*H_2CH$_2$CH$_3$), 35.85 (Ar-*C*H_2), 55.58 (O*C*H_3), 110.09 (Ar*C*), 119.67 (Ar*C*), 120.71 (Ar*C*), 125.28 (Ar*C*), 138.70 (Ar*C*), 147.63 (Ar*C*), 167.94 (*C*=O) ppm.

4.3.39. Synthesis of 2-methoxy-4-pentylaniline (56)

N-(2-methoxy-4-pentylphenyl)acetamide (50 mg, 0.21 mmol) was refluxed in 1 mL methanol and 1 mL 20 % H_2SO_4 at 80 ^oC for 2 hours. Then, the reaction mixture was cooled to room temperature and made weakly alkaline by slowly adding a 5 % aqueous solution of $NaHCO_3$. The resultant solution was then extracted with diethyl ether (two times). The ether layers were combined, washed with water, dried with Na_2SO_4 and filtered. Evaporation of ether gave the pure product as an brown oil at room temperature (33.4 mg, 82.4 % yield). ^{1}H NMR ($CDCl_3$), δ : 0.82 (t, *J*=6.4 Hz, 3H, CH_2CH_3), 1.23 (m, 4H, $CH_2CH_2CH_3$), 1.50 (m, 2H, $CH_2CH_2CH_2CH_3$), 2.43 (t, *J*=7.6 Hz, 3H, ArCH_2), 3.58 (bs, 2H, NH_2), 3.76 (s, 3H, OCH_3), 6.52-6.57 (m, 3H, Ar*H*s) ppm. ^{13}C NMR ($CDCl_3$), δ : 14.07 (CH_2CH_3), 22.58 (*C*H_2CH$_3$), 31.55 (*C*H_2CH$_2$CH$_2$CH$_3$), 31.57 (*C*H_2CH$_2$CH$_3$), 35.61 (Ar-*C*H_2), 55.42 (O*C*H_3), 110.82 (Ar*C*), 115.00 (Ar*C*), 120.55 (Ar*C*), 133.52 (Ar*C*), 133.64 (Ar*C*), 147.31 (Ar*C*) ppm.

4.3.40. Synthesis of *N*-(2-methoxy-4-pentylphenyl)-2-naphthamide (57)

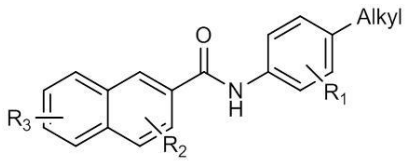
2-Naphthoic acid (86.1 mg, 0.5 mmol) was dissolved in anhydrous CH_2Cl_2 (2 mL). PBr_3 (0.07 mL, 0.75 mmol) was added to the solution under nitrogen. The mixture was stirred at room temperature for 3 hours. Et_3N (0.21 mL, 1.5 mmol) and 2-methoxy-4-pentylaniline (96.5 mg, 1 mmol) were added subsequently, and after stirring for 1 hour at room temperature, the mixture was diluted with CH_2Cl_2, washed with water and dried over anhydrous $MgSO_4$. After evaporation, the crude product was purified by column chromatography on silica gel using CH_2Cl_2-hexane (5:1, v/v) as eluent to give the pure product as a solid (59.5 mg, 34.3 % yield). ^{1}H NMR ($CDCl_3$), δ : 0.83 (t, *J*=Hz, 3H, CH_2CH_3), 1.27 (m, 4H, $CH_2CH_2CH_3$), 1.56 (m, 2H, $CH_2CH_2CH_2CH_3$), 2.53 (t, *J*=Hz, 3H, ArCH_2), 6.69 (d, *J*=1.7 Hz, 1H, Ar*H*), 6.79 (dd, *J*=8.2, 1.7 Hz, 1H, Ar*H*), 7.51 (m, 2H, Ar*H*s), 7.88 (m, 4H, Ar*H*s), 8.33 (s, 1H, Ar*H*), 8.38 (d, *J*=8.2, 1H, Ar*H*), 8.55 (s, 1H, N*H*) ppm. ^{13}C NMR ($CDCl_3$), δ : 14.06 (CH_2CH_3), 22.57 (*C*H_2CH$_3$), 31.27 (*C*H_2CH$_2$CH$_2$CH$_3$),

31.50 ($CH_2CH_2CH_3$), 35.94 (Ar-CH_2), 55.81 (OCH_3), 110.20 (Ar*C*), 119.77 (Ar*C*), 120.89 (Ar*C*), 123.61 (Ar*C*), 125.45 (Ar*C*), 126.82 (Ar*C*), 127.53 (Ar*C*), 127.74 (Ar*C*), 127.79 (Ar*C*), 128.62 (Ar*C*), 129.03 (Ar*C*), 132.68 (Ar*C*), 134.77 (Ar*C*), 139.08 (Ar*C*), 148.15 (Ar*C*), 165.17 (C=O) ppm.

5. CONCLUSIONS

The aim of the study was to synthesize lead compound derivatives to decrease IC_{50} value of the lead compound to nanomolar levels. With computer-aided studies, the syntheses of some lead compound derivatives were planned. Lead compound derivatives have two parts; the left hand side (the naphthyl unit) and the right hand side (the phenyl unit). Some derivatives were successfully synthesized by the coupling reactions of the commercially available naphthyl and phenyl units *via* ester or amide bonds. However, some phenyl derivatives for the left hand side were not commercially available. These compounds were succesfully synthesized *via* multistep reactions, then coupled with naphoic acid to give the final products.

Some of the synthesized lead compound derivatives were subjected to biological tests to see the inhibition effects of them on CYP17. Among them, the IC_{50} value of compound 6 was calculated and it was found to be 2.3 μM, which means that the activity of this compound is about fifteen times higher than the activity of the lead compound. According to biological test results, alkyl substituent on the phenyl ring and amide bond at join are preferable in the derivatization. Nitro and amino groups can be attached to the phenyl unit and metoxy group may be used on the naphyl unit (Figure 5.1).



R_1=- NO_2, -NH_2

R_2, R_3= -H, -OCH_3

Figure 5.1. Derivatization of the lead compound.

PART II

INVESTIGATION OF BIOACTIVE PROPERTIES OF CYCLOPOLYMERS OBTAINED BY RAFT POLYMERIZATION

6. INTRODUCTION

6.1. Conventional Radical Polymerization

Conventional radical polymerization is one of the most common used processes for the commercial production of high molecular weight polymers [51]. The main features of radical polymerization are as follows:

- It can be used with various monomers including (meth)acrylates, styrene, (meth)acrylamides, butadiene, and vinyl acetate
- It is tolerant to a wide range of functional groups such as -OH, $-NR_2$, -COOH, $-CONR_2$ and reaction conditions (bulk, solution, emulsion, miniemulsion, suspension)
- It is simple to put into practice and inexpensive in compared to the competitive methods such as the anionic or cationic polymerization..

However, the conventional process has some remarkable limitations with respect to the degree of control that can be asserted over molecular structure, in particular, the molecular weight distribution, composition, and architecture.

Radical polymerization is a chain reaction. The chains are initiated by radicals (formed from an initiator) adding to monomer. Chain propagation then involves the sequential addition of monomer units to the radical ($P_n^{\cdot}$) so formed. Chain termination occurs when the propagating radicals react by combination or disproportionation. A simplified mechanism is shown in Figure 6.1 [52].

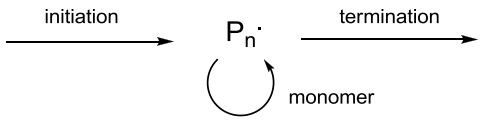


Figure 6.1. Conventional radical polymerization.

The molecular weight of chains formed in the early stages of polymerization is high and will reduce with conversion because of monomer depletion. The polydispersity is broad (M_w/M_n>1.5).

6.2. Living Radical Polymerization

The field of conventional radical polymerization has been revolutionalized by the invention and development of living radical polymerization techniques with respect to the polydispersity, the control of the molecular weights, and the formation of complex macromolecular architectures [53-57].

In an ideal living polymerization, all chains are initiated at the beginning, grow at the same rate, and survive the polymerization. To provide living character on a radical polymerization, it is necessary to suppress or render insignificant all processes that terminate chains irreversibly. Thus, living polymerization only becomes possible in the presence of reagents that react with propagating radicals ($P_n^{\cdot}$) by reversible deactivation (Figure 6.2) and reversible chain transfer (Figure 6.3) so that the majority of chains are maintained in a dormant form (P_n-X) [52]. Rapid equilibrium between the active and dormant forms ensures that all chains possess an equal chance for growth and that all chains will grow. Under these conditions, the molecular weight increases linearly with conversion and the molecular weight distribution can be very narrow (M_w/M_n<1.5).

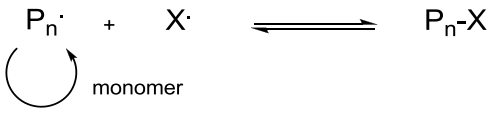


Figure 6.2. Reversible deactivation.

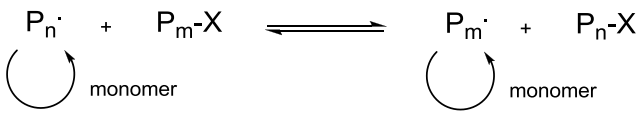


Figure 6.3. Reversible chain transfer.

The living radical polymerization techniques that have recently received greatest attention are nitroxide mediated polymerization (NMP) [58], atom transfer radical polymerization (ATRP) [54, 55], and reversible addition-fragmentation chain transfer (RAFT) polymerization [59]. RAFT polymerization will be presented in details, because it was the method employed in this study.

6.3. RAFT Polymerization

RAFT polymerization can be performed by simply adding a chosen quantity of an appropriate RAFT agent to a conventional free-radical polymerization which includes a free radical initiator and monomer (Figure 6.4) [60-62]. RAFT agents are generally thiocarbonylthio compounds. They can be referred as chain transfer agents (CTAs).

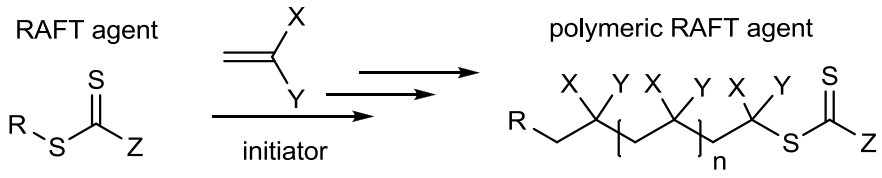


Figure 6.4. Overall reaction in the RAFT polymerization.

Its main potential lies in its versatility towards the types of monomers it can polymerize, including styrenic, (meth)acrylamides, (meth)acrylates, acrylonitrile, vinyl acetates, vinyl formamide, vinyl chlorides as well as a range of other vinyl monomers. Another advantage of the RAFT process is that it is carried out in the same conditions as a classic free radical polymerization except with the addition of a chain transfer agent (CTA). In addition to simple homopolymers, a large variety of macromolecular structures have been synthesized via RAFT including statistical, block, multiblock, gradient, and comb copolymers, telechelic (co)polymers, star, hyperbranched, and network (co)polymers [63-70]. Due to this versatility, RAFT polymerization becomes an increasingly popular technique for the advanced macromolecular designs.

The main features of the ideal RAFT polymerization can be summarized as follows [59]:

- RAFT polymerization processes the characteristics usually associated with the living polymerization. All chains begin to grow at the commemcement of the polymerization and continue to grow until the monomer is comsumed. Molecular weights increase linearly with conversion.
- Molecular weights in RAFT polymerization can be predicted by the molar ratio of the consumed monomer to CTA using the following equation.

$$M_{n,theo} = [M]/[CTA] \times M_{monomer} \times Conv. + M_{CTA}$$

- Active chain ends are retained.
- Narrow molecular weight distributions are achievable (1<PDI<1.5).
- Blocks, stars, telechelics, and complex molecular architectures are accessible.

6.3.1. The Mechanism

The key feature of the mechanism of RAFT polymerization is a sequence of addition-fragmentation equilibrium as shown in Figure 6.5 [59]. Initiation and radical-radical termination occur as in conventional radical polymerization. In the early stages of the polymerization, addition of a propagating radical ($P_n^{\cdot}$) to the thiocarbonylthio compound (1) followed by the fragmentation of the intermediate radical (3) gives rise to a polymeric thiocarbonylthio compound (4) and a new radical ($R^{\cdot}$). Reaction of the radical ($R^{\cdot}$) with the monomer forms a new propagating radical ($P_m^{\cdot}$). Rapid equilibrium between the active propagating radicals ($P_n^{\cdot}$ and $P_m^{\cdot}$) and the dormant polymeric thiocarbonylthio compounds (1 and 4) provides equal probability for all chains to grow, and allows for the production of polymers with narrow polydispersity. When the polymerization is complete (or stopped), most of chains retain the thiocarbonylthio end group and can be isolated as stable materials [59].

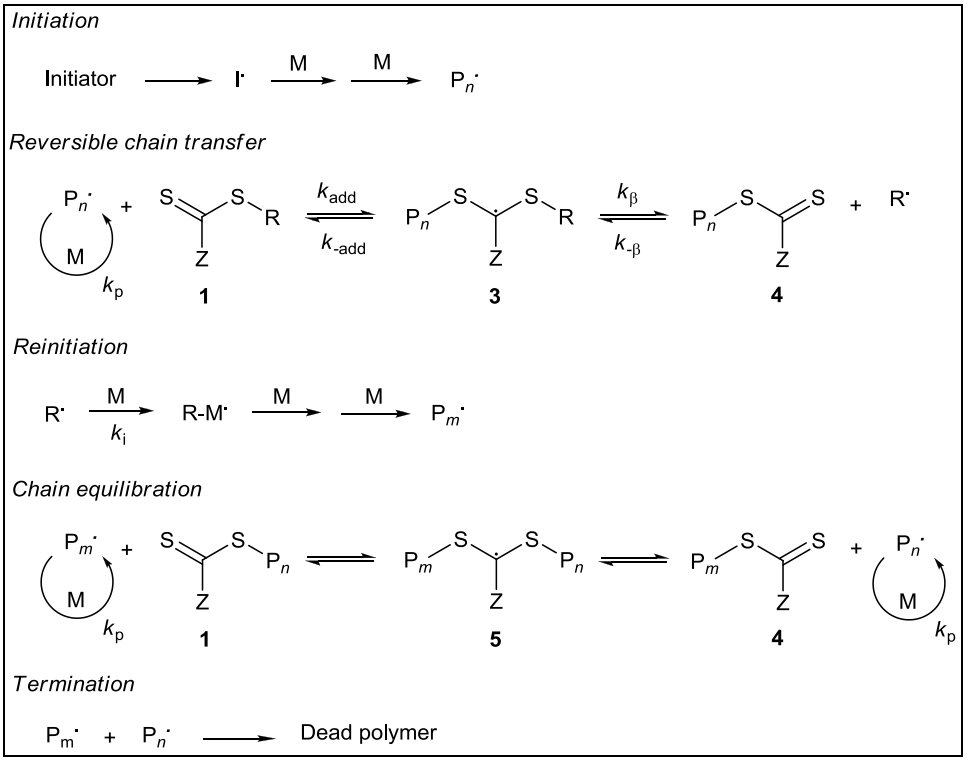


Figure 6.5. The mechanism of the RAFT polymerization [56].

6.3.2. RAFT agents

A wide variety of thiocarbonylthio RAFT agents have now been reported. These include certain trithiocarbonates, dithiocarbonates (xanthates), dithiocarbamates, dithiobenzoates, and other compounds (Figure 6.6) [71-74].

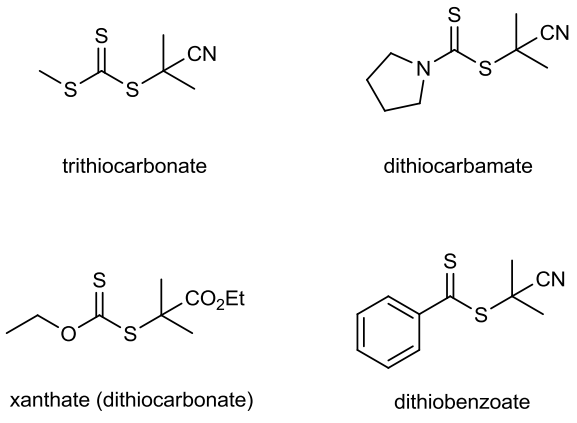


Figure 6.6. Examples of thiocarbonylthio RAFT agents.

The effectiveness of the RAFT agent depends on several factors; the monomer being polymerized, the properties of the free radical leaving group R, the group Z which can be chosen to activate or deactivate the carbonyl double bond and modify the stability of the intermediate radicals (Figure 6.7). For an efficient RAFT polymerization the following requirements should be fullfilled [71]:

- The RAFT agents 1 and 4 should have a reactive C=S double bond (high k_{add}).
- The intermediate radicals 3 and 5 should fragment rapidly (high k_{β}, weak S-R bond) and give no side reactions.
- The intermediate 3 should partition in favour of products ($k_{\beta} \geq k_{-add}$).
- The expelled radicals ($R^{\cdot}$) should efficiently reinitiate polymerization.

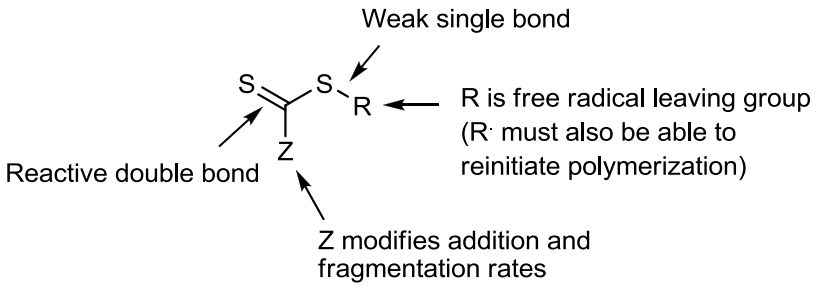


Figure 6.7. Structural features of thiocarbonylthio RAFT agent [71].

Several papers have been published on the on the effects of the substituents R and Z on the effectiveness and transfer coefficients of RAFT agents. The rate of addition of radicals to the C=S double bond is strongly influenced by the substituent Z. This rate is higher when Z=aryl, alkyl (dithioesters), or S-alkyl (trithiocarbonates), and lower when Z=*O*-alkyl (xanthates) or *N*,*N*-dialkyl (dithiocarbamates).

More generally, chain-transfer coefficients decrease in the following order; dithiobenzoates, trithiocarbonates ≈ dithioalkanoates, dithiocarbonates (xanthates), dithiocarbamates.

6.4. Cyclopolymers of Alkyl α-(Hydroxymethyl)acrylate (RHMA) Ether Dimers

The cyclopolymers derived from the alkyl a-(hydroxymethyl)acrylate (RHMA) ether dimers contain tetrahydropyrane repeat units and pendent ester groups (Figure 6.8) [75-77]. The cyclopolymers derived from the RHMA ether dimers exhibit high glass transition temperatures, and therefore can be considered as alternatives to acrylate/methacrylate derived polymers for higher temperature applications such as automotive part and coatings where dimensional stability is important.

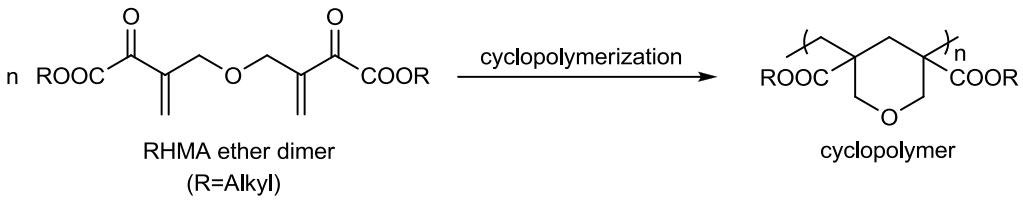


Figure 6.8. Cyclopolymers of RHMA ether dimers.

However, the cyclopolymers produced by conventional radical polymerization are not used based on these advantages. One reason is attributable to the difficulty in getting the cyclopolymers with a well-defined structure. Therefore, for a number of years, we have been interested in the synthesis of controlled cyclopolymers with living end groups and in the factors affecting the cyclization in controlled/living polymerization systems.

The literature reports on the RAFT polymerization have been mostly limited to monomers that contain a single polymerizable double bond. Bifunctional monomers such as diacrylates, dienes which upon polymerization result in polymers with cyclic repeat units and linearlike backbones are not studied much. Only recently, Li *et al.* reported the formation of ring structures in the preparation of hyperbranched polymers from asymmetric divinyl monomers such as allyl methacrylates in low yields [78]. Then, Agarwal *et al.* reported the first studies on RAFT mediated cyclopolymerizations in which alkyl ammonium dienes were used in the preparation of cyclopolymers with five membered heterocyclic repeat units [79, 80]. In a broader sense, there are only few examples of cyclopolymers obtained by the controlled living radical polymerization techniques [81-83]. Therefore, the cyclopolymers reported have been limited to high

polydispersity homopolymers with uncontrolled molecular weights and most importantly dead end groups.

6.4.1. Factors Effecting Cyclization

Aliphatic cyclopolymers derived from alkyl α-(hydroxymethyl)acrylate (RHMA) have been previously synthesized by conventional free radical polymerization technique. We recently reported the successful cyclopolymerization of the TBHMA ether dimer via atom transfer radical polymerization (ATRP). The cyclopolymerization is known to proceed through sequential *intra*-molecular cyclization and *inter*-molecular propagation reactions which leads to the formation of cyclopolymers with six-membered tetrahydropyran repeat units. The main challenge in the cyclopolymerization is the synthesis of cyclopolymers with linearlike backbone since incomplete cyclization leads to pendent group unsaturation which may act as in bound-plasticizer or crosslinking sites (Figure 6.9).

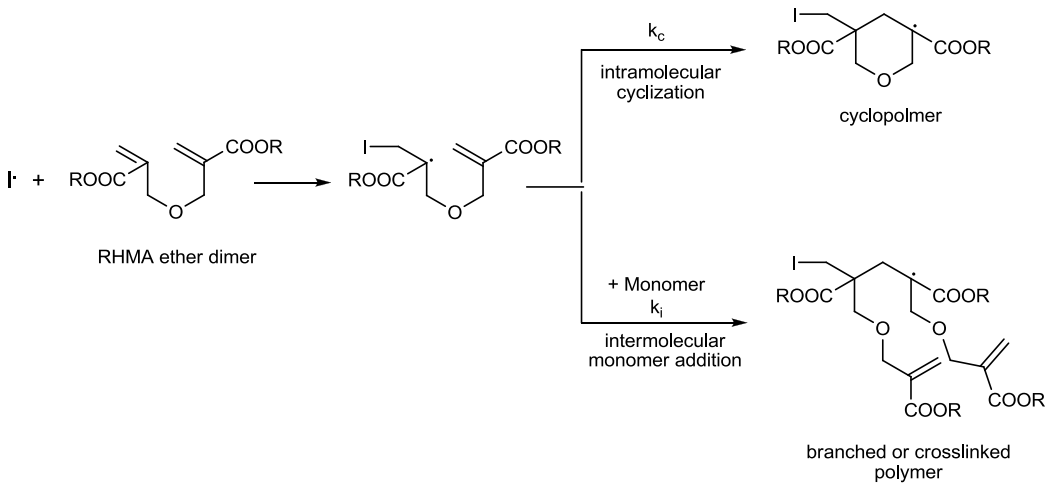


Figure 6.9. Intra- and intermolecular reactions leading to cyclization and crosslinking.

Previous studies with similar difunctional monomers showed that large R-groups such as *tert*-butyl and high temperatures favor cyclization. High temperatures favor cyclization, because monomers can overcome their activation energies for cyclization at high temperatures. Bulky ester substituents also favor cyclization by supressing the competitive intermolecular monomer addition reactions.

6.4.2. Apparent and Effective Bulkiness

The bulkiness of ester substituents in monomers can be defined using two different approaches; apparent bulkiness and effective bulkiness. Apparent bulkiness is the bulkiness according to the total size or volume of the ester substituent. On the other hand, effective bulkiness is the bulkiness according to the number of carbon atoms attached to the central ester carbon, in other words according to the primary, secondary or tertiary nature of the central ester carbon [84].

According to previous conventional free radical polymerization and ATRP studies, the effective bulkiness rather than the apparent bulkiness is important for a high cyclization efficiency.

7. OBJECTIVES

The cyclopolymers derived from the RHMA ether dimers exhibit high glass transition temperatures, and therefore can be considered as alternatives to acrylate/methacrylate derived polymers for higher temperature applications such as automative parts and coatings where dimentional stability is important.

Aliphatic cyclopolymers derived from alkyl α-(hydroxymethyl)acrylate (RHMA) have been previously synthesized by conventional radical polymerization technique.

The aim of the study is to get highly cyclized living aliphatic polymers with controlled molecular weights and low polydispersities. In order to attain this goal, we decided to apply RAFT polymerization to alkyl α-(hydroxymethyl)acrylate (RHMA) ether dimers.

Previous studies with similar difunctional monomers showed that large R-groups such as *tert*-butyl and high temperatures favor cyclization. However, the effects of temperature and bulkiness of ester substituent were not known for the controlled cyclopolymerization systems. Beside targeting high cyclization efficiency, maintaining the controlled/living nature of the cyclopolymerization was the main challenge, which could limit the choice of the monomers. Therefore, the syntheses of monomers with different ester substituents such as ethyl, n-butyl, *tert*-butyl, cyclohexyl and isobornyl and then the RAFT polymerization of these monomers were planned.

In the literature, it is known that tetrahydropyran (THP) and/or tetrahydrofuran (THF) rings as hydrophobic groups on the polymer chain play a significant role in the biological activity of the polymers. Since our cyclopolymers contain tetrahyrofuran rings, we decided to investigate the antibacterial activities of the obtained cyclopolymers.

8. RESULTS AND DISCUSSION

It is known that the success of the RAFT process with a given monomer depends on the proper selection of the chain transfer agent (CTA) and reaction conditions. In the RAFT polymerization of alkyl α-(hydroxymethyl)acrylate (RHMA) ether dimers, cumyl dithiobenzoate (CDB) [85, 86] was chosen as the chain transfer agent and *N,N'*-azobis(isobutyronitrile)(AIBN) was used as the free radical initiator. Polymerizations were carried out in xylene. Monomers with different ester substituents such as ethyl, n-butyl, *tert*-butyl, cyclohexyl and isobornyl were synthesized and subjected to RAFT polymerization (Figure 8.1).

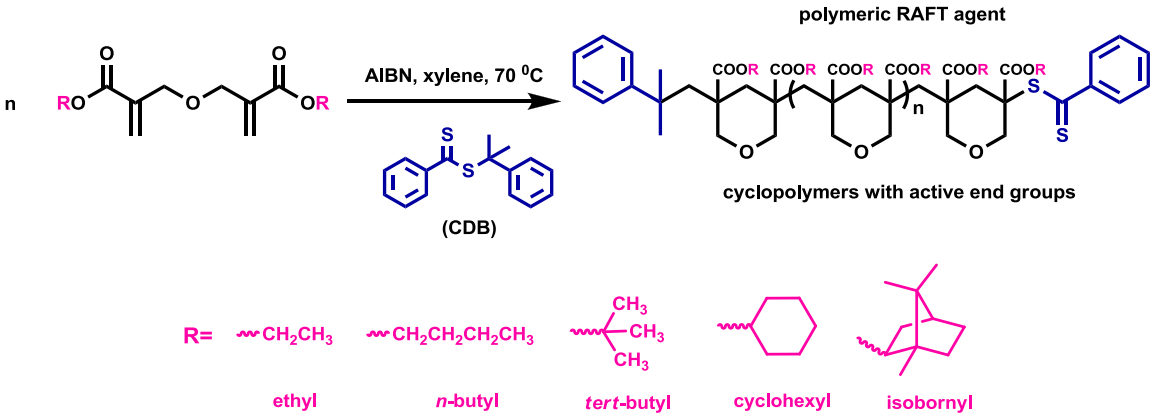


Figure 8.1. RAFT cyclopolmerization of RHMA ether dimers.

8.1. Synthesis of the RAFT Agent (CDB)

The RAFT agent, cumyl dithiobenzoate (CDB), was synthesized by Markownikov addition of produced dithiobenzoic acid across the olefinic double bond of alpha methyl styrene in carbontetrachloride at 70 ^{o}C (Figure 8.2) [87].

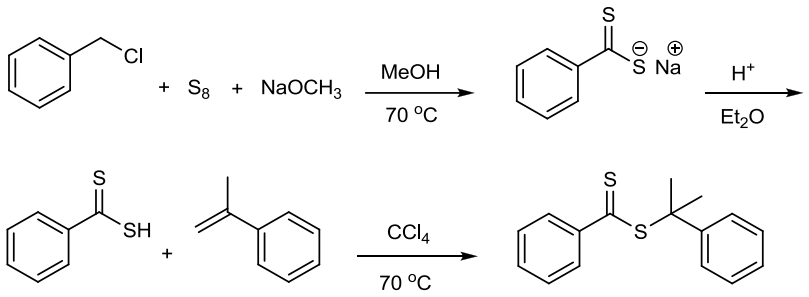


Figure 8.2. Synthesis of RAFT agent (CDB).

8.2. Synthesis of the Monomers

The monomers were synthesized from their corresponding acrylate esters in one pot reaction. The reaction of acrylate esters with formaldehyde is catalyzed by DABCO, which is called as the Baylis-Hillman reaction. Then, the dimerization of Baylis-Hillman product gave the desired monomers (Figure 8.3). The acrylate ester of cyclohexyl was synthesized from the reaction of the corresponding alcohol with acryloyl chloride.

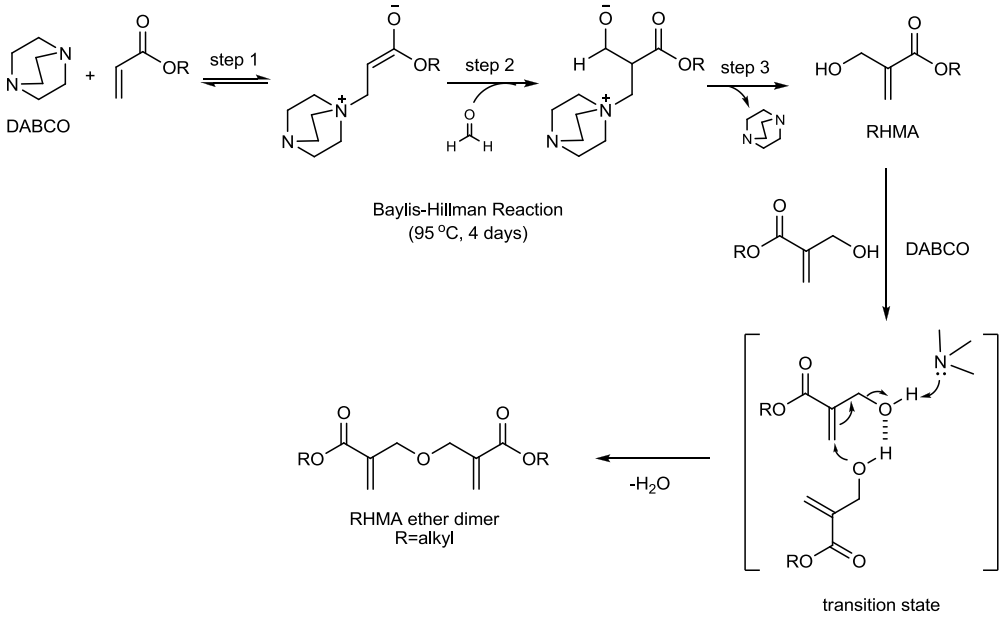


Figure 8.3. Synthesis of RHMA ether dimers via Baylis-Hillman reaction.

Previous studies with similar difunctional monomers showed that large R-groups such as *tert*-butyl and high temperatures favor cyclization. However, the effects of temperature and bulkiness of ester substituent were not known for the controlled cyclopolymerization systems. Beside targeting high cyclization efficiency, maintaining the controlled/living nature of the cyclopolymerization was the main challenge, which could limit the choice of the monomers. Therefore, monomers with sterically different esters were polymerized by RAFT polymerization technique.

Initially, TBHMA ether dimer was employed as the bulky difunctional acrylate since previous conventional radical and atom transfer radical polymerizationsof this monomer resulted in high cyclization efficiencies. Factors affecting the RAFT cyclopolymerization of TBHMA ether dimer were investigated. The concentration of the monomer, [M]/[CDB] and [CDB]/[AIBN] ratios in polymerization mixtures and the polymerization temperature were changed to investigate the effect of the individual RAFT components and to find out the optimum RAFT cyclopolymerization conditions.

8.3. RAFT Cyclopolymerization of the TBHMA Ether Dimer

The initial polymerizations were carried out at 70 ^{o}C at various [M]/[CDB] ratios where [CDB]/[AIBN] ratio was kept constant (1:0.25; Table 8.1) [88]. This ratio, according to the literature, appeared to be a good compromise between a fast polymerization rate and a well controlled radical polymerization process for acrylic monomers. The monomer concentrations were fixed to 1M initially, CDB and thus accordingly the AIBN concentrations were changed and polymers with various molecular weights were obtained (Table 8.1, Entries 1-6). All resulting polymers were soluble in organic solvents such as methylene chloride, which indicated that cyclizations were efficient enough to prevent crosslinking. The polydispersities of the polymers were relatively low (1.25-1.50) and the molecular weights were close to the theoretical values. The ^{1}H and ^{13}C NMR analysis of the polymers showed no peaks corresponding to pendent group unsaturation which may result from incomplete cyclization.

Table 8.1. Results from the RAFT cyclopolymerization of TBHMA ether dimer in xylene at 70 °C.[a,b]

Entry	[M]:[CDB]	[M] (mol/L)	Time (h)	Conv.[c] (%)	$M_{n,theo}$ (10^3 g/mol)	$M_{n,sec}$ (10^3 g/mol)	M_w/M_n[d]
1	200:1	1	2	42.0	25.3	20.6	1.36
2	200:1	1	4	72.2	43.3	39.7	1.48
3	100:1	1	2	36.6	11.2	10.8	1.31
4	100:1	1	4	77.1	23.2	23.8	1.39
5	50:1	1	2	38.7	6.0	5.3	1.25
6	50:1	1	4	78.8	12.0	12.4	1.30
7	150:1	1.5	2	45.0	20.4	16.4	1.35
8	150:1	1.5	3	70.3	31.7	26.4	1.53
9	150:1	1.5	4	82.9	37.3	35.6	1.90
10	50:1	1.5	2	43.5	6.8	6.4	1.33
11	70:1	1.75	1	29.4	6.4	9.1	1.59
12[e]	-	1	2	85.0	25.5	57.5	2.75

[a]Conditions: [CDB]/[AIBN]=1:0.25; TBHMA=*tert*-butyl α-(hydroxymethyl)acrylate, M=monomer, CDB=cumyl dithiobenzoate, AIBN=2,2'-azobis(isobutyronitrile). [b]All polymers were entirely soluble in methylene chloride. [c]Measured by gravimetric methods. [d]Molecular weight distribution (M_w/M_n) was measured by size exclusion chromatography (SEC). [e]Entry 12 was generated by conventional free radical polymerization.

Kinetic experiments were carried out at 1M monomer concentration and three different [M]/[CDB] ratios (Figure 8.4). An induction period of one hour was detected for all the polymerizations. As shown in Figure 8.4, a linear first-order rate plot was observed for conversions up to 80-90% at three different [M]/[CDB] ratios, which indicated a constant free radical concentration during polymerizations. The number average molecular weights increased linearly with monomer conversions while the polydispersities remained relatively low throughout the polymerizations only with a small increase at higher conversions (>80%). These results indicate that the RAFT cyclopolymerizations of the TBHMA ether dimer proceeded in a controlled manner. The control experiment carried out in the absence of the CTA resulted in polymers with high polydispersities (Table 8.1, Entry 12), proving the effect of the CTA in the RAFT cyclopolymerization. The first-order rate

plots also show that the overall polymerization rates were close to each other even though different initiator concentrations were used. We believe that, as previously reported in the literature, the expected increase in polymerization rate which should be observed as a result of the increased AIBN concentration (i.e. [M]/[CDB]=50 *versus* [M]/[CDB]=100, the former contains twice of the initiator since [CDB]/[AIBN] ratio is constant) is compensated by the higher retardation effect of the CDB whose concentration had to be increased to the same extent as AIBN.

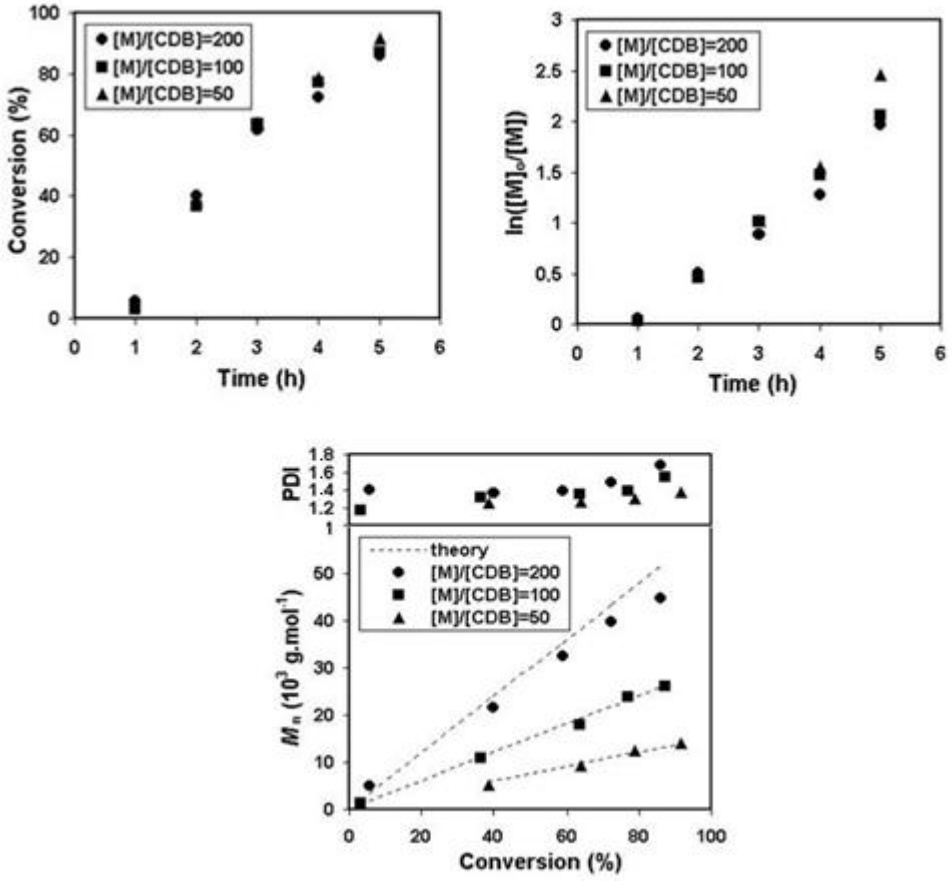


Figure 8.4. Kinetic studies of the RAFT cyclopolymerization of TBHMA ether dimer in xylene at 70 ^{o}C and various [M]/[CDB] ratios ([M]=1 mol.L^{-1}; [CDB]/[AIBN]=1:0.25; TBHMA=*tert*-butyl α-(hydroxymethyl)acrylate, M=monomer, CDB=cumyl dithiobenzoate, AIBN=2,2'-azobis(isobutyronitrile)).

Cyclopolymerizations carried out at more concentrated solutions resulted in polymers with higher polydispersities (Table 8.1, Entries 7-11). Similar results were

reported by *Agarwal et al.* at higher monomer concentrations (4.2 M) and the increase in polydispersity was attributed to diffusion problems and/or changing kinetic parameters. Because the monomer concentrations in the present work were much lower (1.50-1.75 M) than the reported ones, it is most probable that the higher polydispersities are due to the changing kinetic parameters corresponding to intramolecular cyclization and intermolecular branching reactions.

RAFT polymerization of tert-butyl monomer is the second example of a controlled living cyclopolymerization that involves the RAFT process. To the best of our knowledge, this is the first time a diacrylate monomer is used in the RAFT mediated cyclopolymerization.

8.3.1. The Effect of CDB and AIBN Concentrations

To see the effect of the CDB concentration, initially, the monomer and AIBN concentrations were kept constant, and CDB concentration was changed. Increasing the CDB concentration as observed in previous reports resulted in lower conversions at similar polymerization times (Table 8.2, Entries 1 and 2). To demonstrate this effect better, kinetic studies were done. Figure 8.5 shows the pseudo-first-order rate plots of the cyclopolymerizations carried out at constant monomer concentration but various CDB and AIBN concentrations. The results show that when the [CDB]/[AIBN] ratio was kept constant but the absolute concentrations of CDB and AIBN were increased, the polymerization rate remained unchanged (Figure 8.5, [CDB]/[AIBN]= 10:2.5 mM and 20:5 mM). These results are in accordance with the results discussed in Figure 8.4. However, increasing the CDB concentration relative to the AIBN concentration decreases the polymerization rate considerably ([CDB]/[AIBN]=10:2.5 mM compared to 20:2.5 mM). Higher concentrations of AIBN at constant CDB and monomer concentrations resulted in faster polymerizations (Figure 8.5, [CDB]/[AIBN]=20:10 mM compared to 20:5 mM and 20:2.5 mM) but at the expense of higher polydispersities (Table 8.2, Entry 4 compared to 2 and 3) and deviation from theoretical molecular weights. When all polymerizations are compared, as expected, the slowest polymerization rate is observed with the lowest AIBN concentration but highest CDB concentration ([CDB]/[AIBN]=20:2.5 mM); whereas, the highest polymerization rate is observed with

the highest initiator concentration but lowest CDB concentration. A good balance between a fast polymerization rate and control of the RAFT process is attained at 4:1 [CDB]/[AIBN] ratio.

Table 8.2. Effect of CDB and AIBN concentrations on the RAFT cyclopolymerization of TBHMA ether dimer in xylene at 70 ^{o}C.[a,b]

Entry	[M]:[CDB]:[AIBN]	Conv.[c] (%)	$M_{n,theo}$ (10^3 g/mol)	$M_{n,sec}$ (10^3 g/mol)	M_w/M_n[d]
1	1000:10:2.5	77.1	23.2	23.8	1.39
2	1000:20:2.5	48.8	7.5	4.7	1.26
3	1000:20:5	78.8	12.0	12.4	1.30
4	1000:20:10	98.3	14.9	9.9	1.44

[a]Conditions: [M]= 1 mol.L^{-1}; polymerization time= 4h; TBHMA= *tert*-butyl α-(hydroxymethyl)acrylate; M= monomer, CDB= cumyl dithiobenzoate, AIBN=2,2'-azobis(isobutyronitrile). [b]All polymers were entirely soluble in methylene chloride. [c]Measured by gravimetric methods. [d]Molecular weight distribution (M_w/M_n) was measured by size exclusion chromatography (SEC).

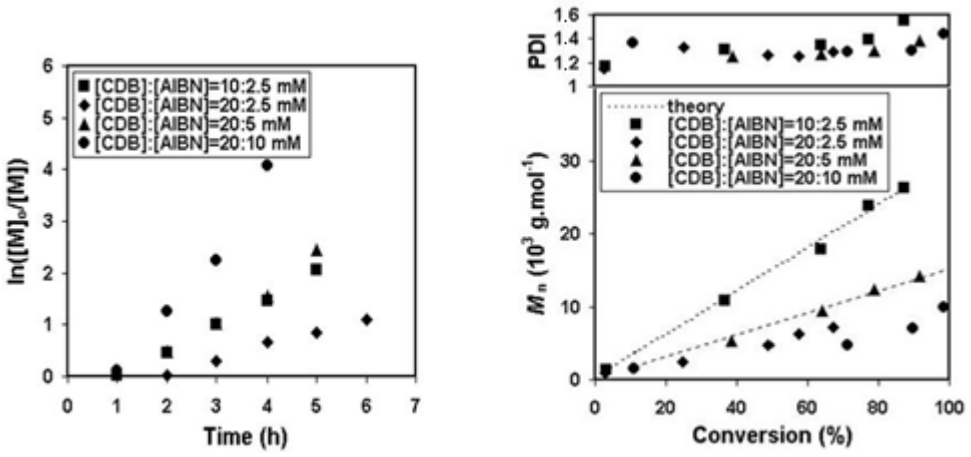


Figure 8.5. Kinetic studies of the RAFT cyclopolymerization of TBHMA ether dimer in xylene at 70 ^{o}C and various CDB and AIBN concentrations ([M]=1 mol.L^{-1}; TBHMA=*tert*-butyl α-(hydroxymethyl)acrylate, M=monomer, CDB=cumyl dithiobenzoate, AIBN=2,2'-azobis(isobutyronitrile)).

8.3.2. The Effect of Temperature

In the conventional free radical polymerization, it is known that high temperatures favor the cyclization process. Previously, we reported that in the ATRP cyclopolymerization of the TBHMA ether dimer an optimum temperature range is present (70-80 ^{o}C). Below this temperature, the branching/crosslinking reactions become significant. On the other hand, when the temperature exceeds these optimum values, a less controlled ATRP process takes place.

To investigate the effect of temperature on the RAFT cyclopolymerization of TBHMA ether dimer, experiments were carried out at various temperatures (60-90 ^{o}C, Table 8.3). All resulting polymers were soluble in organic solvents such as methylene chloride indicating that the intramolecular cyclization was still the dominant pathway. The cyclopolymers obtained at 60 ^{o}C had broader molecular weight distributions than the ones obtained at 70 and 80 ^{o}C, even under more dilute conditions (Table 8.3, Entries 1 and 2). We believe that at lower temperatures, the intermolecular branching reactions become more competitive with the desired intramolecular cyclization reactions that require higher temperatures to overcome the energy of activation for the cyclization. The amount of intermolecular branching reactions increased with the increasing monomer concentration giving rise to polymers with higher polydispersities (Table 8.3, Entry 3). When the polymerizations at 70 and 80 ^{o}C were compared, faster rates of polymerization were observed at 80 ^{o}C as evidenced by the shorter polymerization times (Table 8.3, Entries 4-6) and the first-order rate plots (Figure 8.6). Both polymerizations proceeded in a controlled manner; polydispersities were low and comparable, the molecular weights increased with conversions linearly. Inhibition time, as expected, decreased with increasing temperature. Finally, when the polymerization temperature was increased further to 90 ^{o}C, higher molecular weight distributions were obtained indicating a less controlled RAFT process (Table 8.3, Entry 7). This is most probably due to the changing equilibrium constants involved in the RAFT process.

As a result, similar to the ATRP cyclopolymerization of TBHMA ether dimer, an optimum temperature (70-80 ^{o}C) range seems to exist for the RAFT cyclopolymerization as well.

Table 8.3. Effect of temperature on the RAFT cyclopolymerization of TBHMA ether dimer in xylene.[a,b]

Entry	[M]:[CDB]	[M] (mol/L)	Temp. (^{o}C)	Time (h)	Conv.[c] (%)	$M_{n,theo}$ (10^3 g/mol)	$M_{n,sec}$ (10^3 g/mol)	M_w/M_n[d]
1	100:1	0.75	60	7	9.6	3.1	2.7	1.50
2	100:1	0.75	60	29	83.6	25.2	22.3	1.78
3	200:1	1.5	60	3	5.2	3.4	5.1	3.20
4	100:1	1	70	2	42.0	12.8	9.2	1.32
5	100:1	1	80	1	49.0	14.9	13.3	1.30
6	100:1	1	80	2	80.9	24.4	24.0	1.45
7	100:2	1	90	2	85.6	13.0	15.1	2.23

[a]Conditions: [CDB]/[AIBN]=1:0.25, TBHMA= *tert*-butyl α-(hydroxymethyl)acrylate; M= monomer, CDB= cumyl dithiobenzoate, AIBN=2,2'-azobis(isobutyronitrile). [b]All polymers were entirely soluble in methylene chloride. [c]Measured by gravimetric methods. [d]Molecular weight distribution (M_w/M_n) was measured by size exclusion chromatography (SEC).

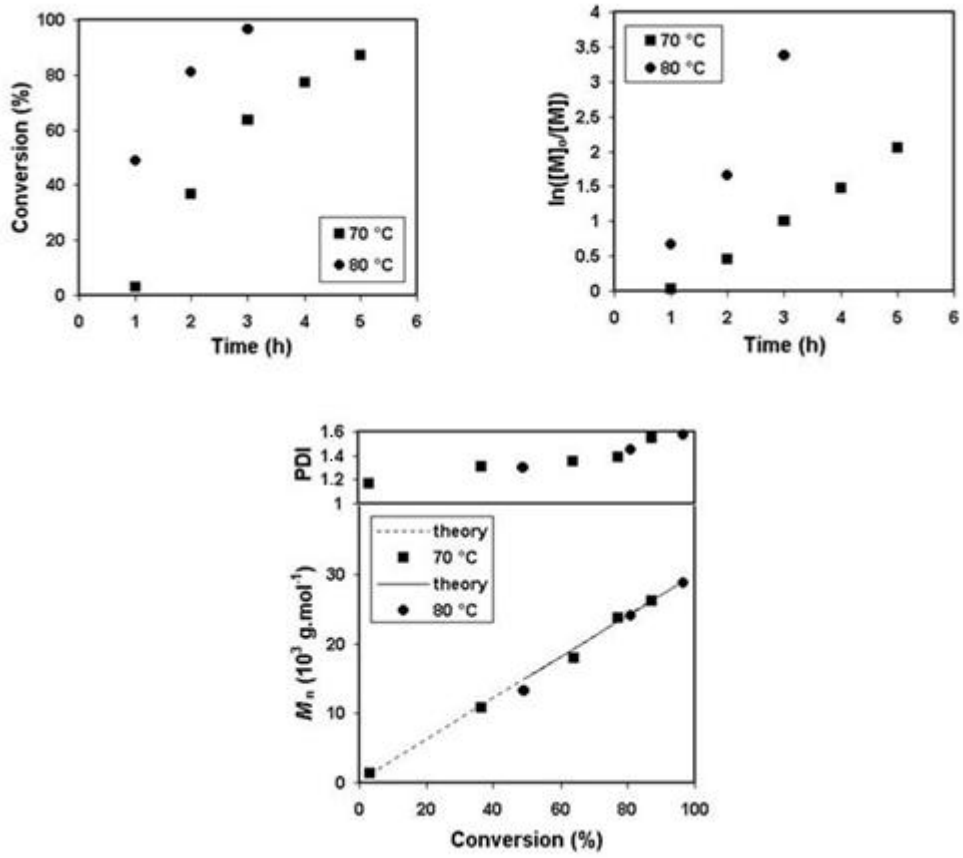


Figure 8.6. Kinetic studies of the RAFT cyclopolymerization of TBHMA ether dimer in xylene at 70 and 80 ^{o}C ([M]=1 mol.L^{-1}; [M]/[CDB]/[AIBN]=100:1:0.25; TBHMA=*tert*-butyl α-(hydroxymethyl)acrylate, M=monomer, CDB=cumyl dithiobenzoate, AIBN=2,2'-azobis(isobutyronitrile)).

8.4. The Effect of Ester Substituent on the RAFT Cyclopolymerization System: The Importance of Apparent and Effective Bulkiness

Optimum conditions on RAFT cyclopolymerization of *tert*-butyl monomer by using CDB as RAFT agent and AIBN as initiator can be summarized as follows:

- [M] = 1M
- [CDB]:[AIBN]=4:1
- Temperature = 70-80 ^{o}C

Therefore, in order to compare the results, monomers with different ester substituents were polymerized under the same conditions to see the effect of ester substituent on the RAFT cyclopolymerization system.

8.5. RAFT Polymerization of the Monomers with Primary Central Ester Carbon

In the RAFT polymerization of monomers with primary ester substituents, ethyl and *n*-butyl derivatives were used. Apparent bulkiness was decreased in addition to effective bulkiness when compared to the *tert*-butyl derivative.

Ethyl and n-butyl monomers gave fully crosslinked insoluble polymers at 80 ^{o}C, which indicated that these groups were not large enough to supress the alternative intermolecular monomer addition pathway which is responsible for the crosslinking (Table 8.4, Entries 1,2).

Table 8.4. Results from the RAFT polymerization of EHMA and BHMA ether dimers in xylene at 80 ^{o}C.[a,b]

Entry	R group	Temp. (^{o}C)	Time (h)	Conv. (%)	$M_{n,theo}$ (10^3 g/mol)	$M_{n,sec}$ (10^3 g/mol)	M_w/M_n
1	Ethyl	80	2	x-linked	x-linked	x-linked	x-linked
2	*n*-Butyl	80	2	x-linked	x-linked	x-linked	x-linked

[a]Conditions: [M]:[CDB]=100:1; [CDB]/[AIBN]=1:0.25; [M]=1M in xylene; EHMA= ethyl α-(hydroxymethyl)acrylate, BHMA= *n*-butyl α-(hydroxymethyl)acrylate; M=monomer, CDB=cumyl dithiobenzoate, AIBN=2,2'-azobis(isobutyronitrile). [b]All polymers were insoluble in methylene chloride.

8.6. RAFT Polymerization of the Monomers with Secondary Central Ester Carbon

In the RAFT polymerization of monomers with secondary ester substituents, cyclohexyl and isobornyl derivatives were used. The effective bulkiness was decreased, but apparent bulkiness was increased in compared to the *tert*-butyl derivative. Within the

same effective bulkiness, cyclohexyl group has lower apparent bulkiness than isobornyl group.

8.6.1. RAFT Cyclopolymerization of the CHHMA Ether Dimer

In the RAFT cyclopolymerization of cyclohexyl monomer at 70 ^{o}C, crosslinked insoluble polymer was obtained after two hours (Table 8.5, Entry 2). Cyclizations were not efficient because the bulkiness most probably did not provide enough steric crowding to suppress the intermolecular addition pathway at 70 ^{o}C.

At 80 ^{o}C, soluble polymers were obtained, even at high monomer conversions, which indicates that cyclization efficiency increased with increasing temperature, but obtained polymers had high polydispersities (Table 8.5, Entries 3-5).

Table 8.5. Results from the RAFT polymerization of CHHMA ether dimer in xylene.[a]

Entry	[M]:[CDB]	Temp. (^{o}C)	Time (h)	Conv.[b] (%)	$M_{n,theo}$ (10^3 g/mol)	$M_{n,sec}$ (10^3 g/mol)	M_w/M_n[c]
1	50:1	70	1	84.5	15.1	21.3	2.76
2	50:1	70	2	x-linked	x-linked	x-linked	x-linked
3	100:1	80	1	45.2	16.1	14.7	1.56
4	100:1	80	1.5	66.3	23.5	21.0	1.63
5	100:1	80	2.5	87.3	30.8	27.8	2.17

[a]Conditions: [CDB]/[AIBN]=1:0.25; [M]=1M in xylene; CHHMA= cyclohexyl α-(hydroxymethyl)acrylate; M=monomer, CDB=cumyl dithiobenzoate, AIBN=2,2'-azobis(isobutyronitrile). [b]Measured by gravimetric methods. [c]Molecular weight distribution (M_w/M_n) was measured by size exclusion chromatography (SEC).

^{1}H-NMR spectrums of the polymers obtained at 80 ^{o}C clearly show the presence of pendent double bonds (Figure 8.7). Therefore, the high polydispersities at 80 ^{o}C can be due to incomplete cyclizations and thus branching.

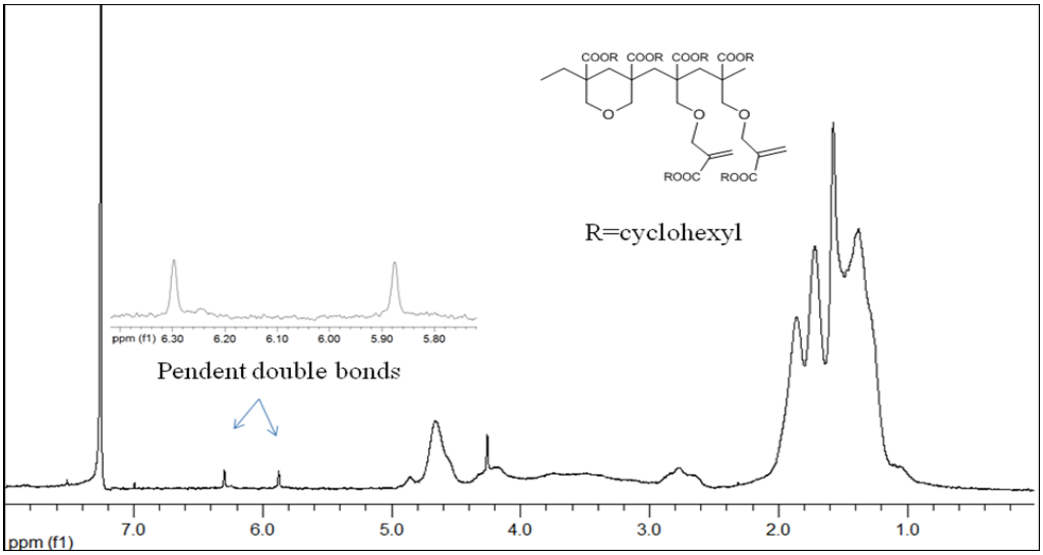


Figure 8.7. ^{1}H-NMR spectrum of poly(CHHMA ether dimer) obtained by RAFT polymerization at 80 ^{o}C.

8.6.2. RAFT Cyclopolymerization of the IBHMA Ether Dimer

In the RAFT polymerization of isobornyl monomer at 70 ^{o}C, soluble polymers were obtained (Table 8.6, Entries 1-3). These results indicated that within the same effective bulkiness compared to cyclohexyl, cyclization efficiency increased with increasing apparent bulkiness. As mentioned previously, at 70 ^{o}C, cyclohexyl monomer resulted in crosslinking.

In the ^{1}H-NMR spectrums of the polymers obtained at 70 ^{o}C, there was no evidence of pendent double bonds, which indicates that cyclizations were efficient (Figure 8.8).

Polydisperties of the polymers were relatively low. However, polymerizations were less controlled when compared to the polymerizations of *tert*-butyl monomer. Polymerization rate increased with increasing temperature and higher PDI polymers were obtained (Table 8.6, Entries 4,5). The source of the high polydispersities in the case of isobornyl derivative polymers seems to be changing equilibrium constants in the RAFT process.

Table 8.6. Results from the RAFT polymerization of IBHMA ether dimer in xylene.[a,b]

Entry	[M]:[CDB]	Temp. (^{o}C)	Time (h)	Conv.[c] (%)	$M_{n,theo}$ (10^3 g/mol)	$M_{n,sec}$ (10^3 g/mol)	M_w/M_n[d]
1	50:1	70	2	43.5	20.2	20.0	1.34
2	50:1	70	3	49.4	22.9	25.7	1.40
3	100:1	70	4	53.7	24.9	26.9	1.47
4	100:1	80	2	56.7	26.2	24.1	1.51
5	100:1	80	3	74.8	34.5	26.7	1.65

[a]Conditions: [CDB]/[AIBN]=1:0.25; [M]=1M in xylene; IBHMA= isobornyl α-(hydroxymethyl)acrylate; M= monomer, CDB= cumyl dithiobenzoate, AIBN=2,2'-azobis(isobutyronitrile). [b]All polymers were entirely soluble in methylene chloride. [c]Measured by gravimetric methods. [d]Molecular weight distribution (M_w/M_n) was measured by size exclusion chromatography (SEC).

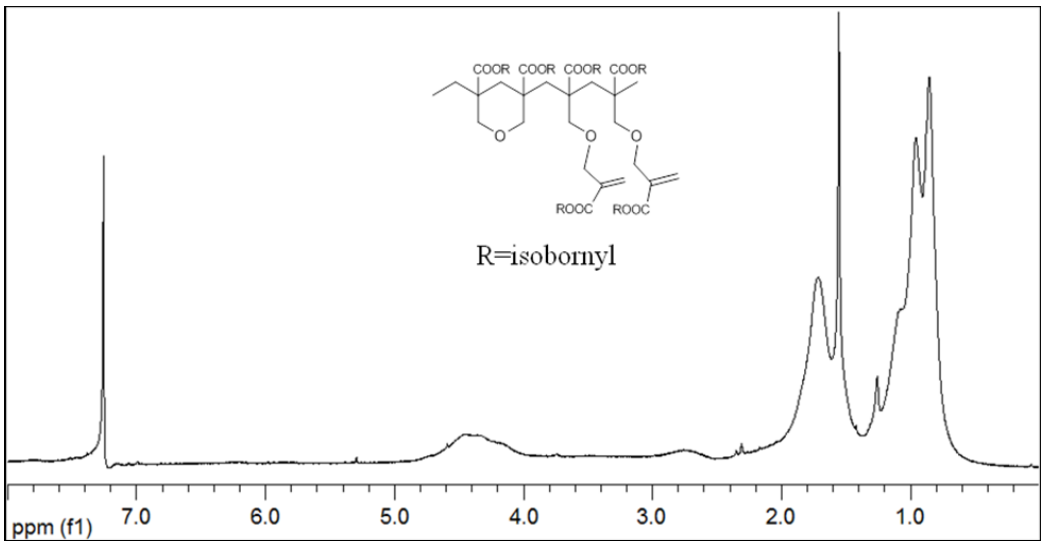


Figure 8.8. ^{1}H-NMR spectrum of poly(IBHMA ether dimer) obtained by RAFT polymerization at 70 ^{o}C.

8.7. Block Copolymerization Studies

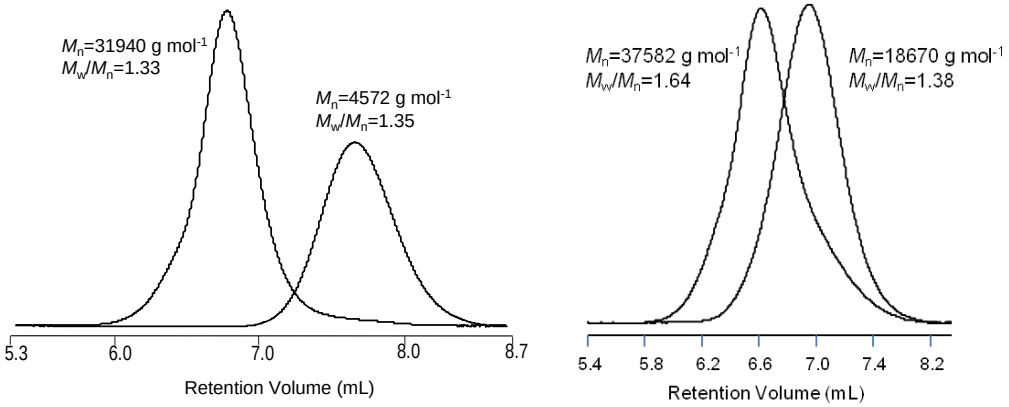
The livingness of the cyclopolymer end groups were investigated through chain extension/block copolymerization studies where the cyclopolymers obtained were used as

macroCTAs. The block copolymerizations were carried out at 60 ^{o}C in bulk with *n*-butyl acrylate (*n*-BA) as the co-monomer (Table 8.7). SEC traces of the block copolymers showed unimodal molecular weight distributions with no evidence of unreacted macroCTA (Figure 8.9), which proved the high efficiency of the macroCTA, and thus the livingness of the cyclopolymers obtained by the RAFT technique. Changing the [macroCTA]/[AIBN] ratio from 1:0.50 to 1:0.25 (Table 8.7, Entry 5) had no significant effect on the polydispersities obtained, but the copolymerization rate was slightly lower than the ones carried out at 1:0.50 [macroCTA]/[AIBN] ratio (Table 8.7, Entry 3) as evidenced by the lower molecular weights obtained at similar copolymerization times.

Table 8.7. Synthesis of block copolymers in bulk using the TBHMA ether dimer and IBHMA ether dimer derived cyclopolymers as the macroCTAs and *n*-butyl acrylate as the co-monomer.[a,b]

Entry	macroCTA			block copolymer		
	Polymer R-	$M_{n,sec}$ (g/mol)	M_w/M_n	Time (h)	$M_{n,sec}$ (g/mol)	M_w/M_n [c]
1	*tert*-butyl	4561	1.30	6	92272	1.55
2	*tert*-butyl	4572	1.35	1	6023	1.28
3	*tert*-butyl	4572	1.35	2	25864	1.37
4	*tert*-butyl	4572	1.35	4	31940	1.33
5	*tert*-butyl	5297	1.33	2	20835	1.37
6	isobornyl	18670	1.38	2	37582	1.64
7	isobornyl	13951	1.35	2	26211	1.59

[a]Conditions: [macroCTA]/[AIBN]=1:0.50 for entries 1-4, 6-7 and [macroCTA]/[AIBN]=1:0.25 for entry 5; Temp=60 ^{o}C; TBHMA= *tert*-butyl α-(hydroxymethyl)acrylate; IBHMA= isobornyl α-(hydroxymethyl)acrylate; AIBN=2,2'-azobis(isobutyronitrile). [b]All polymers were entirely soluble in methylene chloride. [c]Molecular weight distribution (M_w/M_n) was measured by size exclusion chromatography (SEC).



(a) (b)

Figure 8.9. Size-exclusion chromatography (SEC) traces of the copolymerization studies in bulk using *tert*-butyl (a) and isobornyl (b) α-(hydroxymethyl)acrylate ether dimers derived cyclopolymers as the macroCTA and *n*-butyl acrylate as the co-monomer (Table 8.7, Entries 4 and 6).

8.8. Antibacterial Properties of the Cyclopolymers

An antibacterial compound is a compound or substance that kills or slows down the growth of bacteria. There are two types of bacteria; Gram-positive and Gram-negative bacteria. The Gram-positive bacteria cell wall appears as a thick, dense wall 20-80 nm thick and consisting of numerous interconnecting layers of peptidoglycan. Chemically, 60 to 90 % of gram-positive bacteria cell wall is peptidoglycan. The Gram-negative cell wall, on the other hand, contains only 2-3 layers of peptidoglycan and is surrounded by an outher membrane composed of phospholipids, lipopolysaccharide, lipoprotein and proteins. Only 10-20 % of the gram-negative cell wall is peptidoglycan [89-91].

There are several factors that affect the antibacterial activities of the polymers such as [92];

- Constitution
- 3D structure
- Molecular weight

- Concentration
- Hydrophobicity
- Bacteria type

In the literature, it is known that tetrahydropyran (THP) and/or tetrahydrofuran (THF) rings as hydrophobic groups on the polymer chain play a significant role in the biological activity of the polymers [93, 94]. Since the obtained cyclopolymers contain tetrahydrofuran rings, their antibacterial activities were investigated. Cyclopolymers that contain cyclic ether rings as hydrophobic groups together with carboxyl or thiocarbonyl as hydrophilic groups along the polymer chain can exhibit biological activities.

The screening of the obtained controlled cyclopolymers from RHMA ether dimers for antibacterial activity was done using *S. Aureus* and *E. Coli* as test organisms because they represent gram-positive and gram-negative bacteria, respectively. *S. Aureus* and *E. Coli* are also two of the most common nosocomial (originating in a hospital) pathogens. The tests were done at Sabanci University by PhD. student Gonul Kendirci and Dr. Alpay Taralp. The test results are summarized in Table 8.8.

In the controlled cyclopolymers with *tert*-butyl group, the results of antibacterial tests that were done with the same solvent (dichloromethane or tetrahydrofurane) showed that antibacterial activity increased with increasing molecular weight (Table 8.8, entries 1,2 or entries 3,4), which may come from incerasing hydrophobic interactions between cyclopolymer and lipid layer of the cell wall. However, a similar trend could not be established when the results obtained by different solvents were compared (Table 8.8, entries 2, 3 or 2,4 or 1,3). The reason of this may be the differences between the arrangement of the polymer chains and pendent groups of the polymer films formed during evaporation of the two different solvents. The reducing polymer concentrations resulted in the reduction of antibacterial properties. At 10 ppm, none of the cyclopolymers showed antibacterial activity.

Most importantly, the cyclopolymer with tert-butyl group obtained by conventional radical polymerization (Table 8.8, entry 8) and the RAFT agent (CDB) alone showed no antibacterial property. Therefore, it can be considered that the antibacterial activities of the

controlled cyclopolymers obtained by the RAFT process can come from the synergy between the cyclopolymer and thiocarbonylthio end groups. Hydrophobic cyclic units may provide diffusion through the cell and thiocarbonylthio groups may act as the active groups.

Table 8.8. Antibacterial activities of the cyclopolymers.

Entry	poly(RHMA ether dimer)		% inhibation rate						solvent
			at 1000 ppm		at 100 ppm		at 10 ppm		
	R-	$M_{n,sec}$ (g/mol)	*S.aerous*	*E.coli*	*S.aerous*	*E.coli*	*S.aerous*	*E.coli*	
1	*tert*-butyl	5266	65-70	65-70	<15	<20	<15	<20	DCM
2	*tert*-butyl	10762	85-90	85-90	55-60	60-65	<15	<15	DCM
3	*tert*-butyl	14513	40-45	-	<15	-	<15	-	THF
4	*tert*-butyl	21526	70-75	-	45-50	-	<15	-	THF
5	isobornyl	11231	80-85	85-90	45-50	55-60	<15	<15	DCM
6	isobornyl	14885	75-80	-	45-50	-	<15	-	THF
7	isobornyl	22540	70-75	-	45-50	-	<15	-	THF
8	*tert*-butyl[a]	57500	<15	<20	<15	<20	<15	<20	DCM
9	CDB	-	<15	-[b]	<15	-	<15	-	THF

[a]Polymer was synthesized by conventional radical polymerization. [b] "-": not determined.

In the controlled cyclopolymers with isobornyl group, antibacterial activity was also observed at 1000 ppm, but there was no significant change in antibacterial properties of the cyclopolymers at different molecular weights (Table 8.8, entries 6,7). This may be due to more bulky and hydrophobic nature of the isobornyl derivative in compared to the *tert*-butyl derivative. The threshold molecular weight for an effective interaction might be reached at lower molecular weight (i.e>11000 g/mol), above which the molecular weight effect becomes less significant. The reducing polymer concentrations resulted in the reduction of antibacterial properties. At 10 ppm, none of them showed antibacterial activity.

9. EXPERIMENTAL SECTION

9.1. Materials

Xylenes *extra pure* (mixture of isomers, Merck) was purified by distillation over Na and benzophenone. *tert*-Butyl acrylate (Acros Organics, 99%), isobornyl acrylate (Fluka, 99%), ethyl acrylate (Fluka, 99%), n-butyl acrylate (Fluka, ≥99%), acryloyl chloride (Merck, 96%), cyclohexanol (Fluka, 99%), triethylamine (TEA) (Merck, >99%) paraformaldehyde (Sigma-Aldrich), 1,4-diazabicyclo[2.2.2]octane (DABCO) (Fluka, ≥ 95.0%), *tert*-butyl alcohol (Merck, 99%), benzyl chloride (Acros Organics, 99.5+%), elemental sulfur (Acros Organics, 99.5+%), sodium methoxide (Acros Organics, 30 wt % solution in methanol), α-methylstyrene (Acros Organics, 99%) were used as received without any purification. *N,N'*-azobis(isobutyronitrile) (AIBN) was recrystallized from ethanol. All glassware, needles, and stirring bars were dried overnight in an oven at 150 ^{o}C and purged with nitrogen before use.

9.2. Instrumentation

^{1}H-NMR and ^{13}C-NMR spectra were recorded on Varian 400-MHz NMR spectrometer (Varian Associates, Palo Alto, CA). Size exclusion chromatograhy (SEC) analyses were done using a Viscotek GPCmax VE-2001 Analysis System with a PL Gel 5 μm MIXED-C column that was calibrated against polystyrene standards.

9.3. Synthesis of RAFT Agent (CDB)

CDB was synthesized according to the published literature [60, 87].

9.3.1. Step 1: Synthesis of Dithiobenzoic Acid (DTBA)

Sodium methoxide (30 % solution in methanol, 90 g, 0.5 mol) was put into 500 mL three-necked round bottom flask fitted with a magnetic stirring bar and additional funnel.

Anhydrous methanol (125 g) was added to the flask followed by rapid addition of elemental sulfur (32 g, 0.5 mol). Benzyl chloride (31.5 g, 0.25 mol) was then added dropwise via the additional funnel over a period of 1 hour, at room temperature under a dry nitrogen atmosphere. The reaction mixture was heated at 67 ^{o}C for 12 hours. After this time, the reaction mixture was cooled using an ice bath. The precipitated sodium dithiobenzoate salt was removed by vacum filtration. The salt was dissolved 250 mL deionized water. The solution was filtered a second time. The crude sodium dithiobenzoate solution was washed three times with 100 mL of diethyl ether. Then, 100 mL diethyl ether and 1 N HCl (250 mL) were added to the sodium dithiobenzoate solution. Dithiobenzoic acid was extracted into the ether layer. The solution was washed three times with 150 mL of deionized water. The organic layer was separated and solvent was evaporated under reduced pressure. Note that dithiobenzoic acid is unstable and should be used immediately or stored at low temperature.

9.3.2. Step 2: Synthesis of Cumyl Dithiobenzoate (CDB)

A mixture of dithiobenzoic acid (4.62 g, 0.03 mol), excess α-methylstyrene (3.65 g, 0.031 mol) was heated in 25 mL carbon tetrachloride at 70 ^{o}C for 4 hours. The solvent was evaporated under reduced pressure. Purification was done by flash chromatography on silica with n-hexane as eluent to give cumyl dithiobenzoate (CDB) as a dark puple oil. The purity was estimated by ^{1}H NMR to be >99 %, 19 % yield based on dithiobenzoic acid. ^{1}H NMR ($CDCl_3$), δ: 1.93 (s, 6H, C*H*$_3$), 7.23 (m, 1H, Ar*H*), 7.33 (m, 4H, Ar*H*), 7.47 (m, 1H, Ar*H*), 7.56 (dd, 2H, Ar*H*), 7.87 (dd, 2H, Ar*H*) ppm. ^{13}C NMR ($CDCl_3$), δ; 27.26 (*C*H$_3$C*C*H$_3$), 55.47 (CH$_3$*C*CH$_3$), 125.58 (Ar*C*), 125.60 (Ar*C*), 125.72 (Ar*C*), 127.02 (Ar*C*), 127.11 (Ar*C*), 127.29 (Ar*C*), 130.77 (Ar*C*), 143.15 (Ar*C*), 145.25 (Ar*C*), 227.38 (*C*=S) ppm.

9.4. Syntheses of Monomers

9.4.1. Synthesis of Ethyl α-(Hydroxymethyl) Acrylate (EHMA) Ether Dimer

Ethyl acrylate (25.0 g, 0.25 mol), paraformaldehyde (7.50 g, 0.25 mol) and 1,4-diazabicyclo[2.2.2]octane (DABCO) (1.95 g, 6.0 wt%) were added into a 50 mL three-

necked round-bottom flask fitted with a condenser and a magnetic stirrer. The mixture was stirred at 95 ^{o}C for 4 days. The reaction progress was monitored by TLC. The mixture was then diluted with 100 mL of hexane, washed three times with 50 mL of 3 % HCl, and then three times with 50 mL of water. The organic layer was separated and solvent was evaporated under reduced pressure to give crude monomer. Column chromatography on silica with methylene chloride: hexane (4:3) as eluent gave the pure monomer as a clear liquid in 42 % yield. ^{1}H NMR ($CDCl_3$), δ: 1.25 (t, 6H, C*H*$_3$), 4.16 (m, 4H, OC*H*$_2$CH$_3$) , 4.20 (s, 4H, OC*H*$_2$), 5.85 (s, 2H, C*H*=C), 6.26 (s, 2H, C*H*=C) ppm. ^{13}C NMR ($CDCl_3$), δ: 14.34 (*C*H$_3$), 60.88 (O*C*H$_2$CH$_3$), 69.07 (O*C*H$_2$), 125.75 (C=*C*H$_2$), 137.41 (CH$_2$=*C*), 165.92 (*C*=O) ppm.

9.4.2. Synthesis of *n*-Butyl α-(Hydroxymethyl) Acrylate (BHMA) Ether Dimer

n-Butyl acrylate (64.0 g, 0.50 mol), paraformaldehyde (15.0 g, 0.50 mol) and 1,4-diazabicyclo[2.2.2]octane (DABCO) (4.74 g, 6.0 wt %) were added to a 250 mL three-necked round bottom flask fitted with a condenser and a magnetic stirring bar. The mixture was stirred at 95 ^{o}C for 4 days. The reaction progress was monitored by TLC. The mixture was then diluted with 150 mL of methylene chloride, washed three times with 100 mL of 3 % HCl and three times with 100 mL of water. The organic layer was separated and solvent was evaporated under reduced pressure to give crude monomer. Vacuum distillation in the presence of a free-radical inhibitor, CuCl, gave the pure monomer as a clear liquid in 47 % yield. ^{1}H NMR ($CDCl_3$), δ: 0.90 (t, 6H, C*H*$_3$), 1.36 (m, 4H, OCH$_2$CH$_2$C*H*$_2$CH$_3$), 1.61 (m, 4H, OCH$_2$C*H*$_2$CH$_2$CH$_3$), 4.12 (t, 4H, OC*H*$_2$CH$_2$CH$_2$CH$_3$), 4.21 (s, 4H, OC*H*$_2$), 5.85 (s, 2H, C*H*=C), 6.26 (s, 2H, C*H*=C) ppm. ^{13}C NMR ($CDCl_3$), δ: 13.88 (*C*H$_3$), 19.37 (OCH$_2$CH$_2$*C*H$_2$CH$_3$), 30.80 (OCH$_2$*C*H$_2$CH$_2$CH$_3$), 64.79 (O*C*H$_2$CH$_2$CH$_2$CH$_3$), 69.09 (O*C*H$_2$), 125.72 (C=*C*H$_2$), 137.42 (CH$_2$=*C*), 165.99 (*C*=O) ppm.

9.4.3. Synthesis of *tert*-Butyl α-(Hydroxymethyl) Acrylate (TBHMA) Ether Dimer

t-Butyl acrylate (64.0 g, 0.50 mol), paraformaldehyde (15.0 g, 0.50 mol), 1,4-diazabicyclo[2.2.2]octane (DABCO) (2.50 g, 0.02 mol) and *t*-butyl alcohol (5.0 mL, 0.05 mol) were added to a 250 mL three-necked round bottom flask fitted with a condenser and magnetic stirring bar. The mixture was stirred at 95 ^{o}C for 4 days. The reaction progress

was monitored by TLC. The mixture was then diluted with 150 mL of methylene chloride, washed three times with 100 mL of 3 % HCl and three times with 100 mL of water. The organic layer was separated and solvent was evaporated under reduced pressure to give 63.9 g of crude monomer in 86 % yield. Column chromatography on silica with *n*-hexane:methanol (99:1) as eluent gave the pure monomer as a clear liquid in 57 % yield. ^{1}H NMR ($CDCl_3$), δ : 1.46 (s, 18H, C*H*$_3$), 4.17 (s, 4H, OC*H*$_2$), 5.78 (s, 2H, C*H*=C), 6.17 (s, 2H, C*H*=C) ppm. ^{13}C NMR ($CDCl_3$), δ : 28.26 (*C*H$_3$), 69.19 (O*C*H$_2$), 81.13 [*C*-(CH$_3$)$_3$], 124.69 (C=*C*H$_2$), 138.83 (CH$_2$=*C*), 165.26 (*C*=O) ppm.

9.4.4. Synthesis of Cyclohexyl α-(Hydroxymethyl) Acrylate (CHHMA) Ether Dimer

They were synthesized according to the literature [84].

Cyclohexyl acrylate. ^{1}H NMR ($CDCl_3$), δ: 1.25 (br, C*H*$_2$CH$_2$CHO, 2H), 1.32-1.48 (br, C*H*$_2$CH$_2$CH$_2$CHO, 2H), 1.55 (br, C*H*$_2$CH$_2$CHO, 2H), 1.72 (br, C*H*$_2$CHO, 2H), 1.86 (br, C*H*$_2$CHO, 2H), 4.82 (br, C*H*-O, 1H), 5.78 (dd, C*H*=CH$_2$, 1H), 6.11 (dd, C*H*$_2$=CH, 1H), 6.38 (dd, C*H*=CH$_2$, 1H) ppm. ^{13}C NMR ($CDCl_3$), δ: 23.95 (*C*H$_2$CH$_2$CHO), 25.59 (*C*H$_2$CH$_2$CH$_2$CHO), 31.81 (*C*H$_2$CH-O), 72.96 (*C*HO), 129.37 (*C*H=CH$_2$), 130.33 (*C*H$_2$=CH), 165.91 (*C*=O) ppm.

Cyclohexyl α-(Hydroxymethyl) Acrylate (CHHMA) Ester Ether Dimer. ^{1}H NMR ($CDCl_3$), δ: 1.18-1.50 (br, 12H, C*H*$_2$C*H*$_2$CH$_2$CHO), 1.70 (br, 4H, C*H*$_2$CHO), 1.82 (br, 4H, C*H*$_2$CHO), 4.24 (s, 4H, C*H*$_2$-O), 4.84 (br, 2H, C*H*-O), 5.86 (s, 2H, C*H*=CH), 6.26 (s, 2H, C*H*=CH) ppm. ^{13}C NMR ($CDCl_3$), δ: 23.80 (*C*H$_2$CH$_2$CHO), 25.63 (*C*H$_2$CH$_2$CH$_2$CHO), 31.72 (*C*H$_2$CHO), 69.22 (O*C*H$_2$), 73.07 (*C*H-O), 125.40 (C=*C*H$_2$), 138.00 (CH$_2$=*C*), 165.41 (*C*=O)ppm**.**

9.4.5. Synthesis of Isobornyl α-(Hydroxymethyl) Acrylate (IBHMA) Ether Dimer

They were synthesized according to the literature [84].

Isobornyl α-(Hydroxymethyl) Acrylate (IBHMA) Ether Dimer. ^{1}H NMR ($CDCl_3$), δ: 0.86 (s, 12H, C*H*$_3$), 1.02 (s, 6H, C*H*$_3$), 1.05-1.25 (m, 8H, C*H*$_2$C*H*$_2$), 1.57 (m, 2H,

C*H*CH_2), 1.7-1.9 (m, 4H, C*H*$_2$CHO), 4.24 (s, 4H, C*H*$_2$O), 4.75 (t, 2H, C*H*O), 5.87 (s, 2H, C*H*=CH), 6.27 (s, 2H, (C*H*=CH) ppm. ^{13}C NMR ($CDCl_3$), δ: 11.5 (*C*H_3), 19.9 (*C*H_3), 20.1 (*C*H_3), 27.0 (*C*H_2CH_2), 33.6 (*C*H_2C), 38.7 (*C*H_2CH), 45.0 (*C*HCH_2), 46.9 (*C*$(CH_3)_2$), 48.8 (*C*CH_3), 68.9 (*C*H_2O), 81.2 (*C*HO), 125.2 (*C*H_2=C), 137.5 (*C*=CH_2), 165.0 (*C*=O) ppm.

9.5. Syntheses of Polymers

9.5.1. Raft Solution Polymerization of TBHMA Ether Dimer (Table 8.1, Entry 3)

The monomer (5.03 g, 16.9 mol), CDB (45.9 mg, 0.169 mmol), AIBN (6.92 mg, 0.042 mmol) and 11.4 mL xylene were put in a round bottom flask fitted with a magnetic stirring bar. The flask was sealed with rubber septa and the solution was purged with nitrogen for 45 minutes. Then, the flask was immersed into a preheated oil bath at 70 ^{o}C. Polymerization was carried out under nitrogen for 2 hours. The final polymer was dissolved in 2 mL methylene chloride, precipitated into 60 mL of methanol/water (5/1, v/v) and dried in a vacuum oven overnight to give a pink powder (1.84 g, 36.6 % yield, $M_{n,sec}$=10.8x10^3, $M_{n,th}$=11.2x10^3 g/mol, $M_w/M_{n,sec}$=1.31). The theoretical molecular weight was calculated by the equation ($M_{n,th.}$)=(MW of Monomer)x(Conv.)x([M]/[CTA])+(MW of CTA).

In the ^{1}H-NMR characterization of poly(TBHMA ether dimer), the spectrum clearly shows characteristic aromatic peaks of CDB between 7-8 ppm.

In the ^{13}C-NMR characterization of poly(TBHMA ether dimer), the spectrum clearly shows characteristic peaks of backbone carbons, cyclic ether groups, and ester carbonyls. The backbone quaternary carbon peak is at 45.3 ppm and ether methylenes of the pyran units are at 71.0 ppm. The methyl and quaternary carbon peaks of the ester alkyls are at 28.1 and 82.1 ppm and the ester carbonyl is at 174.2 ppm.

^{1}H NMR ($CDCl_3$), δ: 1.40 (OC(C*H*$_3$)$_3$), 1.80 (*backbone* C*H*$_2$), 2.40-4.40 (m-br, *tetrahydropyran H*'s), 7.09 (Ar-*H*), 7.23 (Ar-*H*), 7.31 (Ar-*H*), 7.74 (Ar-*H*) ppm. ^{13}C NMR ($CDCl_3$), δ: 28.1 (OC(*C*H_3)$_3$), 45.3 (backbone *C*$_q$), 71.0 (O*C*H_2C_q), 82.1 (O*C*$(CH_3)_3$), 174.2 (C_q*C*OOC$(CH_3)_3$) ppm.

9.5.2. Conventional Free Radical Polymerization of TBHMA Ether Dimer (Table 8.1, Entry 12)

The monomer (2.01 g, 6.74 mmol), AIBN (11.0 mg, 0.067 mmol) and 4.6 mL xylene were put in a 25 mL single necked round bottom flask fitted with a magnetic stirring bar. The flask was sealed with rubber septa and the solution was purged with nitrogen for 45 minutes. Then, the flask was immersed into a preheated oil bath at 70 ^{o}C. Polymerization was carried out under nitrogen for 2 hours. The final polymer was dissolved in 2 mL methylene chloride, precipitated into 60 mL methanol/water (5/1, v/v) and dried in a vacuum oven overnight (1.71 g, 85.0 % yield, $M_{n,sec}$=57.5x10^3, $M_{n,th}$=25.5x10^3 g/mol, $M_w/M_{n,sec}$=2.75). The theoretical molecular weight was calculated by the equation ($M_{n,th.}$)=(MW of Monomer)x(Conv.)x([M]/[AIBN]).

^{1}H NMR, δ: 1.40 (OC(C*H*$_3$)$_3$), 1.85 (br, *backbone* C*H*$_2$), 2.40-4.40 (m-br, *tetrahydropyran H*'s) ppm.^{13}C NMR, δ: 28.1 (OC(*C*H$_3$)$_3$), 45.3 (backbone *C*$_q$), 71.0 (O*C*H$_2$C$_q$), 82.1 (O*C*(CH$_3$)$_3$), 174.2 (C$_q$*C*OOC(CH$_3$)$_3$) ppm.

9.5.3. Bulk Block Copolymerization of Poly(TBHMA Ether Dimer) with *n*-BA (Table 8.7, Entry 4)

The copolymerization was conducted in a single necked round bottom flask fitted with a stirring bar and which had been sealed with rubber septa and purged with nitrogen for 15 minutes. In a separate vial, the solid macroCTA poly(TBHMA ether dimer) ($M_{n,sec}$=4572 g/mol) (0.150 g, 0.033 mmol) and AIBN (2.7 mg, 0.016 mmol) was dissolved in 8 mL *n*-BA (7.20 g, 56.3 mmol). The solution was transferred to the reaction flask by syringe and degassed with nitrogen for 30 minutes. Then the flask was immersed into a preheated oil bath at 60 ^{o}C. Polymerization was carried out under nitrogen for 4 hours. The final polymer was dissolved in 2 mL methylene chloride, precipitated into 60 mL of methanol/water (5/1, v/v) and dried in a vacuum oven overnight (0.69 g, 7.5 % yield, $M_{n,sec}$=31940 g/mol, $M_w/M_{n,sec}$=1.33). The theoretical molecular weight was calculated by equation ($M_{n,th.}$)=(MW of *n*-BA)x(Conv.)x([*n*-BA]/[macroCTA])+(MW of macroCTA).

^{1}H NMR, δ : 0.86 (t, $OCH_2CH_2CH_2CH_3$), 1.30 (m, $OCH_2CH_2CH_2CH_3$), 1.40 (s-br, $OC(CH_3)_3$), 1.52 (br, $OCH_2CH_2CH_2CH_3$), 1.84 (br, backbone CH_2-CH), 2.21 (br, backbone CH_2-CH), 3.96 (t, $OCH_2CH_2CH_2CH_3$) ppm.^{13}C NMR, δ : 13.9 ($OCH_2CH_2CH_2CH_3$), 19.3 ($OCH_2CH_2CH_2CH_3$), 28.1 ($OC(CH_3)_3$), 30.8 ($OCH_2CH_2CH_2CH_3$), 34.5-36.8 (*n*-BA-backbone CH_2-CH) 41.6 (*n*-BA-backbone CH_2-CH), 45.3 (cyclopoymer backbone C_q), 64.6 ($OCH_2CH_2CH_2CH_3$), 82.1 ($OC(CH_3)_3$), 174.7 (COO) ppm.

9. CONCLUSIONS

The results indicate that the RAFT process was applied successfully to the synthesis of cyclopolymers with sixmembered tetrahydropyran repeat units using a diacrylate monomer such as the TBHMA ether dimer. An optimum polymerization temperature is attained around 70-80 ^{o}C, below and above which the controlled RAFT cyclopolymerization process becomes less efficient. Cyclopolymers with tunable molecular weights, low polydispersities, and most importantly, living end groups were obtained under tuned conditions.

RAFT cyclopolmerization system was affected by apparent and effective bulkiness of the ester substituents. The results can be summarized by the graph in Figure 9.1. When both apparent and effective bulkiness were low, cyclization efficency was lost. Effective bulkiness seems to be more important than apparent bulkiness for cyclization. Within the same effective bulkiness, with increasing apparent bulkiness, cyclization efficiency increases but the control of the polymerization is lost.

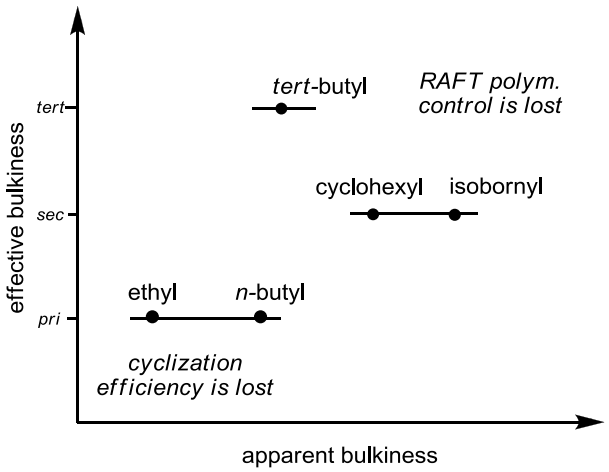


Figure 9.1. Summary on the effect of the apparent and effective bulkiness on the RAFT cyclopolymerization.

The cyclopolymers obtained from *tert*-butyl and isobornyl monomers showed living character that allowed the synthesis of block copolymers. The livingness of the cyclopolymers obtained may open new possibilities in the desing of new materials, especially targeting high temperature applications.

Finally, the antibacterial properties of controlled cyclopolymers were investigated by using *S. Aureus* and *E. Coli* as test organisms. Results indicated that cyclopolmers obtained by RAFT polymerization had antibacterial activity whereas RAFT agent and cyclopolmer obtained by conventional radical polymerization did not have any activities alone which indicate a potential synergy between the dithioester end groups and cyclopolymer chain.

APPENDIX A: SPECTROSCOPY DATA

^{1}H and ^{13}C NMR data for the synthesized compounds are given. Required regions of NMR data are expanded.

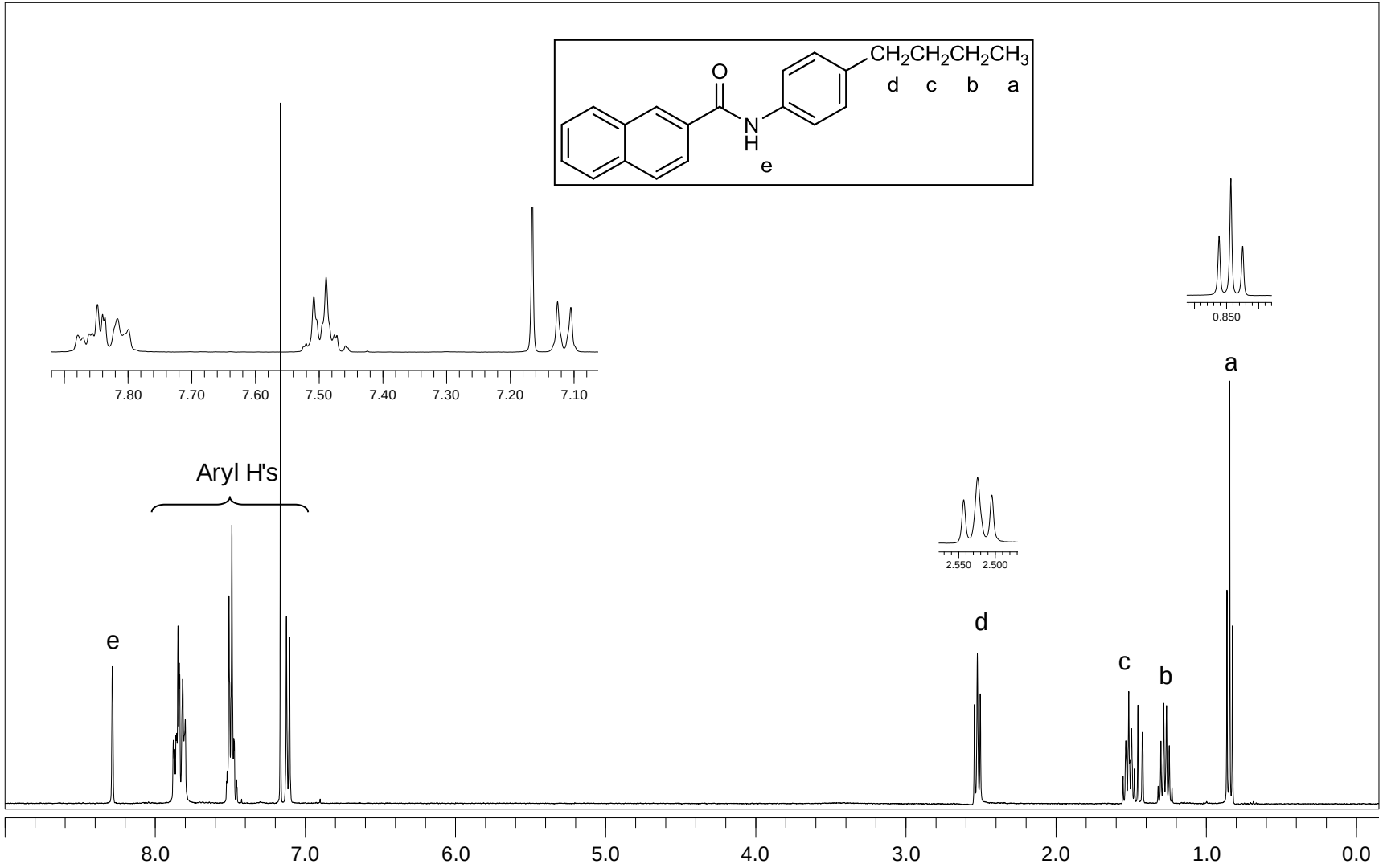


Figure A.1. ^{1}H-NMR ($CDCl_3$) spectrum of compound 6.

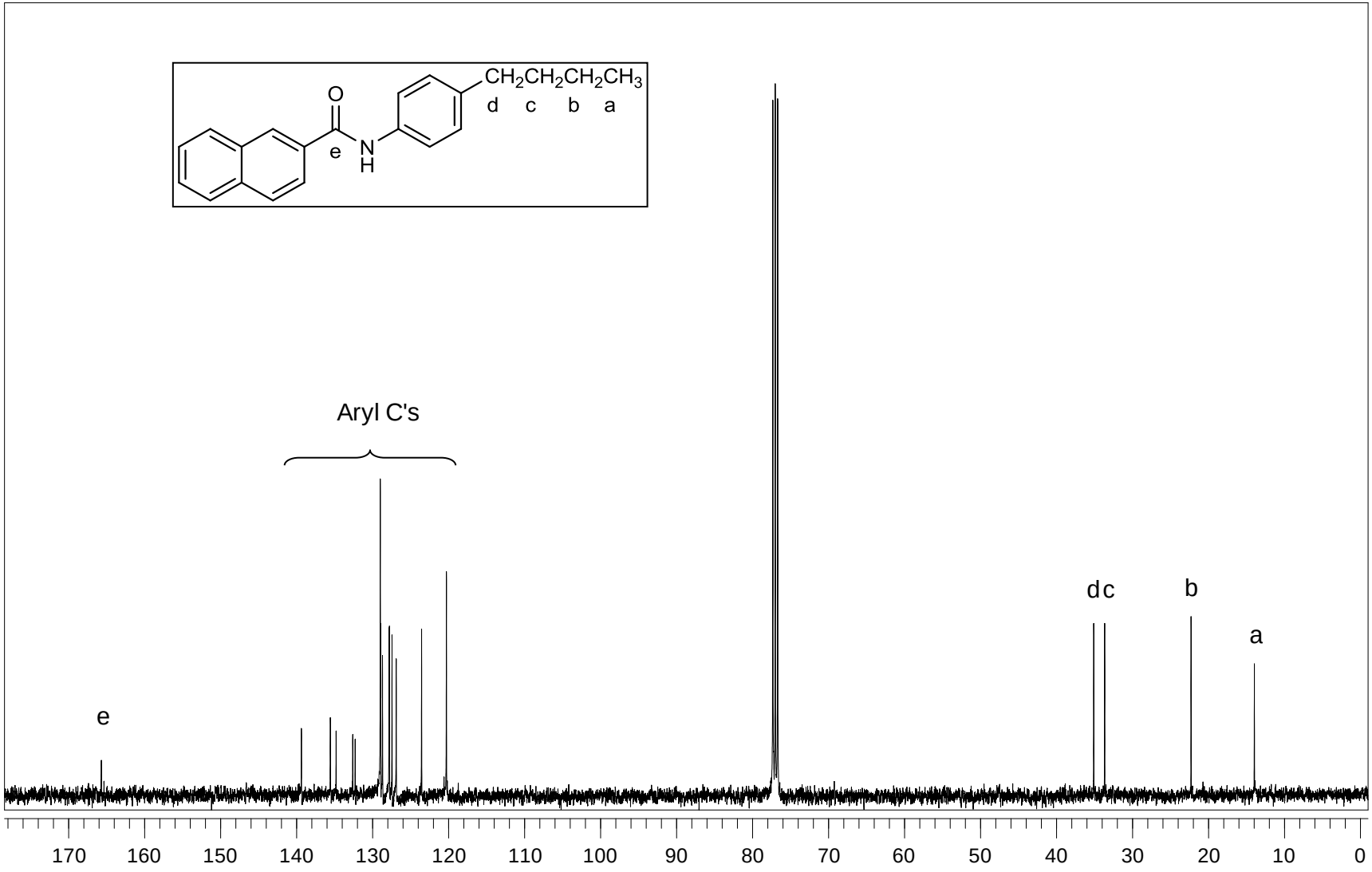


Figure A.2. ^{13}C-NMR ($CDCl_3$) spectrum of compound 6.

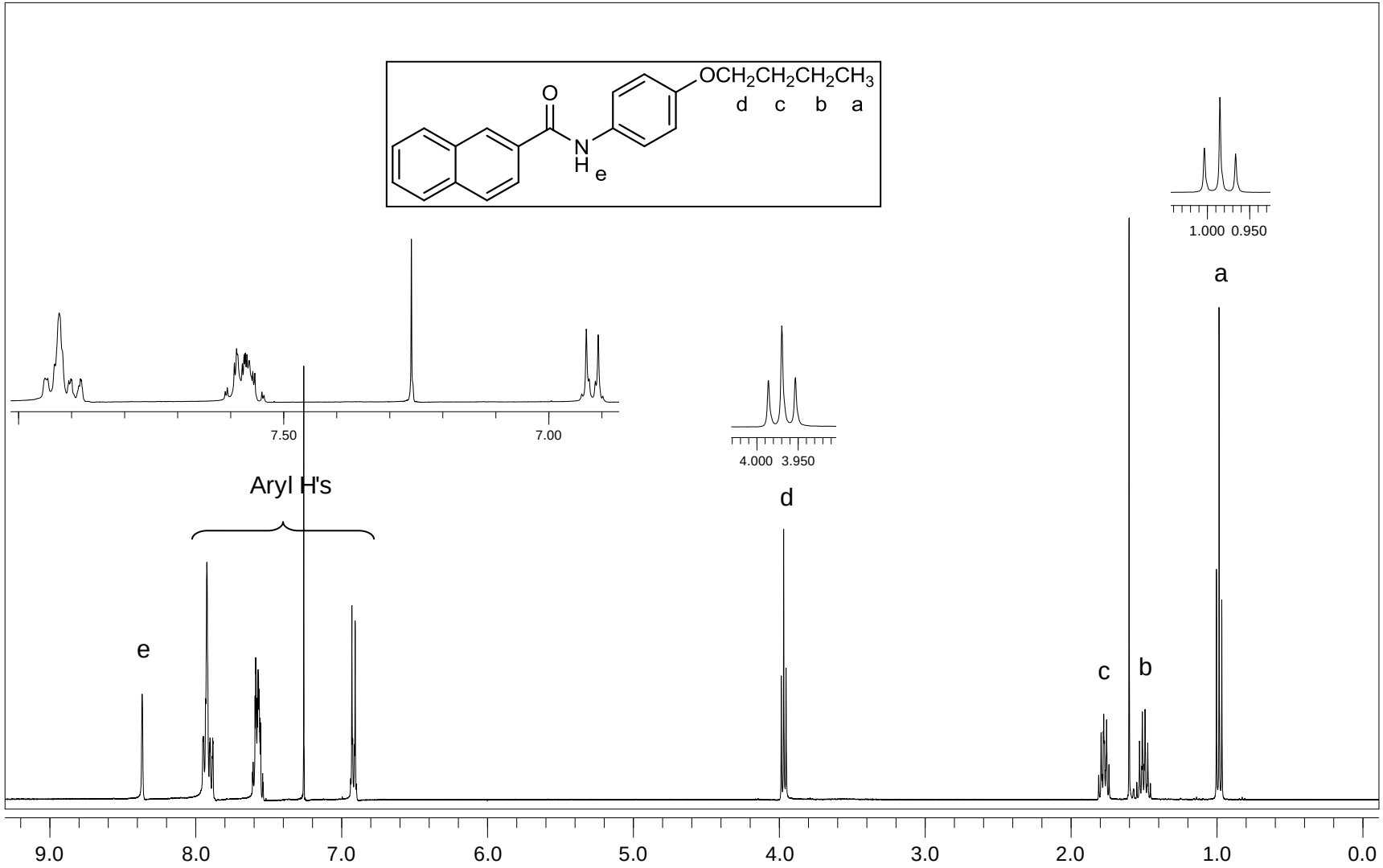


Figure A.3. ^{1}H-NMR ($CDCl_3$) spectrum of compound 7.

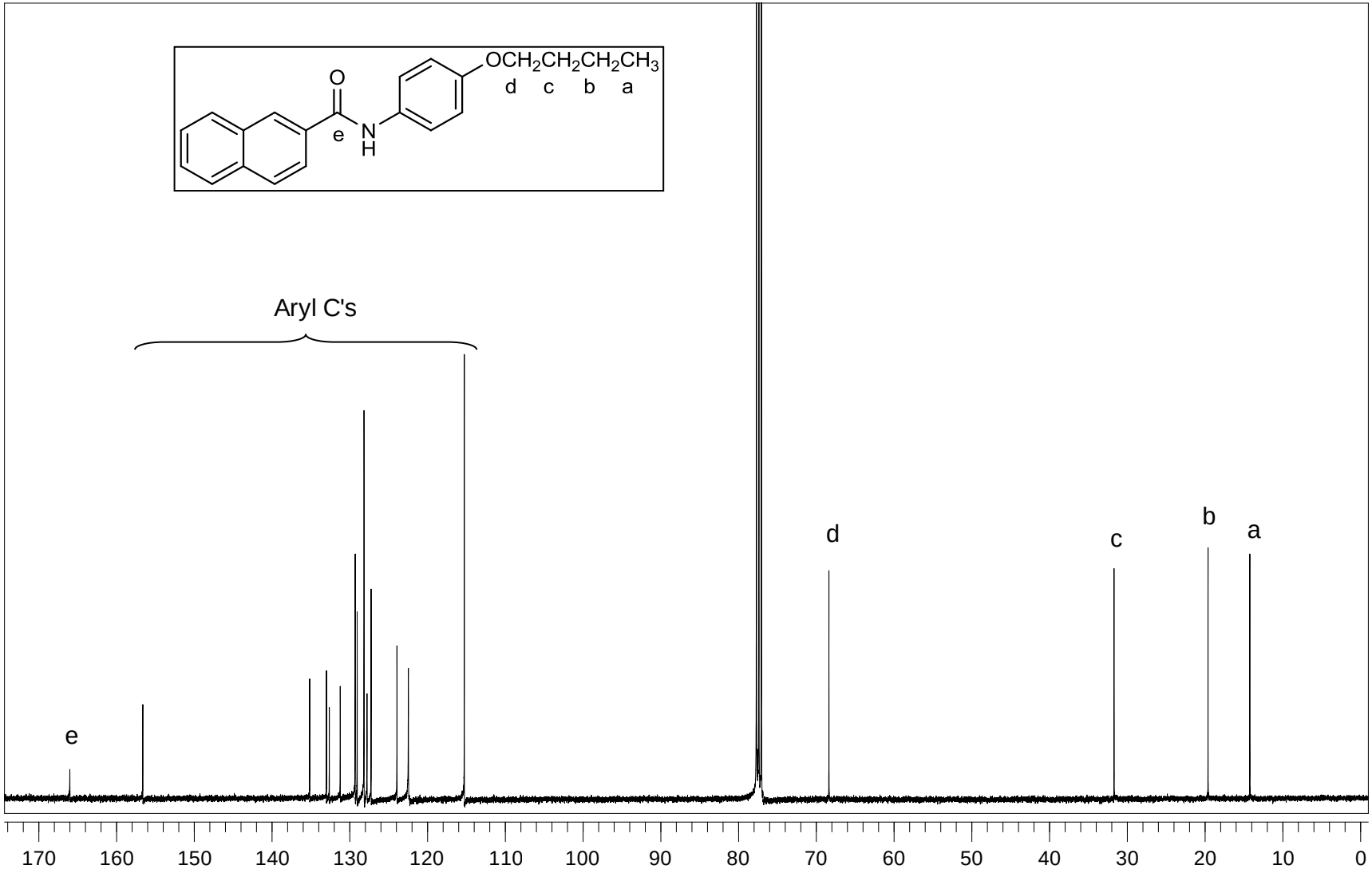


Figure A.4. ^{13}C-NMR ($CDCl_3$) spectrum of compound 7.

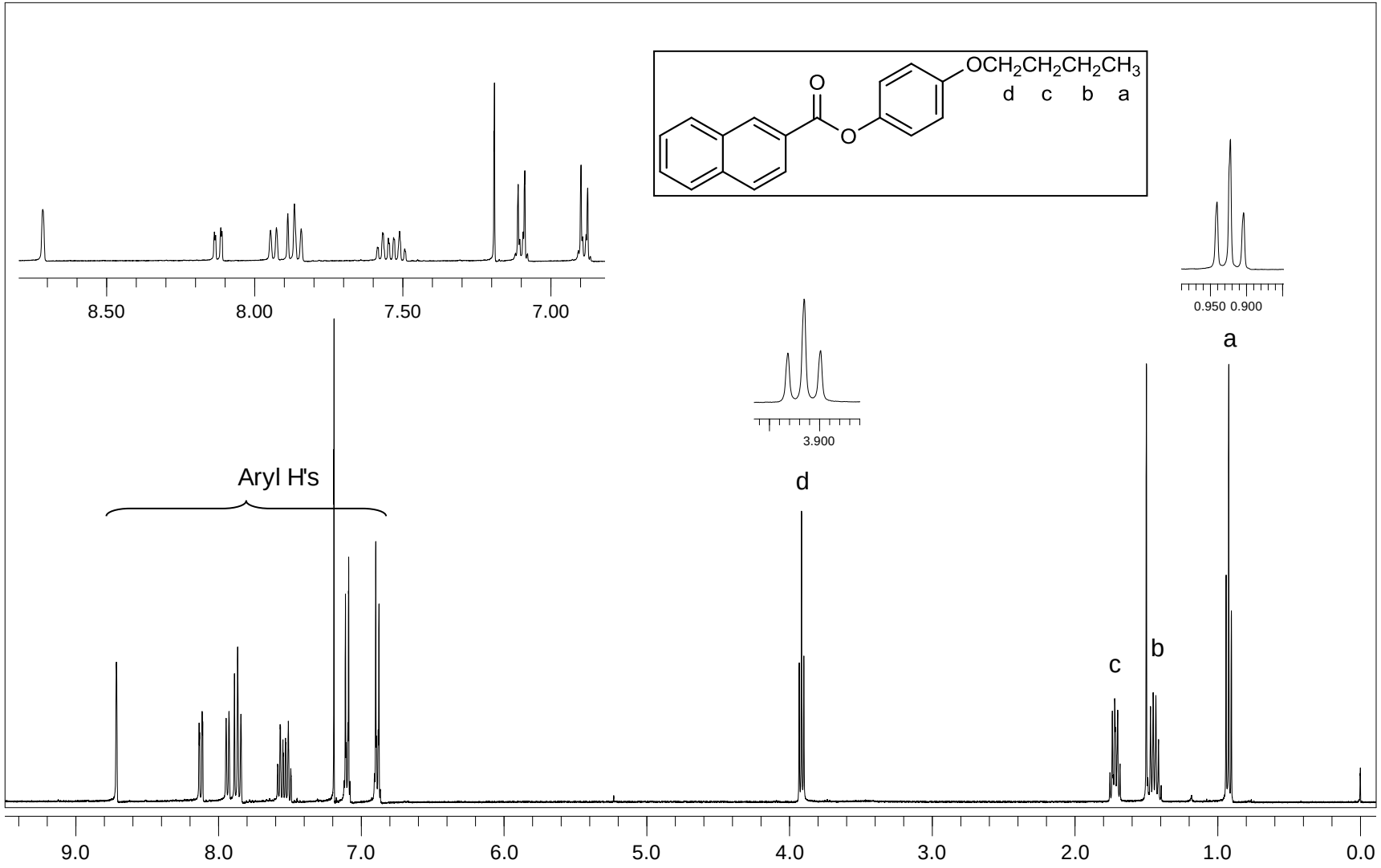


Figure A.5. ^{1}H-NMR ($CDCl_3$) spectrum of compound 8.

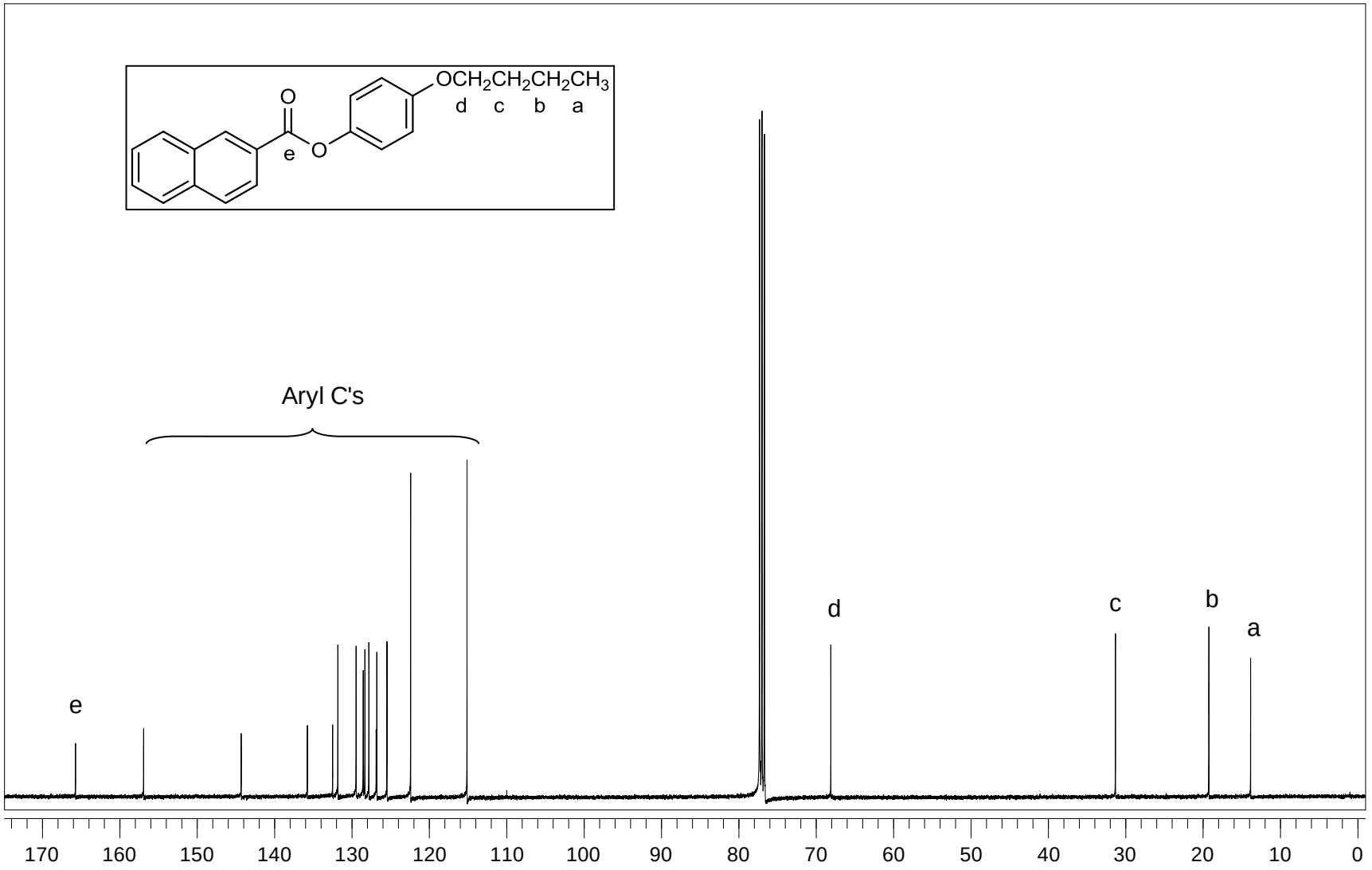


Figure A.6. ^{13}C-NMR ($CDCl_3$) spectrum of compound 8.

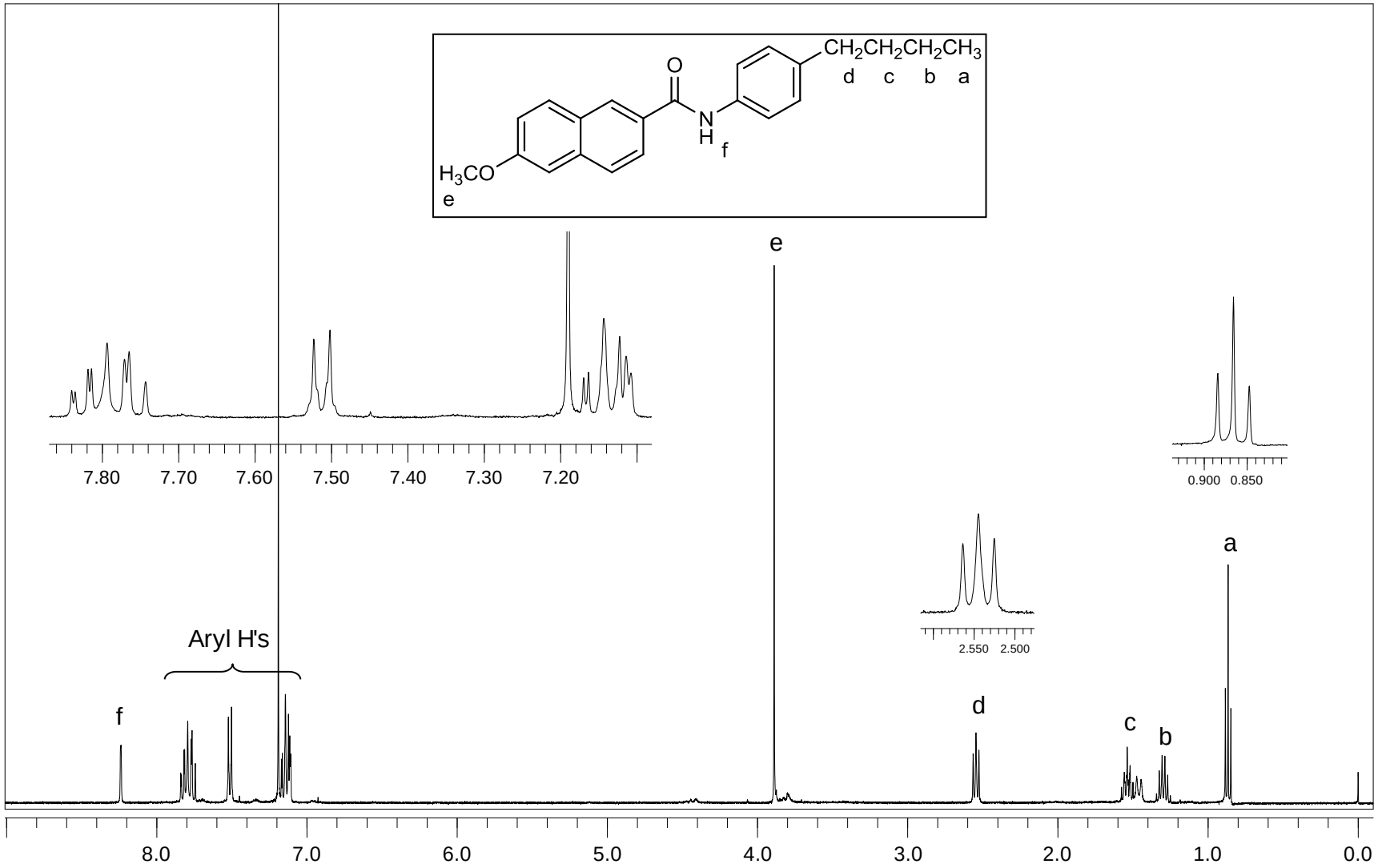


Figure A.7. ^{1}H-NMR ($CDCl_3$) spectrum of compound 10.

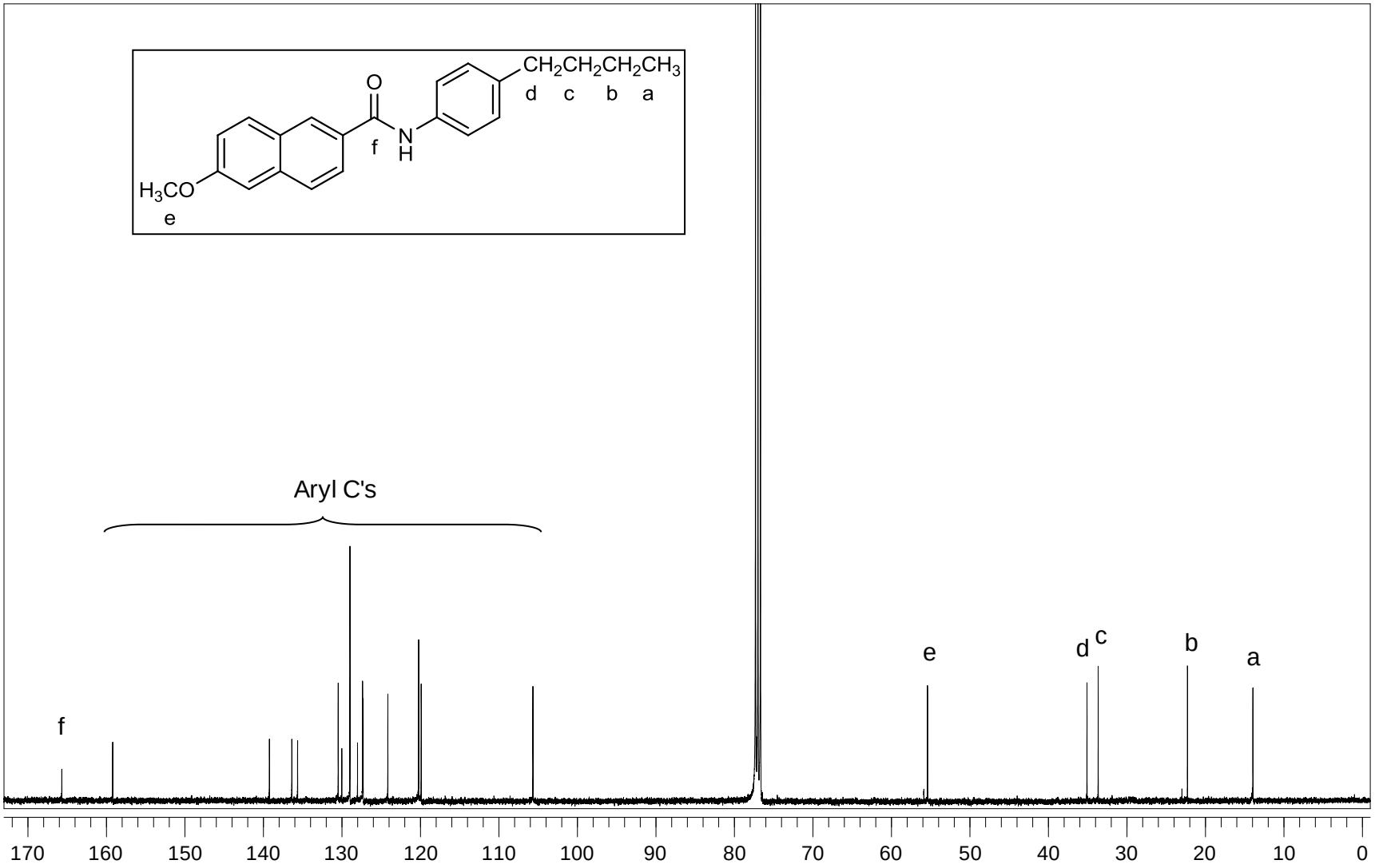


Figure A.8. ^{13}C-NMR ($CDCl_3$) spectrum of compound 10.

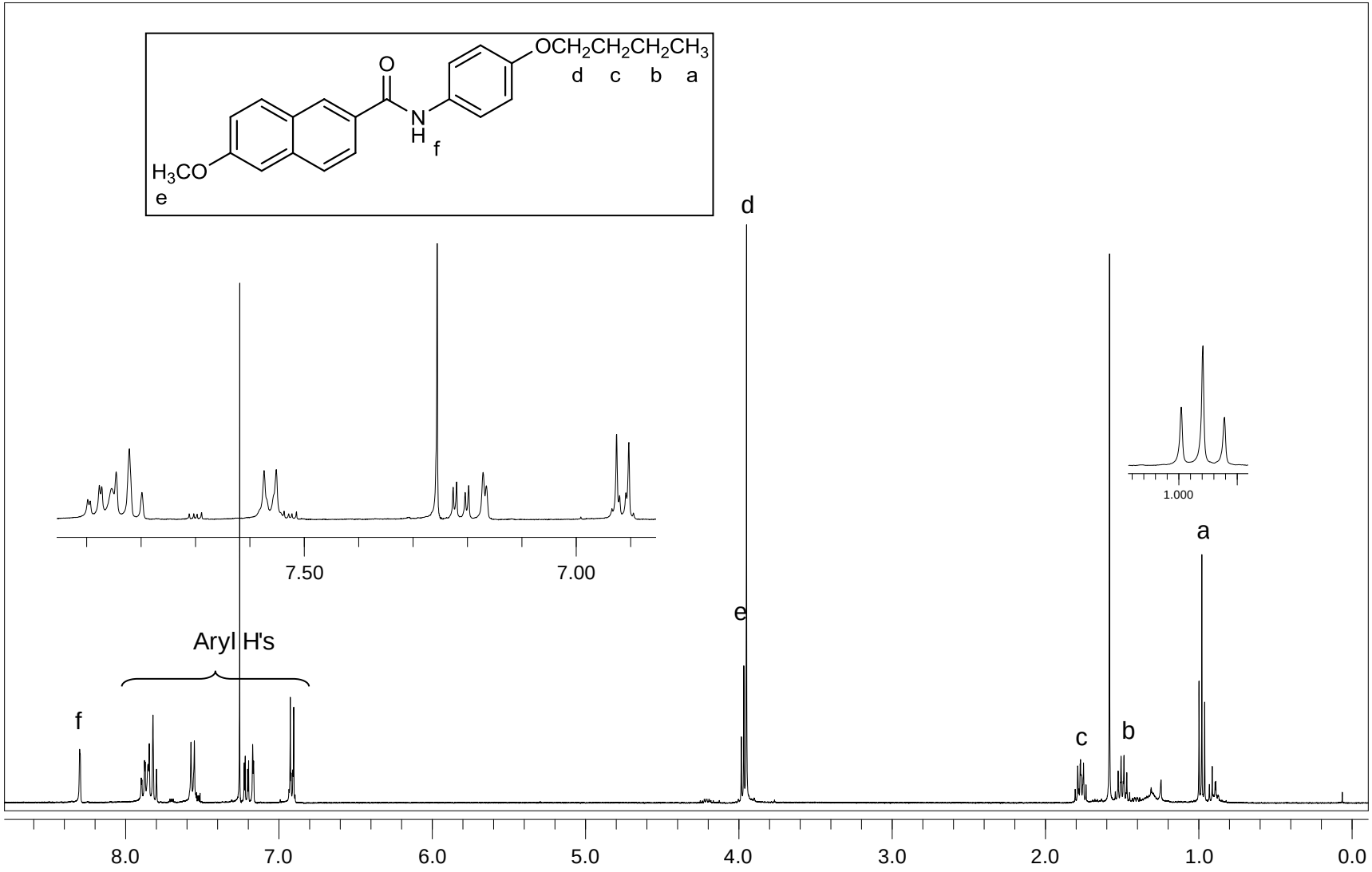


Figure A.9. ^{1}H-NMR ($CDCl_3$) spectrum of compound 11.

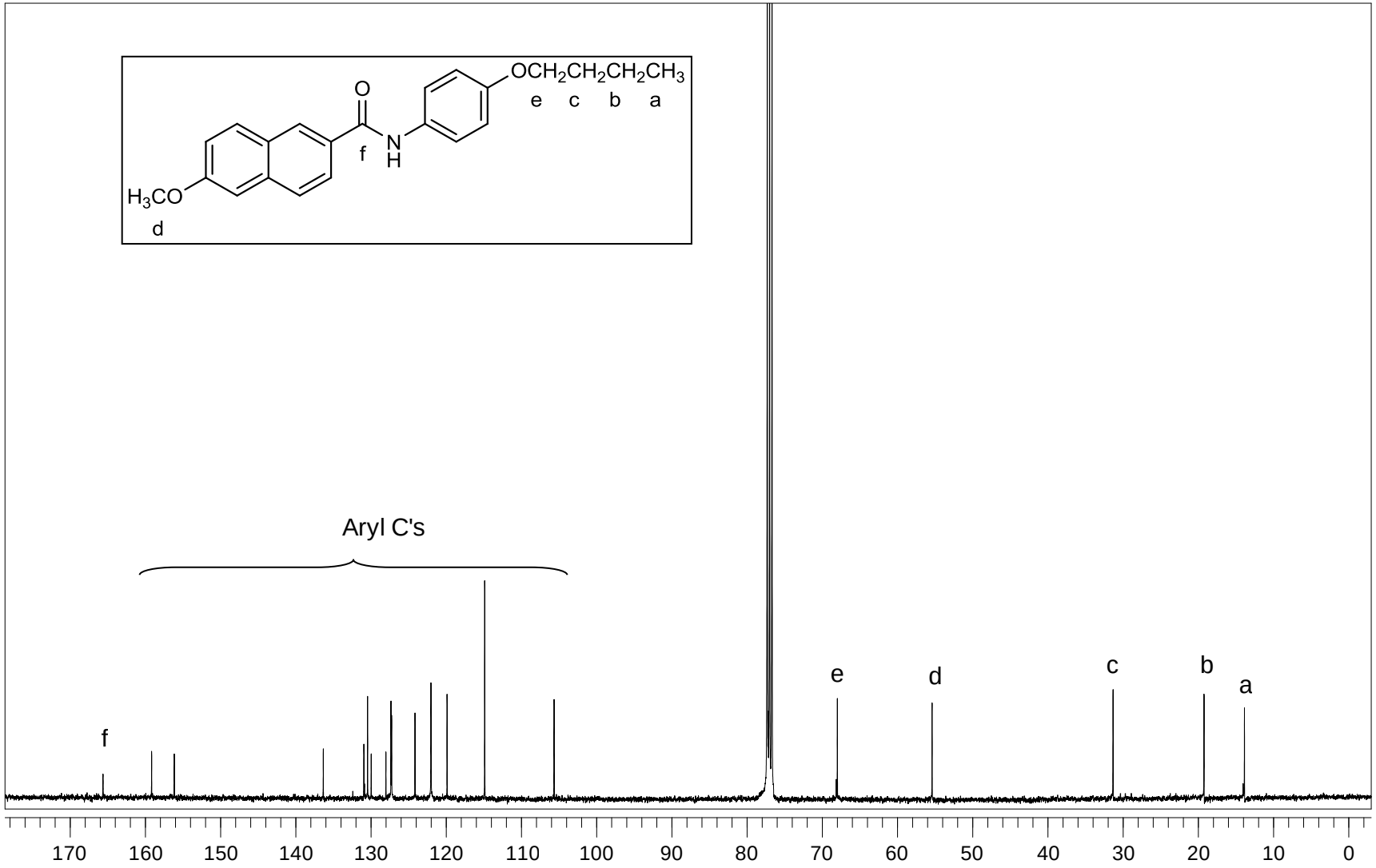


Figure A.10. ^{13}C-NMR ($CDCl_3$) spectrum of compound 11.

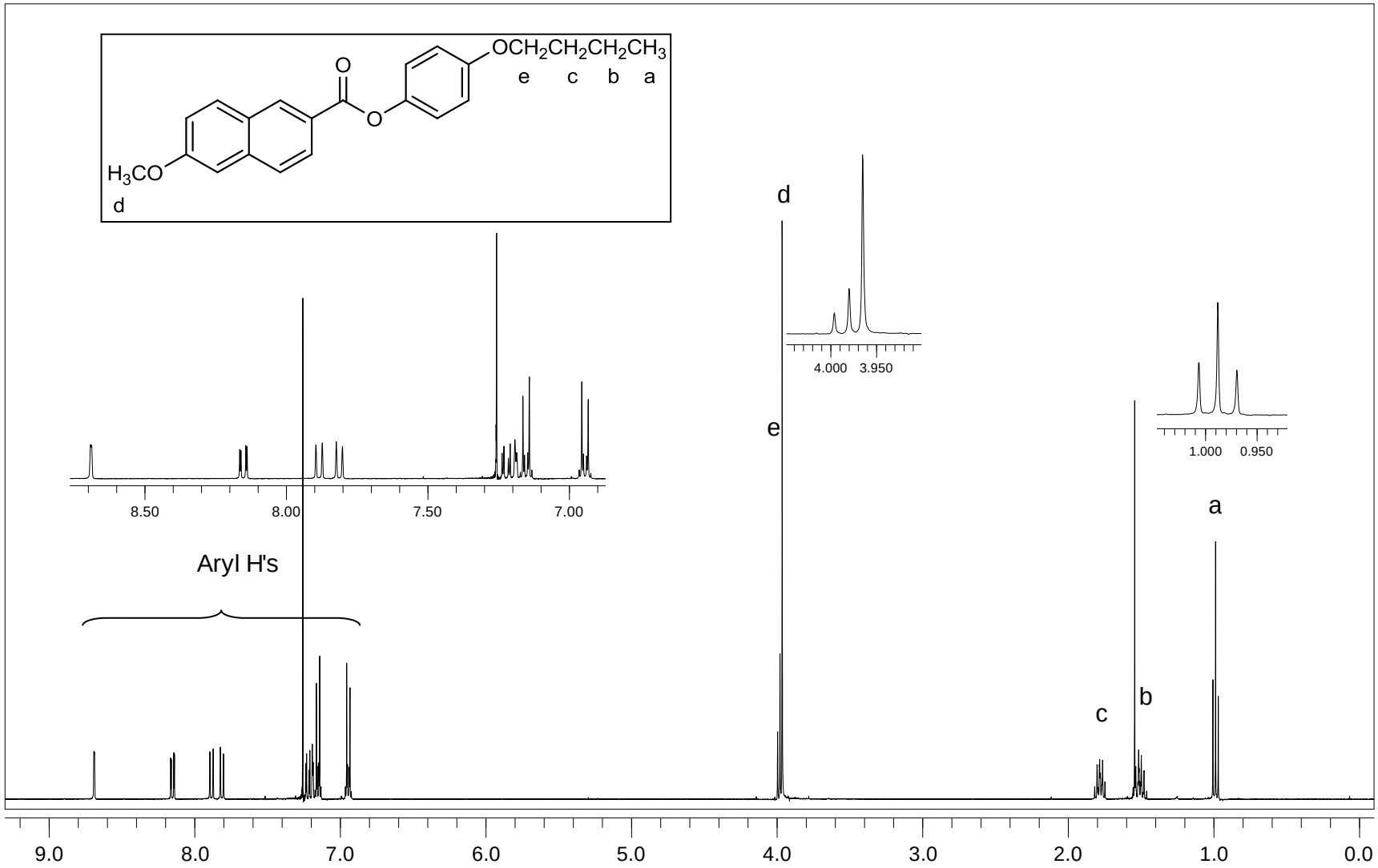


Figure A.11. ^{1}H-NMR ($CDCl_3$) spectrum of compound 12.

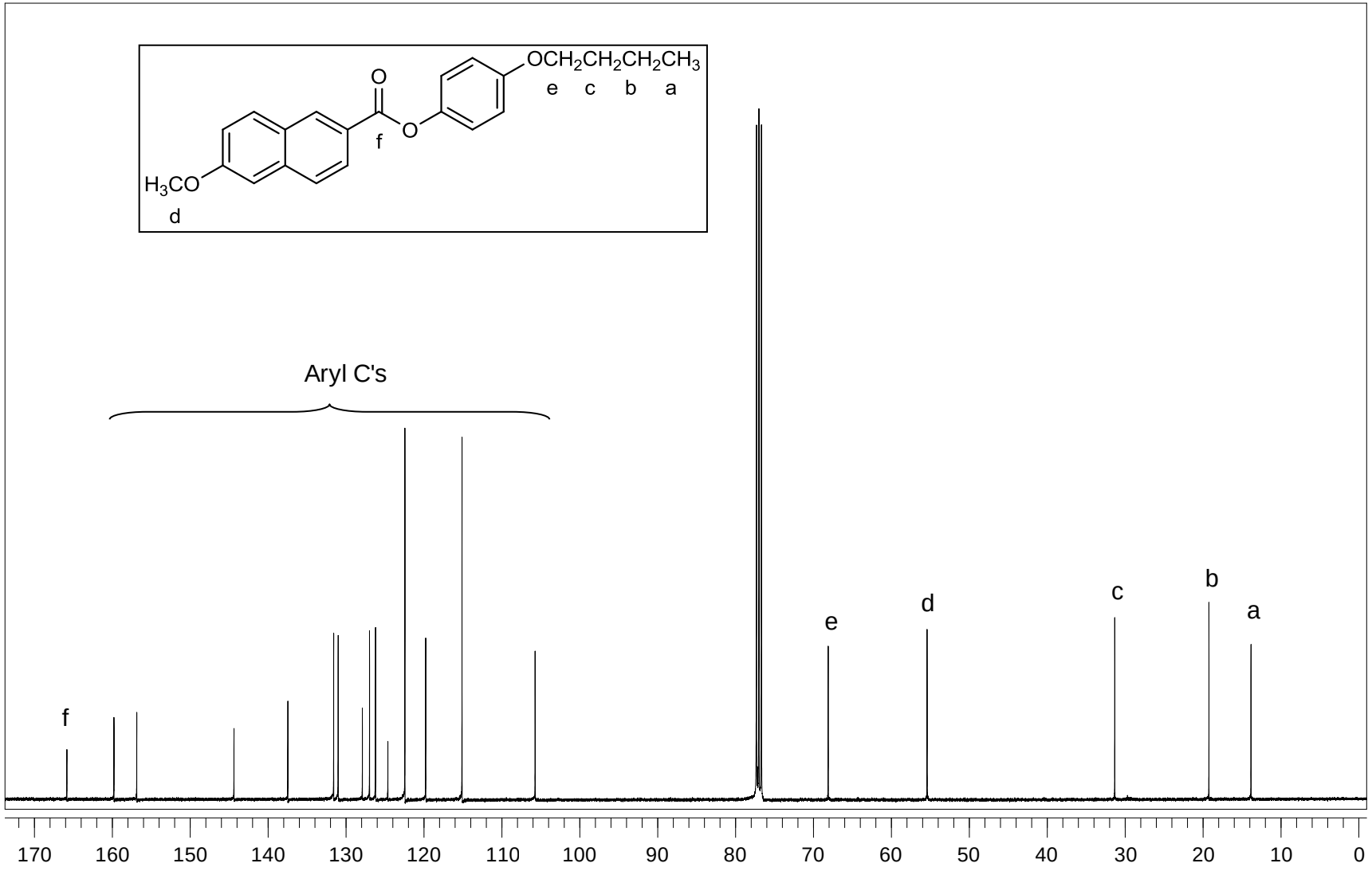


Figure A.12. ^{13}C-NMR ($CDCl_3$) spectrum of compound 12.

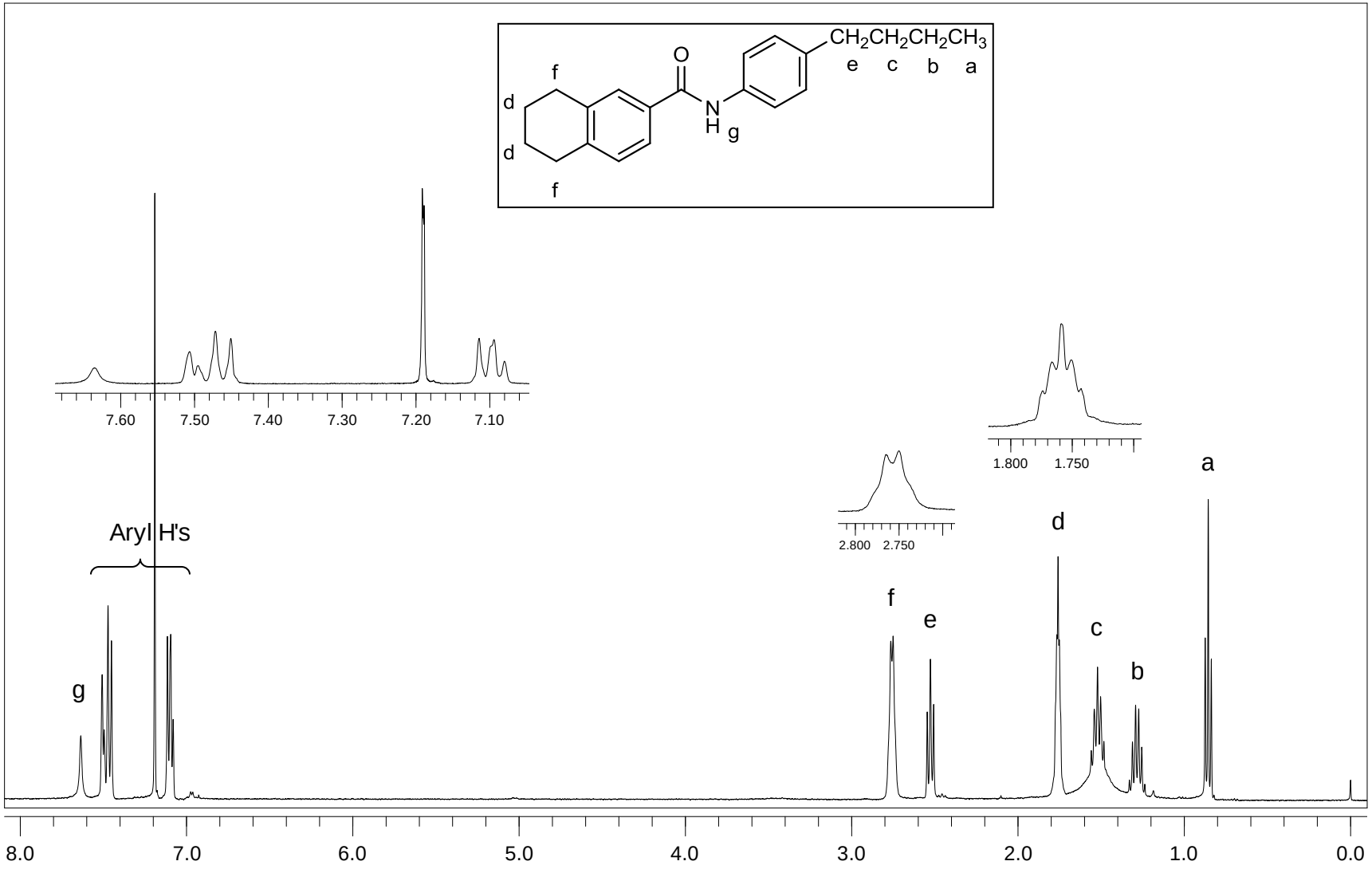


Figure A.13. ^{1}H-NMR ($CDCl_3$) spectrum of compound 18.

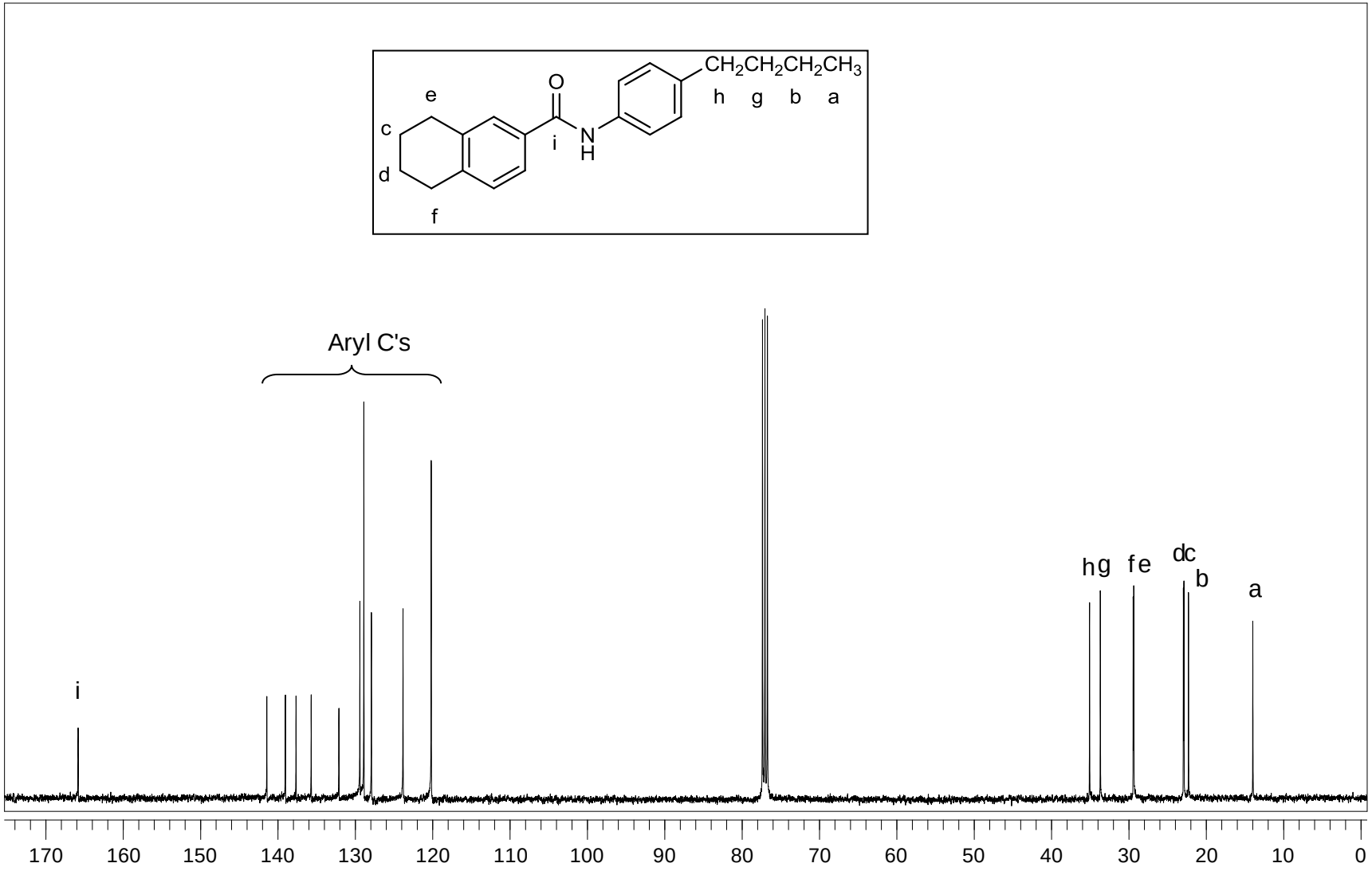


Figure A.14. ^{13}C-NMR ($CDCl_3$) spectrum of compound 18.

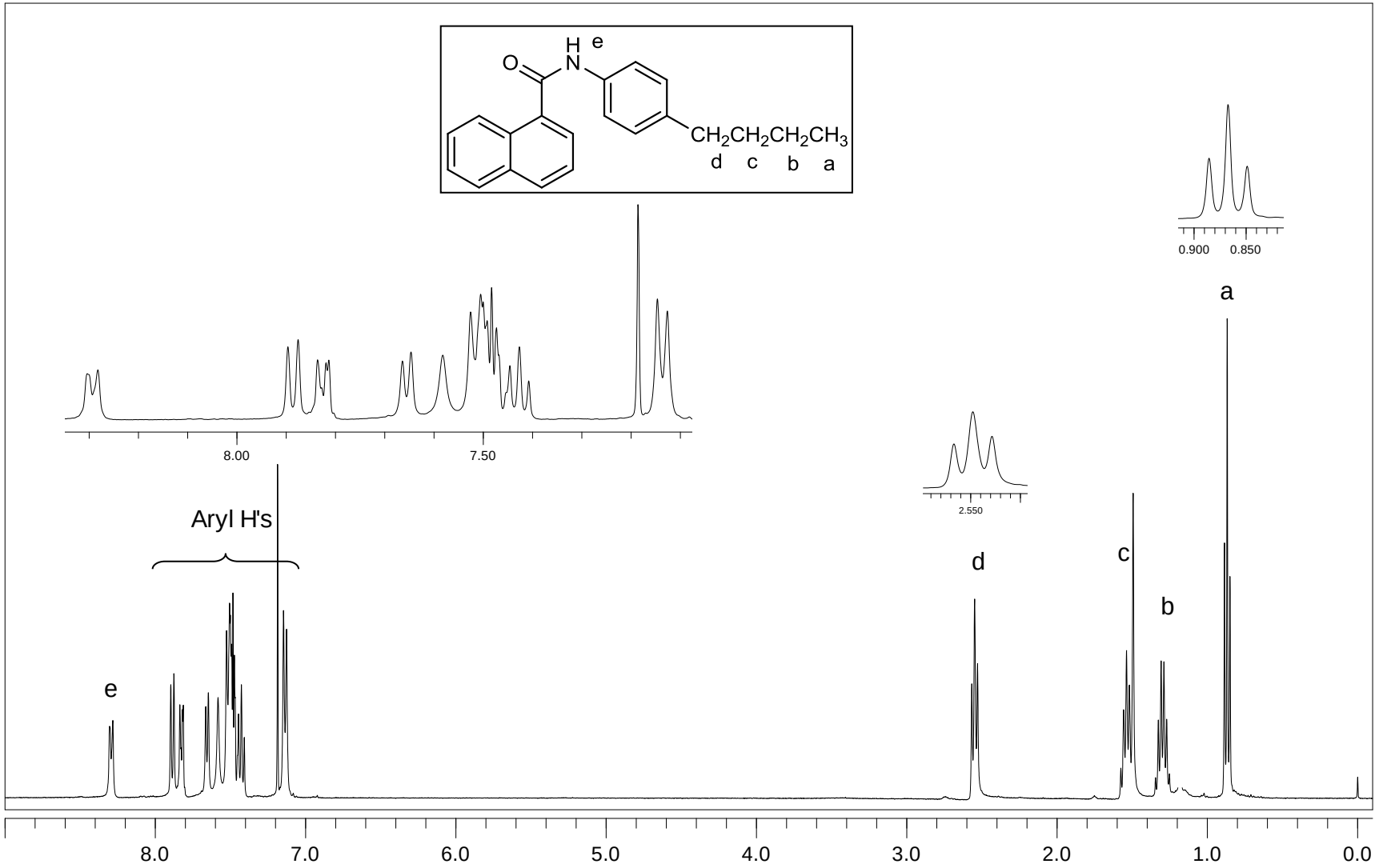


Figure A.15. ^{1}H-NMR ($CDCl_3$) spectrum of compound 19.

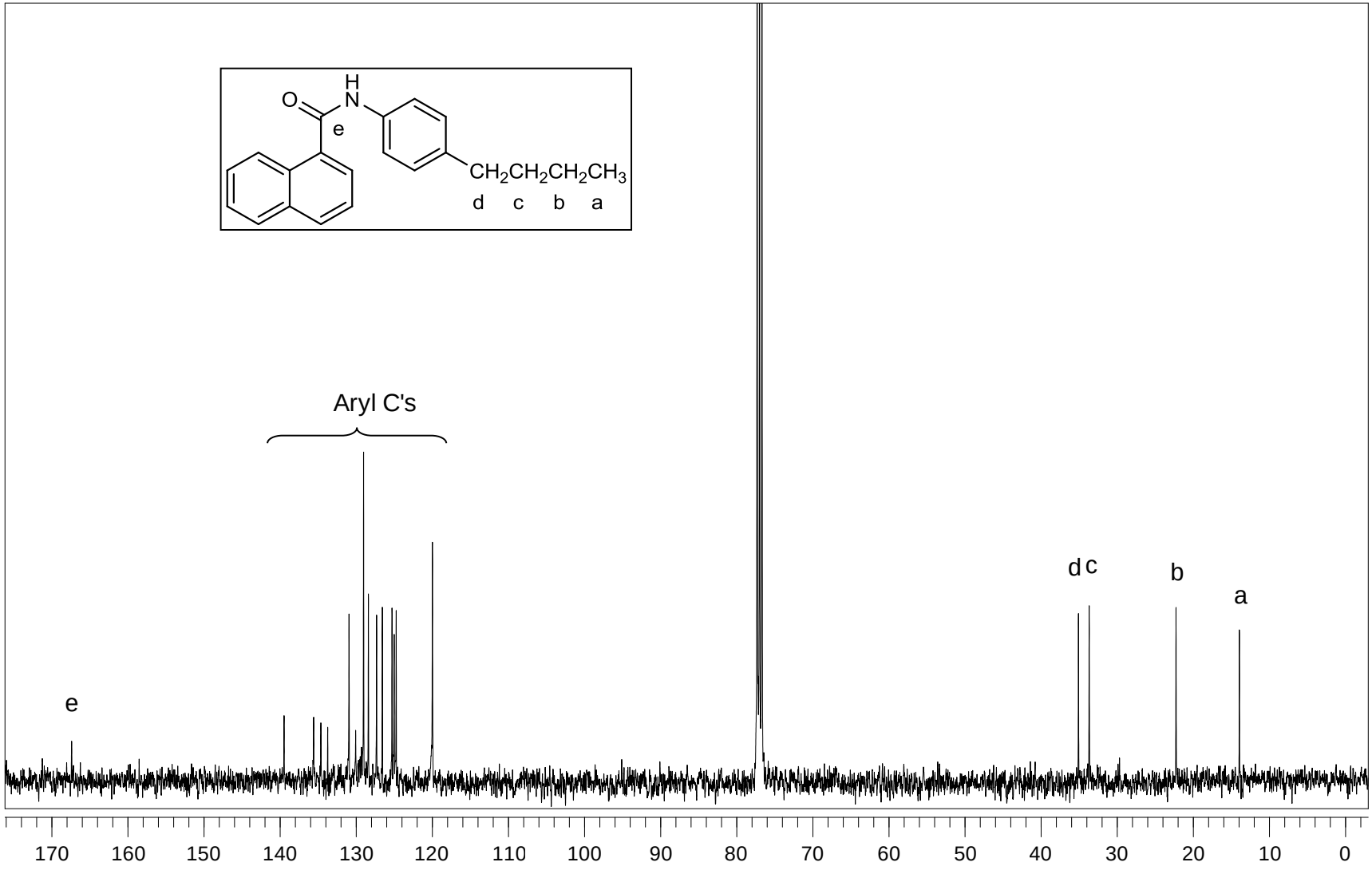


Figure A.16. ^{13}C-NMR ($CDCl_3$) spectrum of compound 19.

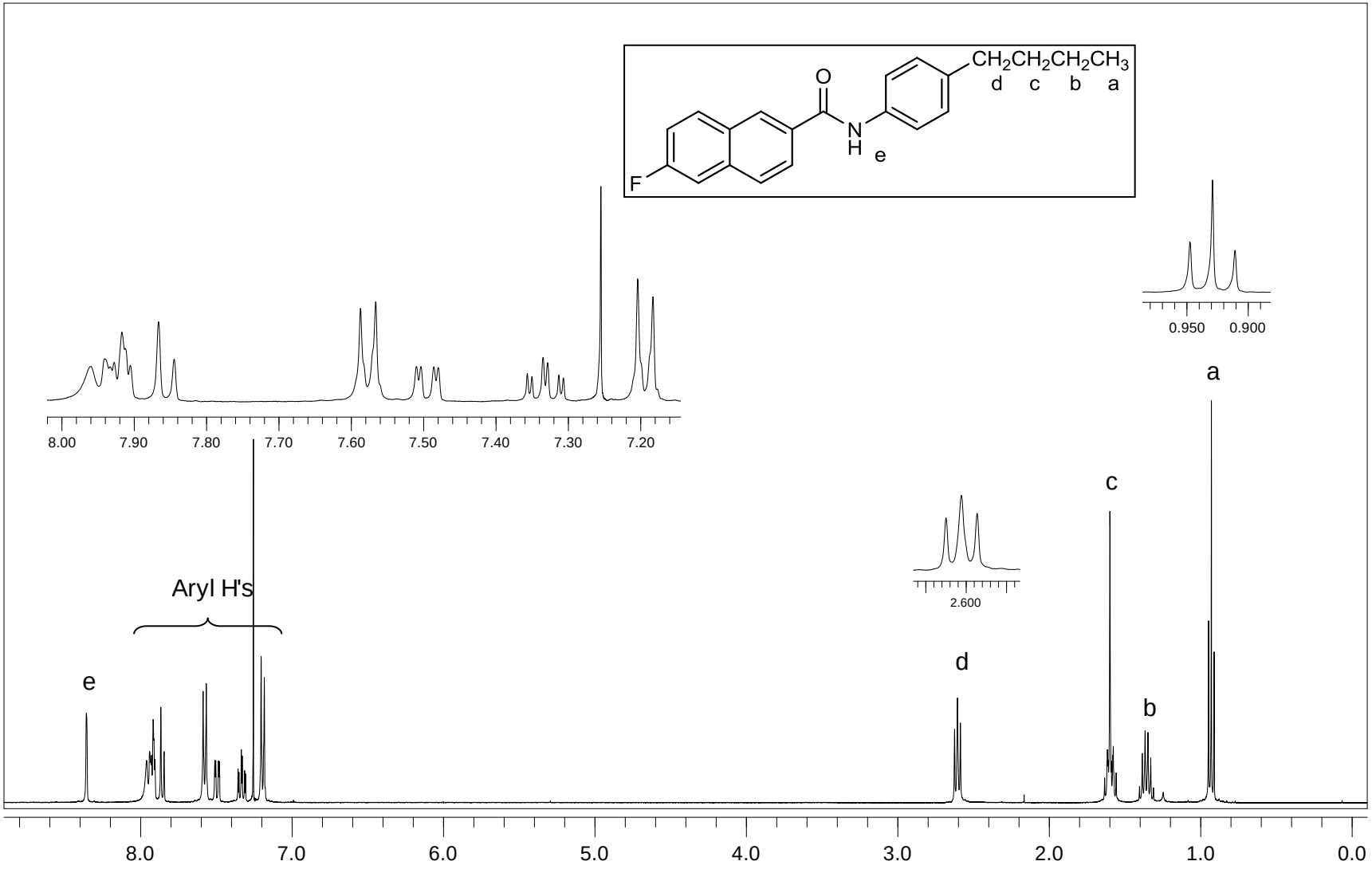


Figure A.17. ^{1}H-NMR ($CDCl_3$) spectrum of compound 20.

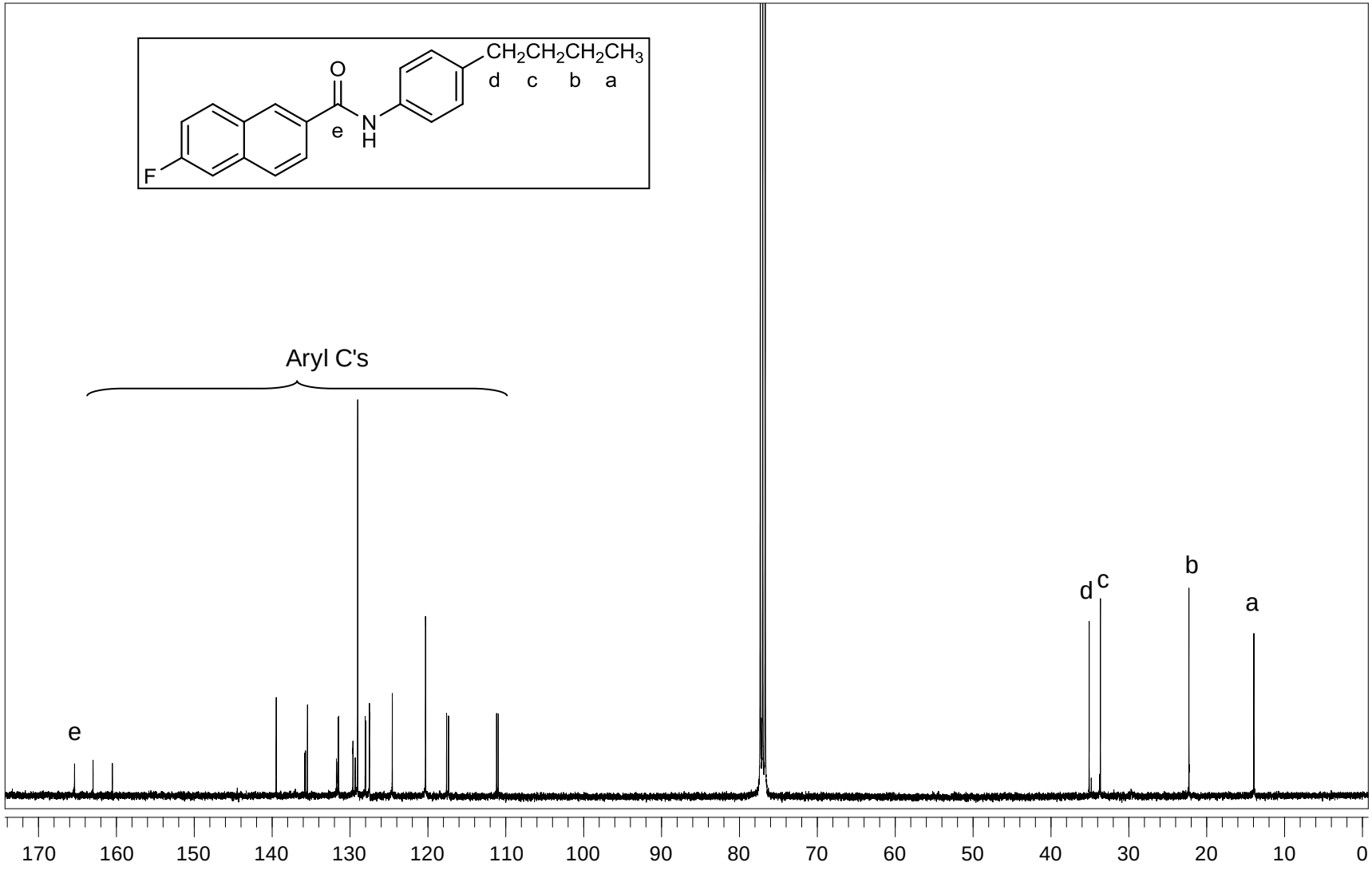


Figure A.18. ^{13}C-NMR ($CDCl_3$) spectrum of compound 20.

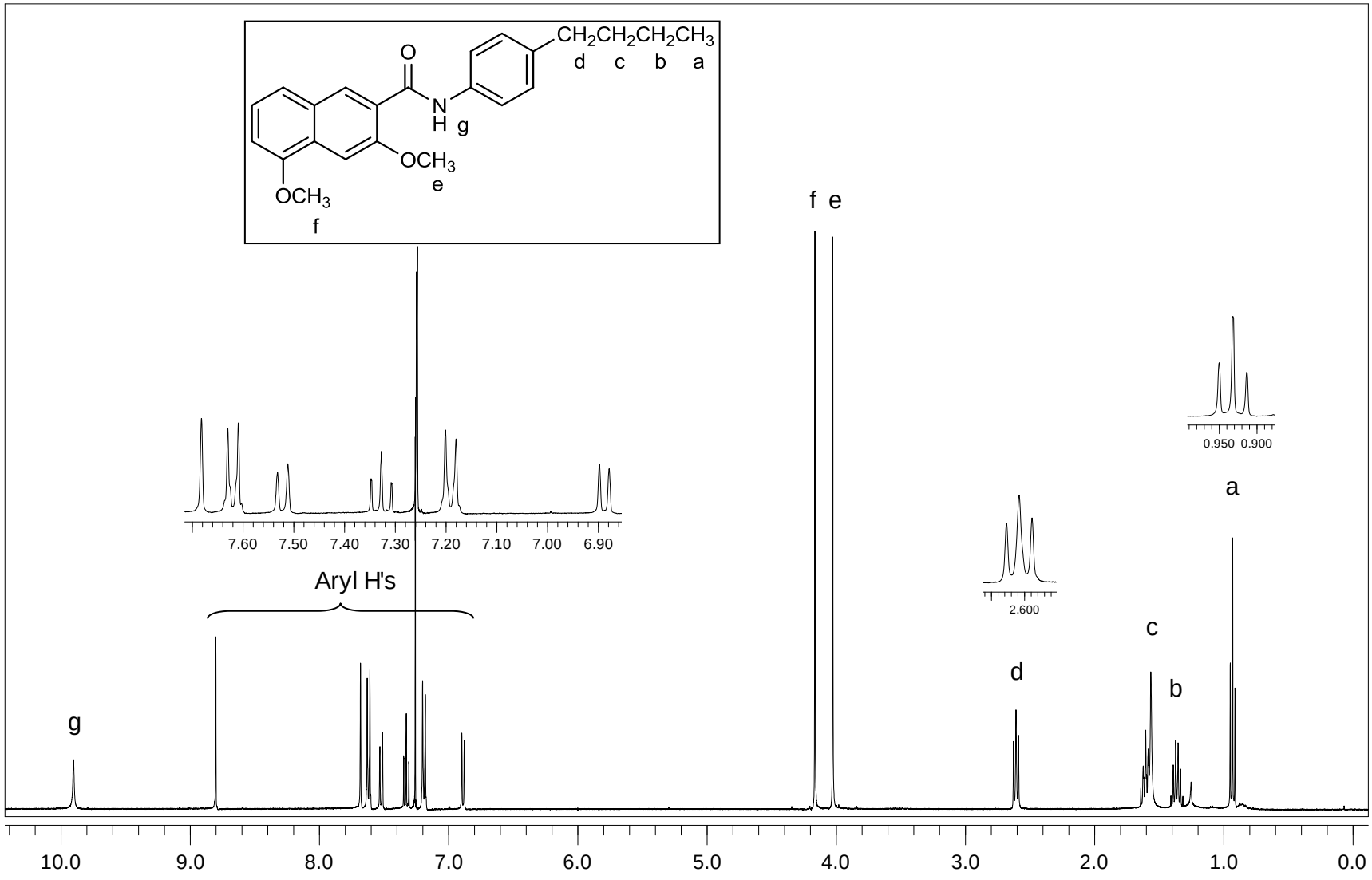


Figure A.19. ^{1}H-NMR ($CDCl_3$) spectrum of compound 21.

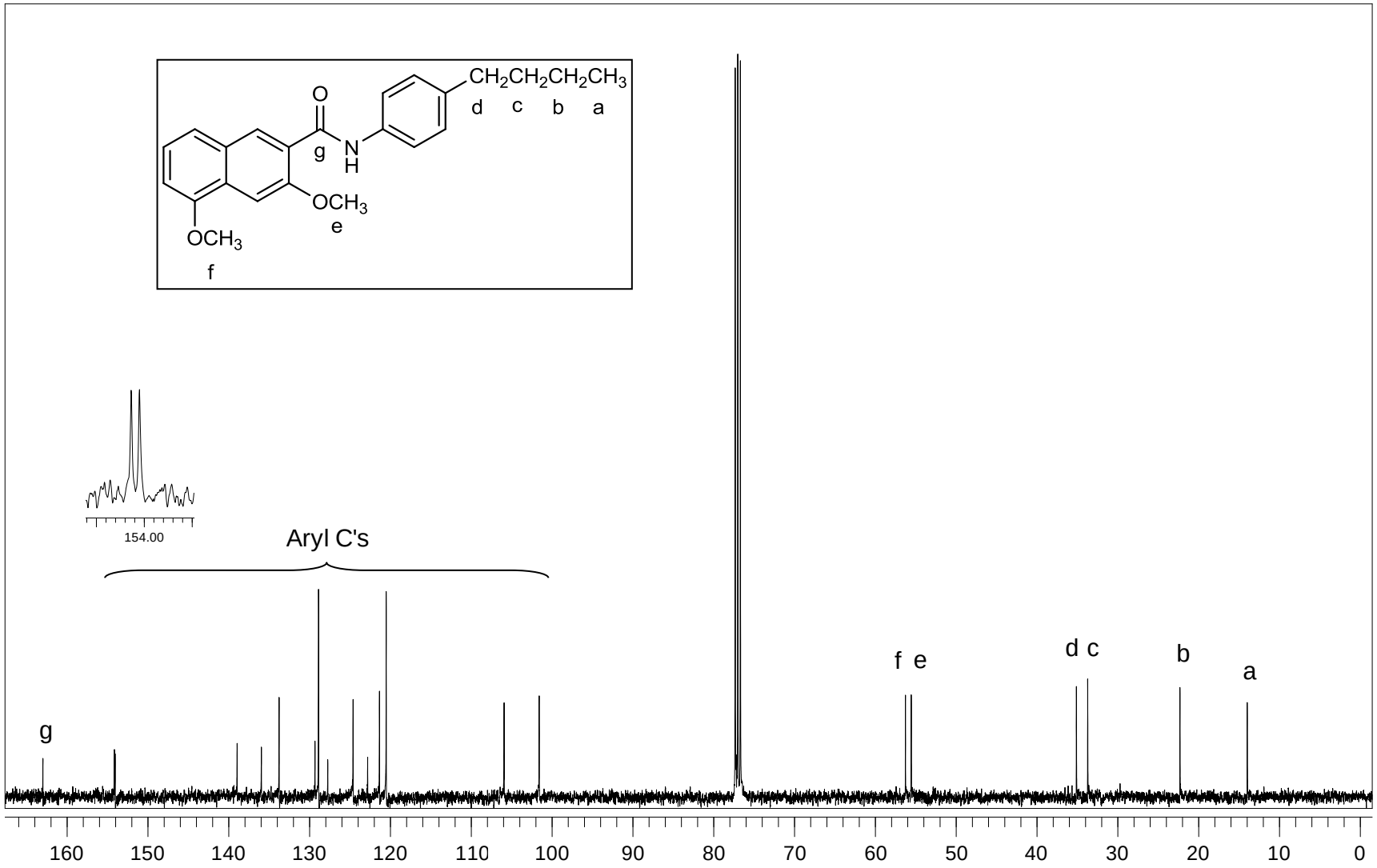


Figure A.20. ^{13}C-NMR ($CDCl_3$) spectrum of compound 21.

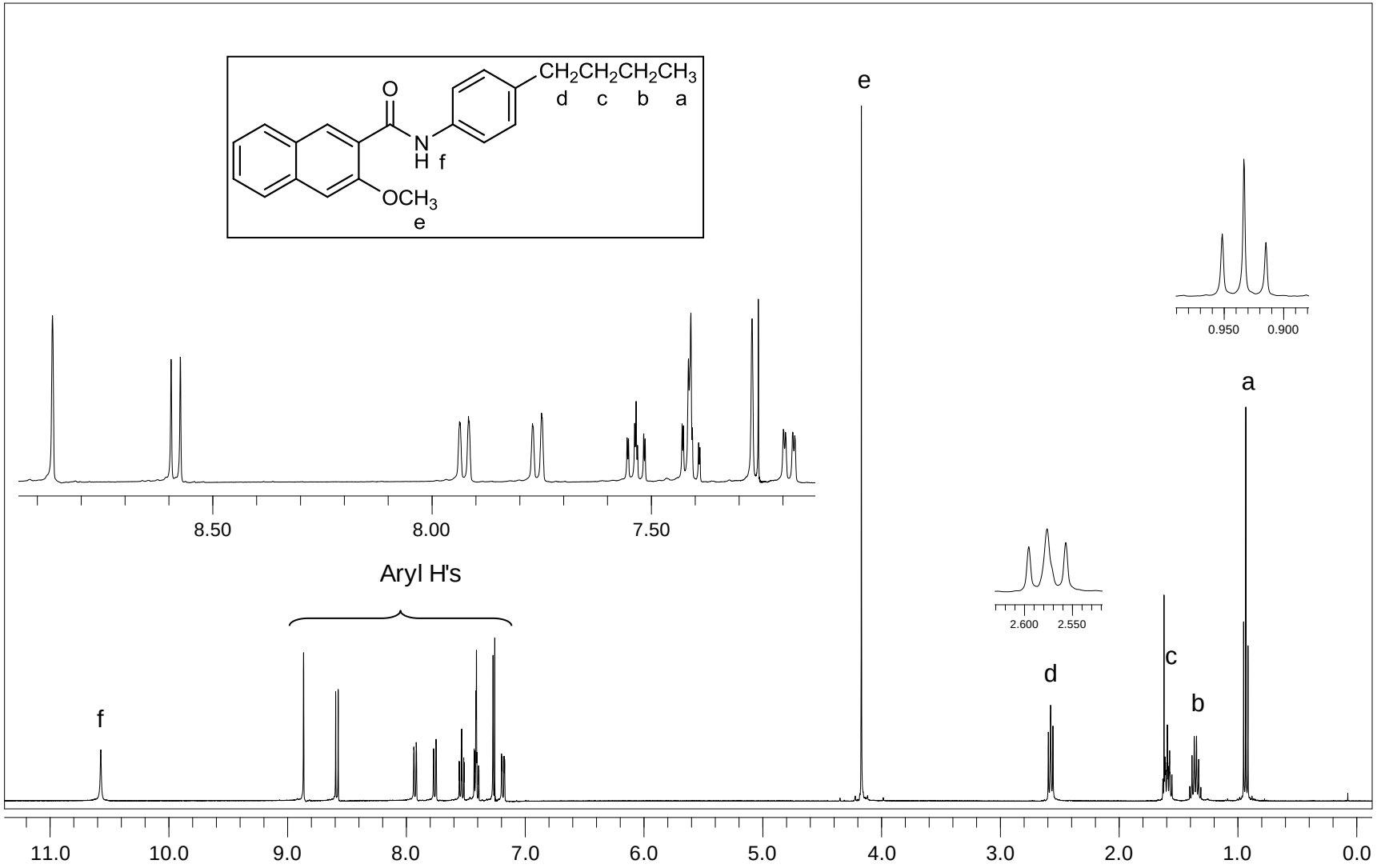


Figure A.21. ^{1}H-NMR ($CDCl_3$) spectrum of compound 22.

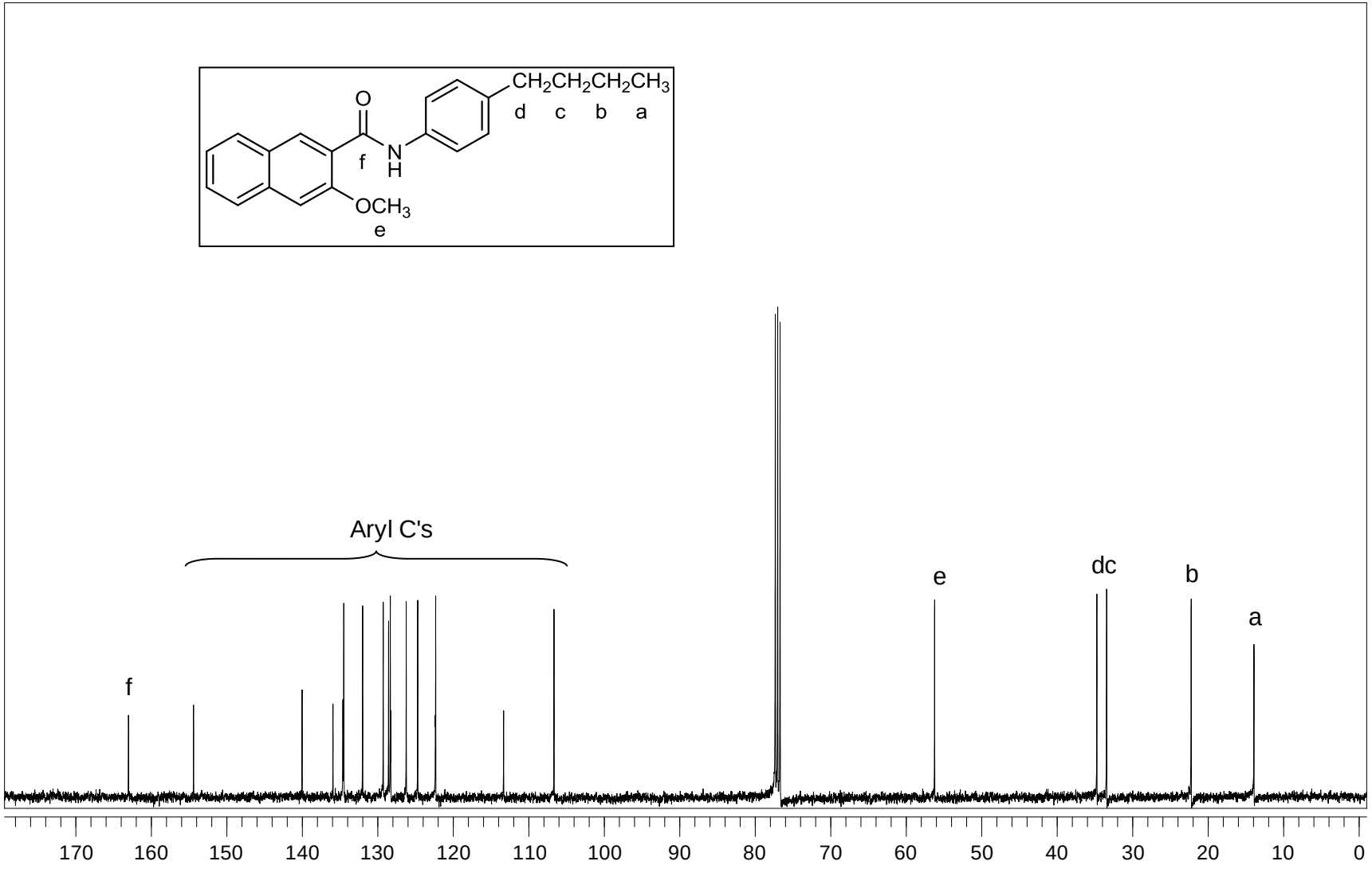


Figure A.22. ^{13}C-NMR ($CDCl_3$) spectrum of compound 22.

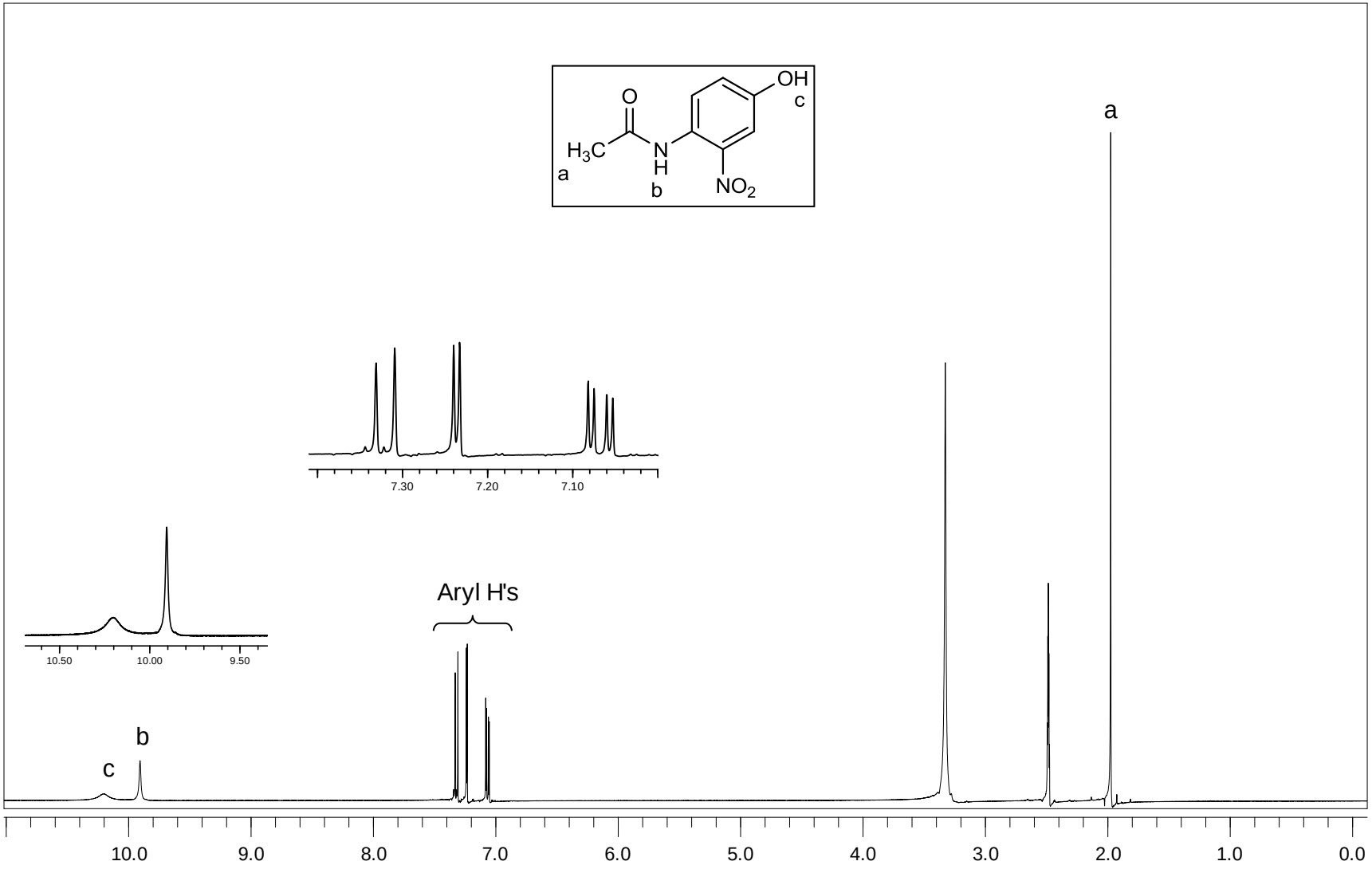


Figure A.23. ^{1}H-NMR (DMSO-d_6) spectrum of compound 24.

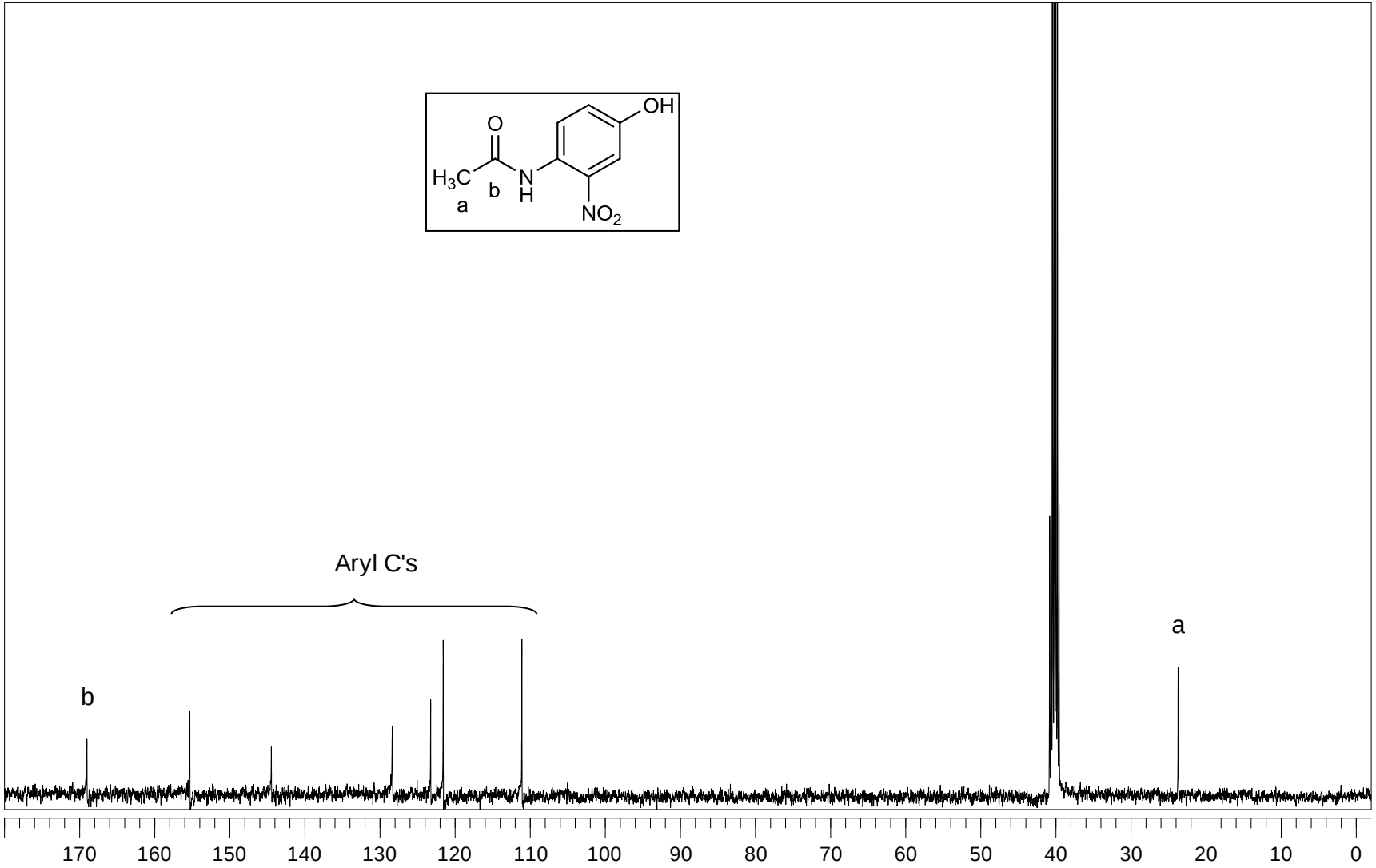


Figure A.24. ^{13}C-NMR (DMSO-d_6) spectrum of compound 24.

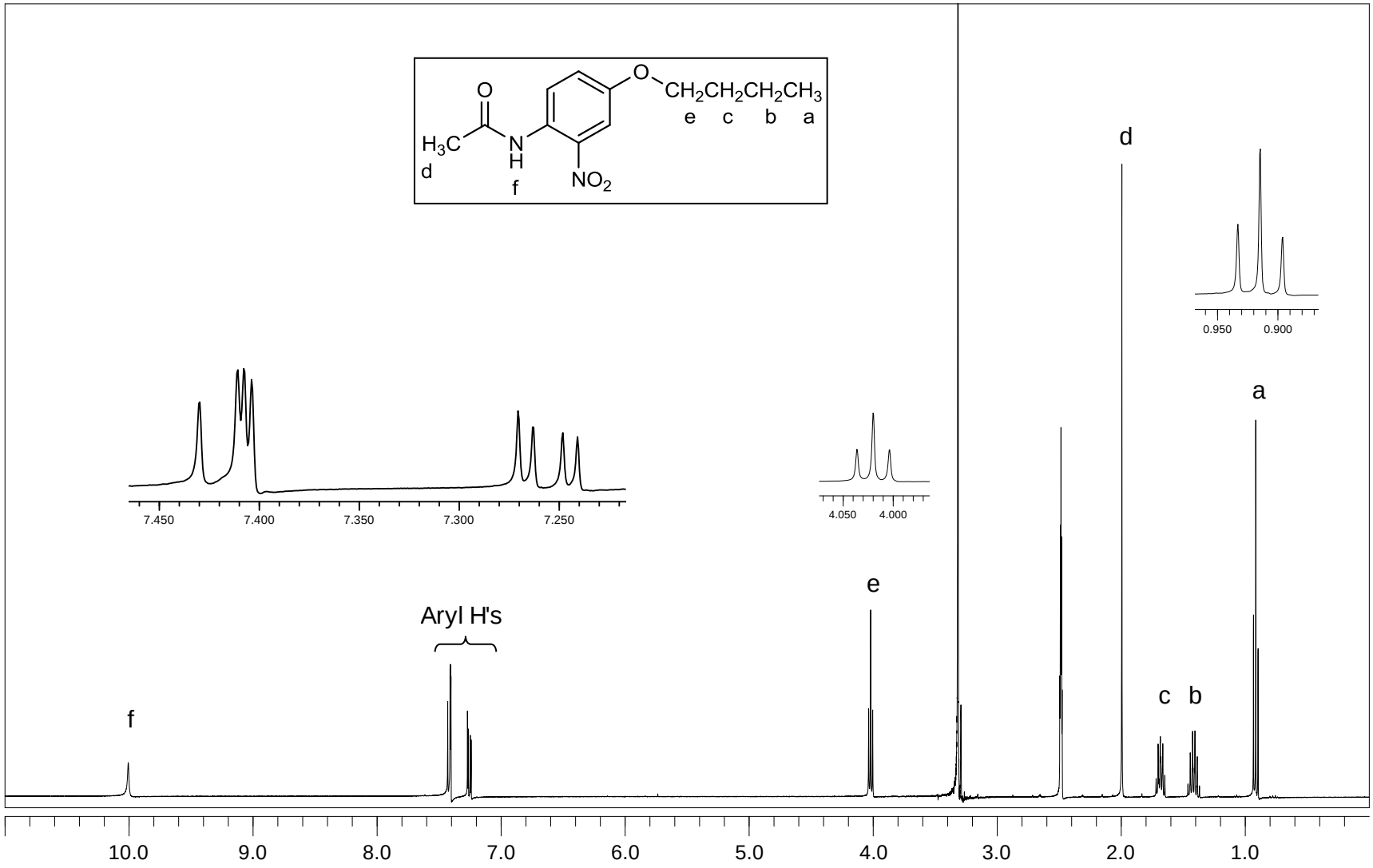


Figure A.25. ^{1}H-NMR (DMSO-d_6) spectrum of compound 25.

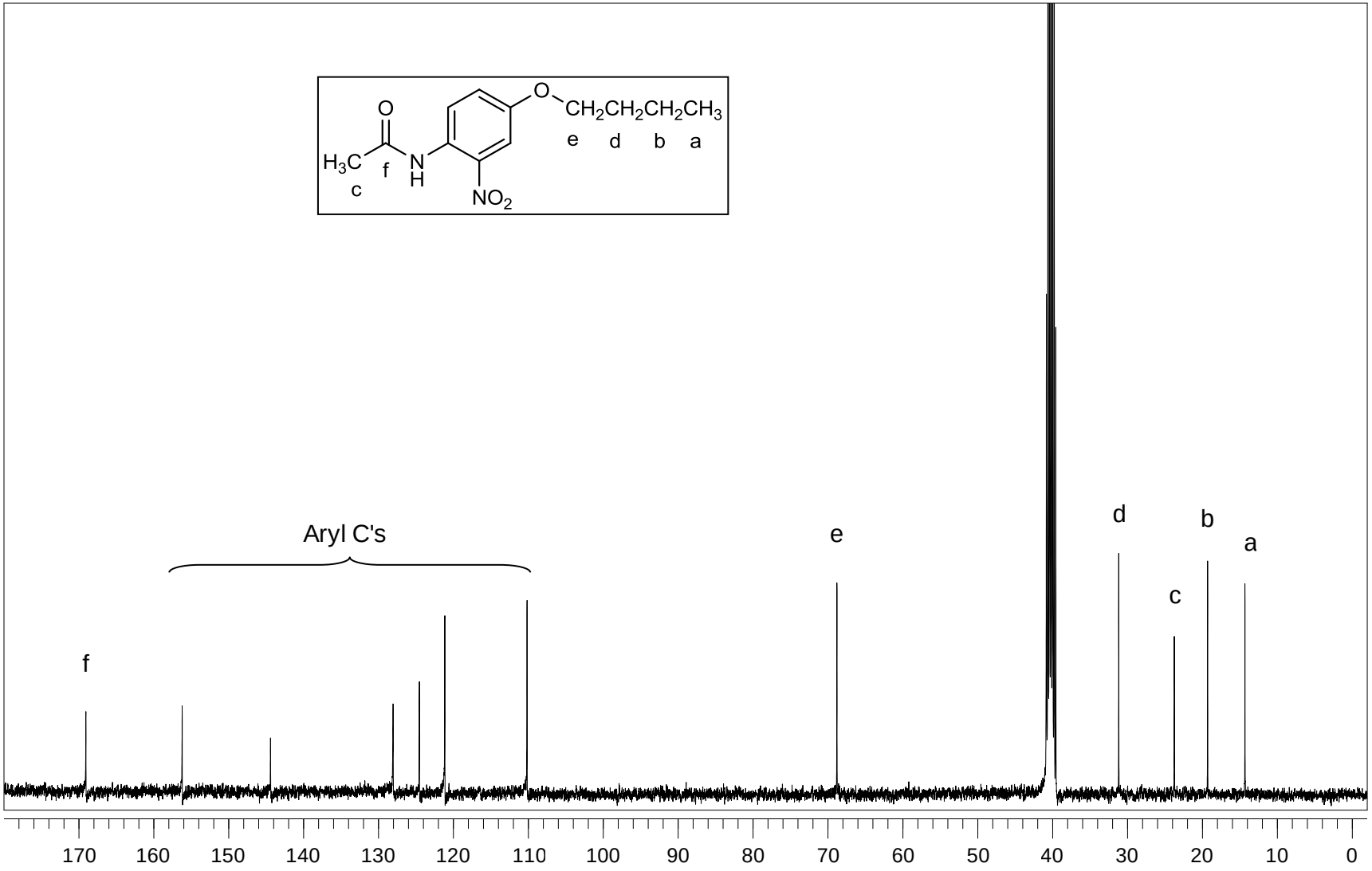


Figure A.26. ^{13}C-NMR (DMSO-d_6) spectrum of compound 25.

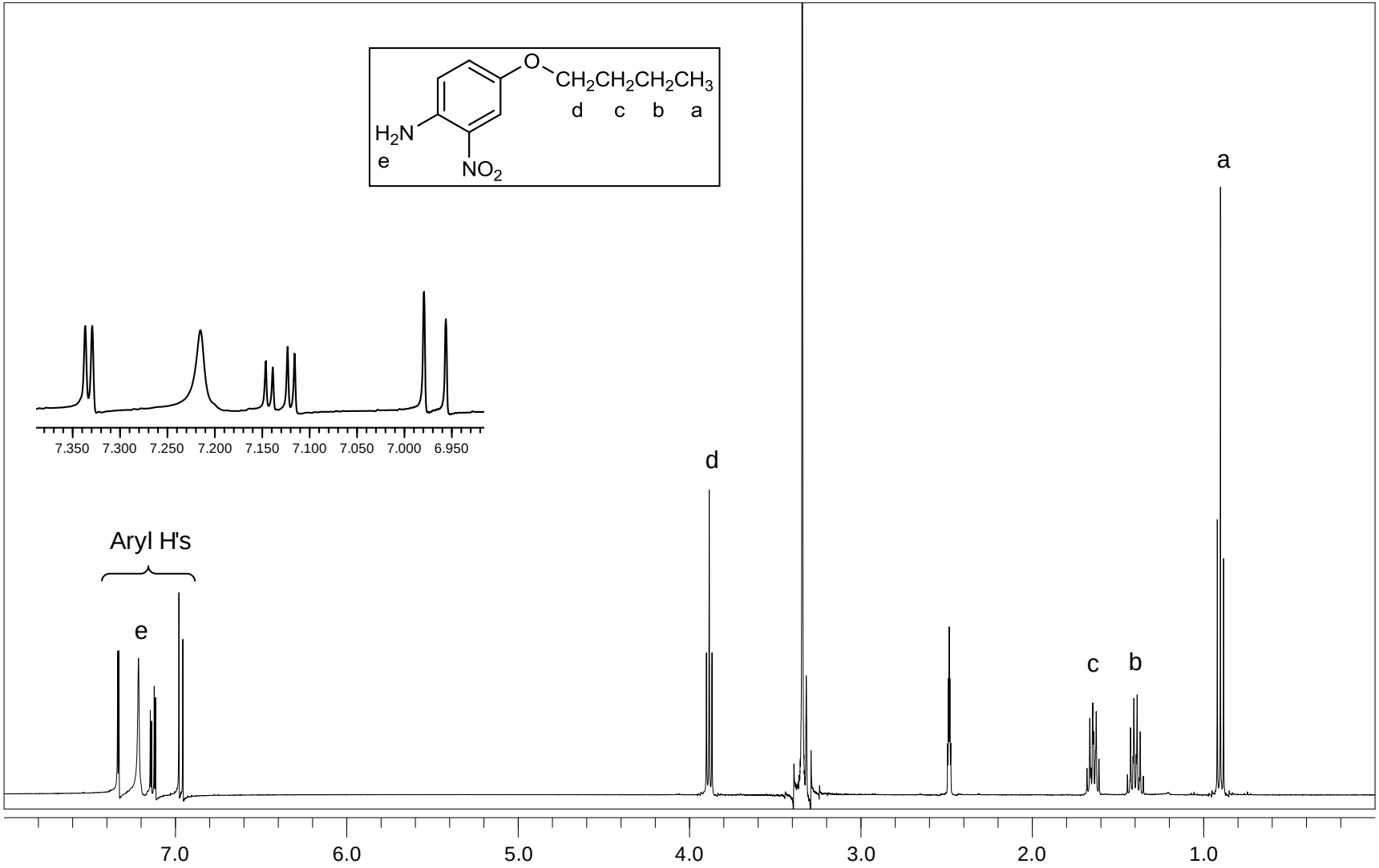


Figure A.27. ^{1}H-NMR (DMSO-d_6) spectrum of compound 26.

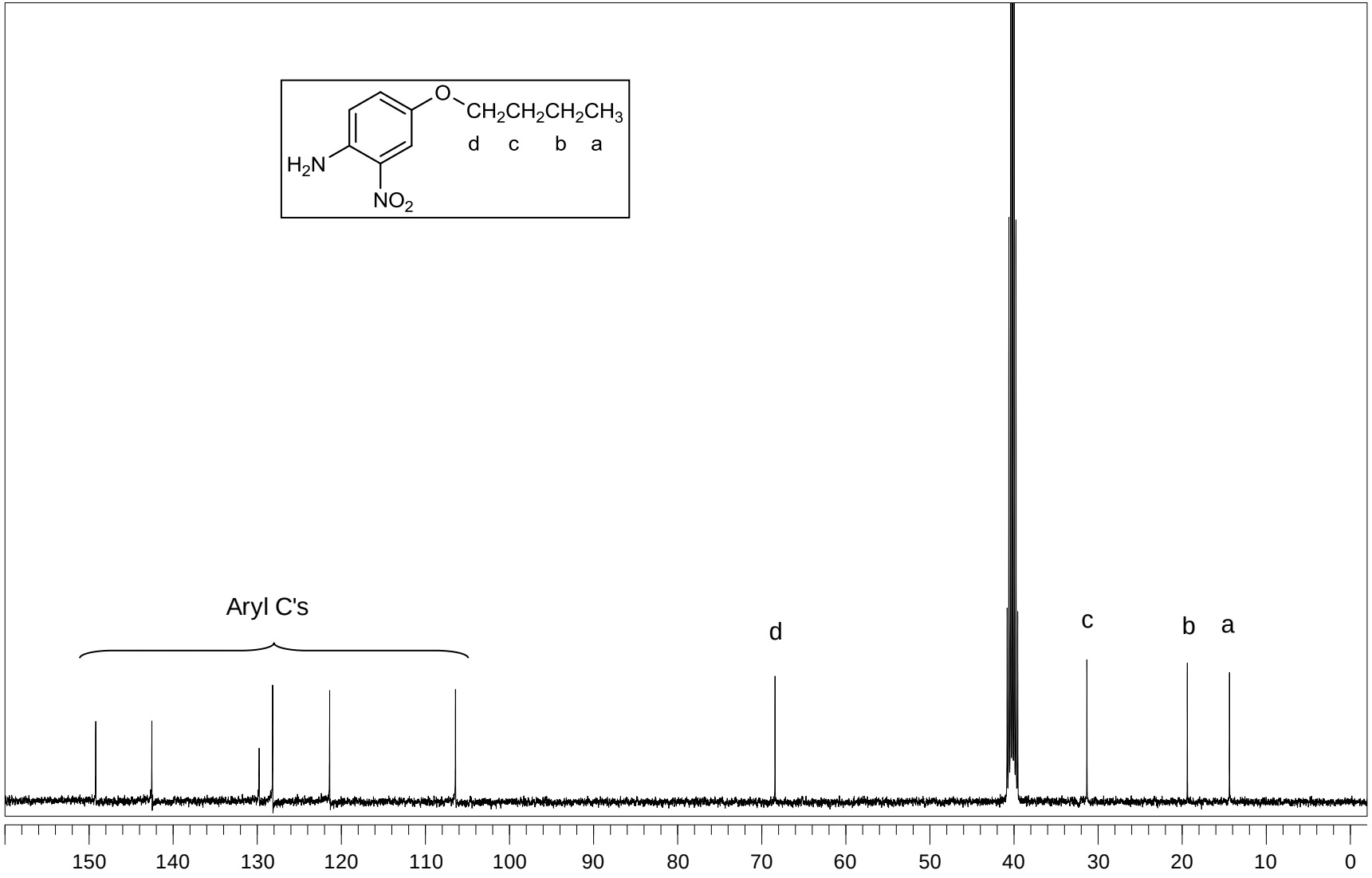


Figure A.28. ^{13}C-NMR (DMSO-d_6) spectrum of compound 26.

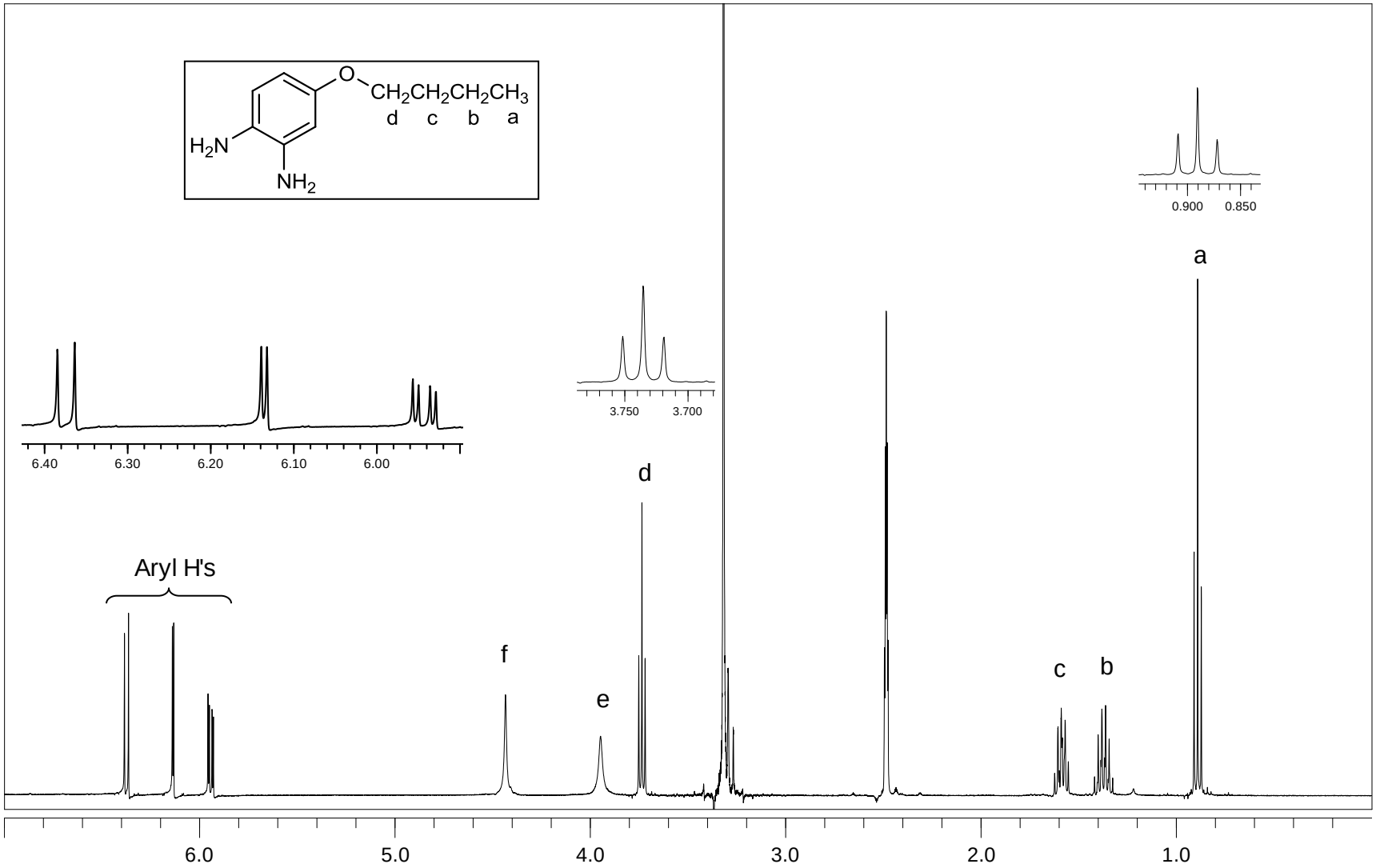


Figure A.29. ^{1}H-NMR (DMSO-d_6) spectrum of compound 27.

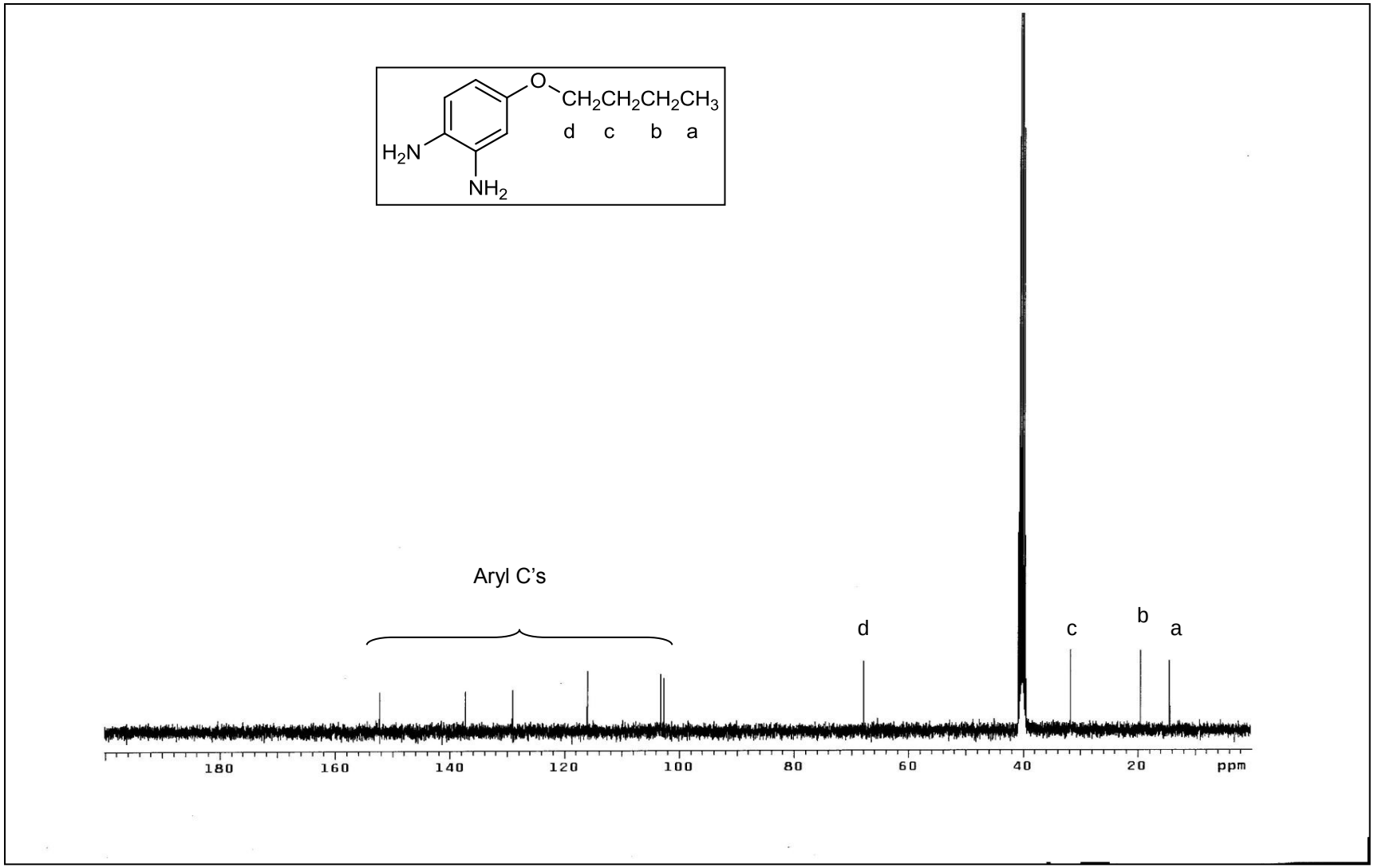


Figure A.30. ^{13}C-NMR (DMSO-d_6) spectrum of compound 27.

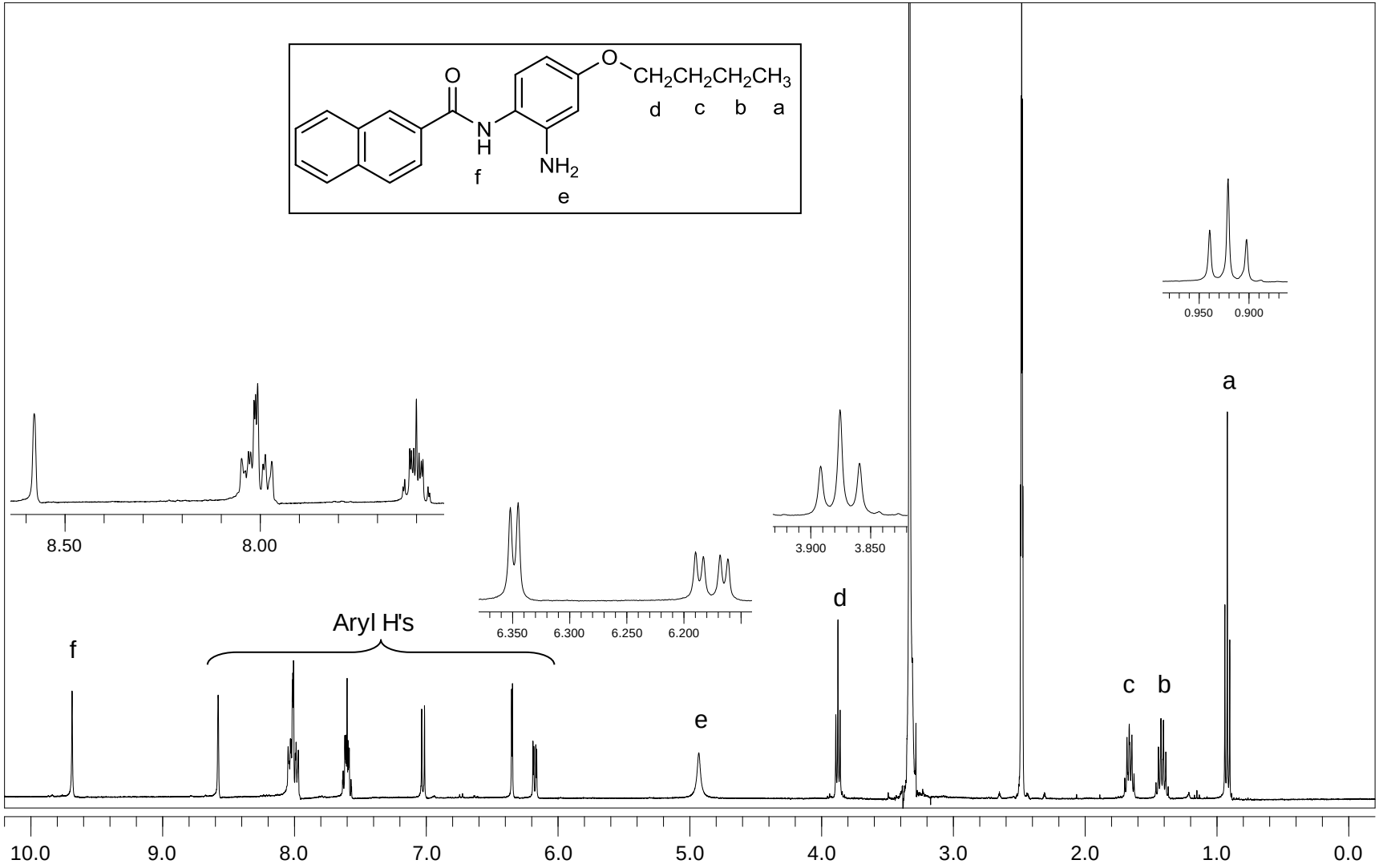


Figure A.31. ^{1}H-NMR (DMSO-d_6) spectrum of compound 28a.

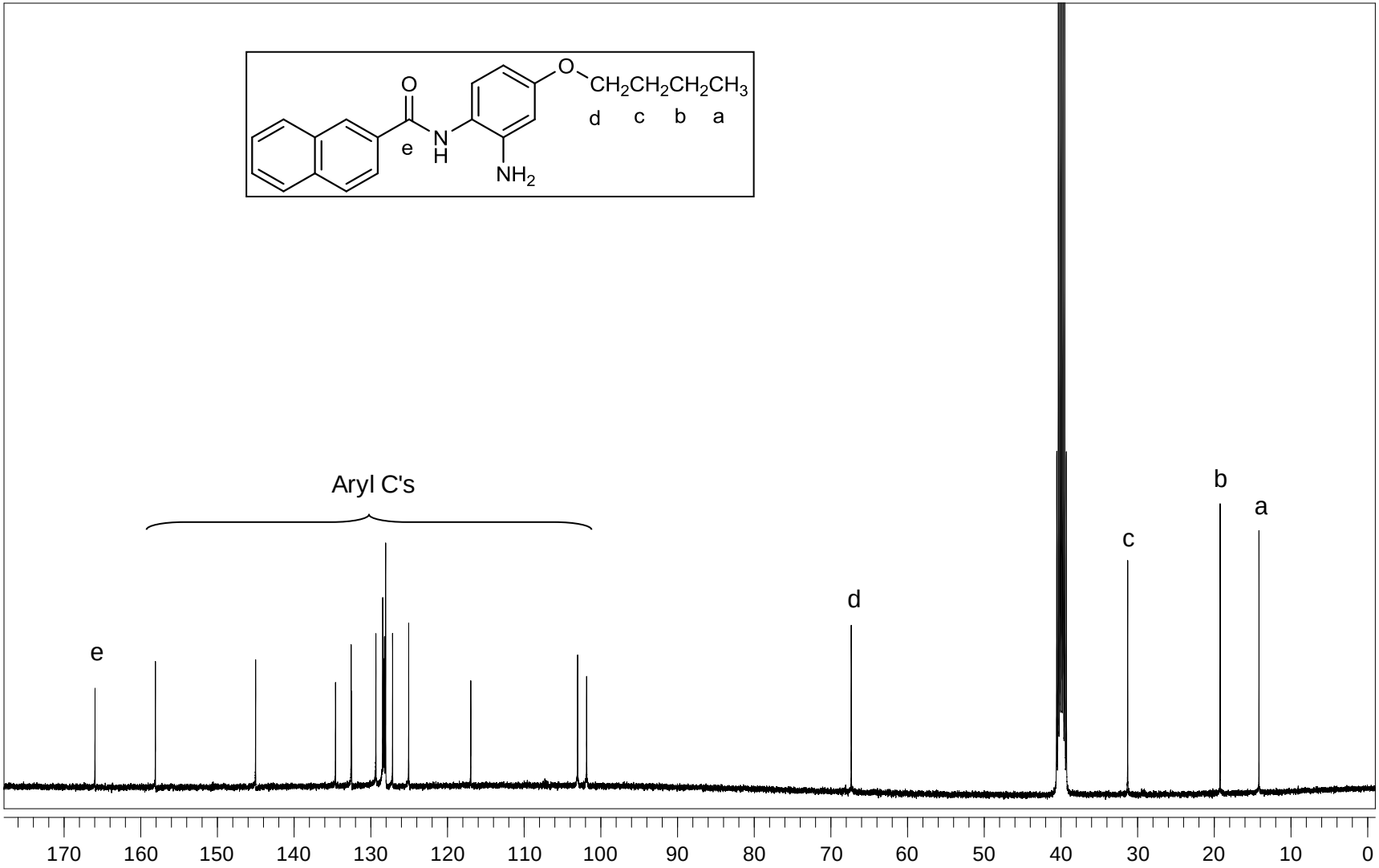


Figure A.32. ^{13}C-NMR (DMSO-d_6) spectrum of compound 28a.

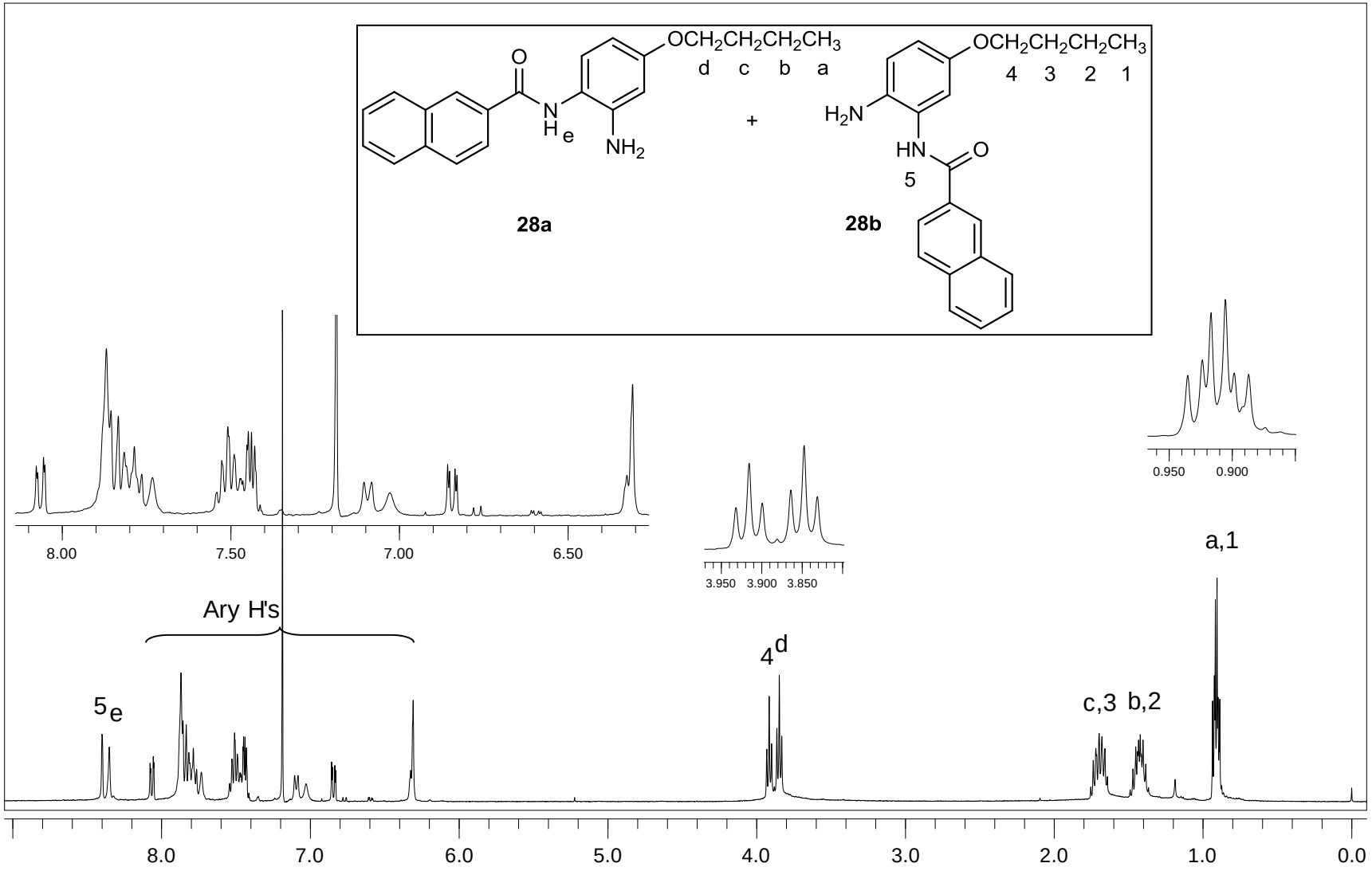


Figure A.33. ^{1}H-NMR ($CDCl_3$) spectrum of compound 28a and 28b.

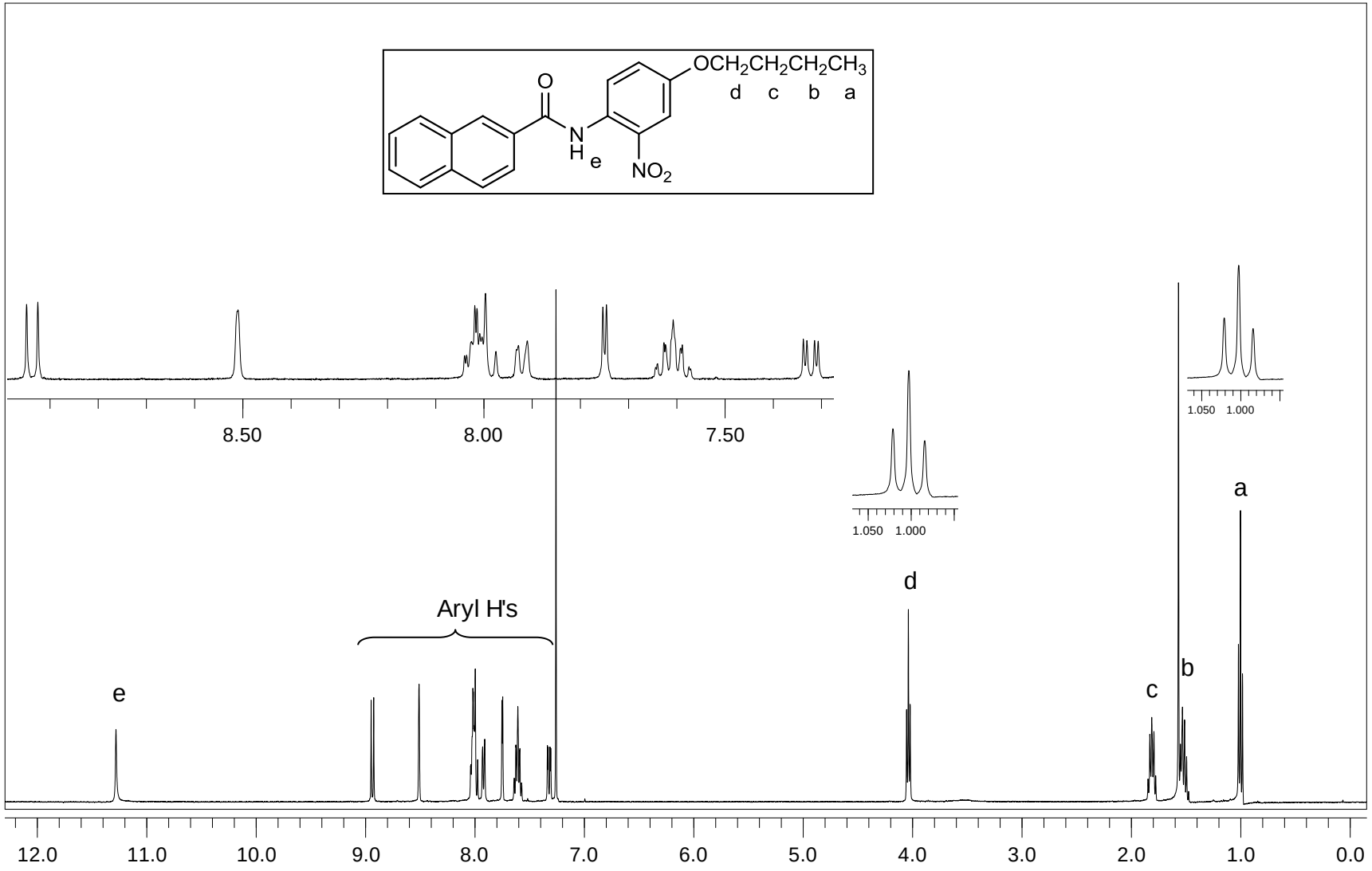


Figure A.34. ^{1}H-NMR ($CDCl_3$) spectrum of compound 30.

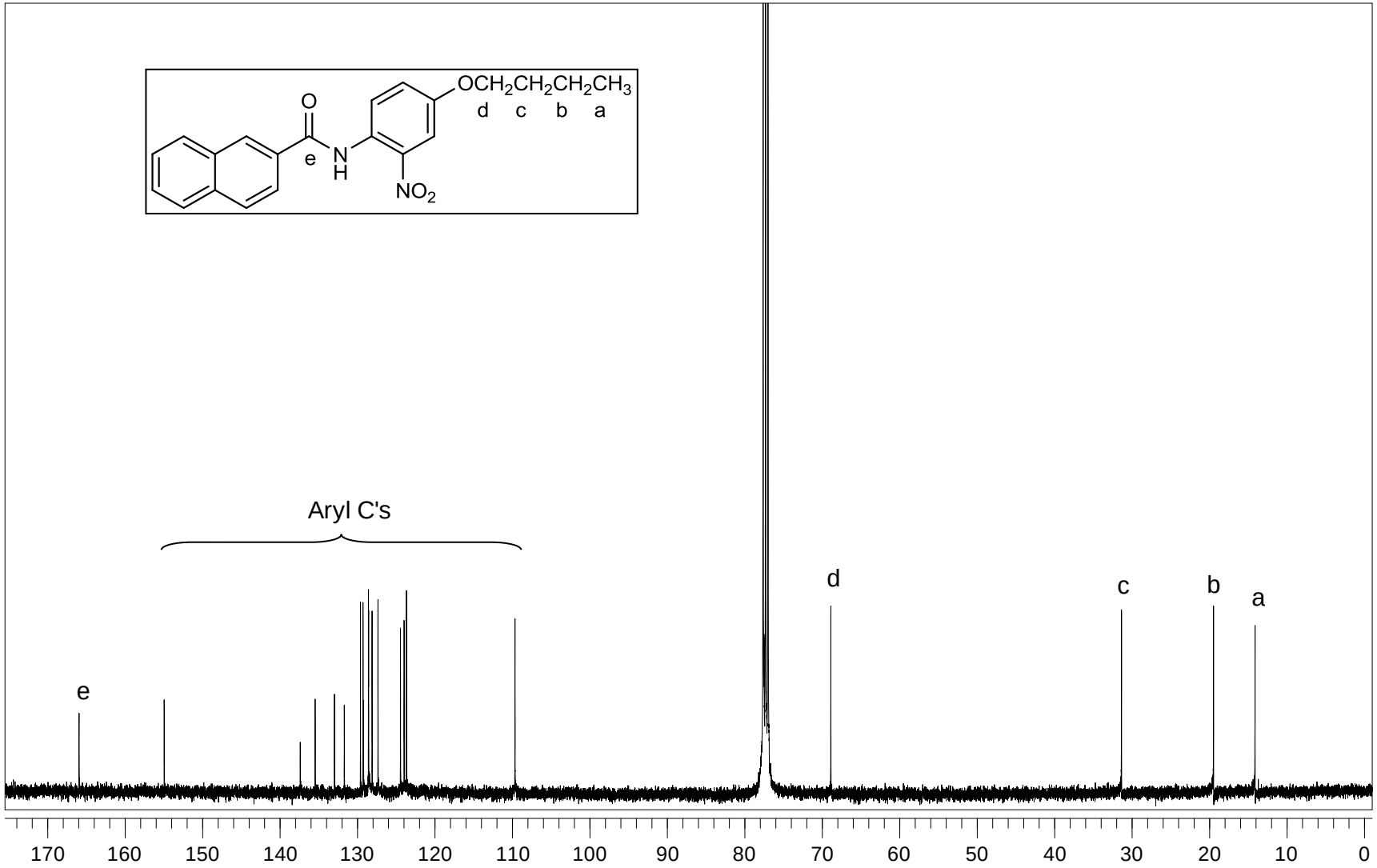


Figure A.35. ^{13}C-NMR ($CDCl_3$) spectrum of compound 30.

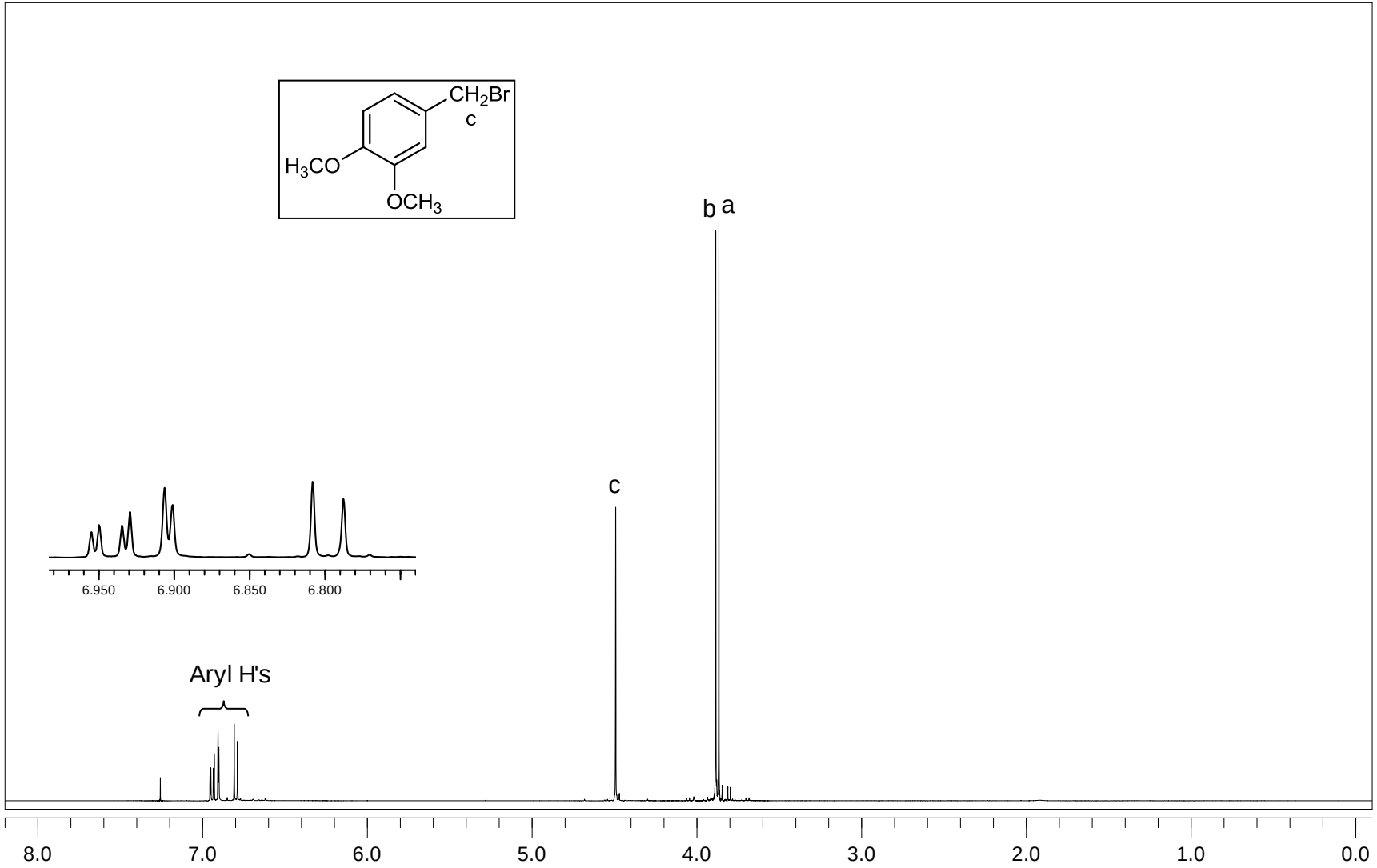


Figure A.36. ^{1}H-NMR ($CDCl_3$) spectrum of compound 32.

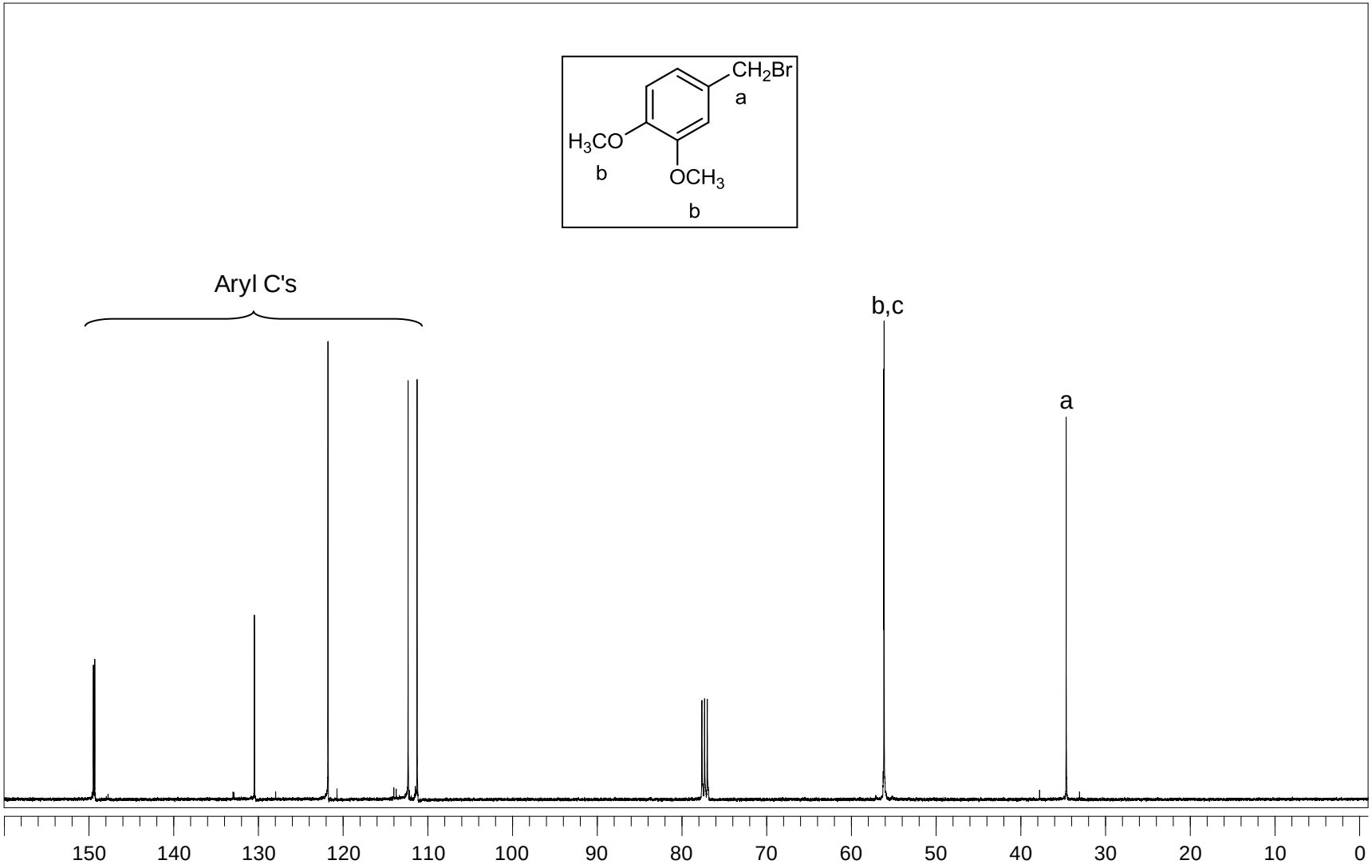


Figure A.37. ^{13}C-NMR ($CDCl_3$) spectrum of compound 32.

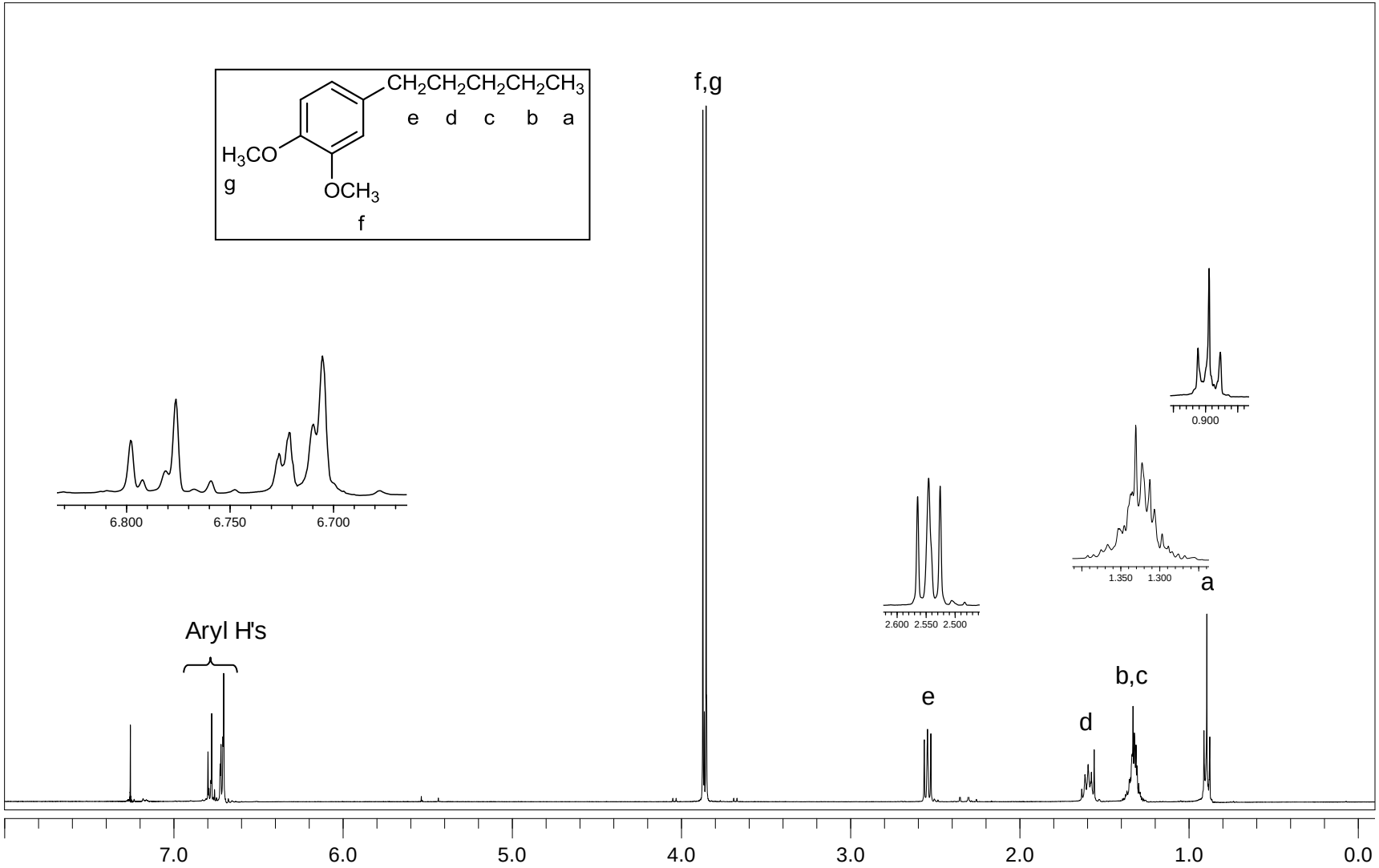


Figure A.38. ^{1}H-NMR ($CDCl_3$) spectrum of compound 33.

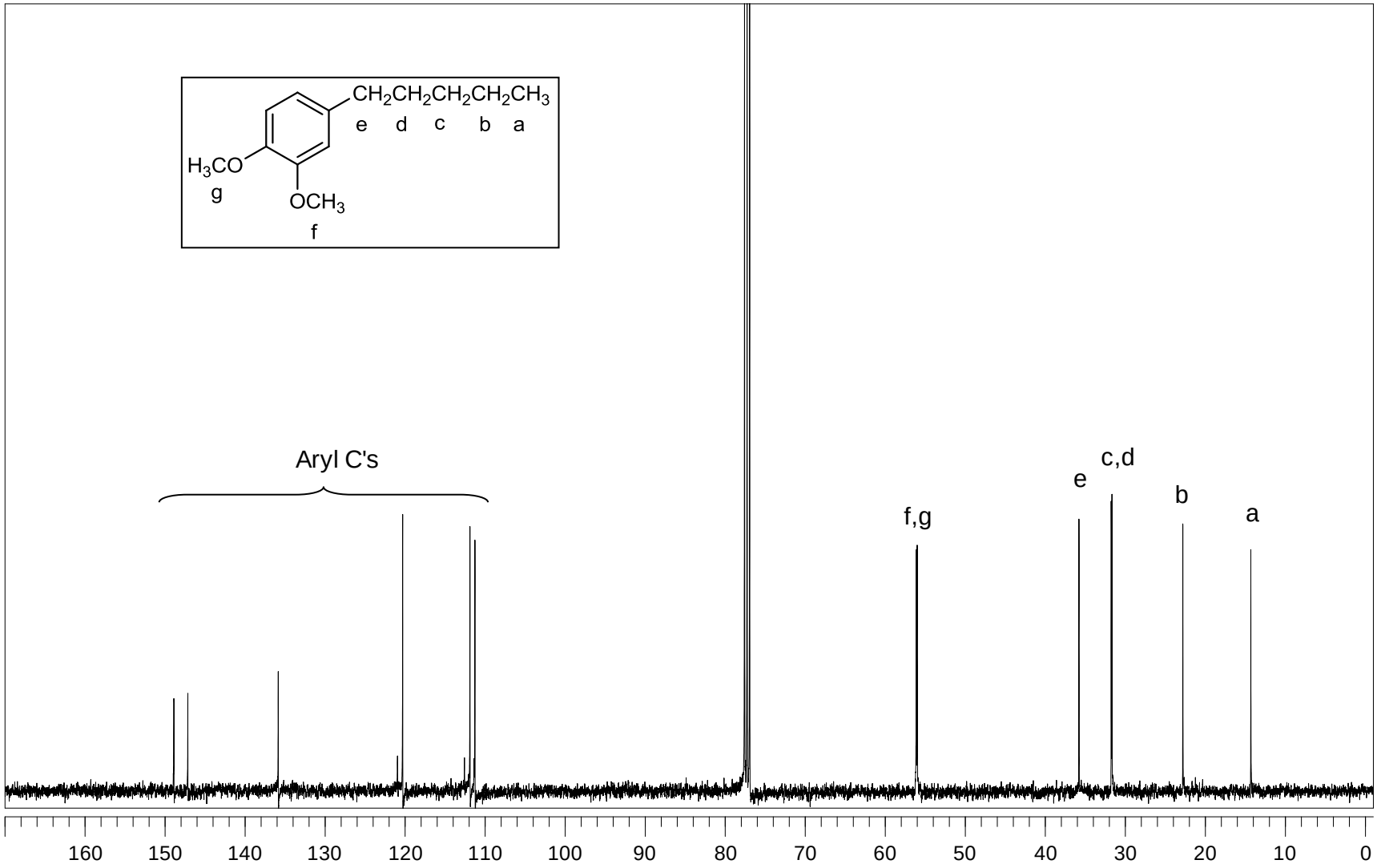


Figure A.39. ^{13}C-NMR ($CDCl_3$) spectrum of compound 33.

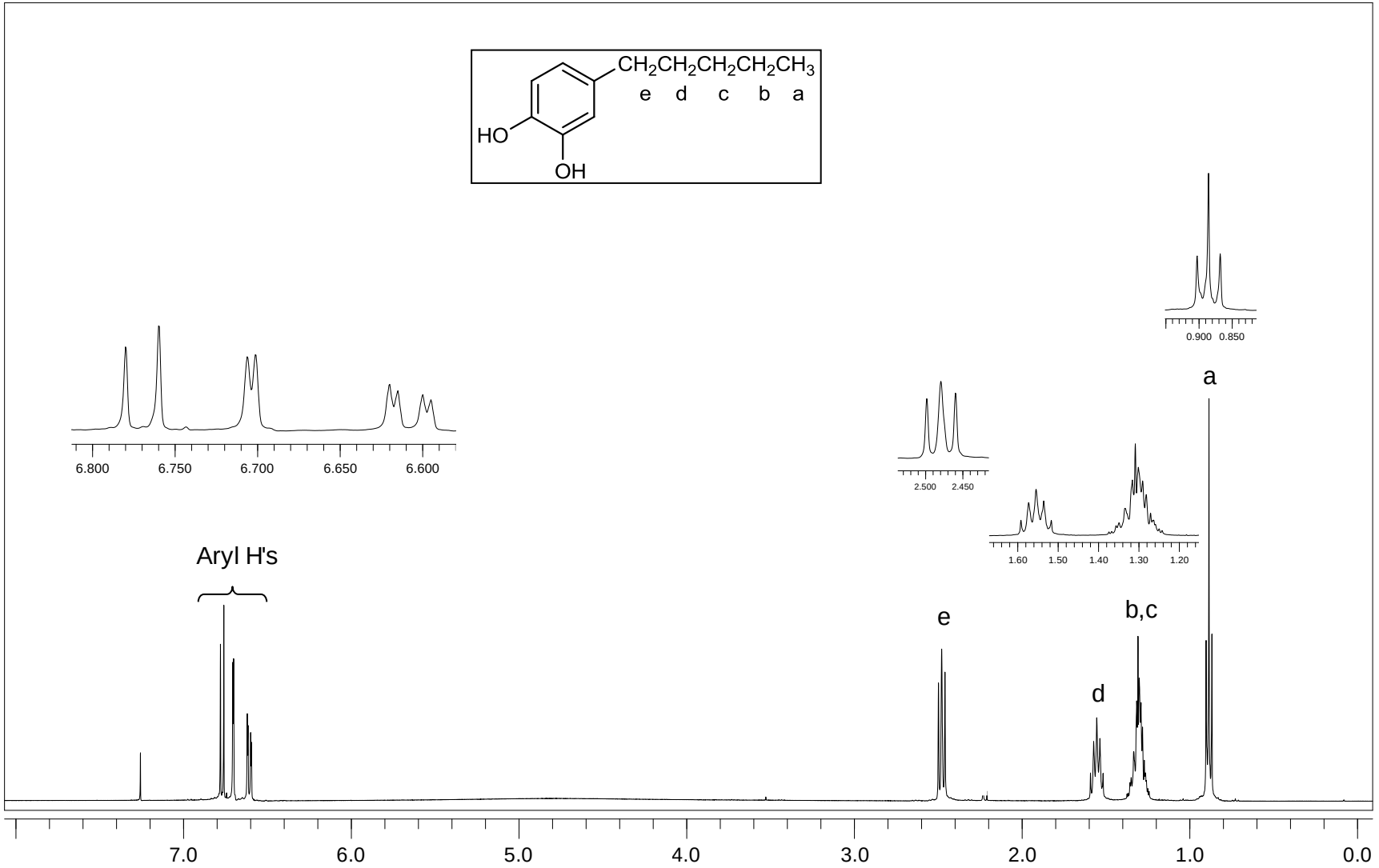


Figure A.40. ^{1}H-NMR ($CDCl_3$) spectrum of compound 34.

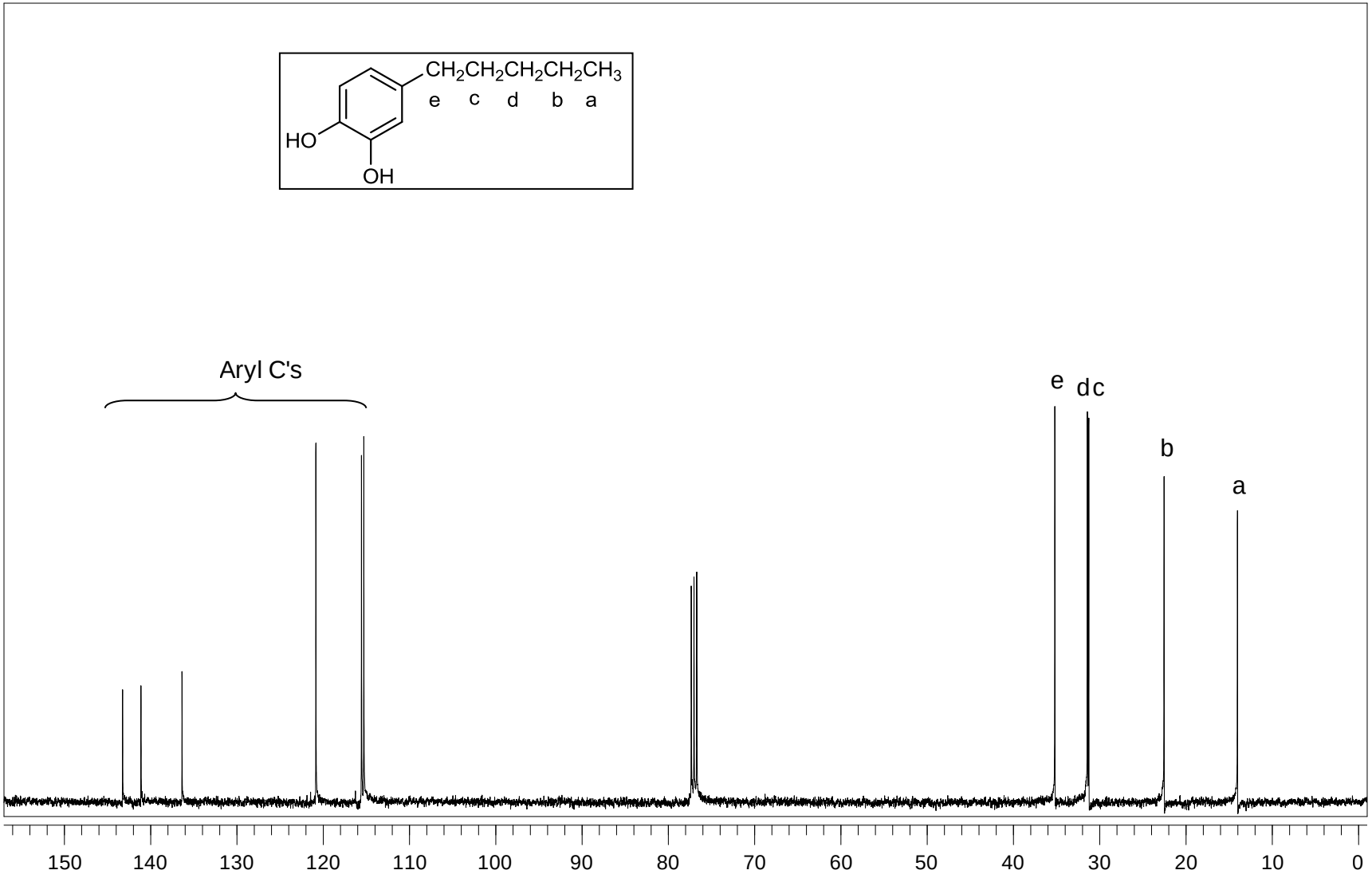


Figure A.41. ^{13}C-NMR ($CDCl_3$) spectrum of compound 34.

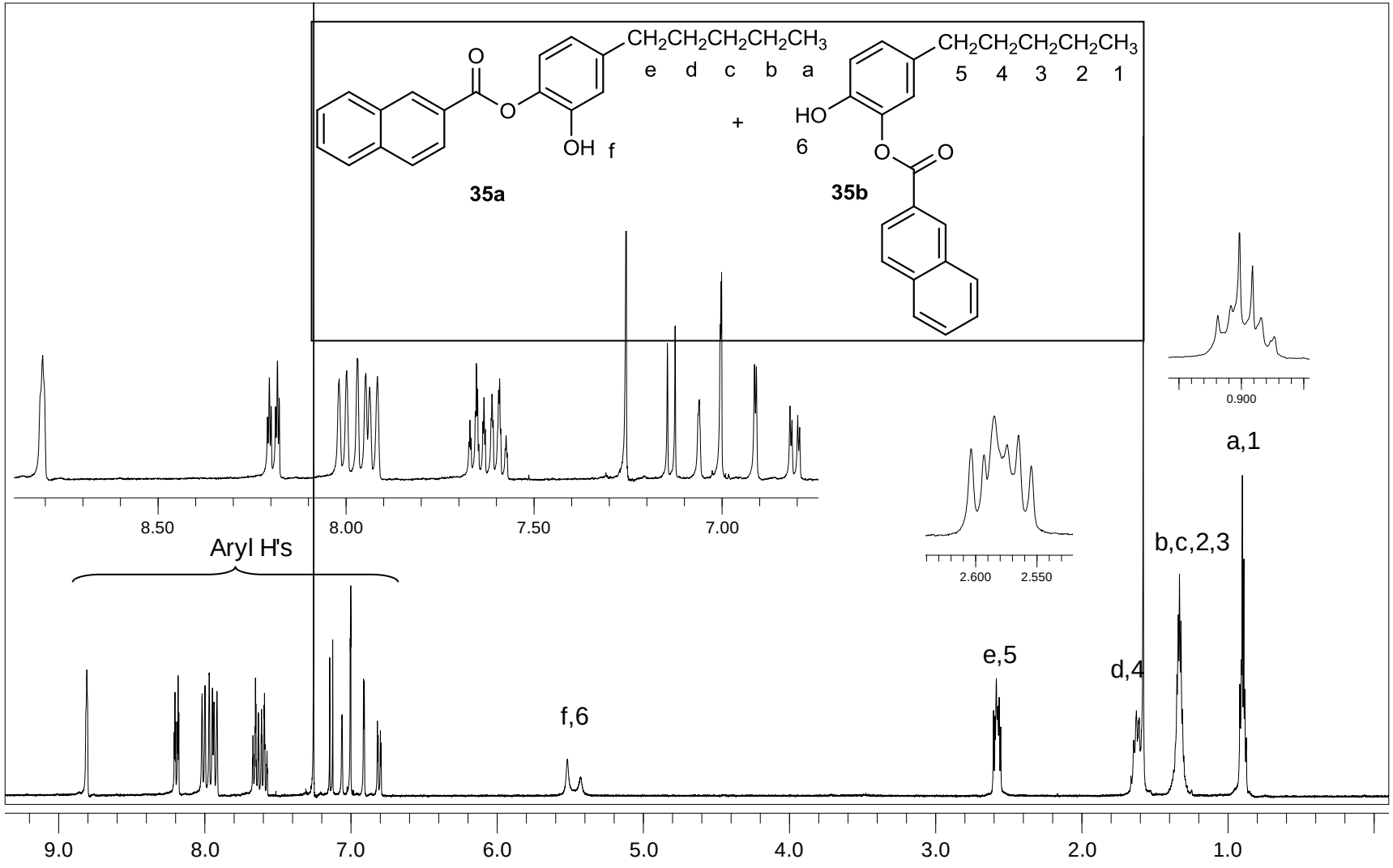


Figure A.42. ^{1}H-NMR ($CDCl_3$) spectrum of compound 35a and 35b.

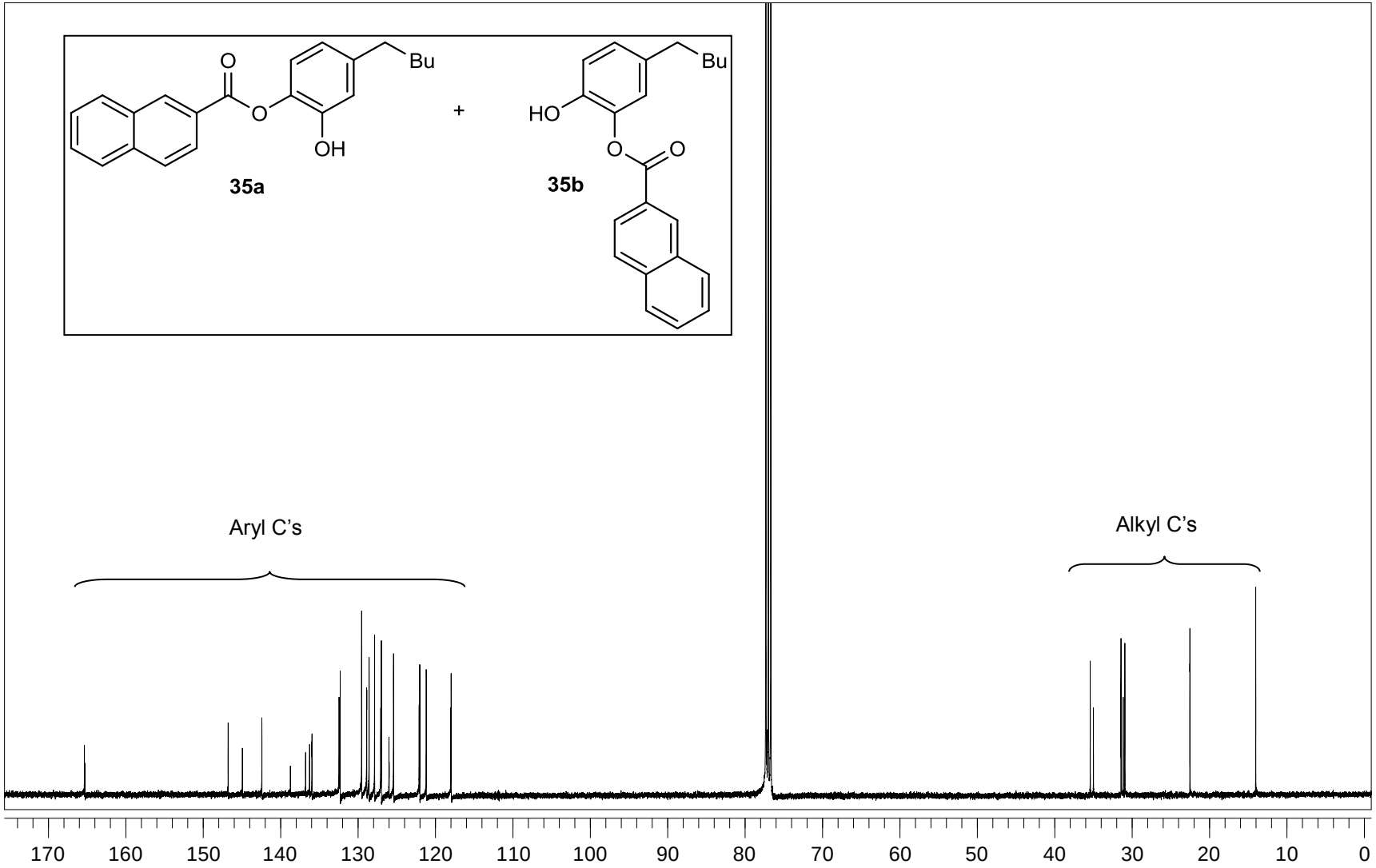


Figure A.43. ^{13}C-NMR ($CDCl_3$) spectrum of compound 35a and 35b.

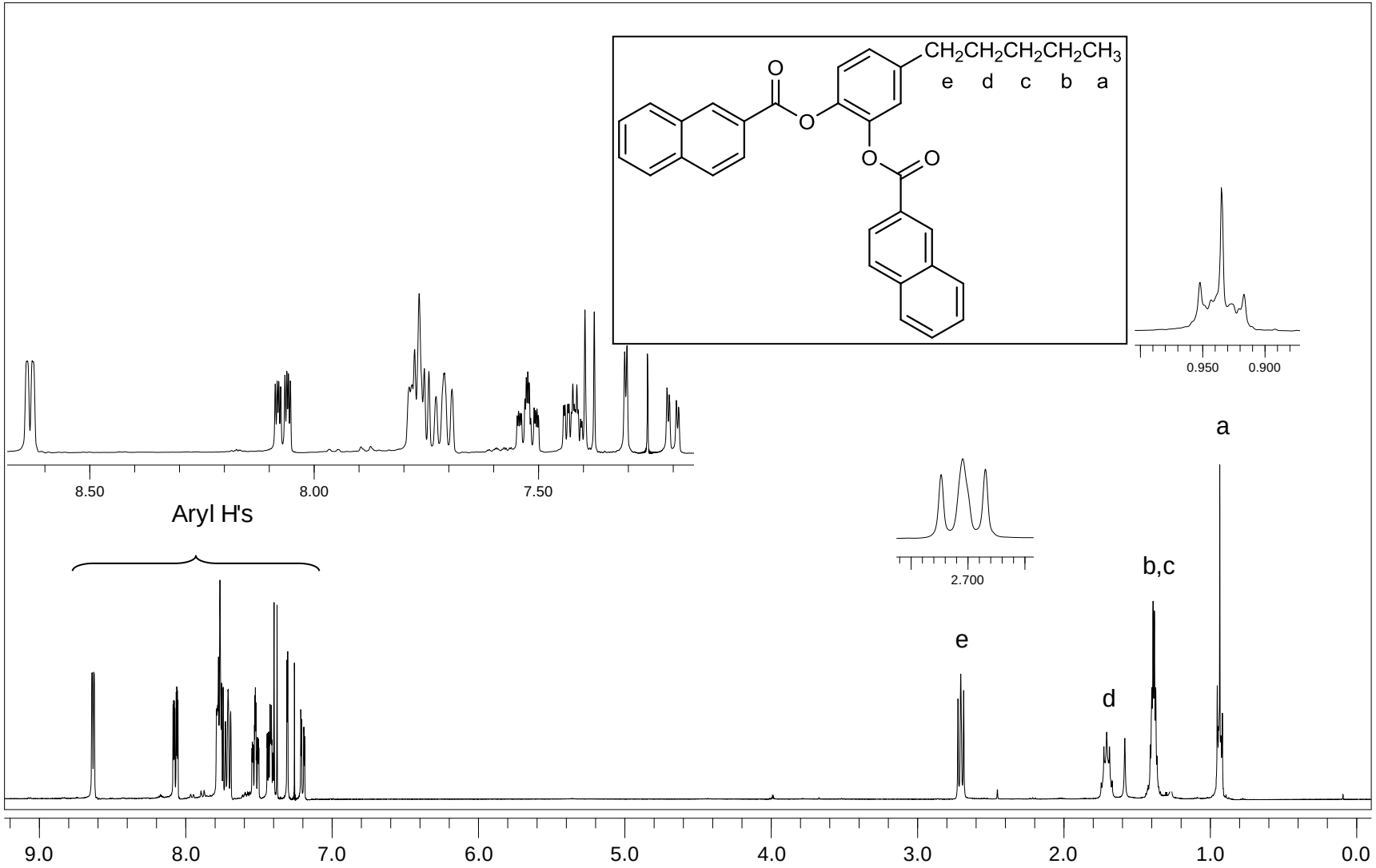


Figure A.44. ^{1}H-NMR ($CDCl_3$) spectrum of compound 36.

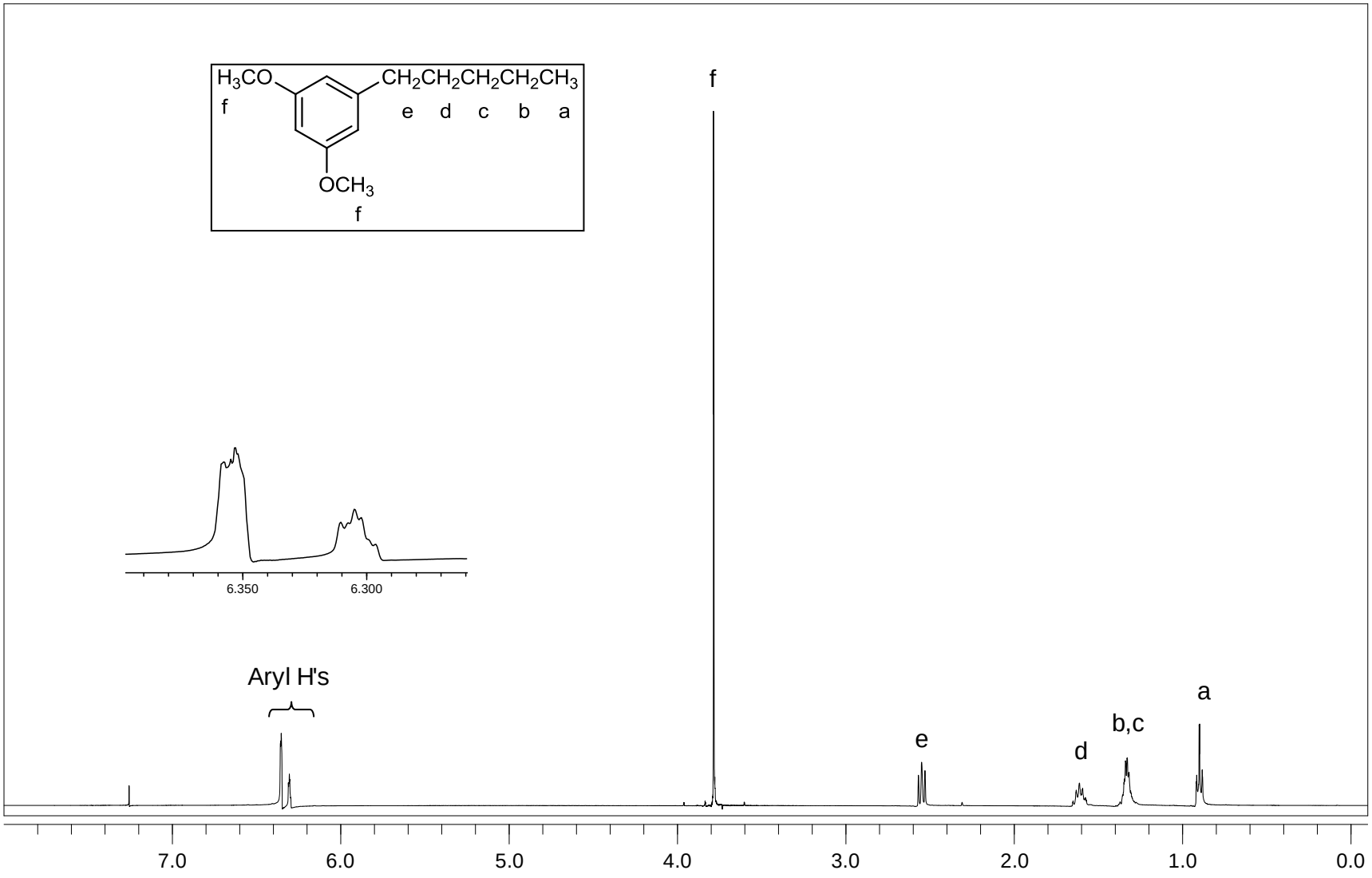


Figure A.45. ^{1}H-NMR ($CDCl_3$) spectrum of compound 38.

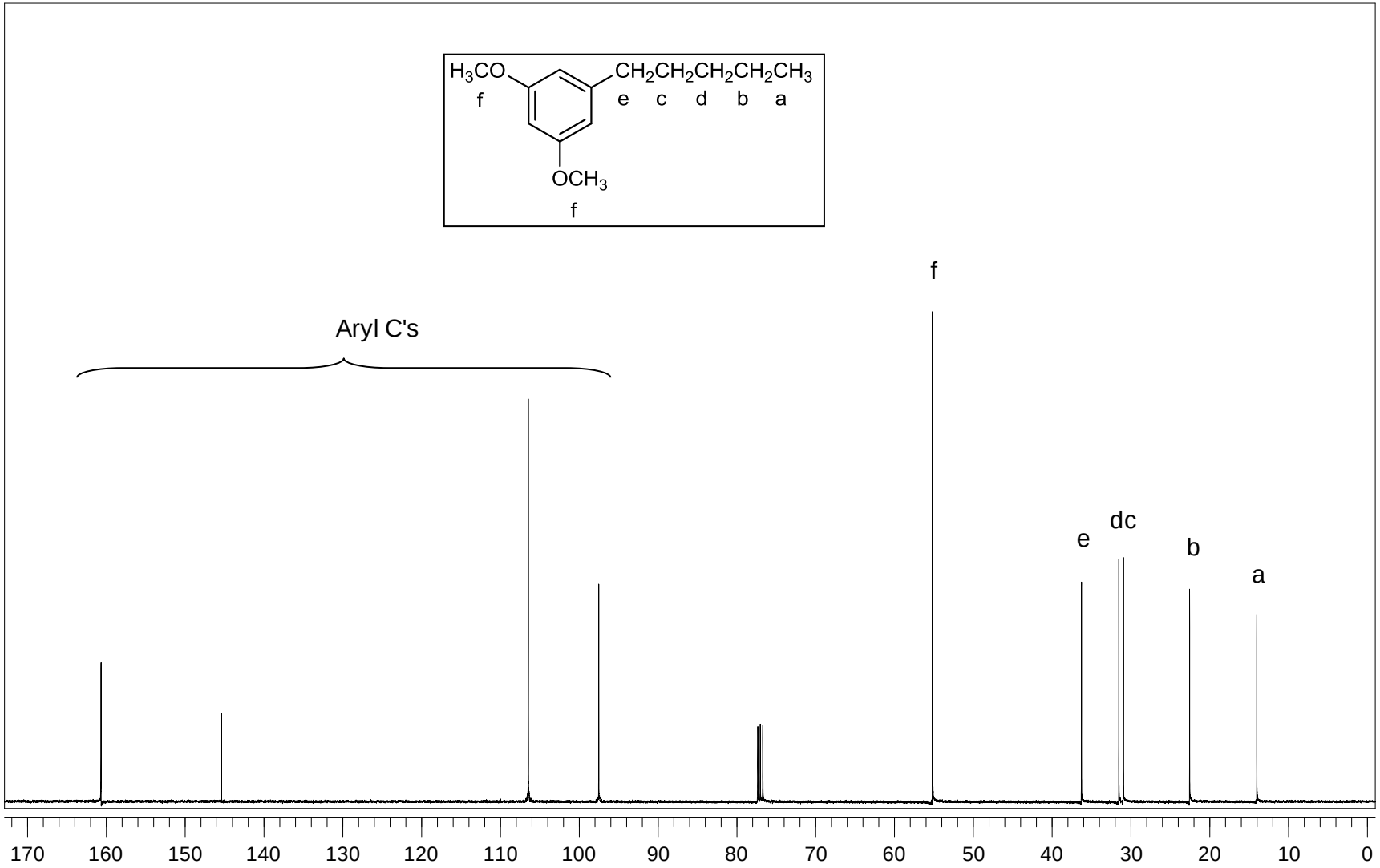


Figure A.46. ^{13}C-NMR ($CDCl_3$) spectrum of compound 38.

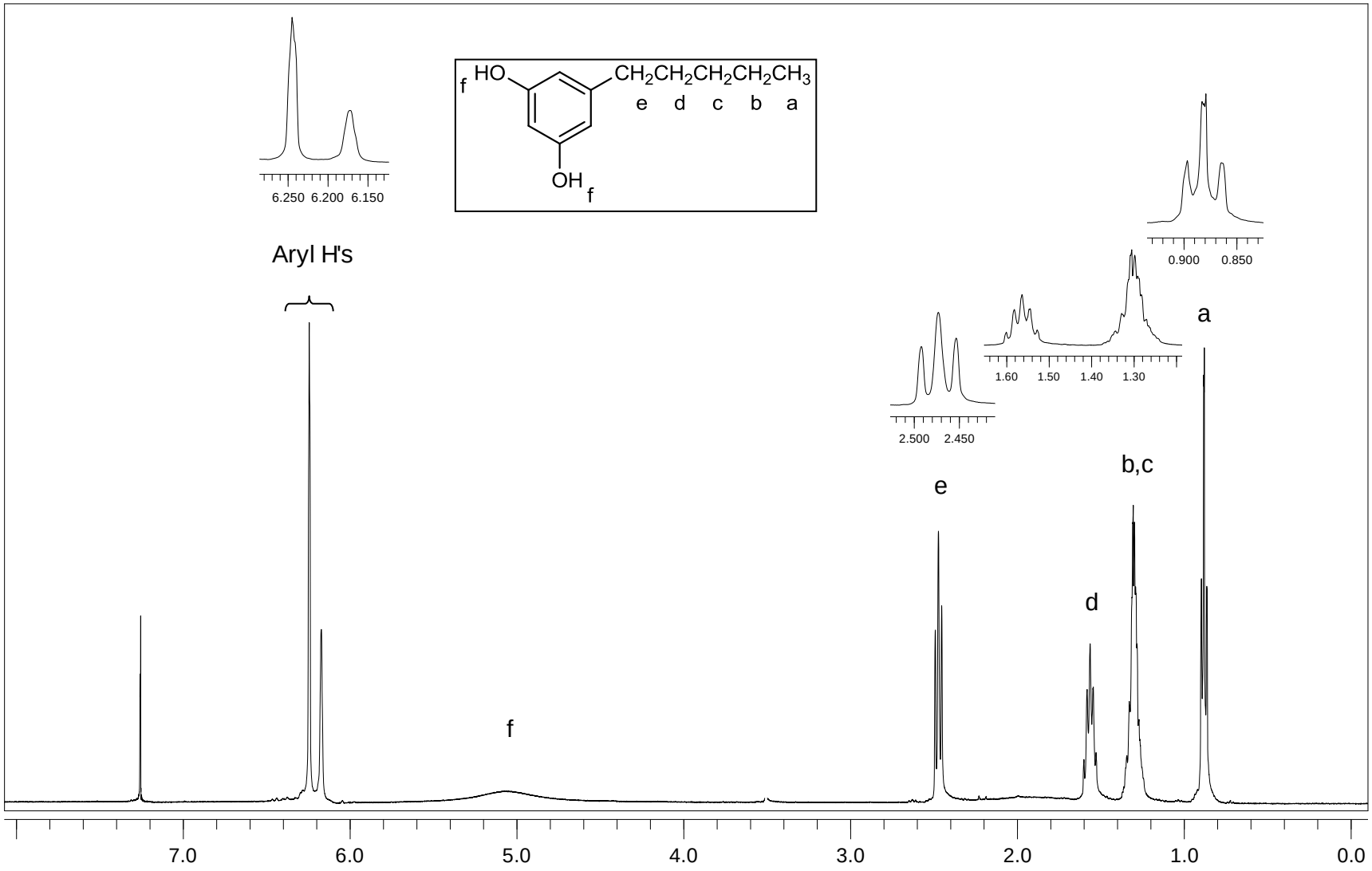


Figure A.47. ^{1}H-NMR ($CDCl_3$) spectrum of compound 39.

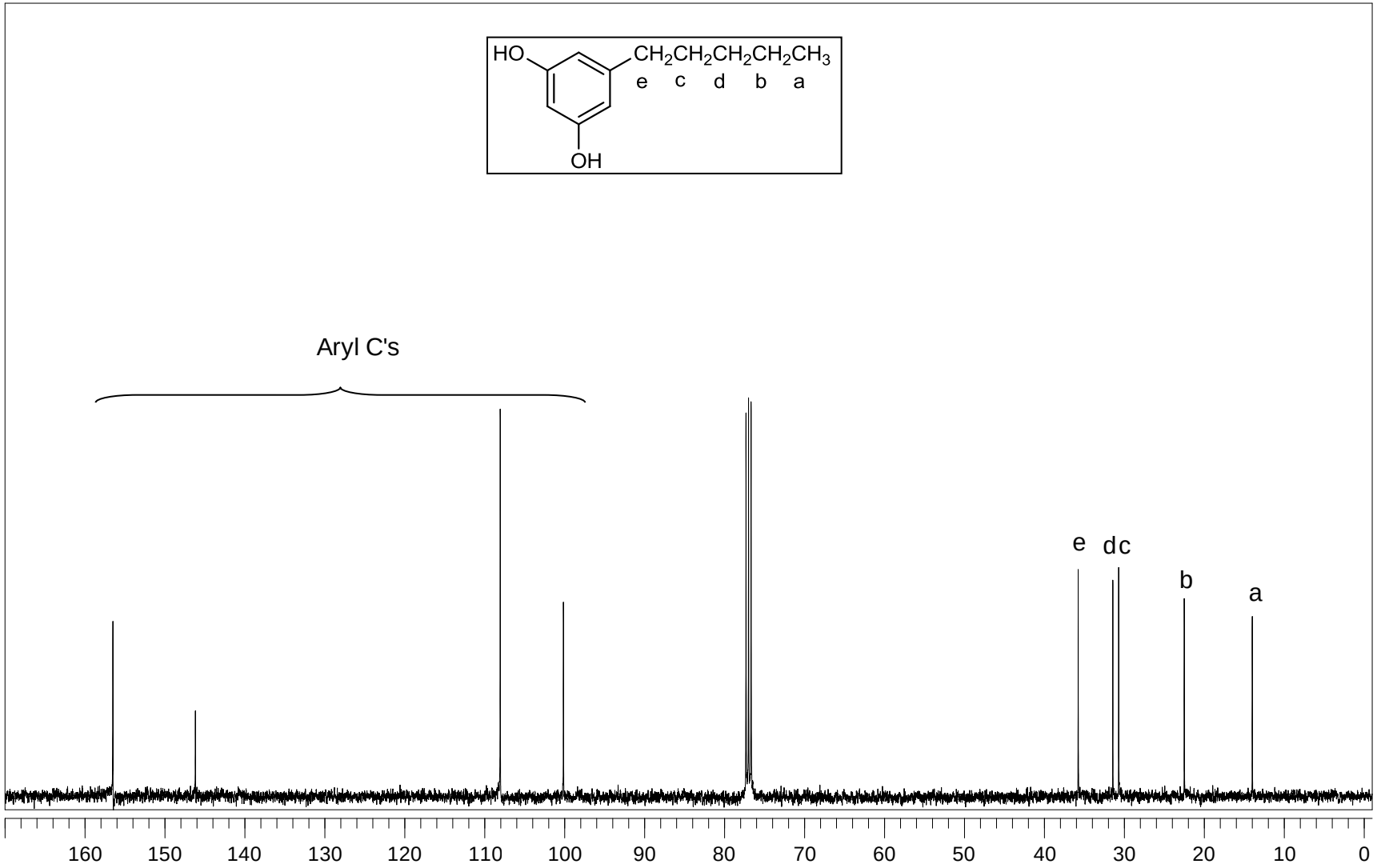


Figure A.48. ^{13}C-NMR ($CDCl_3$) spectrum of compound 39.

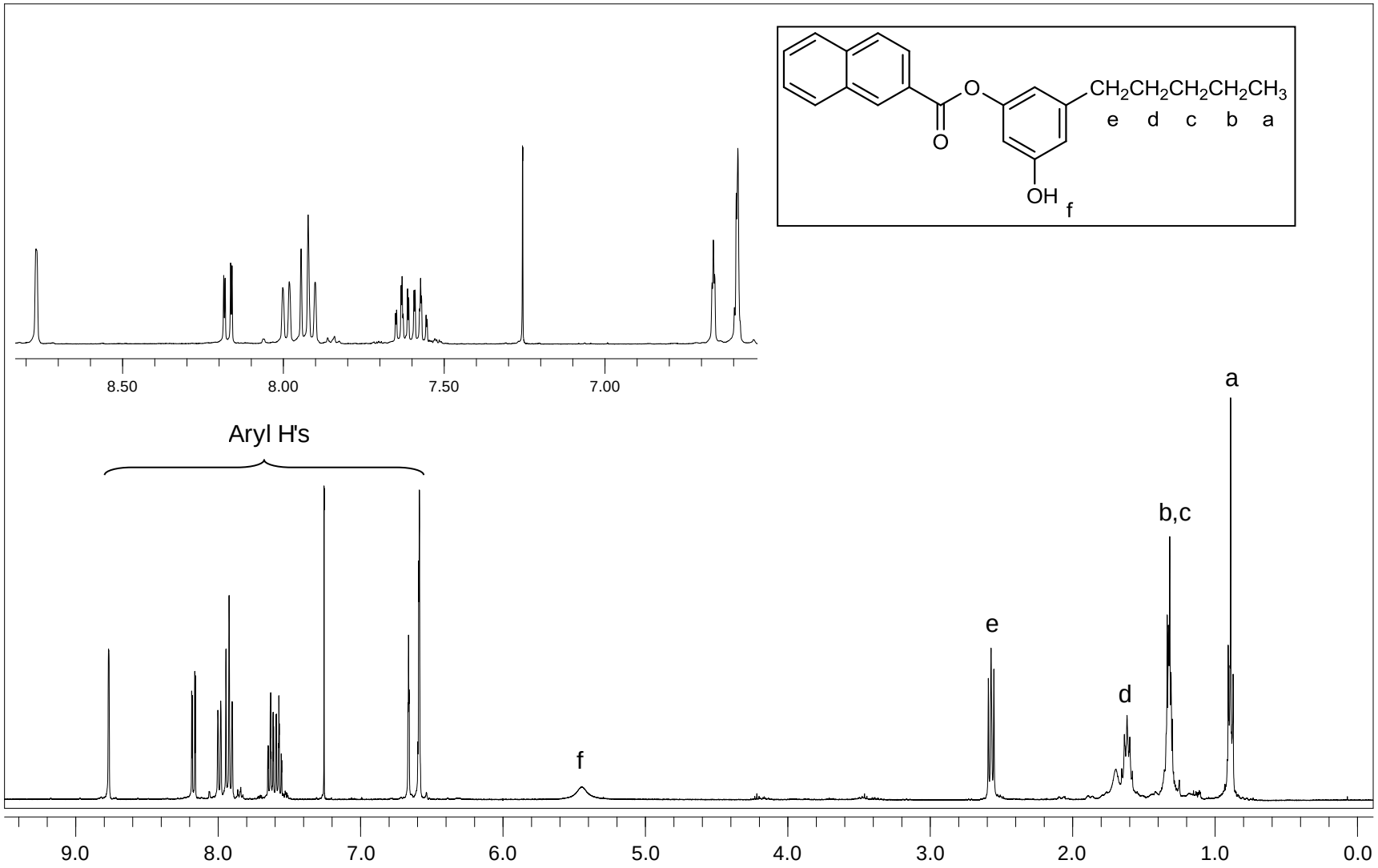


Figure A.49. ^{1}H-NMR ($CDCl_3$) spectrum of compound 40.

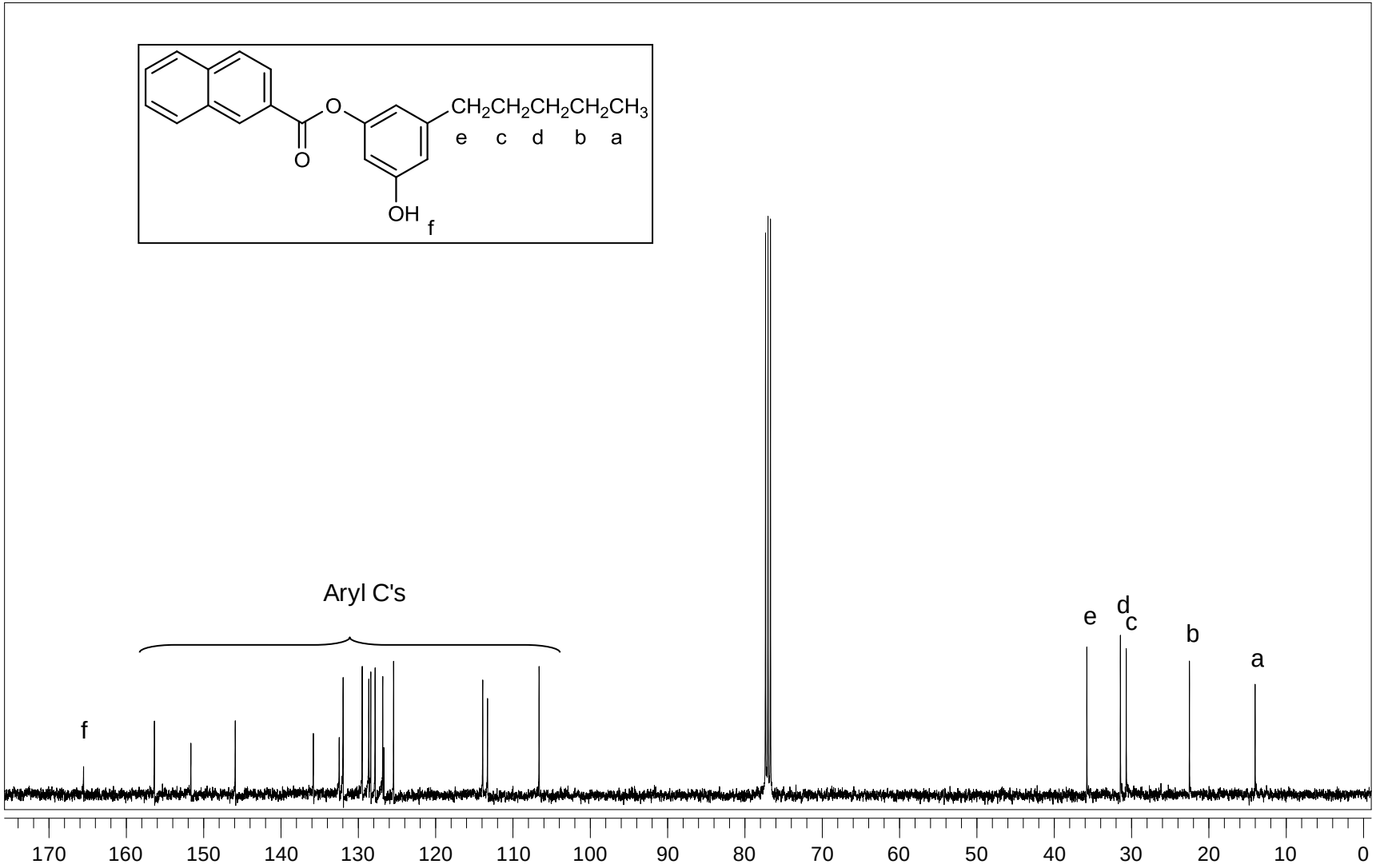


Figure A.50. ^{13}C-NMR ($CDCl_3$) spectrum of compound 40.

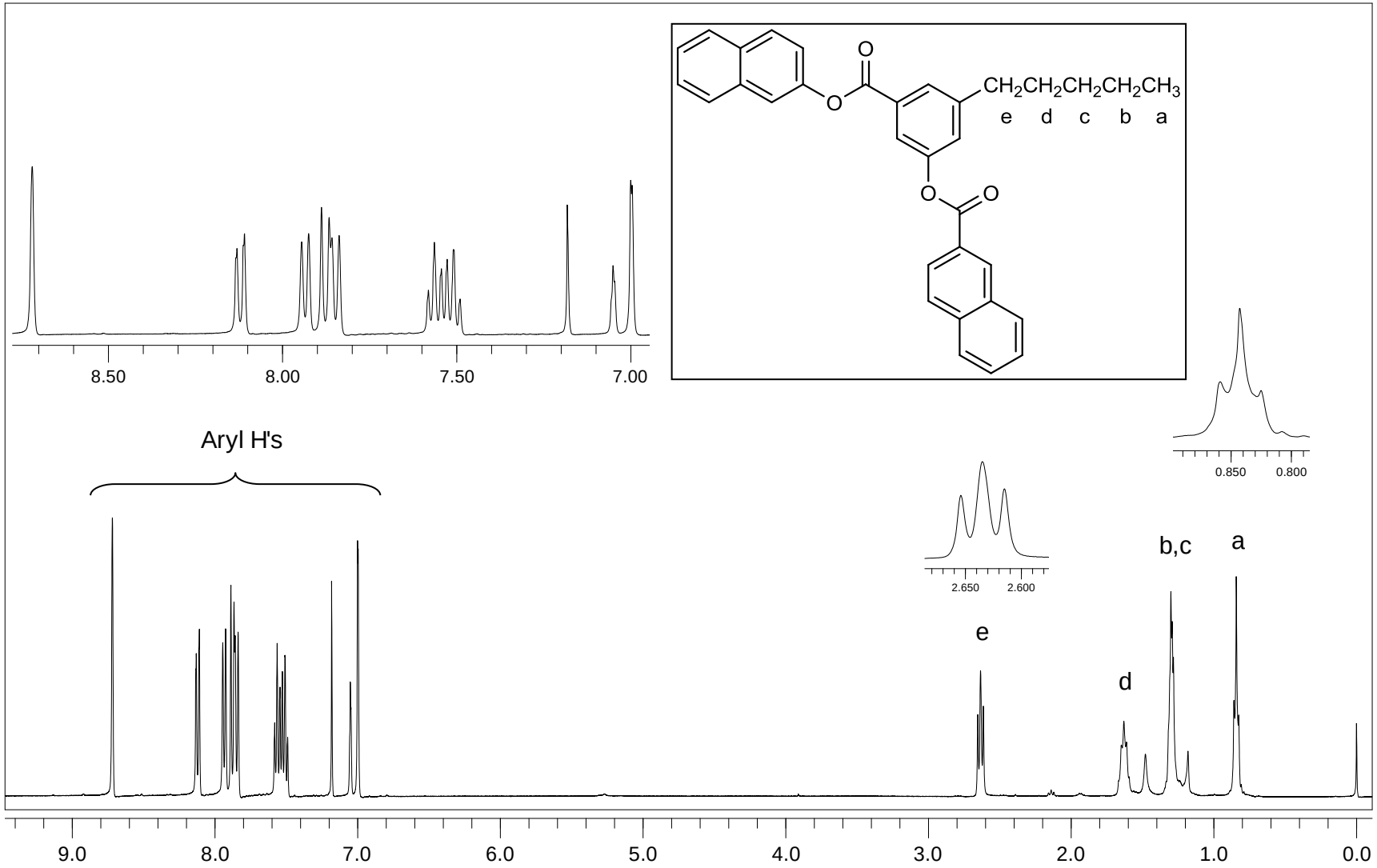


Figure A.51. ^{1}H-NMR ($CDCl_3$) spectrum of compound 41.

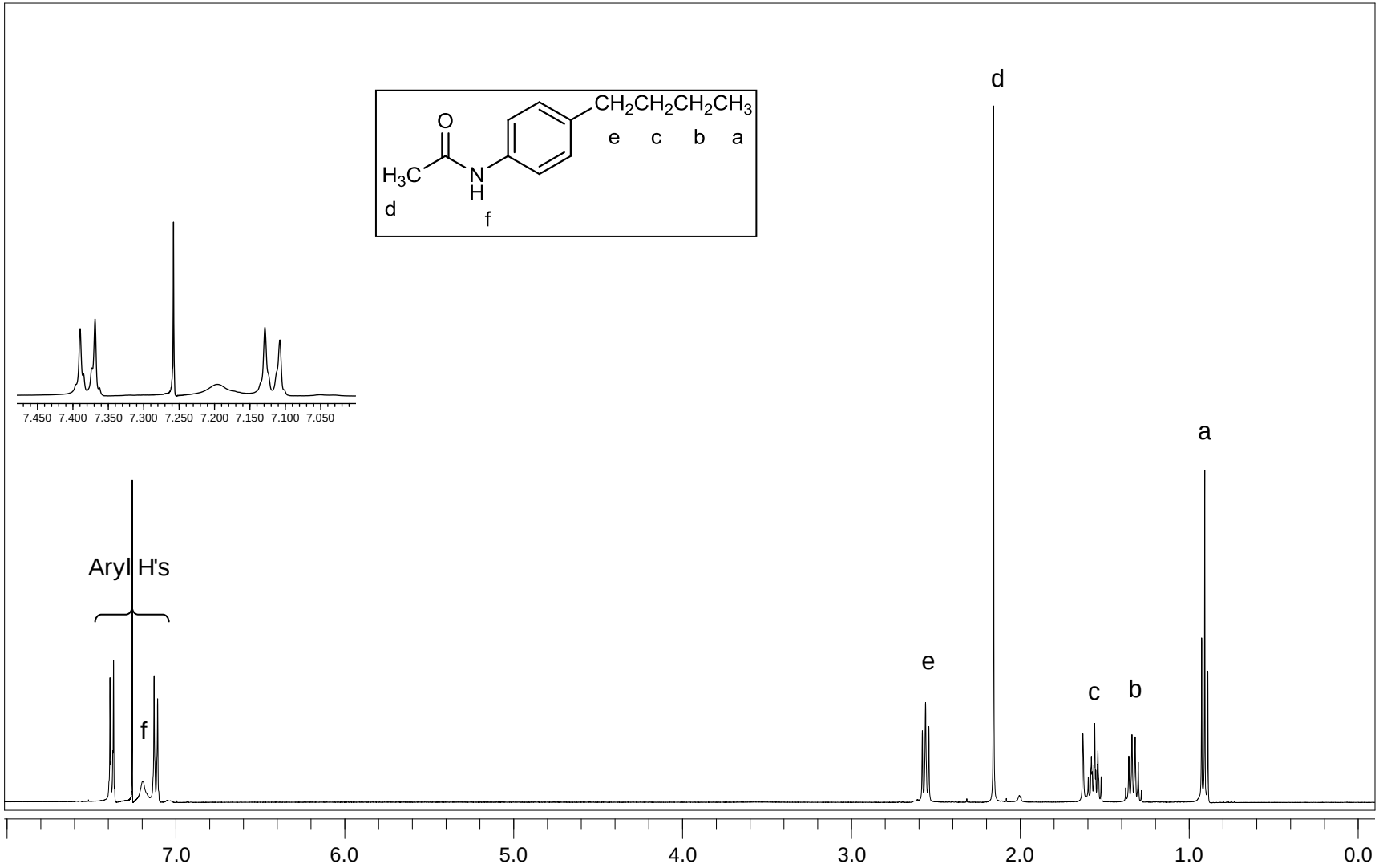


Figure A.52. ^{1}H-NMR ($CDCl_3$) spectrum of compound 43.

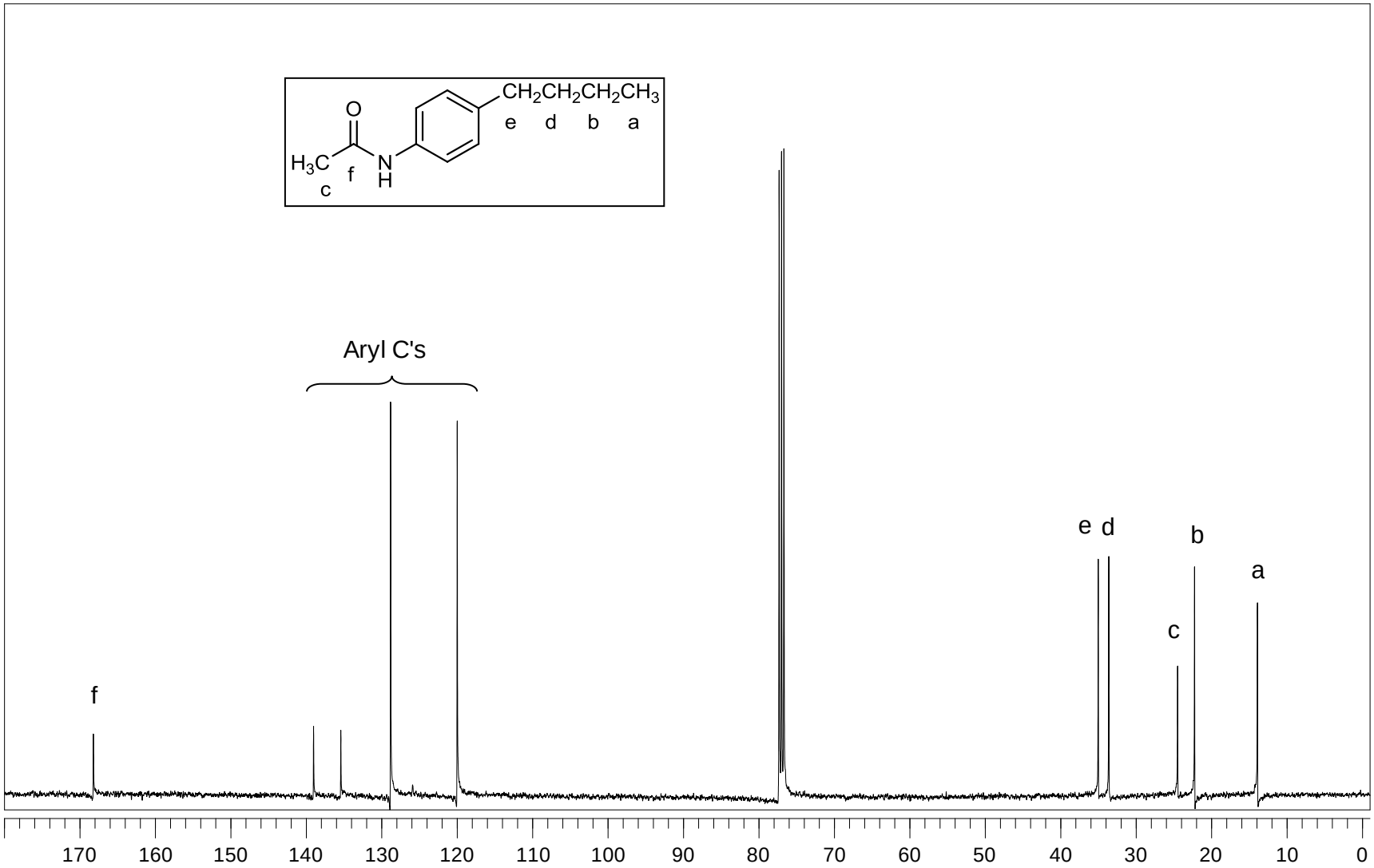


Figure A.53. ^{13}C-NMR ($CDCl_3$) spectrum of compound 43.

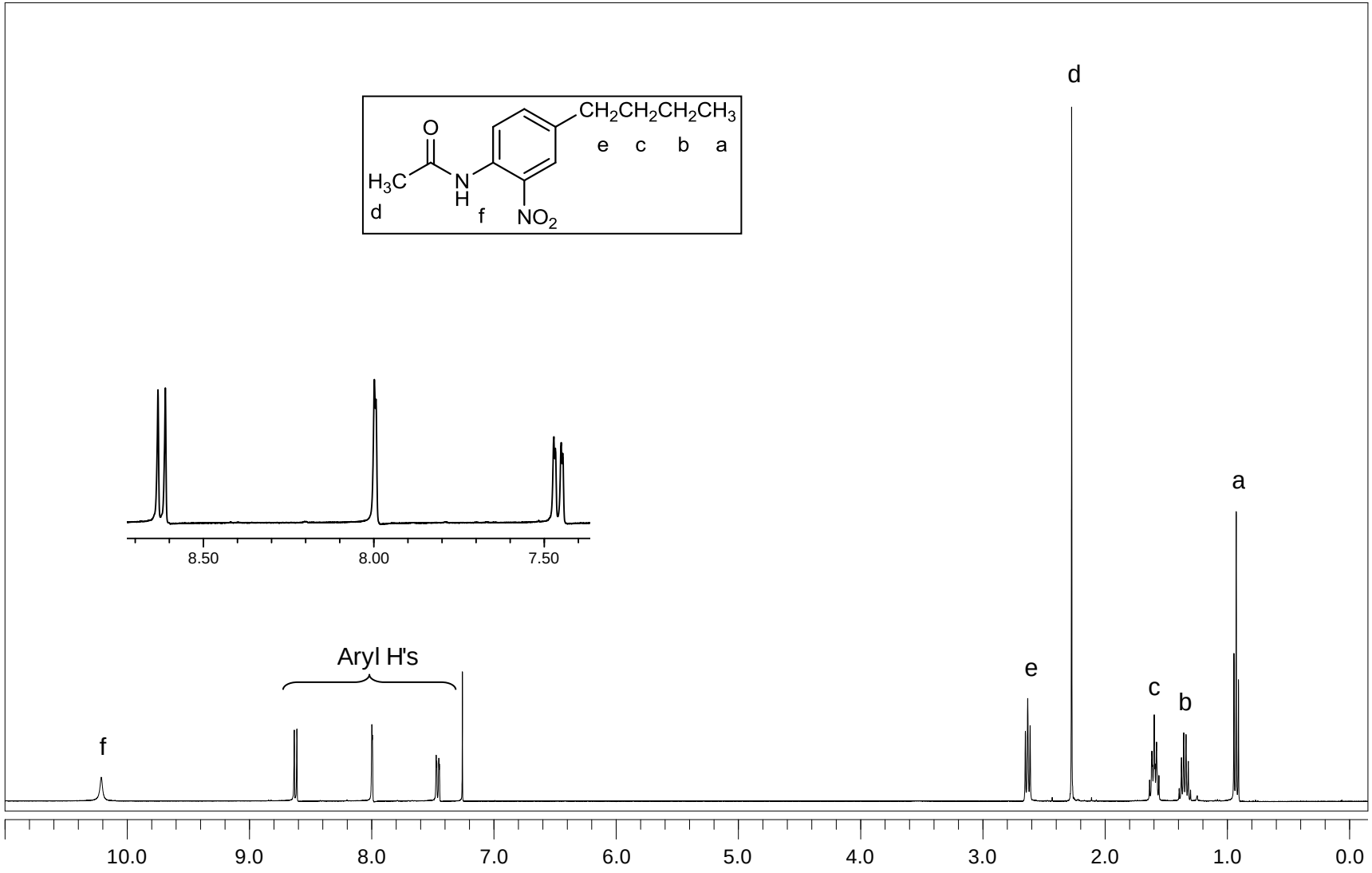


Figure A.54. ^{1}H-NMR ($CDCl_3$) spectrum of compound 44.

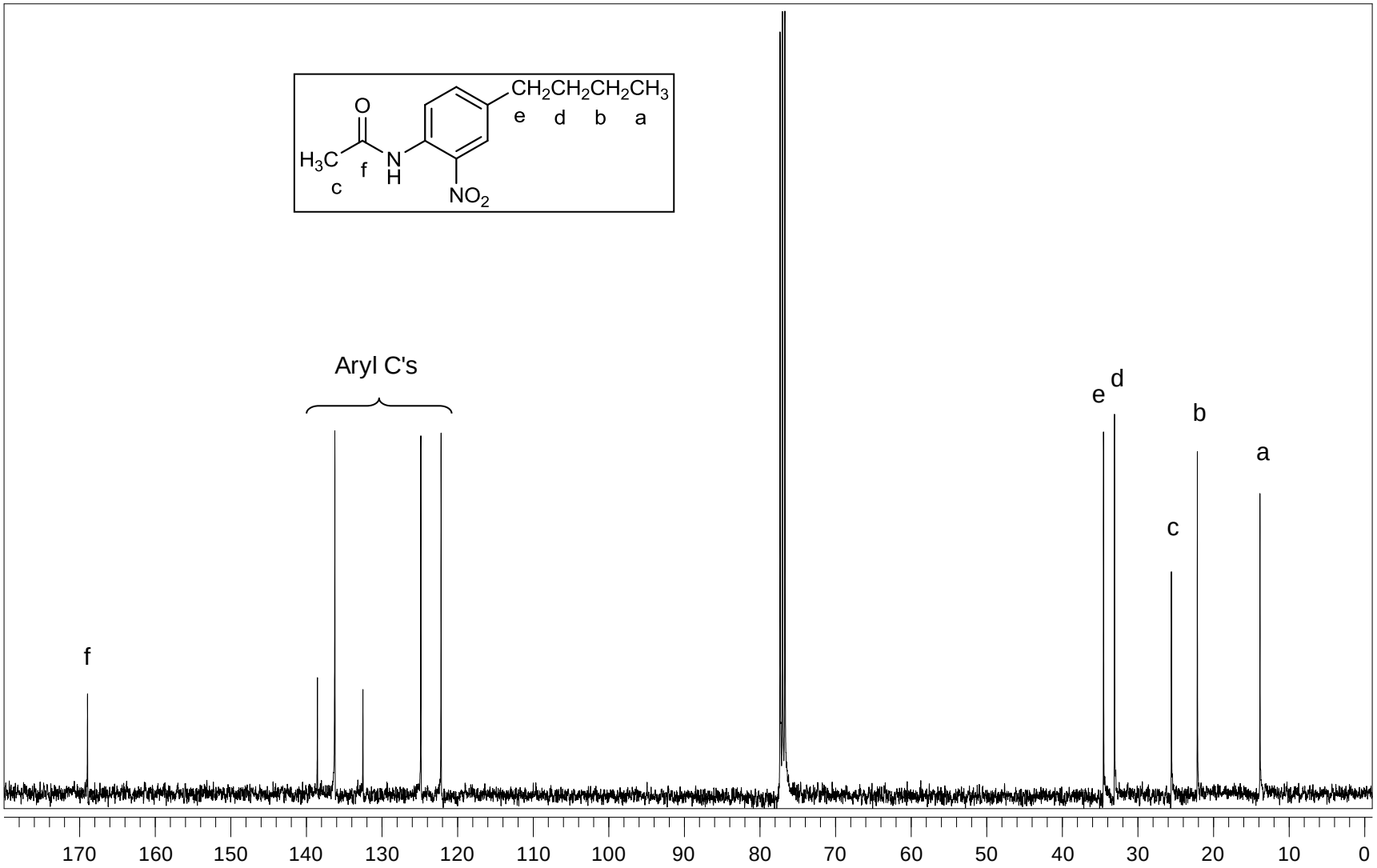


Figure A.55. ^{13}C-NMR ($CDCl_3$) spectrum of compound 44.

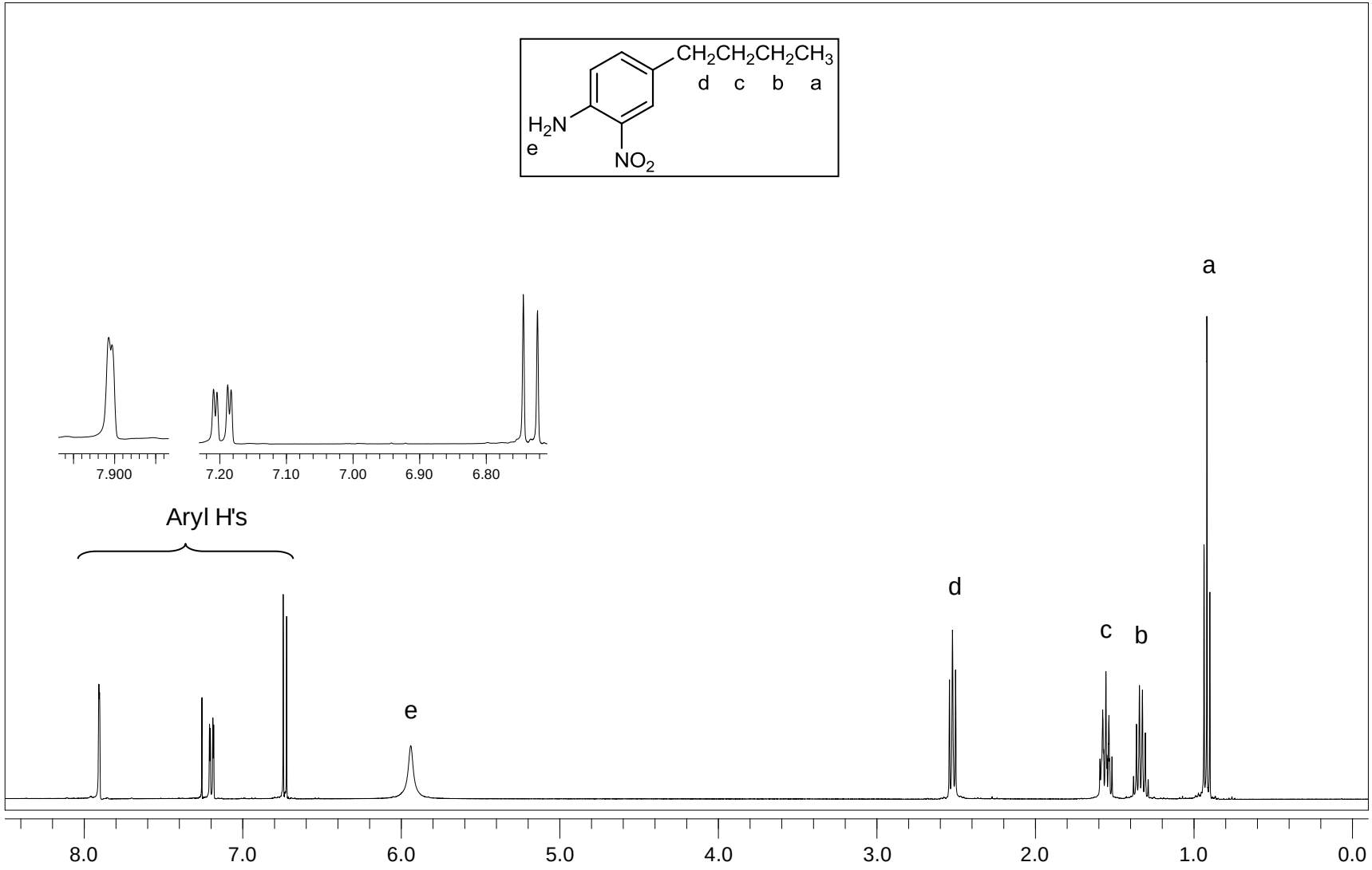


Figure A.56. ^{1}H-NMR ($CDCl_3$) spectrum of compound 45.

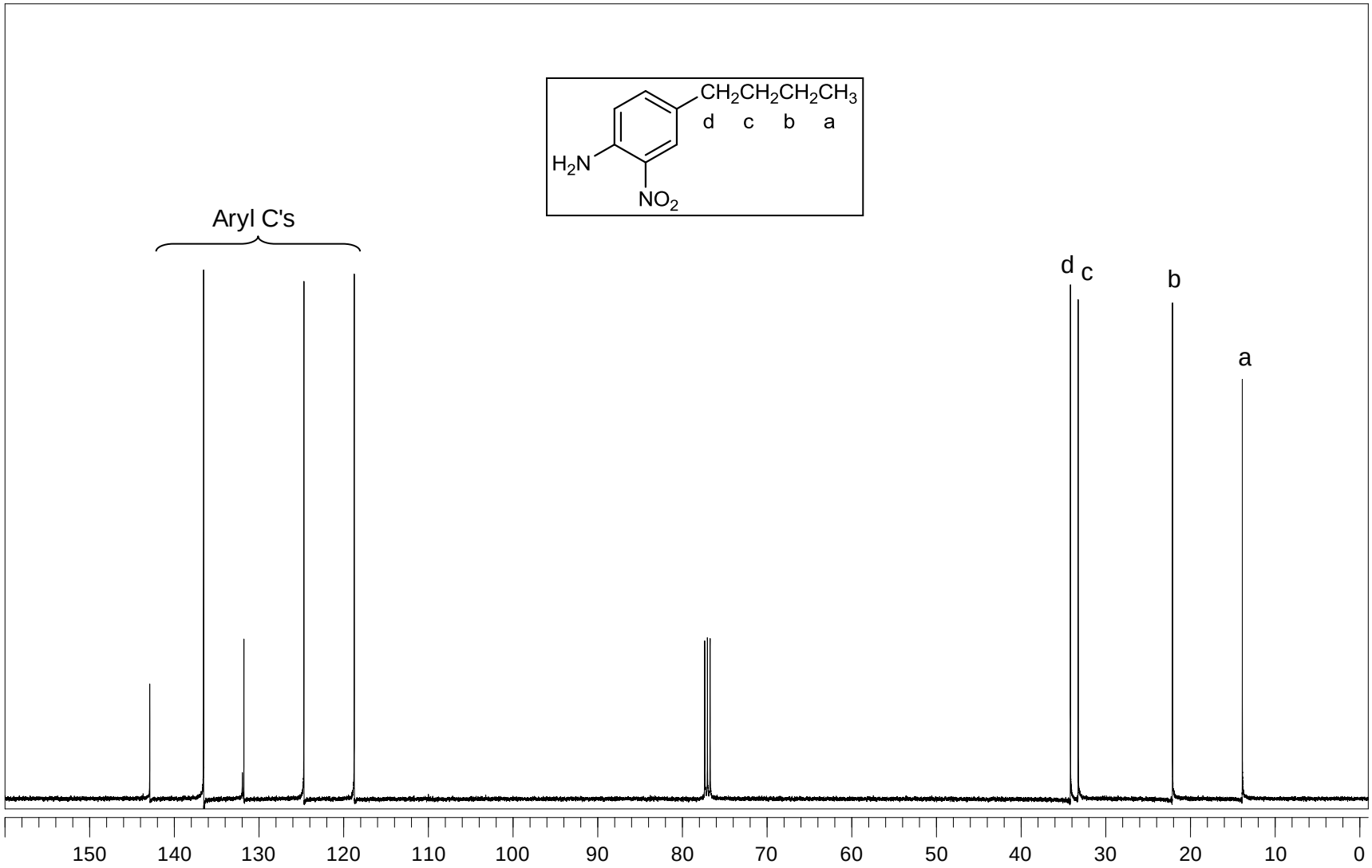


Figure A.57. ^{13}C-NMR ($CDCl_3$) spectrum of compound 45.

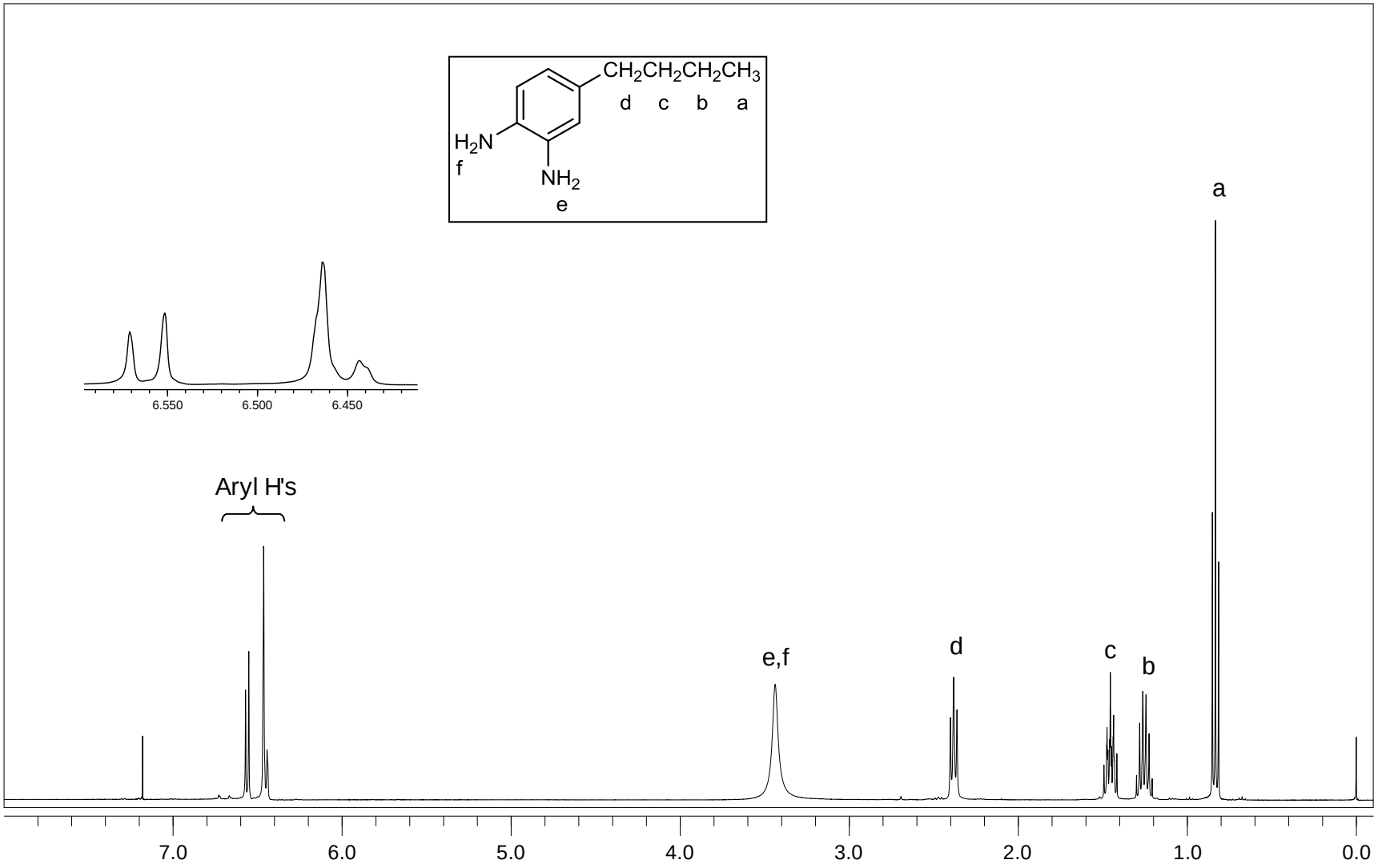


Figure A.58. ^{1}H-NMR ($CDCl_3$) spectrum of compound 46.

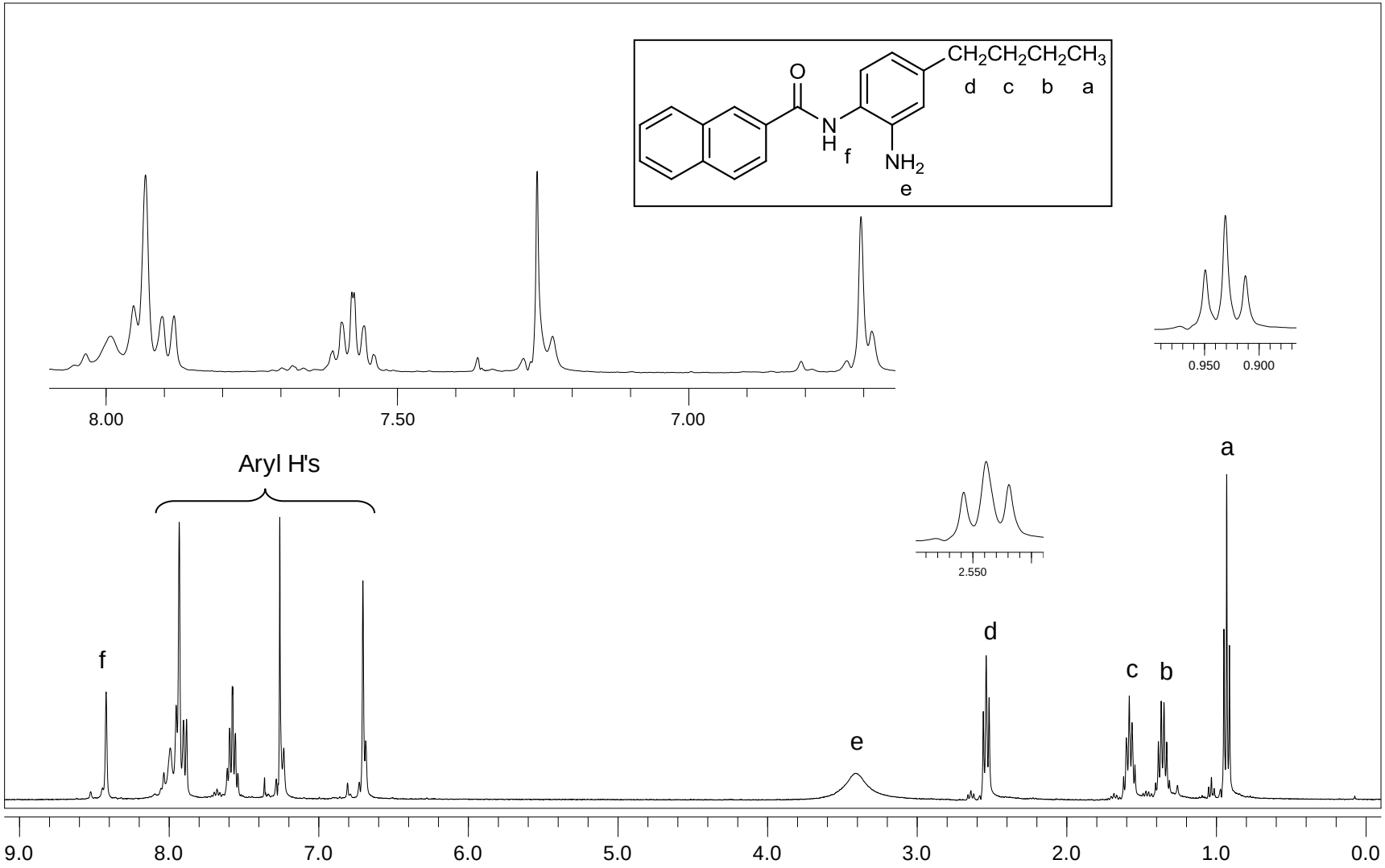


Figure A.59. ^{1}H-NMR ($CDCl_3$) spectrum of compound 47a.

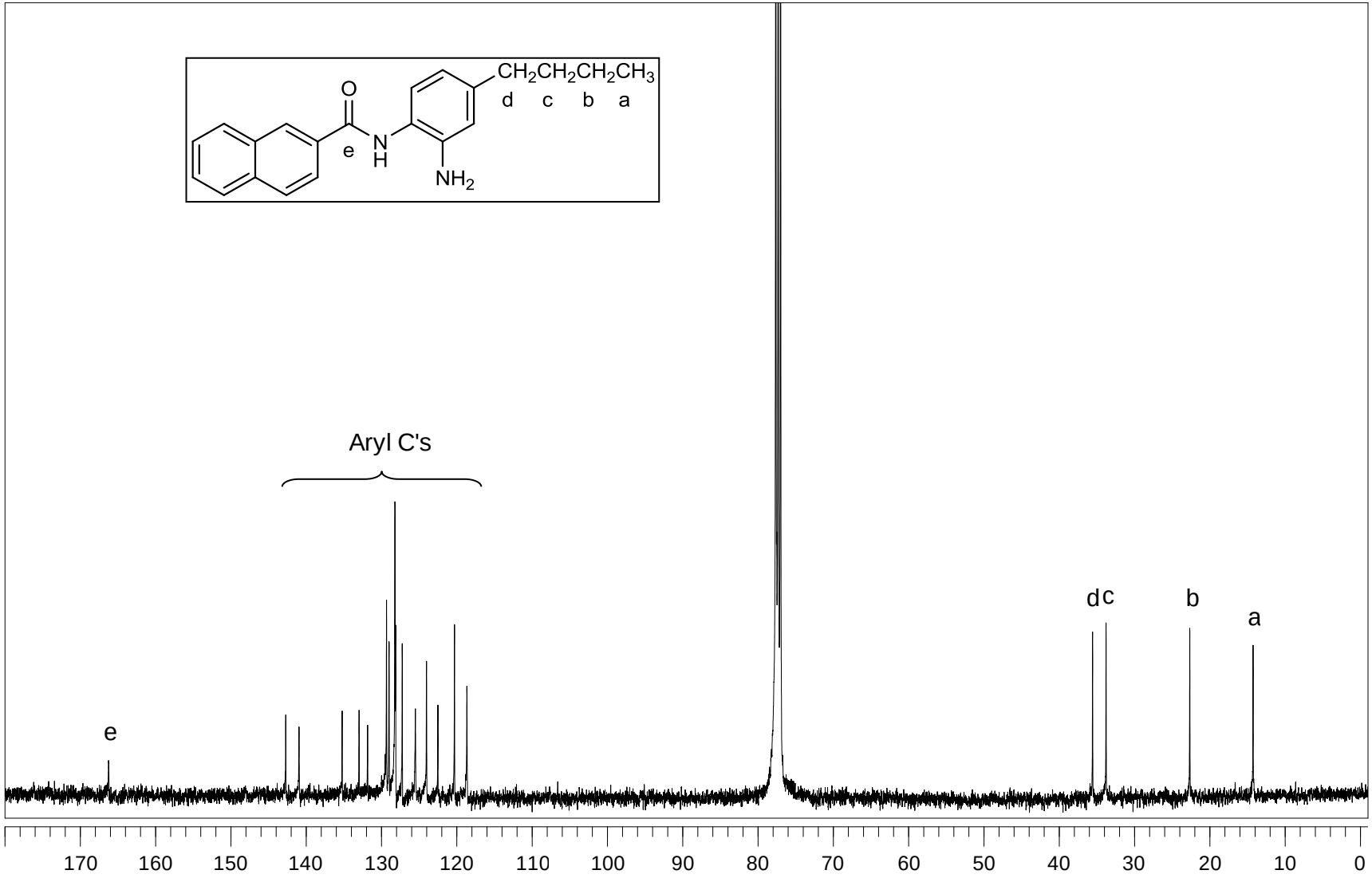


Figure A.60. ^{13}C-NMR ($CDCl_3$) spectrum of compound 47a.

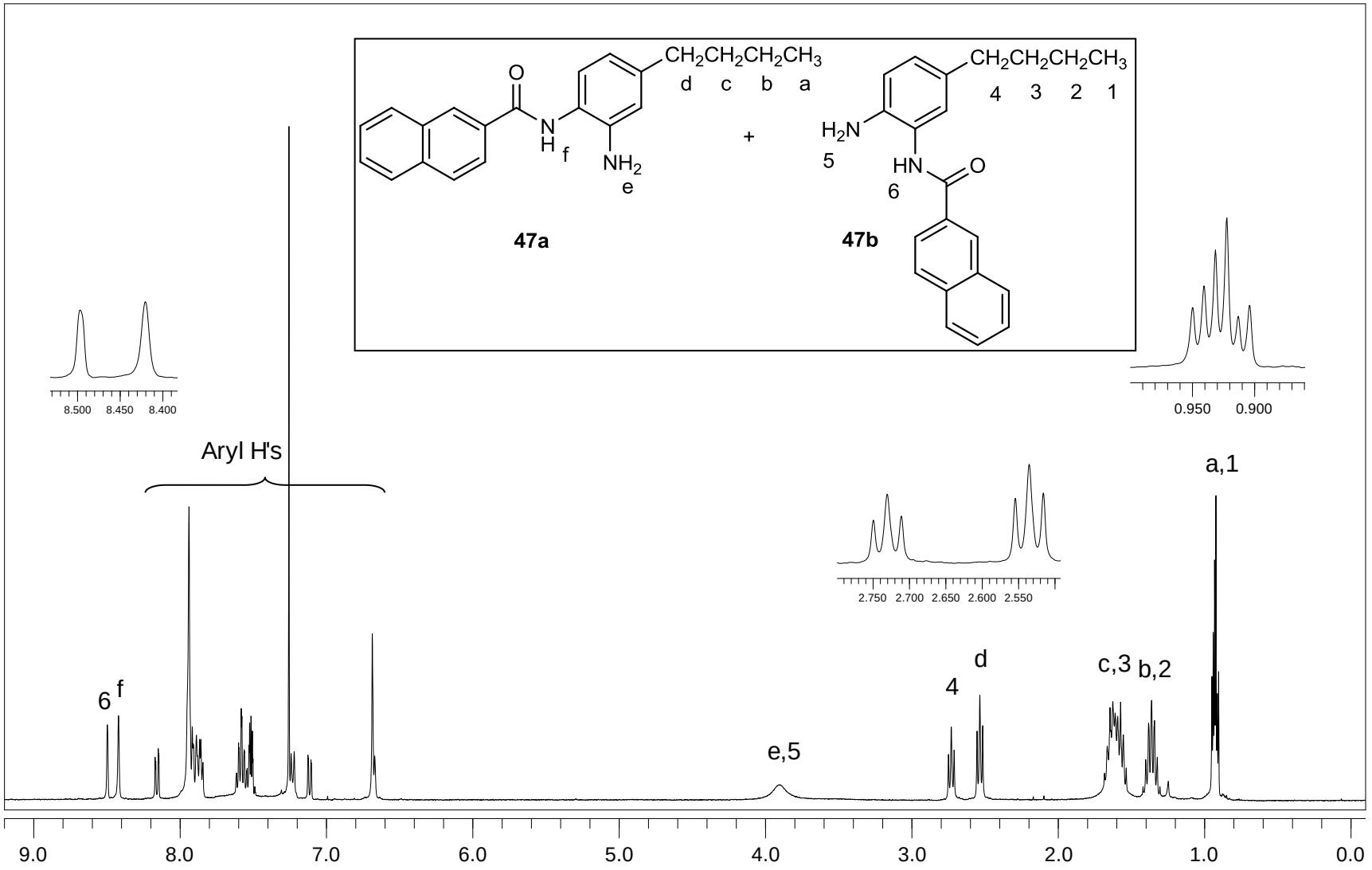


Figure A.61. ^{1}H-NMR ($CDCl_3$) spectrum of compounds 47a and 47b.

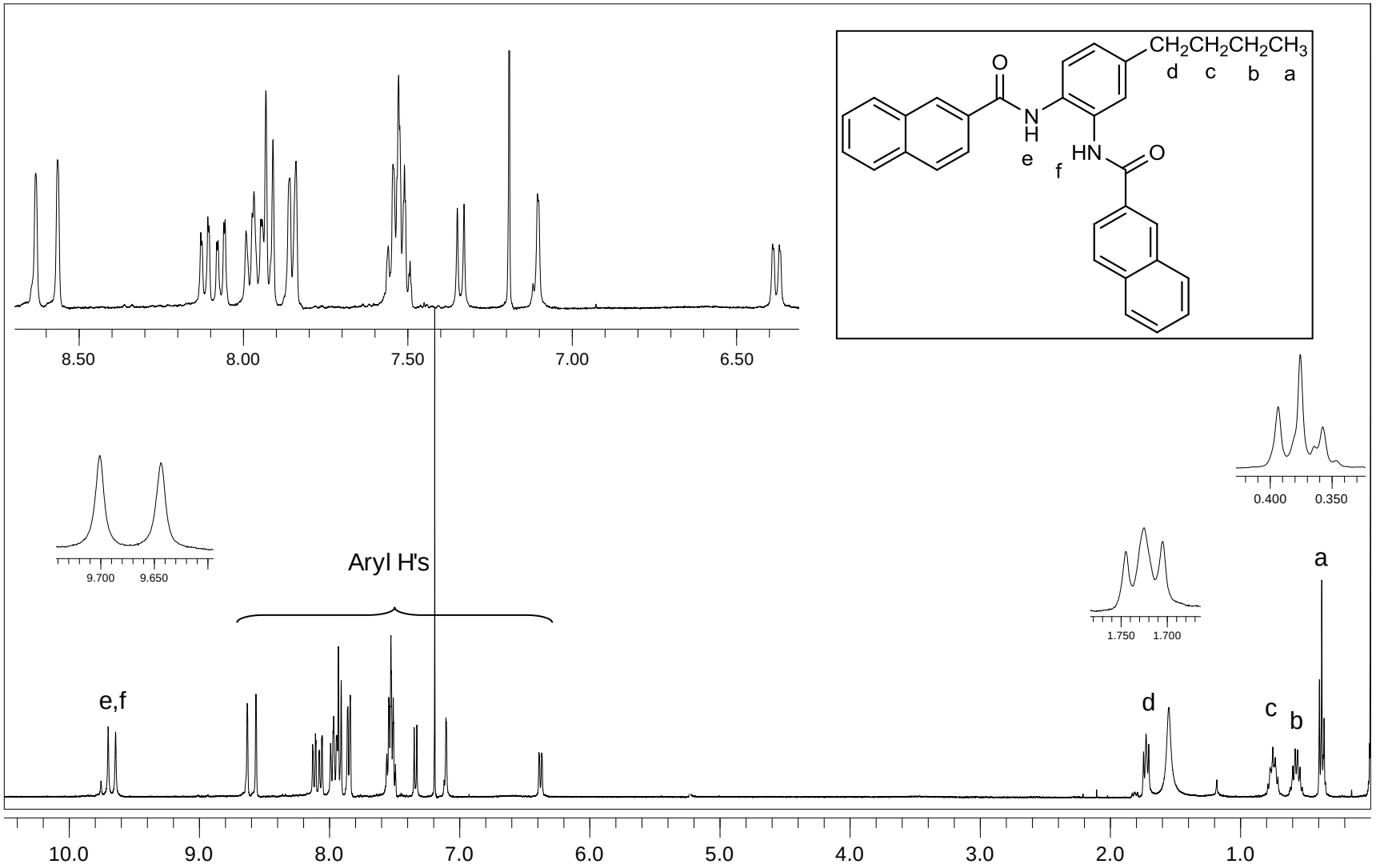


Figure A.62. ^{1}H-NMR ($CDCl_3$) spectrum of compound 48.

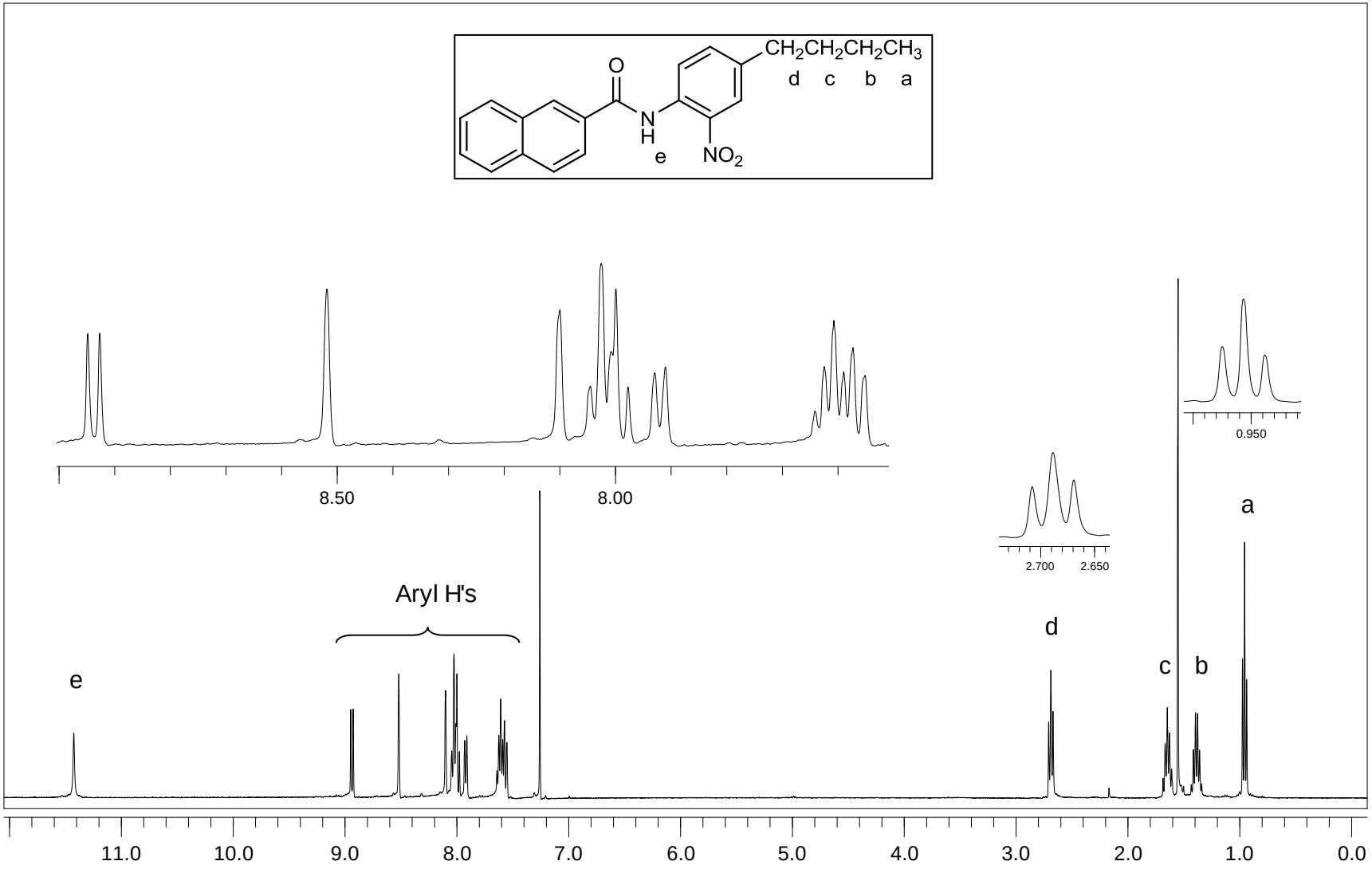


Figure A.63. ^{1}H-NMR ($CDCl_3$) spectrum of compound 49.

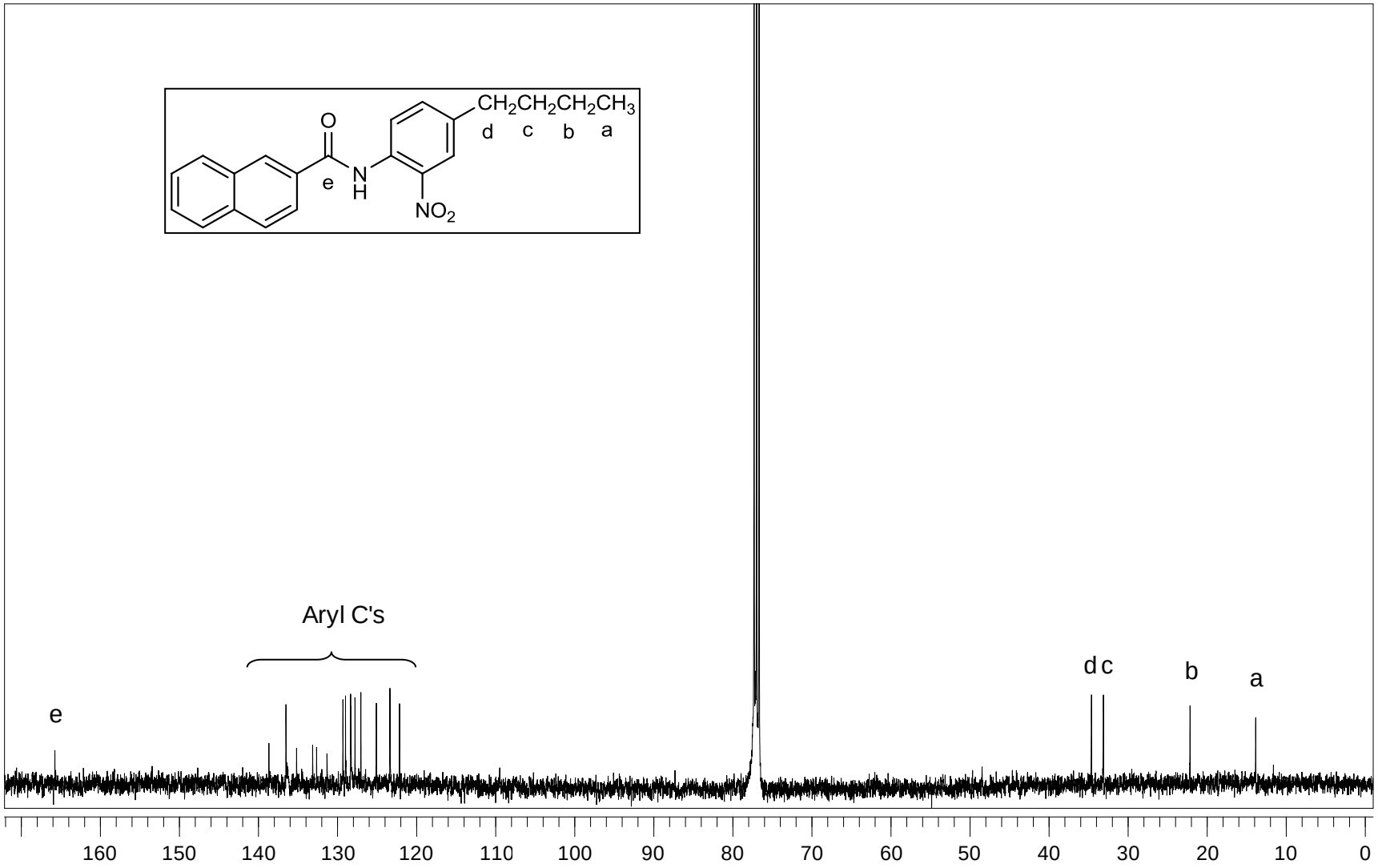


Figure A.64. ^{13}C-NMR ($CDCl_3$) spectrum of compound 49.

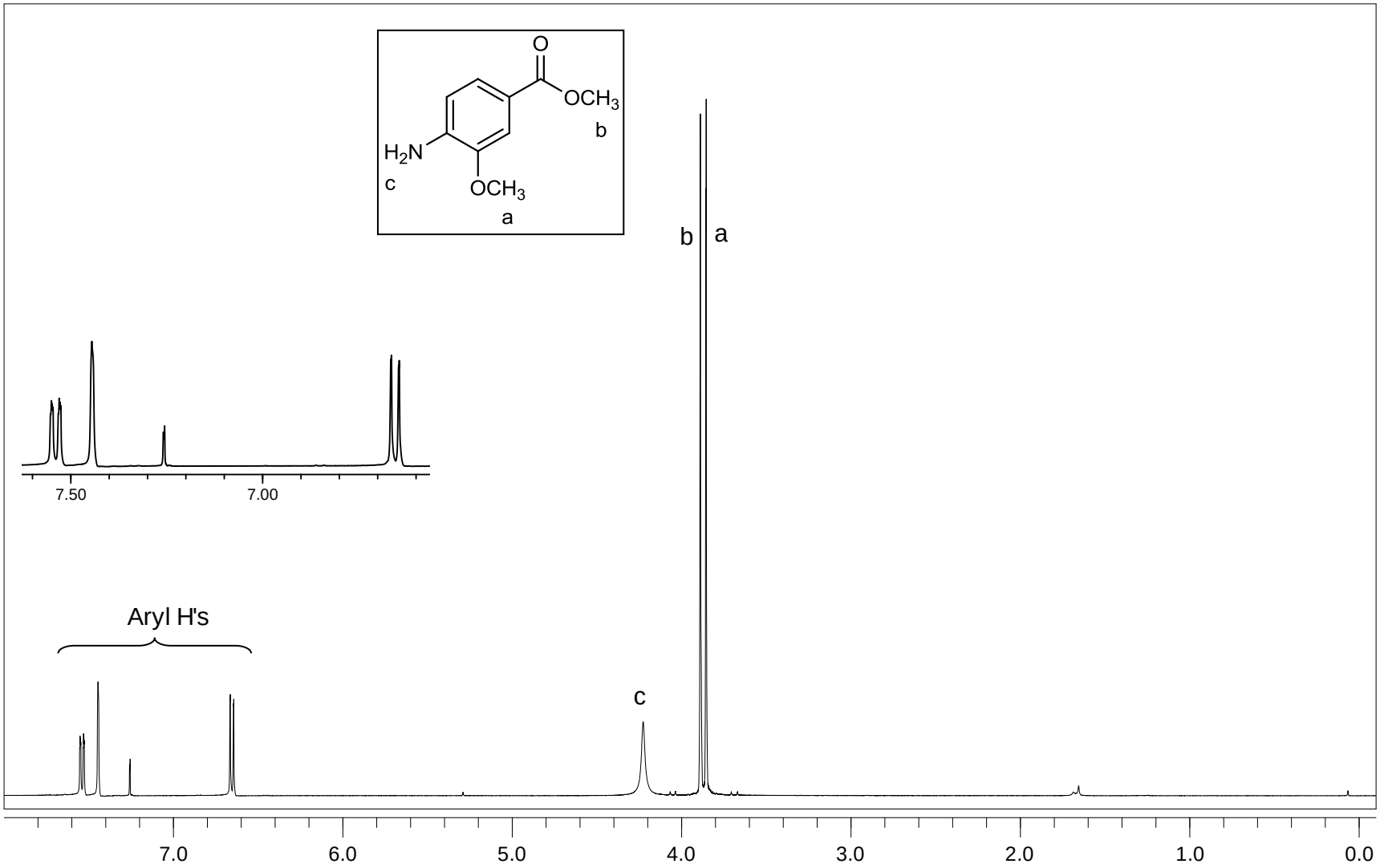


Figure A.65. ^{1}H-NMR ($CDCl_3$) spectrum of compound 51.

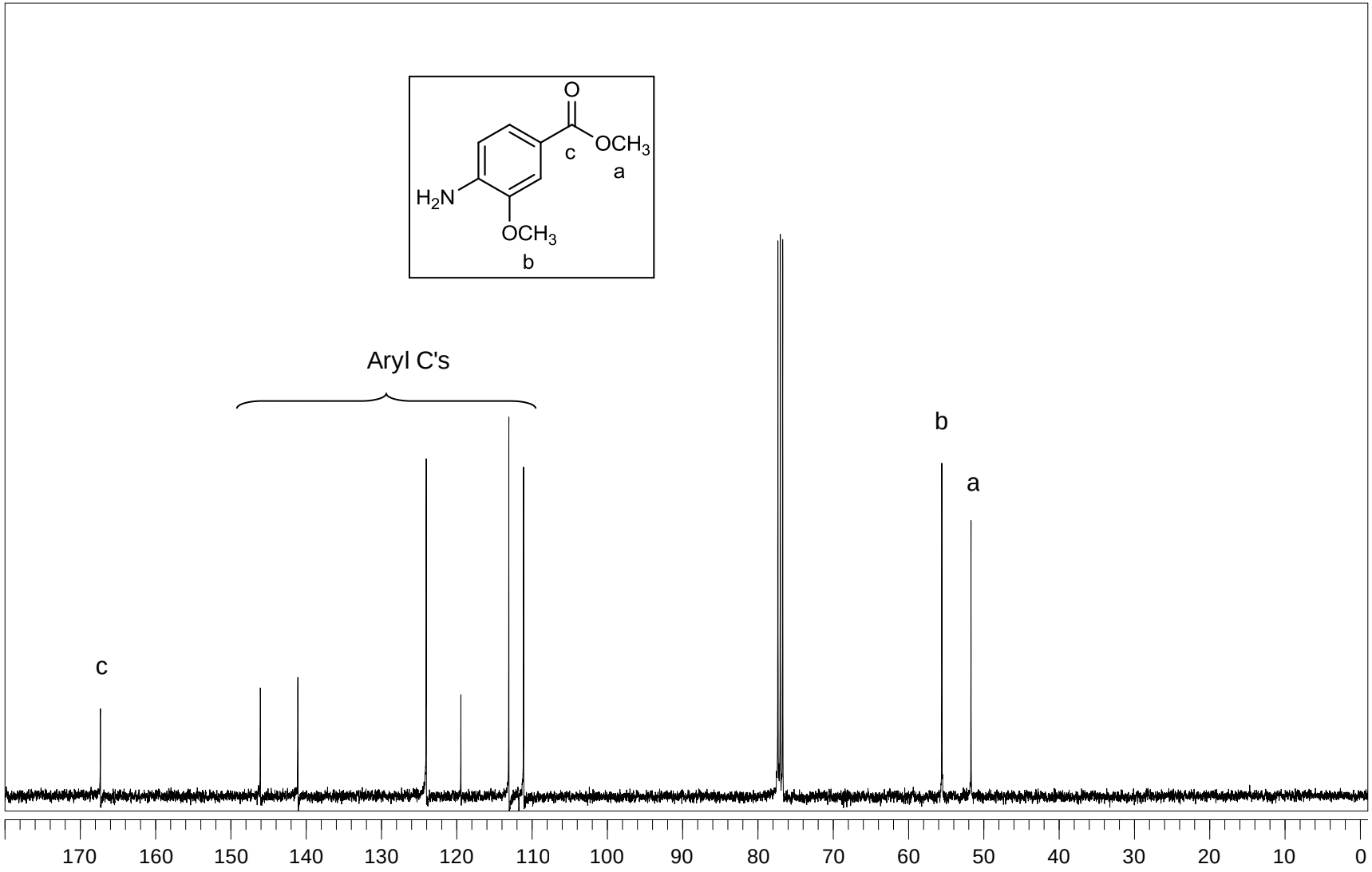


Figure A.66. ^{13}C-NMR ($CDCl_3$) spectrum of compound 51.

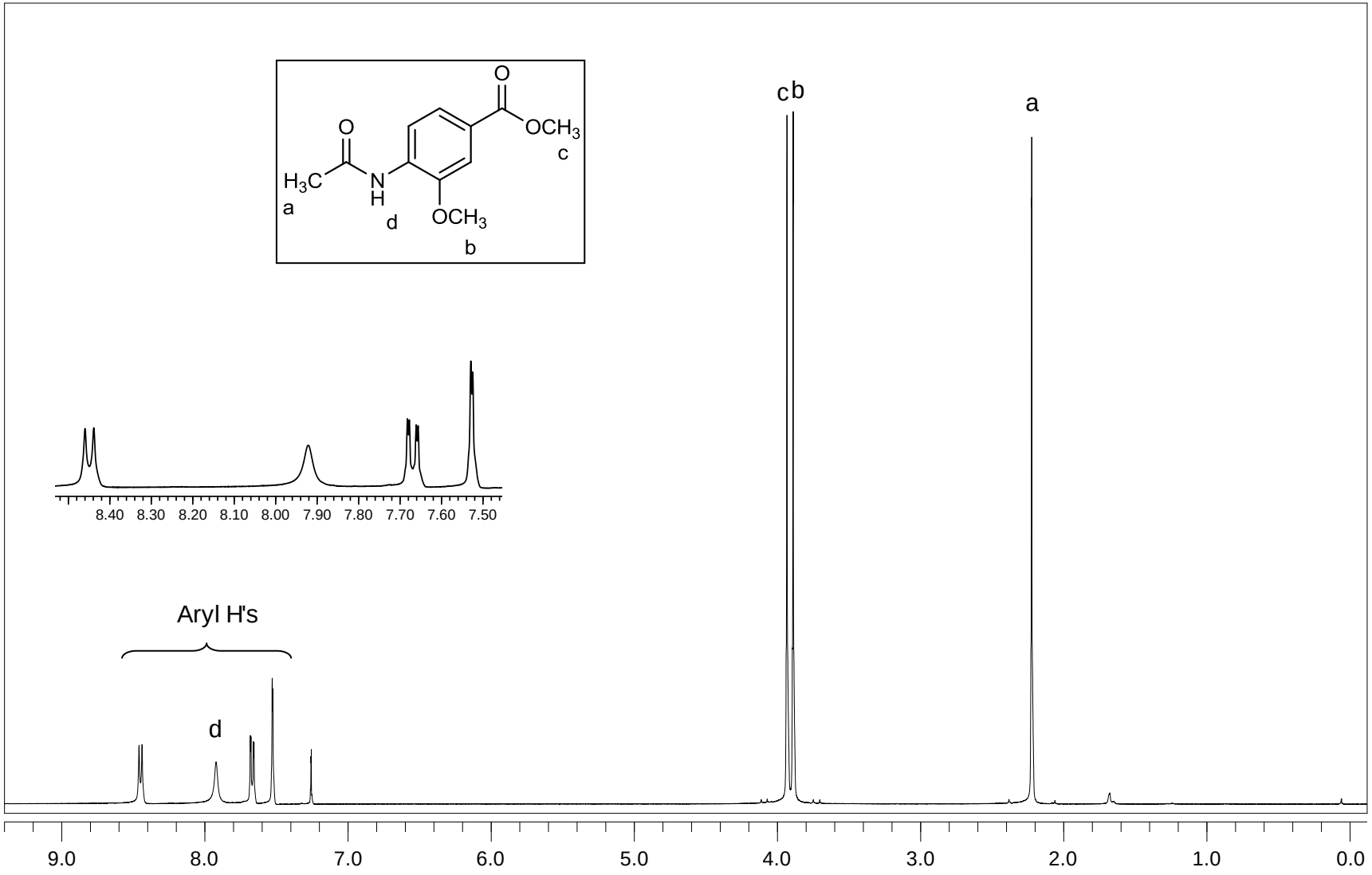


Figure A.67. ^{1}H-NMR ($CDCl_3$) spectrum of compound 52.

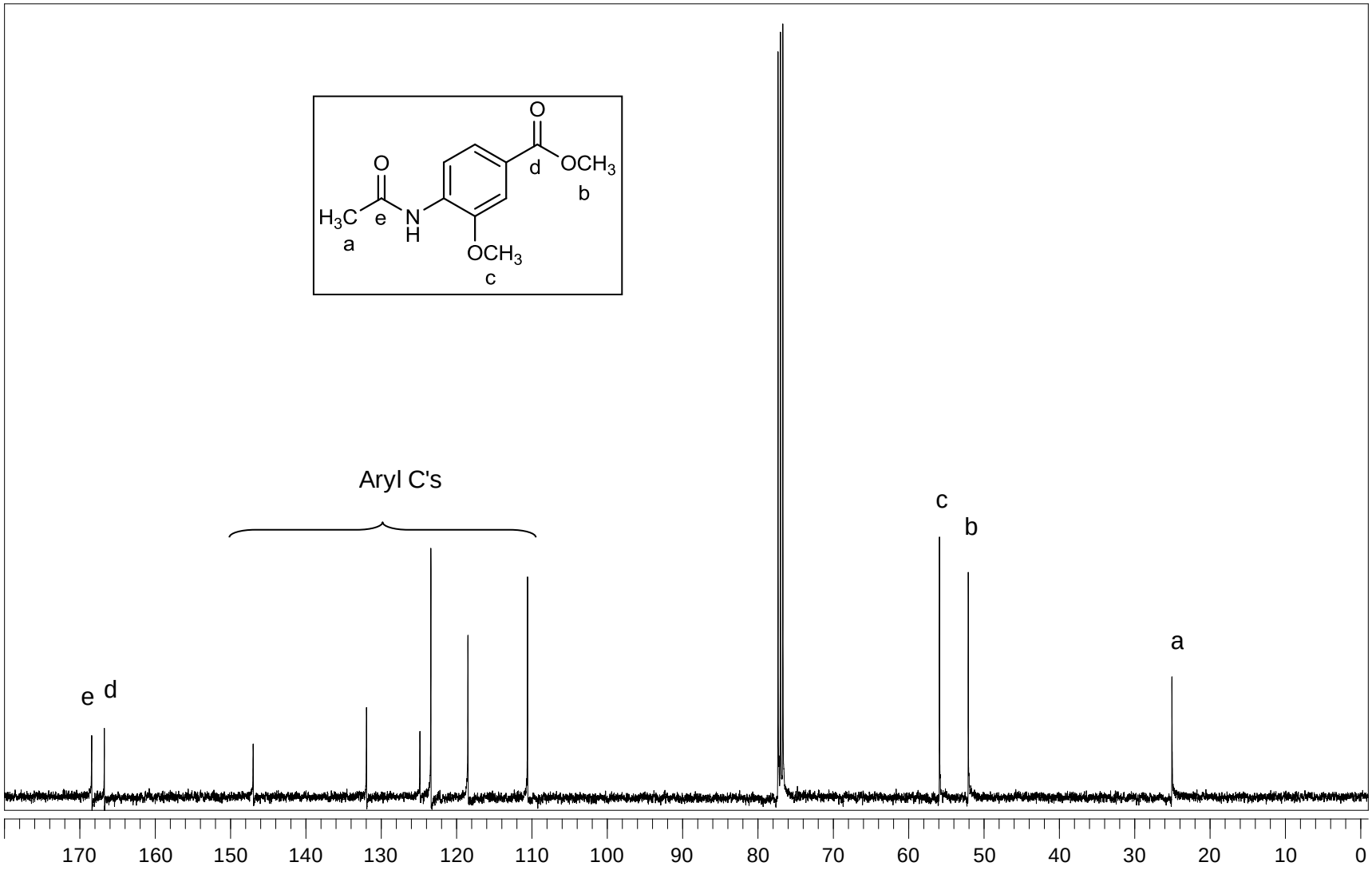


Figure A.68. ^{13}C-NMR ($CDCl_3$) spectrum of compound 52.

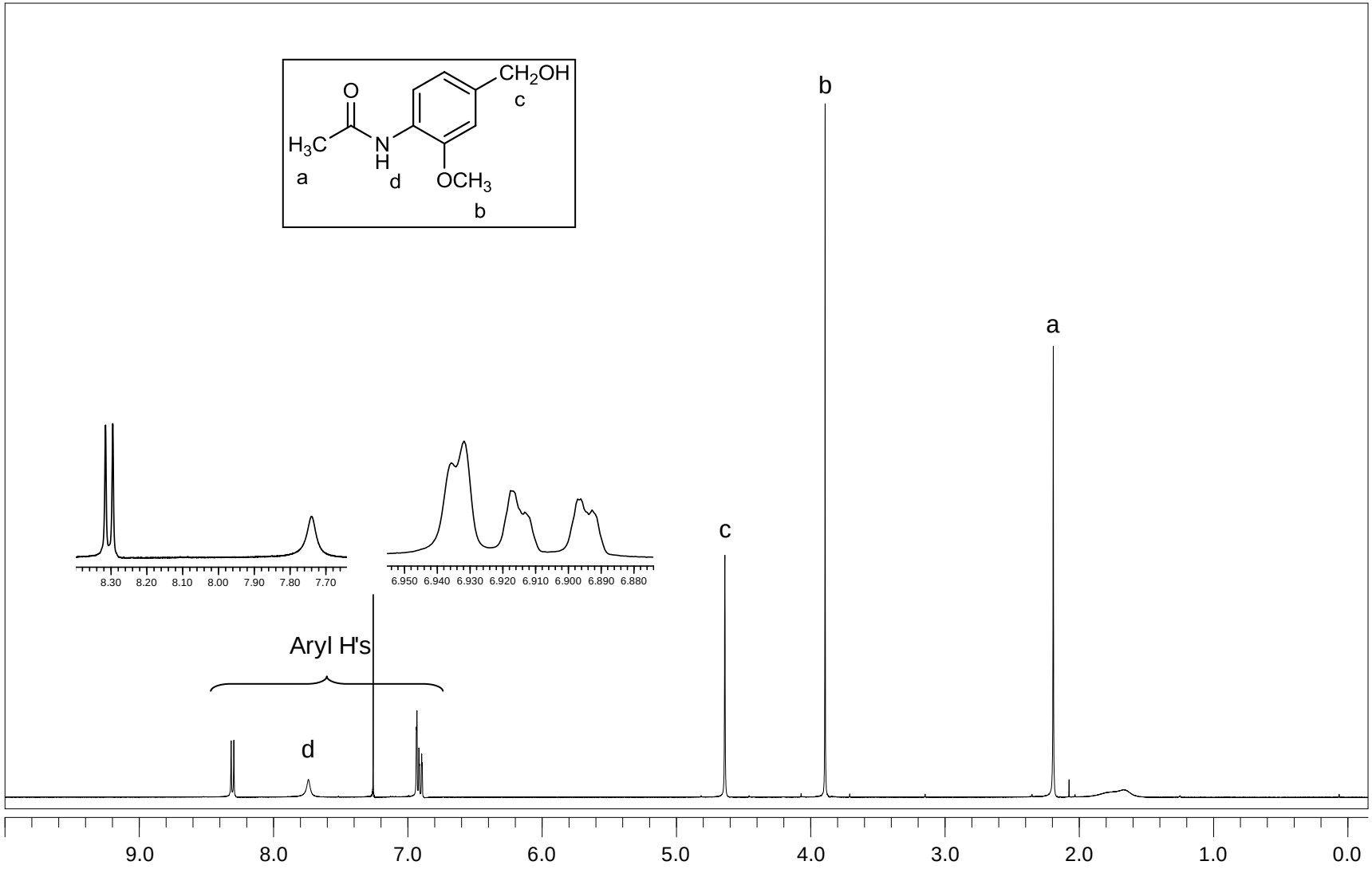


Figure A.69. ^{1}H-NMR ($CDCl_3$) spectrum of compound 53.

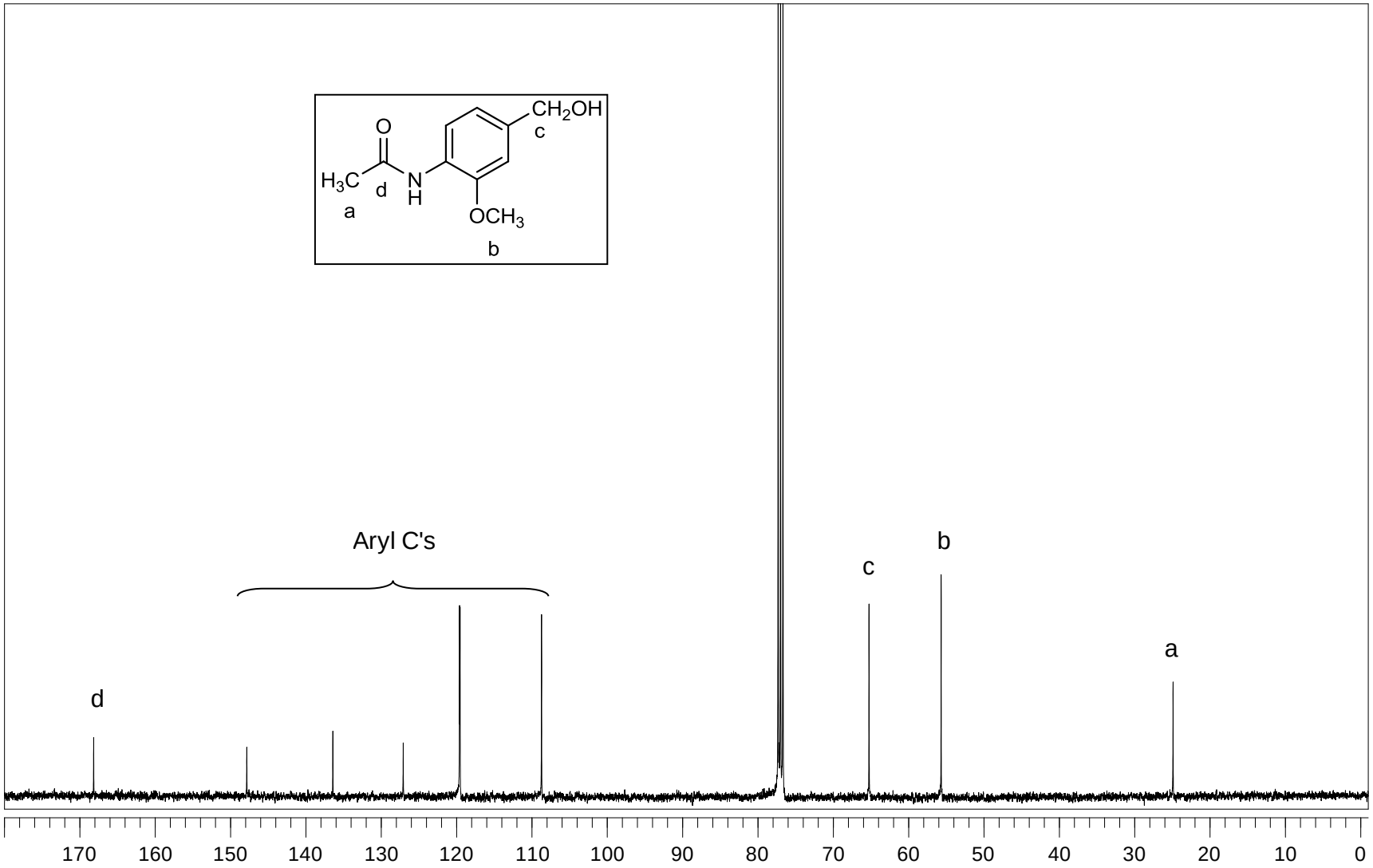


Figure A.70. ^{13}C-NMR ($CDCl_3$) spectrum of compound 53.

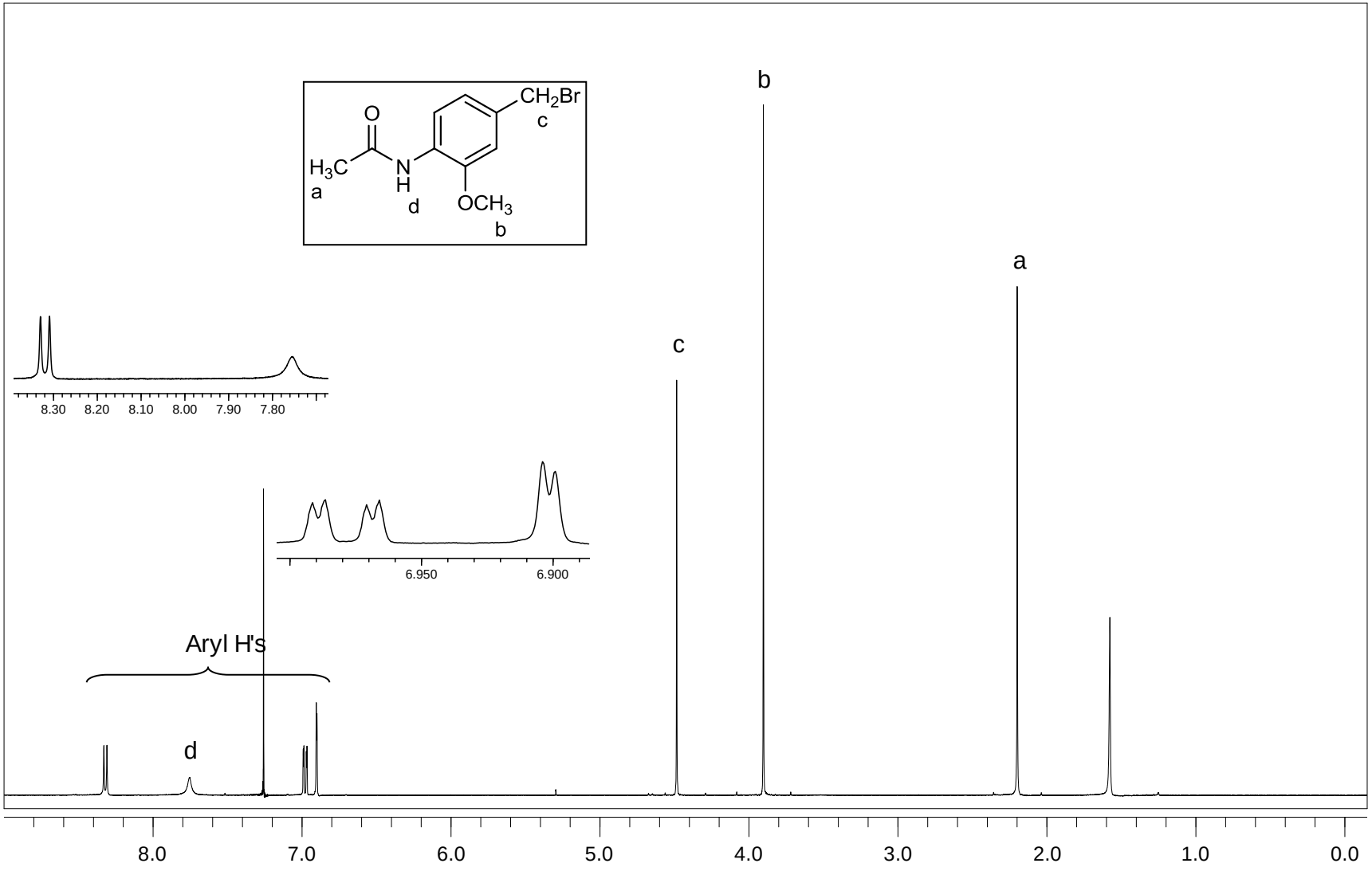


Figure A.71. ^{1}H-NMR ($CDCl_3$) spectrum of compound 54.

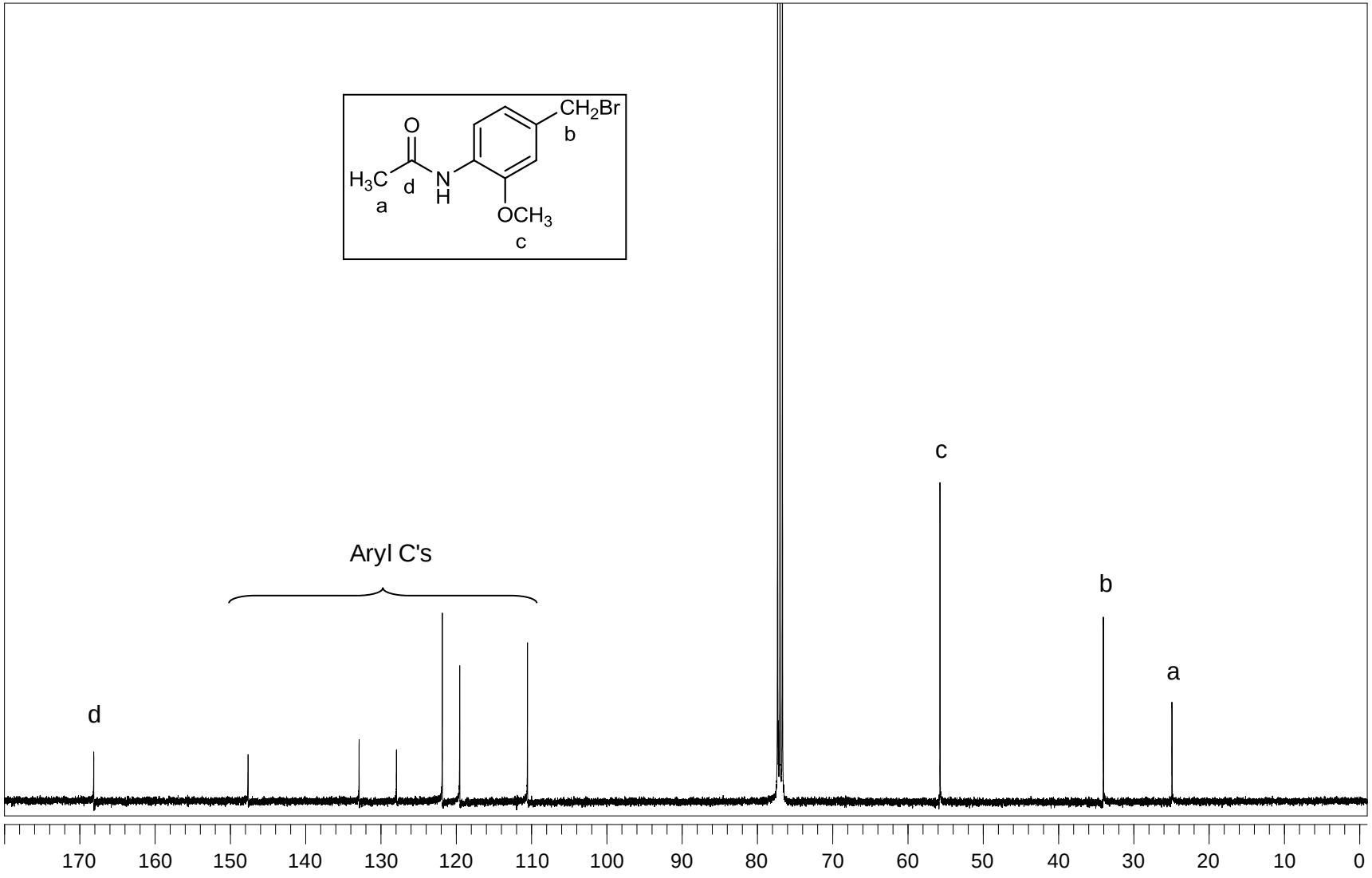


Figure A.72. ^{13}C-NMR ($CDCl_3$) spectrum of compound 54.

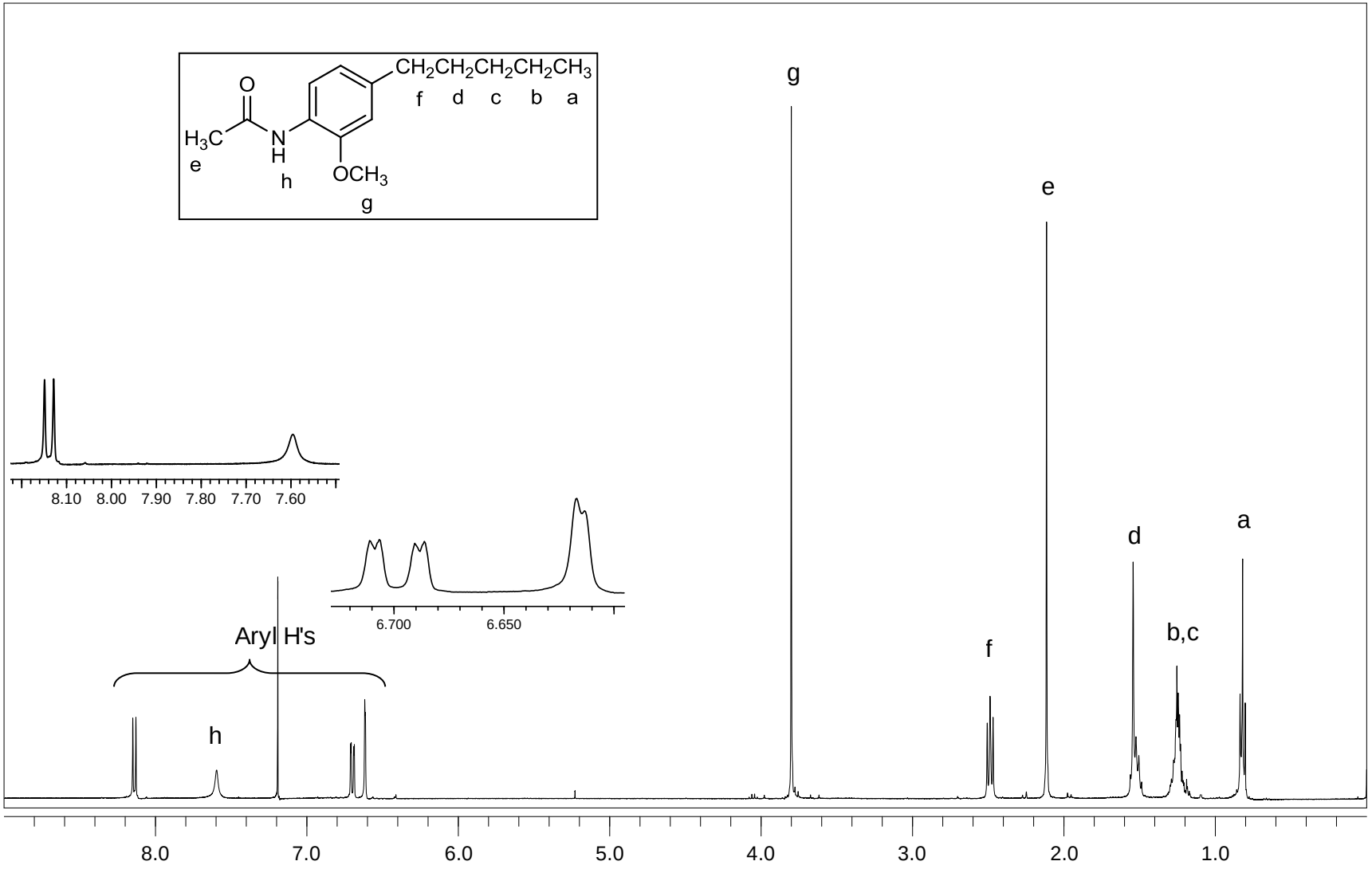


Figure A.73. ^{1}H-NMR ($CDCl_3$) spectrum of compound 55.

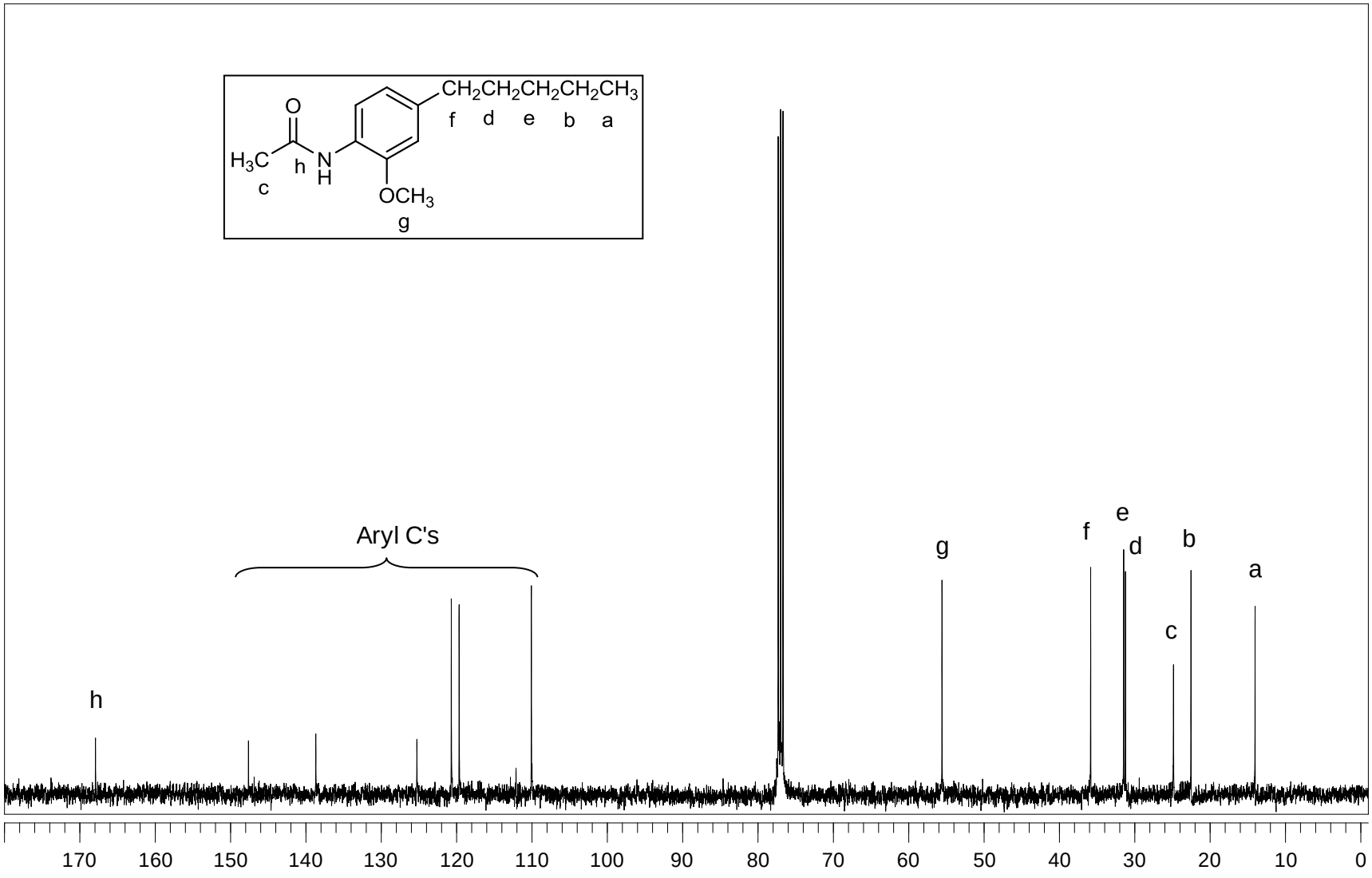


Figure A.74. ^{13}C-NMR ($CDCl_3$) spectrum of compound 55.

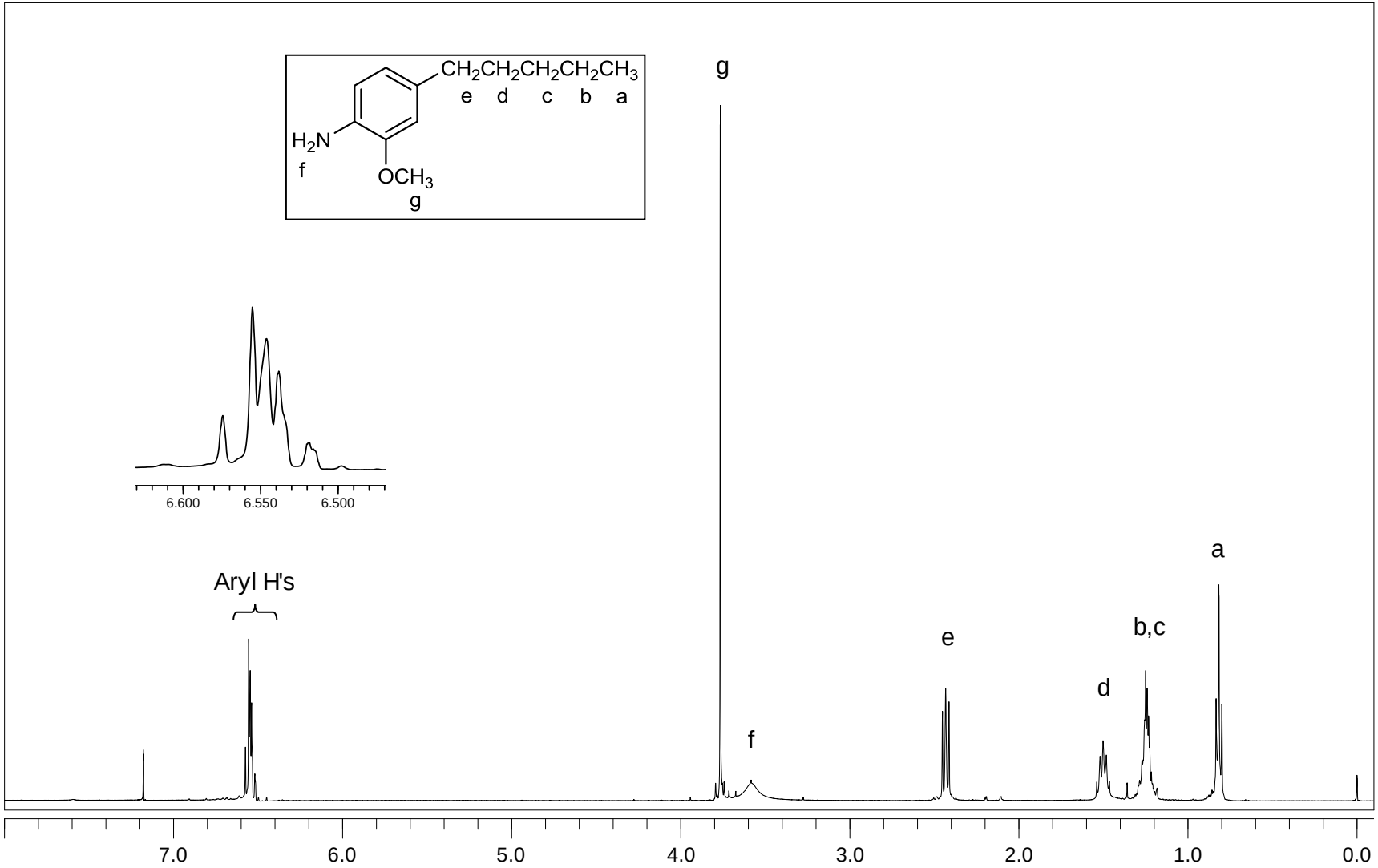


Figure A.75. ^{1}H-NMR ($CDCl_3$) spectrum of compound 56.

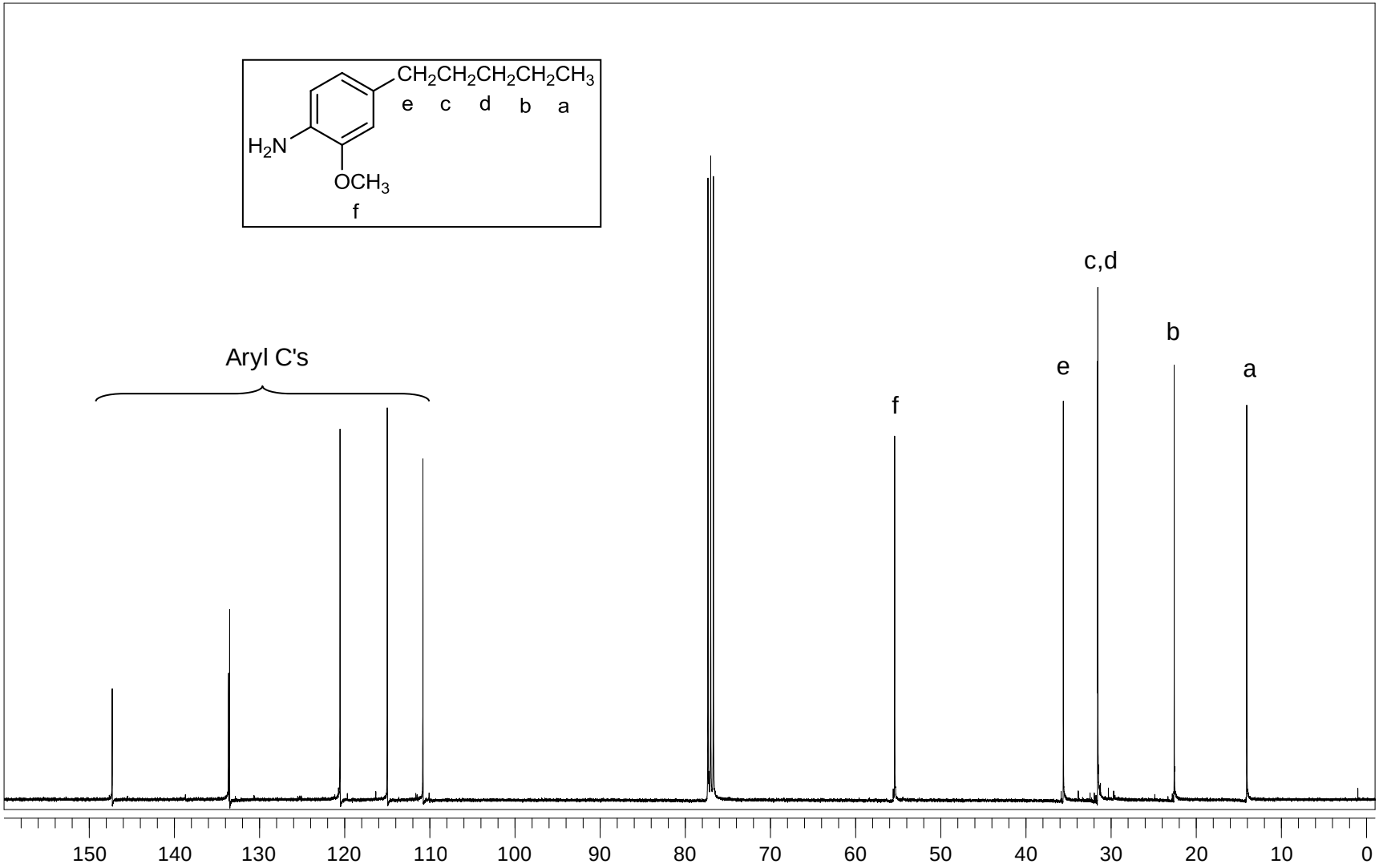


Figure A.76. ^{13}C-NMR ($CDCl_3$) spectrum of compound 56.

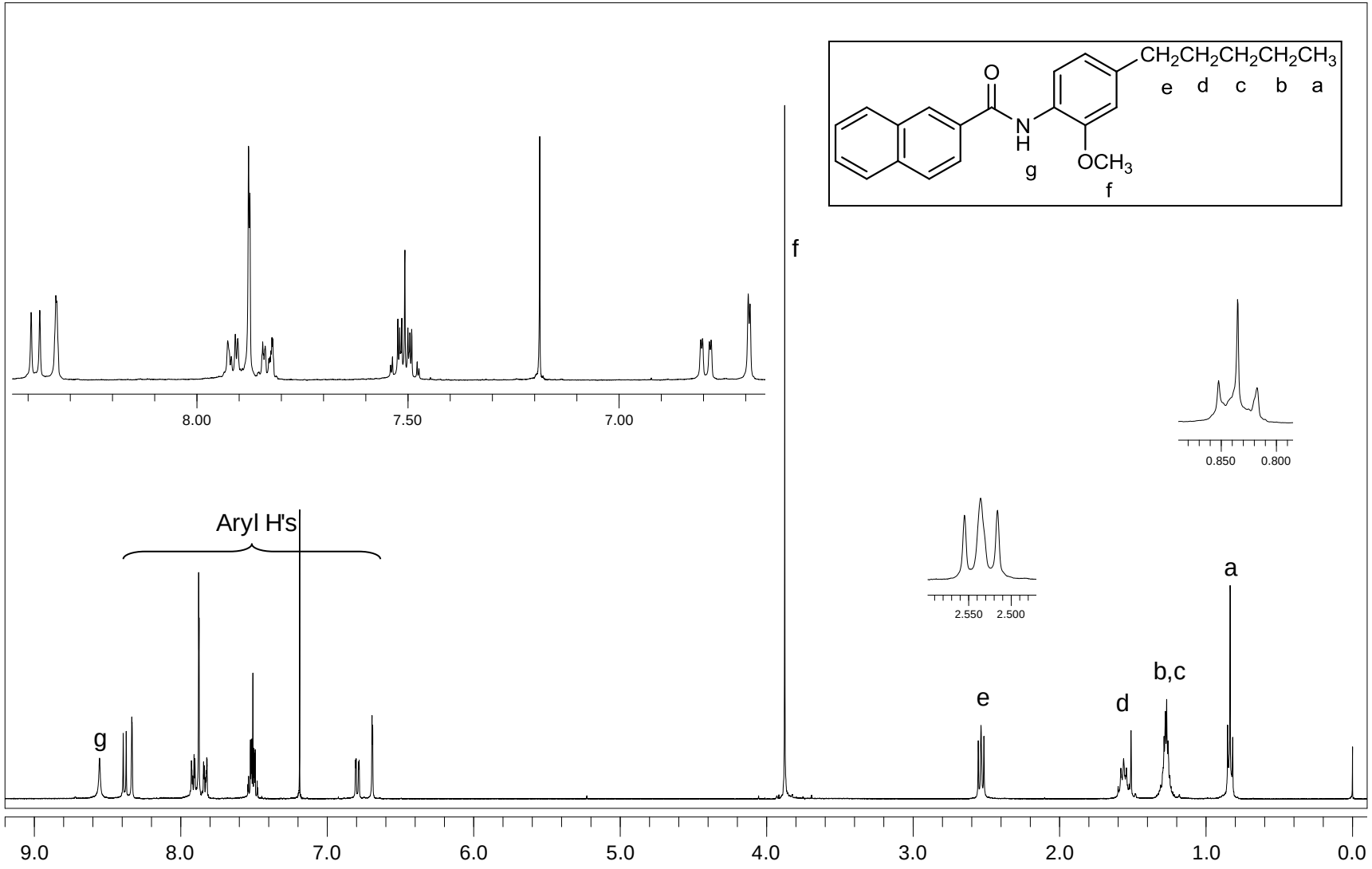


Figure A.77. ^{1}H-NMR ($CDCl_3$) spectrum of compound 57.

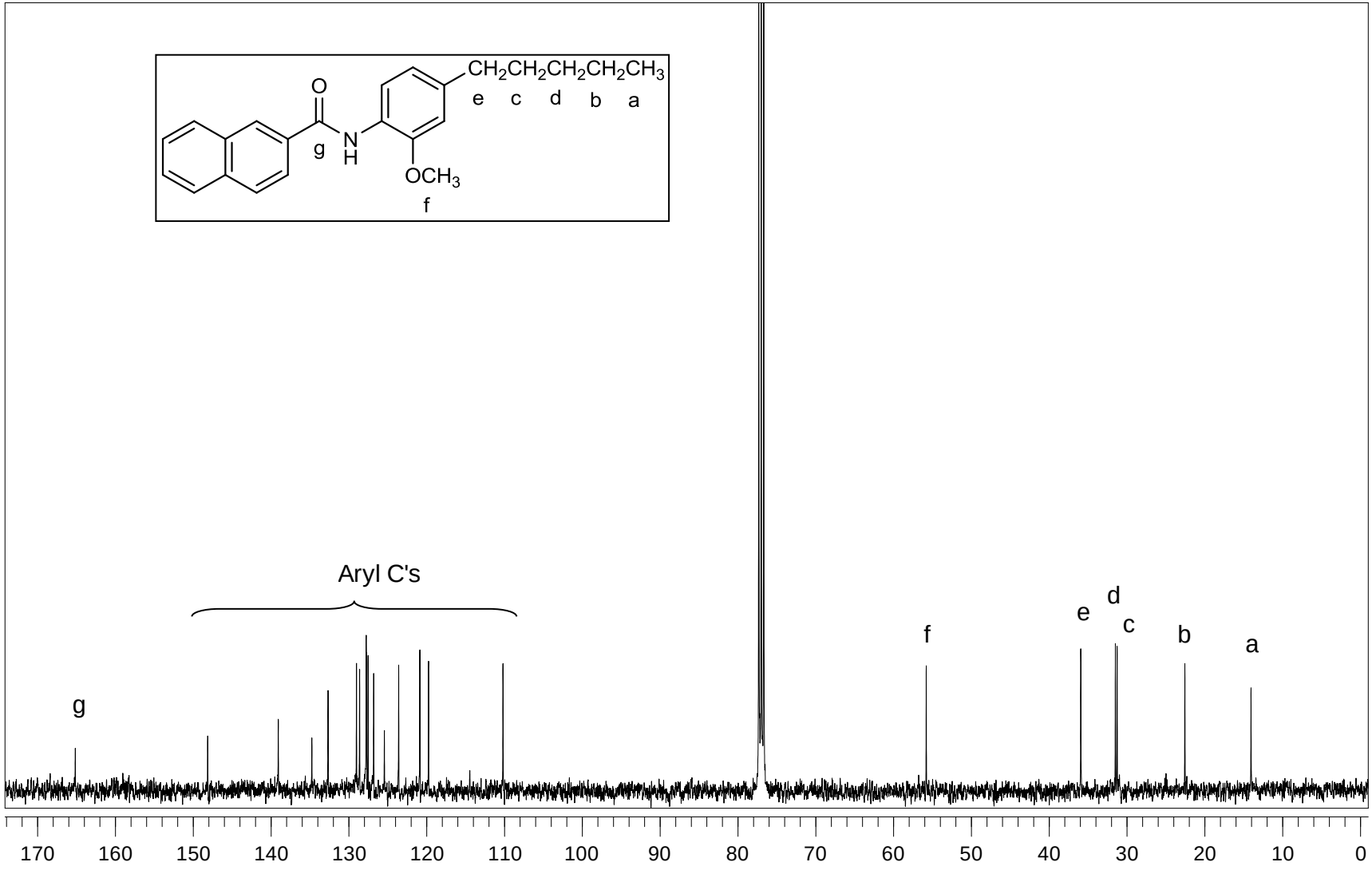


Figure A.78. ^{13}C-NMR ($CDCl_3$) spectrum of compound 57.

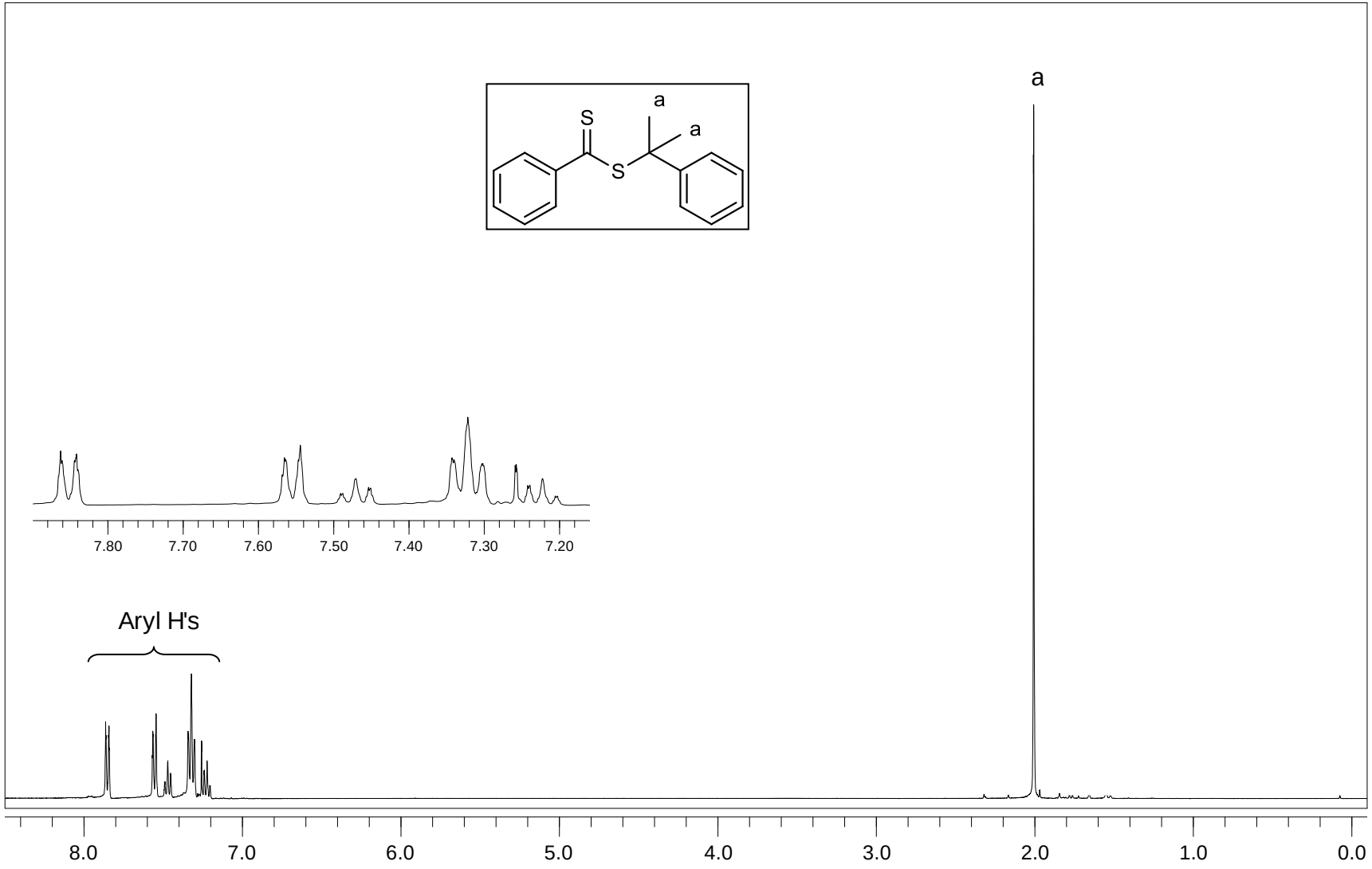


Figure A.79. ^{1}H-NMR ($CDCl_3$) spectrum of RAFT agent (CDB).

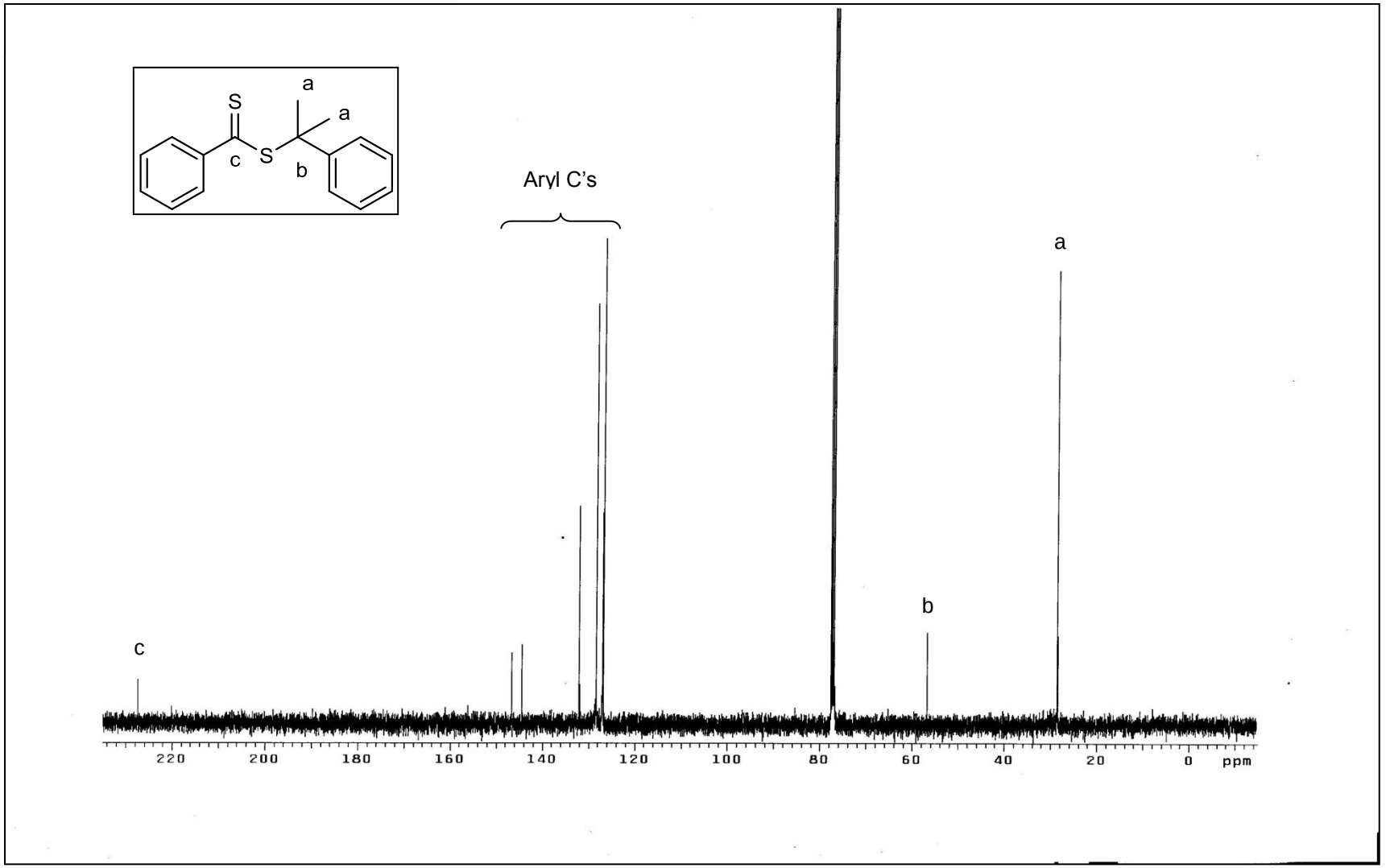


Figure A.80. ^{13}C-NMR ($CDCl_3$) spectrum of RAFT agent (CDB).

REFERENCES

1. Mettlin, C., "Recent developments in epidemiology of prostate cancer", *European Journal of Cancer*, Vol. 33, No. 3, pp. 340-347, 1997.

2. Hayat, M. J., N. Howlader, M. E. Reichman and B. K. Edwards, "Cancer statistics, trends, and multiple primary cancer analyses from surveillance, epidemiology, and end results (SEER) program", *Oncologist*, Vol. 12, No.1, pp. 20-37, 2007.

3. Jemal, A., R. Siegel, E. Ward, Y. Hao, J. Xu, T. Murray and M. J. Thun, "Cancer statistics", *CA: A Cancer Journal for Clinicians*, Vol. 58, No. 2, pp. 71-96, 2008.

4. Ferlay, J., P. Autier, M. Boniol, M. Heanue, M. Colombet and P. Boyle, "Estimates of the cancer incidence and mortality in Europe in 2006", *Annals of Oncology*, Vol. 18, No.3, pp. 581-592, 2007.

5. Pienta, K. J and P. S. Esper, "Risk factors for prostate cancer", *Annals of Internal Medicine*, Vol. 118, No. 10, pp. 793-803, 1993.

6. McConnell, J. D., "Physiological basis of endocrine therapy for prostatic cancer", *Urologic Clinics of North America*, Vol. 18, pp. 1-13, 1991.

7. Bruchovsky, N and J. D. Wilson, "The conversion of testosterone to 5α-androstan-17β-ol-3-one by rat prostate *in vivo* and *in vitro*", *The Journal of Biological Chemistry*, Vol. 243, pp. 2012-2021, 1968.

8. Denmeade, S. R. and J. T. Isaacs, "A history of prostate cancer treatment", *Nature Reviews Cancer*, Vol. 2, pp. 389-396, 2002.

9. Huggins, C., R. C. Stephens and C. V. Hudges, "Studies on prostatic cancer: 2. The effects of castration on advanced carcinoma of the prostate gland", *Archives of Surgery*, Vol. 43, pp. 209-223, 1941.

10. Penta, K. J. and D. Bradley, "Mechanisms underlying the development of androgen-independent prostate cancer", *Clinical Cancer Research*, Vol. 12, pp. 1665-1671, 2006.

11. Hartmann, R. W., P. B. Ehmer, S. Haidar, M. Hector, J. Jose, C. D. P. Klein, S. B. Seidel, T. F. Sergejew, B. G. Wachall, G. A. Wachter and Y. Zhuang, "Inhibition of CYP17, a new strategy for the treatment of prostate cancer", *Archiv der Pharmazie*, Vol. 335, pp. 119-128, 2002.

12. Huhtaniemi, I., H. Nikula, M. Parvinen and S. Rannikko, "Histological and functional changes of the testis tissue during GnRH agonist treatment of prostate cancer", *American Journal of Clinical Oncology*, Vol. 11, pp. 11-15, 1988.

13. Chen, C. D., D. S. Welsbie, C. Tran, S. H. Baek, R. Chen, R. Vessella, M. G. Rosenfeld and C. L. Sawyers, "Molecular determinants of resistance to antiandrogen therapy", *Nature Medicine*, Vol. 10, pp. 33-39, 2004.

14. Labrie, F., A. Dupont, A. Belanger, L. Cusan, Y. Lacourciere, G. Monfette, J. G. Laberge, J. P. Emond, A. T. Fazekas, J. P. Raynoud and J. M. Husson, "New hormonal therapy in prostatic carcinoma: combined treatment with LHRH agonist and antiandrogen", *Clinical and Investigate Medicine*, Vol. 5, pp. 267-275, 1982.

15. Miller, W. L., R. J. Auchus and D. H. Geller, "The regulation of 17,20 lyase activity", *Steroids*, Vol. 62, pp. 133-142, 1997.

16. Leroux, F., "Inhibition of P450 17 as a new strategy for the treatment of prostate cancer", *Current Medicinal Chemistry*, Vol. 12, pp. 1623-1629, 2005.

17. O'Shaughnessy, P. J., P. J. Baeker, M. Heikkila, S. Vainio and A. P. McMahon, "Localization of 17beta-hydroxysteroid dehydrogenase/17-ketosteroid reductase isoform expression in the developing mouse testis-androstenedione is the major androgen secreted by fetal/neonatal Leydig cells", *Endocrinology*, Vol. 141, pp. 2631-2637, 2000.

18. Bruno, R. D. and V. C., Njar, "Targeting cytochrome P450 enzymes, a new approach in anti-cancer drug development", *Bioorganic and Medicinal Chemistry*, Vol. 15, pp. 5047-5060, 2007.

19. De Coster, R., W. Wouters and J. Bruynseels, "P450-dependent enzymes as targets for prostate cancer therapy", *Journal of Steroid Biochemistry and Molecular Biology*, Vol. 56, pp. 133-143, 1996.

20. Moreira, V. M., J. A. R. Salvador, T. S. Vasaitis and V. C. O. Njar, "CYP17 inhibitors for prostate cancer treatment-an update", *Current Medicinal Chemistry*, Vol. 15, pp. 868-899, 2008.

21. Potter, G. A., S. E. Barrie, M. Jarman and M. G. Rowlands, "Novel steroidal inhibitors of human cytochrome P45017 alpha(17 alpha-hyroxylase-C17, 20-lyase): Potential agents for the treatment of prostate cancer", *Journal of Medicinal Chemistry*, Vol. 38, pp. 2463-2471, 1995.

22. Barrie, S. E., G. A. Potter, P. M. Goddard, B. P. Haynes, M. Dowsett and M. Jarman, "Pharmacology of novel steroidal inhibitors of cytochrome P450(17) alpha (17 alpha-hydroxylase/C17-20 lyase", *Journal of Steroid Biochemistry and Molecular Biology*, Vol. 50, pp. 267-273, 1994.

23. Jarman, M., S. E. Barrie and J. M. Llera, "The 16,17-double bond is needed for irreversible inhibition of human cytochrome p45017alpha by abiraterone (17-(3-pyridyl)androsta-5,16-dien-3beta-ol) and related steroidal inhibitors", *Journal of Medicinal Chemistry*, Vol. 41, pp. 5375-5381, 1998.

24. Loose, D. S., P. B. Kan, M. A. Hirst, R. A. Marcus and D. Feldman, "Ketoconazole blocks adrenal steroidogenesis by inhibiting cytochrome P450-dependent enzymes", *Journal of Clinical Investigation*, Vol. 71, pp. 1495-1499, 1983.

25. Amery, W., R. De Coster and I. Caers, "Ketoconazole: from an antimycotic to a drug for prostate cancer", *Drug Development. Research*, Vol. 8, pp. 299-307, 1986.

26. Armutlu, P., M. E. Özdemir, Ş. Özdaş, İ. H. Kavakli and M. Türkay, "Discovery of novel CYP17 inhibitors for the treatment of prostate cancer with structure-based drug design", *Letters in Drug Design & Discovery*, Vol. 6, pp. 337-344, 2009.

27. Anderson, A. C. and D. College, "The process of structure based drug design", *Chemistry and Biology*, Vol. 10, pp. 787–797, 2003.

28. http://www.proxychem.com/sbdd.html

29. Auchus, R. and W. L. Miller, "Molecular modeling of human P450c17 (17 alpha-hydroxylase/17,20-lyase): Insights into reaction mechanisms and effects of mutations", *Molecular Endocrinology*, Vol. 13, pp. 1169-1182, 1999.

30. Gaspari, P., T. Banerjee, W. P. Malachowski, A. J. Muller, G. C. Prendergast, J. DuHadaway, S. Bennett and A. M. Donovan, "Structure-activity study of brassinin derivatives as indoleamine 2,3-dioxygenase inhibitors", *Journal of Medicinal Chemistry*, Vol. 49, pp. 684-692, 2006.

31. Heikkila, T, C. Ramsey, M. Davies, C. Galtier, A. M. W. Stead, A. P. Johnson, C. W. G. Fishwick, A. N. Boa and G. A. McConkey, "Design and synthesis of potent inhibitors of the malaria parasite dihydroorotate dehydrogenase", *Journal of Medicinal Chemistry*, Vol. 50, pp. 186-191, 2007.

32. Wang, H., Y. Wang, H. Hu, G. Lee and C. K. Lai, "Novel metallomesogens derived from heterocyclic benzoxazoles", *Tetrahedron*, Vol. 64, pp. 4939-4948, 2008.

33. Kang, D. H., T. Y. Joo, E. H. Lee, S. Chaysripongkul, W. Chavasiri and D. O. Jang, "A mild and efficient reaction for conversionof carboxylic acids into acid bromides with ethyl tribromoacetate/triphenylphosphine under acid-free conditions", *Tetrahedron Letters*, Vol. 47, pp. 5693-5696, 2006.

34. Bose, A. K., M. S. Manhas, S. Pednekar, S. N. Ganguly, H. Dang, W. He and A. Mandadi, "Large scale Biginelli reaction via water-based biphasic media: a green chemistry strategy", *Tetrahedron Letters*, Vol. 46, pp. 1901-1903, 2005.

35. Rivara, M., V. Zuliani, G. Cocconcelli, G. Morini, M. Comini, S. Rivara, M. Mor, F. Bordi, E. Barocelli, V. Ballabeni, S. Bertoni and P. V. Plazzi, "Synthesis and biological evaluation of new non-imidazole H_3-receptor antagonists of the 2-aminobenzimidazole series", *Biorgonic and Medicinal Chemistry*, Vol. 14, pp. 1413-1424, 2006.

36. Kumar J. S. D., M. M. Ho and T. Toyokuni, "Simple and chemoselective reduction of aromatic nitro compounds to aromatic amines: reduction with hydriodic acid revisited", *Tetrahedron Letters*, Vol. 42, pp. 5601-5603, 2001.

37. Eldred, S. E., D. A. Stone, S. H. Gellman and S. S. Stahl, "Catalytic transamidation under moderate conditions", *Journal of American Chemical Society*, Vol. 125, pp. 3422-3423, 2003.

38. Beste, L. F. and R. C. Houtz, "Amide interchange reactions", *Journal of Polymer Science*, Vol. 8, No. 4, pp. 395-407, 1952.

39. Miller, L. K., "Amide-exchange reactions in mixtures of N-alkyl amides and in polyamide melt blends", *Journal of Polymer Science, Polymer Chemistry Edition*, Vol. 14, No. 6, pp. 1403-1417, 1976.

40. Bon, E., D. C. H. Bigg, G. Bertrand, "Aluminum chloride-promoted transamidation reactions", *Journal of Organic Chemistry*, Vol. 59, No. 15, pp. 4035-4036, 1994.

41. Meth-Cohn, O., "A simple, powerful, and efficient method for transesterification", *Journal of the Chemical Society, Chemical Communications*, Vol. 9, pp. 695-697, 1986.

42. Otera, J., "Transesterification", *Chemical Reviews*, Vol. 93, pp. 1449-1470, 1993.

43. Stanton, M. G. and M. R. Gagne, "The remarkable catalytic activity of alkali-metal alkoxide clusters in the ester interchange reaction", *Journal of the American Chemical Society*, Vol. 119, pp. 5075-5076, 1997.

44. Stanton, M. G., C. B. Allen, R. M. Kissling, A. L. Lincoln and M. R. Gagne, "The role of alkali-metal alkoxide clusters in achieving unprecedented reaction rates", *Journal of the American Chemical Society*, Vol. 120, pp. 5981-5989, 1998.

45. Kissling, R. M. and M. R. Gagne, "Improved ester interchange catalysts", *Organic Letters*, Vol. 2, pp. 4209-4212, 2000.

46. Maier, M. E. and T. Mayer, "Design and synthesis of a tag-free chemical probe for photoaffinity labeling", *European Journal of Organic Chemistry*, Vol. 2007, No. 28, pp. 4711-4720, 2007.

47. Huffman, J. W., S. M. Bushell, S. N. Joshi, J. L. Wiley and B. R. Martin, "Enantioselective synthesis of 1-metoxy- and 1-deoxy-2'-methyl-A^8-tetrahydrocannabinols: new selective ligands for the CB_2 receptor", *Bioorganic and Medicinal Chemistry*, Vol. 14, pp. 247262, 2006.

48. Nikas, S. P., G. A. Thakur and A. Makriyannis, "Regiospecifically deuterated (-)-A^9-tetrahydrocannabivarins", *Journal of the Chemical Society, Perkin Transactions*, Vol. 1, pp. 2544-2548, 2002.

49. Buszek, K. R., N. Brown and D. Luo, "Concise total synthesis of (±)-*cis*-trikentrin A and (±)-herbindole A via intermolecular indole aryne cycloaddition", *Organic Letters*, Vol. 11, pp. 201, 2009.

50. Katsuyama, I. and M. Kubo, "The first synthesis of protected 5-hydroxymethyl-2-cyanomethylbenzimidazole", *Heterocycles*, Vol. 71, pp. 2491, 2007.

51. Moad, G. and D. H. Solomon, *The chemistry of free radical polymerization*, Pergamon; Oxford, 1995.

52. Moad, G., E. Rizzardo and S. H. Thang, "Living radical polymerization by the RAFT process", *Australian Journal of Chemistry*, Vol. 58, No. 6, pp. 379-410, 2005.

53. Hawker, C. J., A. W. Bosman and E. Harth, "New polymer synthesis by nitroxide mediated living radical polymerizations", *Chemical Reviews*, Vol. 101, No. 12, pp. 3661-3688, 2001.

54. Matyjaszewski, K. and J. Xia, "Atom transfer radical polymerization", *Chemical Reviews*, Vol. 101, No. 9, pp. 2921-2990, 2001.

55. Kamigaito, M., T. Ando and M. Sawamoto, "Metal-catalyzed living radical polymerization", *Chemical Reviews.*, Vol. 101, No. 12, pp. 3689-3746, 2001.

56. Rizzardo, E., J. Chiefari, Y. K. Chong, F. Ercole, J. Krstina, J. Jeffery, T. P. T. Le, R. T. A. Mayadunne, G. F. Meijs, C. L. Moad, G. Moad and S. H. Thang, "Tailored polymers by free radical processes", *Macromolecular Symposia*, Vol. 143, No. 1, pp. 291-307, 1999.

57. Rizzardo, E., J. Chiefari, R. T. A. Mayadunne, G. Moad and S. H. Thang, "Synthesis of defined polymers by reversible addition-fragmentation chain transfer: The RAFT process", *ACS Symposium Series*, Vol. 768, No. 20, pp. 278-296, 2000.

58. Moad, G. and E. Rizzardo, "Alkoxyamine-initiated living radical polymerization: Factors affecting alkoxyamine homolysis rates", *Macromolecules*, Vol. 28, No. 26, pp. 8722-8728, 1995.

59. Chiefari, J., Y. K. Chong, F. Ercole, J. Krstina, J. Jeffery, T. P. Le, R. T. Mayadunne, G. F. Meijs, C. L. Moad, G. Moad, E. Rizzardo and S. H. Thang, "Living *free* radical polymerization by reversible addition fragmentation chain transfer: The RAFT process", *Macromolecules*, Vol. 31, No. 16, pp. 5559–5562, 1998.

60. Moad, G., J. Chiefari, B. Y. Chong, J. Krstina, R. T. Mayadunne, A. Postma, E. Rizzardo and S. H. Thang, "Living free radical polymerization with reversible addition fragmentation chain transfer (the life of RAFT), *Polymer International*, Vol. 49, No. 9, pp. 993–1001, 2000.

61. Moad, G., Y. K. Chong, A. Postma, E. Rizzardo and S. H. Thang, "Advances in RAFT polymerization: The synthesis of polymers with defined end groups", *Polymer*, Vol. 46, No. 19, pp. 8458–8468, 2005.

62. Barner-Kowollik, C., T. P. Davis, J. P. A. Heuts, M. H. Stenzel, P. Vana and M. J. Whittaker, "RAFTing down under: tales of missing radicals, fancy architectures, and mysterious holes", *Journal of Polymer Science Part A: Polymer Chemistry*, Vol. 41, No. 3, pp. 365–375, 2003.

63. Fijten, M. W., R. M. Paulus and U. S. Schubert, "Systematic parallel investigation of RAFT polymerizations for eight different (meth)acrylates: A basis for the designed synthesis of block and random copolymers", *Journal of Polymer Science Part A: Polymer Chemistry*, Vol. 43, No. 17, pp. 3831–3839, 2005.

64. Gao, J., Y. Luo, R. Wang, B. Li and S. Zhu, "Kinetics of methyl methacrylate and n-butyl acrylate copolymerization mediated by 2-cyanoprop-2-yl dithiobenzoate as a RAFT agent", *Journal of Polymer Science Part A: Polymer Chemistry*, Vol. 45, No. 14, pp. 3098–3111, 2007.

65. Arita, T., M. Buback and P. Vana, "Cumyl Dithiobenzoate Mediated RAFT Polymerization of Styrene at High Temperatures", *Macromolecules*, Vol. 38, No. 19, pp. 7935–7943, 2005.

66. Goto, A., K. Sato, Y. Tsuji, T. Fukuda, G. Moad, E. Rizzardo and S. H. Thang, "Mechanism and kinetics of RAFT-based living radical polymerizations of styrene and methyl methacrylate", *Macromolecules*, Vol. 34, No. 3, pp. 402–408, 2001.

67. Favier, A., M. T. Charreyne and C. Pichot, "A detailed kinetic study of the RAFT polymerization of a bi-substituted acrylamide derivative: Influence of experimental parameters", *Polymer*, Vol. 45, No. 26, pp. 8661–8674, 2004.

68. Liu, X. H., G. B. Zhang, X. F. Lu, J. Y. Liu, D. Pan and Y. S. Li, "Dibenzyl trithiocarbonate mediated reversible addition-fragmentation chain transfer

polymerization of acrylonitrile", *Journal of Polymer Science Part A: Polymer Chemistry*, Vol. 44, No. 1, pp. 490–498, 2006.

69. Lambert, B., M. T. Charreyne, C. Chaix and C. Pichot, "RAFT polymerization of hydrophobic acrylamide derivatives", *Polymer*, Vol. 46, No. 3, pp. 623–637, 2005.

70. Nguyen, M. N., C. Bressy and A. Margaillan, "Controlled radical polymerization of a trialkylsilyl methacrylate by reversible addition-fragmentation chain transfer polymerization", *Journal of Polymer Science Part A: Polymer Chemistry*, Vol. 43, No. 22, pp. 5680–5689, 2005.

71. Chong, Y. K., J. Krstina, T. P. T. Le, G. Moad, E. Rizzardo and S. H. Thang, "Thiocarbonylthio compounds [S:C(Ph)S-R] in free radical polymerization with reversible addition-fragmentation chain transfer (RAFT polymerization). Role of the free-radical leaving group (R)", *Macromolecules*, Vol. 36, No. 7, pp. 2256–2272, 2003.

72. Chiefari, J., R. T. A. Mayadunne, C. L. Moad, G. Moad, E. Rizzardo, A. Postma, M. A. Skidmore and S. H. Thang, "Thiocarbonylthio compounds (S:C(Z)S-R) in free radical polymerization with reversible addition-fragmentation chain transfer (RAFT polymerization). Effect of the activating group (Z)", *Macromolecules*, Vol. 36, No. 7, pp. 2273–2283, 2003.

73. Barner-Kowollik, C., M. Buback, B. Charleux, M. L. Coote, M. Drache, T. Fukuda, A. Goto, B. Klumperman, A. B. Lowe, J. B. Mcleary, G. Moad, M. J. Monteiro, R. D. Sanderson, M. P. Tonge and P. Vana, "Mechanism and kinetics of dithiobenzoate-mediated RAFT polymerization. I. The current situation", *Journal of Polymer Science Part A: Polymer Chemistry*, Vol. 44, No. 20, pp. 5809–5831, 2006.

74. Benaglia, M., E. Rizzardo, A. Alberti and M. Guerra, "Searching for more effective agents and conditions for the RAFT polymerization of MMA: Influence of dithioester substituents, solvent, and temperature", *Macromolecules*, Vol. 38, No. 8, pp. 3129–3140, 2005.

75. Tsuda, T. and L. J. Mathias, "Cyclopolymerization of ether dimers of α-(hydroxymethyl)acrylic acid and its alkyl esters: substituent effect on cyclization efficiency and microstructures", *Polymer*, Vol. 35, No. 15, pp. 3317–3328, 1994.

76. Mathias, L. J., R. M. Warren and S. Huang, "*tert*-Butyl α-(hydroxymethyl)acrylate and its ether dimer: Multifunctional monomers giving polymers with easily cleaved ester groups", *Macromolecules*, Vol. 24, No. 8, pp. 2036–2042, 1991.

77. Mathias, L. J., S. H. Kusefoglu, A. O. Kress, S. Lee, C. W. Dickerson and S. F. Thames, "New acrylate-containing dimers and oligomers for crosslinking vinyl polymers", *Polymer News*, Vol. 17, No. 2, pp. 36–42, 1992.

78. Lin, Y., X. Liu, X. Li, J. Zhan and Y. Li, "Reversible addition-fragmentation chain transfer mediated radical polymerization of asymmetrical divinyl monomers targeting hyperbranched vinyl polymers", *Journal of Polymer Science Part A: Polymer Chemistry*, Vol. 45, No.1, pp. 26–40, 2007.

79. Assem, Y., H. Chaffey-Millar, C. Barner-Kowollik, G. Wegner and S. Agarwal, "Controlled/living ring-closing cyclopolymerization of diallyldimethylammonium chloride via the reversible addition fragmentation chain transfer process", *Macromolecules*, Vol. 40, No. 11, pp. 3907–3913, 2007.

80. Assem, Y., A. Greiner and S. Agarwal, "Microwave-assisted controlled ring-closing cyclopolymerization of diallyldimethylammonium chloride via the RAFT process", *Macromolecular Rapid Communications*, Vol. 28, No. 18-19, pp. 1923–1928, 2007.

81. Erkoc, S., L. J. Mathias and A. E. Acar, "Cyclopolymerization of *tert*-butyl α-(hydroxymethyl) acrylate ether dimer via atom transfer radical polymerization (ATRP)", *Macromolecules*, Vol. 39, No. 26, pp. 8936–8942, 2006.

82. Tsuji, M., R. Sakai, T. Satoh, H. Kaga and T. Kakuchi, "Enantiomer-selective radical cyclopolymerization of rac-2,4-pentanediyl dimethacrylate using ATRP initiating

system with chiral amine ligand", *Macromolecules*, Vol. 35, No. 22, pp. 8255–8257, 2002.

83. Tsuji, M., T. Aoki, R. Sakai, T. Satoh, H. Kaga and T. Kakuchi, "Enantiomer-selective radical cyclopolymerization of rac-2,4-pentanediyl dimethacrylate using a ruthenium-mediated chiral atom transfer radical polymerization initiating system", *Journal of Polymer Science Part A: Polymer Chemistry*, Vol. 42, No. 18, pp. 4563–4569, 2004.

84. Bayrak, S., S. Erkoc, P. Ulus and A. E. Acar, "Atom transfer radical cyclopolymerization of *alkyl-α-(hydroxymethyl) acrylate (RHMA) ester ether dimers*: Effect of ester (R) substituent and temperature on cyclization efficiency", *239th ACS National Meeting*, San Francisco, CA, United States, March 21-25, 2010.

85. Plummer, R., Y. K. Goh, A. K. Whittaker and M. J. Monteiro, "Effect of impurities in cumyl dithiobenzoate on RAFT-mediated polymerizations", *Macromolecules*, Vol. 38, No. 12, pp. 5352–5355, 2005.

86. Xu, J., J. He, D. Fan, W. Tang and Y. Yang, "Thermal decomposition of dithioesters and its effect on RAFT polymerization", *Macromolecules*, Vol. 39, No. 11, pp. 3753–3759, 2006.

87. Mitsukami, Y., M. S. Donovan, A. B. Lowe and C. L. McCormick, "Water-soluble polymers. 81. Direct synthesis of hydrophilic styrenic-based homopolymers and block copolymers in aqueous solution via RAFT", *Macromolecules*, Vol. 34, No. 7, pp. 2248–2256, 2001.

88. Erkoc, S. and A. E. Acar, "Controlled/living cyclopolymerization of *tert*-butyl α-(hydroxymethyl) acrylate ether dimer via reversible addition fragmentation chain transfer polymerization", *Macromolecules*, Vol. 41, No. 23, pp. 9019-9024, 2008.

89. Ayfer, B. S., *Synthesis of Photopolymerizations of New Methacrylate Crosslinkers and Antibacterial Quaternary Ammonium Monomers*, M.S. Thesis, Bogazici University, 2004.

90. Lugtenberg, S. and L. Van Alphen, “Molecular architecture and functioning of the outer membrane of Escherichia coli and other gram-negative bacteria”, *Biochimica et Biophysica Acta: Protein Structure and Molecular Enzymology*, Vol. 737, pp. 51-115, 1983.

91. Salton, M. R., “Studies of the bacterial cell wall. IV. The composition of the cell walls of some Gram-positive and Gram-negative bacteria”, *Biochimica et Biophysica Acta.*, Vol. 10, pp. 512-523, 1953.

92. Drobnik, J. and F. Rypacek, “Soluble synthetic polymers in biological systems”, *Advances in Polymer Science*, Vol. 57, pp. 1-50, 1984.

93. Han, M. J., S. D. Kang and Y. L. Lee, “Synthesis and biological activities of the alternating copolymers containing cyclic ether rings along with carboxyl or hydroxyl groups on their backbones”, *Bulletin of the Korean Chemical Society*, Vol. 11, pp. 154-156, 1990.

94. Han, M. J., K. H. Kim, T. J. Cho and B. K. Choi, “Synthesis and characterization of poly[(3,4-dihydro-2H-pyran)-alt-(maleic anhydride)] and its derivatives: biologically active polymers”, *Journal of Polymer Science Part A: Polymer Chemistry*, Vol. 28, pp. 2719-2728, 1990.